UNIVERSITY OF SOUTHERN QUEENSLAND

Modifying Function and Fibrosis of Cardiac and Skeletal Muscle from *mdx* Mice

A Dissertation submitted by

Christel van Erp, BSc (Hons)

For the award of

Doctor of Philosophy

2005

ABSTRACT

Duchenne Muscular Dystrophy (DMD) is a fatal condition occurring in approximately 1 in 3500 male births and is due to the lack of a protein called dystrophin. Initially DMD was considered a skeletal myopathy, but the pathology and consequences of cardiomyopathy are being increasingly recognised. Fibrosis, resulting from continual cycles of degeneration of the muscle tissues followed by inadequate regeneration of the muscles, is progressive in both cardiac and skeletal dystrophic muscle. In the heart fibrosis interferes with contractility and rhythm whereas it affects contractile function and causes contractures in skeletal muscles. This study utilised the *mdx* mouse which exhibits a pathological loss of muscle fibres and fibrosis characteristic of DMD, to examine a range of mechanisms that can influence muscle function and fibrosis.

Ageing and workload both appear to contribute to the development of dystrophic features in cardiac and skeletal muscle of the *mdx* mouse. Therefore the effect of eccentric exercise on cardiac and skeletal muscle was examined in older *mdx* mice. Mice ran in 30 minute sessions for five months, 5 days per week. Downhill treadmill running did not exacerbate the contractile function or fibrosis of the *mdx* heart or the EDL, SOL or diaphragm muscles suggesting that cytokines influence function and fibrosis to a greater extent than workload alone.

The role of the cytokine TGF-β was examined by treating *mdx* mice with the TGF-β antagonist pirfenidone at 0.4, 0.8 or 1.2 % in drinking water for six months. Pirfenidone improved cardiac contractility ($P<0.01$) and coronary flow ($P<0.05$), to levels comparable to control mice, despite no reduction in cardiac fibrosis. Pirfenidone did not reduce fibrosis or improve function in skeletal muscle.

A deficiency of neuronal nitric oxide synthase (nNOS) in DMD and *mdx* mice causes a lowered production of nitric oxide indicating that the substrate of nNOS, l-arginine, may be beneficial to cardiac and skeletal muscle function in *mdx* mice. Oral l-arginine (5 mg/g bw) improved cardiac contractility, coronary flow and reduced cardiac fibrosis ($P<0.05$) without improving skeletal muscle function or fibrosis. In contrast, 10 mg/g bw l-arginine improved cardiac function and coronary flow ($P<0.01$), despite also elevating cardiac collagen. This increment in collagen was prevented by co-administration of prednisone.

The experiments described in this dissertation reveal for the first time that pharmacological treatments in *mdx* mice can improve cardiac structure and function. Further elucidation of the optimum time and doses of such treatments may result in future pharmacological treatments to improve cardiac function and fibrosis in DMD.

CERTIFICATION OF DISSERTATION

I certify that the ideas, experimental work, results, analysis and conclusions reported in this dissertation are entirely my own effort, except where otherwise acknowledged. I also certify that the work is original and has not been previously submitted for any other award, except where otherwise acknowledged.

_____ _____

Signature of Candidate **Date**

ENDORSEMENT

_____ _____

Signature of Supervisor/s **Date**

_____ _____

Date

ACKNOWLEDGEMENTS

During my PhD journey, there are many people I need to acknowledge for their non-stop encouragement, support and guidance.

Firstly, my principal supervisor, Associate Professor Andrew Hoey, thank you so much for your dedication, motivation and knowledge. Your positive attitude helped me through some challenging times and for that I am grateful.

Dr Mike Watson, my associate supervisor thanks for your down to earth nature, for reading my drafts and for making the laboratory a pleasant place to work.

Dr. Renée Cornford-Nairn, thank you for your invaluable friendship and support for the past years. I also wish to acknowledge Renée for completing the skeletal muscle experiments in Chapters 2, 3 and 4. Thank you for your contributions to these projects. The analysis of these experiments was completed by me.

Nicole Irwin, thank you for your friendship and your support over the last months. You have become a wonderful friend in a short time. I also wish to acknowledge Nicole for doing the TGF-β RNA experiments in Chapter 3.

Without the past and present members of the lab, this journey would have been very different, much longer and very lonely. All your friendships are appreciated and I will never forget your encouragement. Lisa, Peter, Nicki and Connie, thank you for your friendship, assistance in getting started on my projects and continuous support. Scott, Garth, Helen, Xiao and Rebecca, thank you for your distractions and for keeping my feet on the ground. At times when things would not work, especially the Langendorff experiments, you were always there to encourage me, so I would succeed eventually. Thanks for making sure I did not forget to laugh regularly!

Thank you to the ladies in the animal house, Julie Murphy and especially Sandra Sharp for looking after the mice and for your friendship and support and keeping me company in the many hours I spent treating the mice.

Also a big thank you to the technical and administrative staff of Biological and Physical Sciences, Debbie White, Pat McConnell, Vic Schultz, Adele Jones, Mo Boddington and Ros Gill and the ladies from Nursing (Kath, Angela, Joy and Lyn) for your friendship and support.

Thank you to Ruth Hilton, Chris Bartlett and Carla Hamilton from the Office of Research and Higher Degrees for their support and assistance throughout my postgraduate studies.

Thanks to Oliver Kinder (workshop manager) for your handyman work, you never cease to amaze me with your skills. Graham Holmes, thank you so much for the many times you helped me with the electronics involved with the treadmill.

Thanks to the IT guys, Sammy Quattromani, Phil Hallas, Stephen Payne and especially Chris de Byl. For all the times you helped to solve MAC problems, converted files, fixed profiles and attended to any other annoying computer problems that seemed to arise, I am grateful for your assistance.

Thank you to Laura Willems, Shirley Wee and John Headrick from Griffith University for your time and assistance with the Langendorff technique and thank you to Glen Harrison (also from Griffith University) for the loan of the treadmill.

Thank you to all my other friends. Without your support, I don't know what I would have done. You all kept me grounded during these past years. Whenever I needed a coffee, chat or a break, you were always there and understood. Even though you may not have fully understood many of the scientific terminology I used when things in the lab just didn't work!

Finally, the biggest acknowledgement and thank you goes to David and my family, Mum, Dad and Michael. Without your love, support, encouragement and guidance, I don't think this journey would have been what it was. Thanks especially to Mum and Dad for providing me with the knowledge that I can succeed in whatever it is I wish to do.

Table of Contents

List of Figures

List of Tables

PUBLICATIONS

van Erp, C. and Hoey, A. (2004). Effect of L-Arginine on cardiac function in *mdx* mice. J Mol Cell Cardiol, 37(1): 170 (presented at the XVIII World Congress of the International Society for Heart Research, Brisbane, August 2004).

Hoey, A., van Erp, C., Laws, N and Lu, S (2004). The aging *mdx* mouse as a model of cardiomyopathy for Duchenne Muscular Dystrophy. J Mol Cell Cardiol, 37(1): 174 (presented at the XVIII World Congress of the International Society for Heart Research, Brisbane, August 2004).

van Erp C. and Hoey, A (2005). The effect of long term administration of L-Arginine and Prednisone on cardiac function in *mdx* mice. (submitted).

van Erp C., Cornford-Nairn R. and Hoey, A. (2005). The effect of long term administration of Pirfenidone on cardiac and skeletal muscle function of *mdx* mice (in draft).

van Erp C., Cornford-Nairn R. and Hoey, A. (2005). The effect of long term l-arginine on cardiac and skeletal muscle function in *mdx* mice. (in draft).

PRESENTATIONS

van Erp C. (2002). The prevention and reversal of fibrosis in Duchenne Muscular Dystrophy. *Department of Biological and Physical Sciences, University of Southern Queensland Postgraduate Conference, Toowoomba*.

van Erp C. (2003). The prevention and reversal of fibrosis in Duchenne Muscular Dystrophy. *Department of Biological and Physical Sciences, University of Southern Queensland Postgraduate Conference, Toowoomba*. (Winner- best presentation voted by peers)

van Erp C. (2004). The prevention and reversal of fibrosis in Duchenne Muscular Dystrophy. *Department of Biological and Physical Sciences, University of Southern Queensland Postgraduate Conference, Toowoomba*. (Winner – best presentation voted by peers)

van Erp C. (2005). The prevention and reversal of fibrosis in Duchenne Muscular Dystrophy. *University of Iowa, Iowa*.

van Erp C. (2004). The prevention and reversal of fibrosis in Duchenne Muscular Dystrophy. *Johns Hopkins Hospital, Baltimore, Maryland*.

ABBREVIATIONS

BDM	2,3-butanedione monoxime
BMD	Becker Muscular Dystrophy
C57	C57BL10ScSn
DAGPC	Dystrophin Associated Glycoprotein Complex
DMD	Duchenne Muscular Dystrophy
DP	Developed Pressure
+dP/dt	Rate of Contraction over time
-dP/dt	Rate of Relaxation over time
ECM	Extra Cellular Membrane
EDL	Extensor Digitorum Longus
ESP	End Systolic Pressure
FOC	Force of Contraction
g	gram
H&E	Haematoxylin and Eosin
HP	Hydroxyproline
Hz	Hertz
IGF-1	Insulin-like Growth Factor -1
LV	left ventricle
M	molar
Mdx	C57BL10ScSn *mdx* (muscular dystrophic x-linked)
mg	milligram
min	minute

mL	millilitre
mM	millimolar
MMP	Matrix metalloproteinases
mN	milliNewton
mRNA	messenger RNA
ms	millisecond
nNOS	neuronal Nitric Oxide Synthase
NO	Nitric Oxide
NOS	Nitric Oxide Synthase
PSR	Picrosirius Red
ROS	Reactive Oxygen Species
SDH	Succinate Dehydrogenase
SEM	Standard Error of Mean
SERCA	Sarco-endoplasmic Reticulum Ca^{2+} ATP-ase
SOL	Soleus
sPo	Specific Tetanus Force
sPt	Specific Twitch Force
SR	Sarcoplasmic Reticulum
TGF-β	Transforming Growth Factor Beta
TNF-α	Tumour Necrosis Factor Alpha
vs.	versus

CHAPTER 1 : INTRODUCTION: DUCHENNE MUSCULAR DYSTROPHY

1.1 Brief History of Duchenne Muscular Dystrophy

Duchenne Muscular Dystrophy (DMD) was first described by English physician Edward Meryon in 1851. He described the clinical presentation as onset in childhood with progressive weakness and death in early adulthood and showed it to be a familial disease with a predilection for males. Most importantly, Meryon found the muscle sarcolemma in these patients was broken down and destroyed, which is where the protein deficiency is now known to occur (Emery 2002). Meryon's clear description of the disorder and understanding of its nature were very significant contributions. In 1861 Meryon's work was surpassed by French neurologist Duchenne de Boulogne, who studied the disease pathogenesis extensively and after whom DMD was named. Duchenne developed a biopsy technique that enabled him to study material from the same patient at different stages of the disease, thereby allowing a diagnosis of the disease during their life. In 1879, William R Gowers discussed the clinical features, pathology, prognosis and possible treatment of DMD. He is most widely known for his detailed presentation of the clinical features of the disease and describes what is now commonly referred to as the Gower's manoeuvre (Emery & Muntoni 2003).

1.2 What is Duchenne Muscular Dystrophy?

Duchenne Muscular Dystrophy is the most common form of muscular dystrophy, affecting 1 in 3500 live male births. The disorder is an X-linked recessive genetic disorder most often affecting boys. Patients affected by this disease usually present at 3-

5 years of age with pseudo-hypertrophic calf muscles, decreased levels of physical activity and in one third of cases, non-progressive cognitive impairment. The muscle degeneration evident in DMD is severe, involving all three muscle types (skeletal, cardiac and smooth) and leading to a shortened life expectancy. Most patients are wheelchair dependent by the age of 12 due to the progressive skeletal muscle wasting and death occurs in early to mid twenties as a result of respiratory or cardiac failure (O'Brien & Kunkel 2001).

1.3 Becker Muscular Dystrophy

A similar, yet milder, form of dystrophy known as Becker Muscular Dystrophy (BMD) is phenotypically more variable and usually follows a less severe course than DMD. BMD patients display a wide range of clinical signs, ranging from individuals losing the ability to walk in their late teens, to some only experiencing mild proximal muscle weakness or cramps on exercise and never become significantly physically impaired during the course of their lives (Emery & Muntoni 2003). The most common form of death in BMD is cardiac failure. This form of muscular dystrophy has an incidence of between one tenth of DMD (1 in 35 000) (Finsterer & Stollberger 2003) and 1 in 18 450 in the United Kingdom (Bushby, Thambyayah & Gardner-Medwin 1991).

1.4 Clinical Symptoms of DMD

DMD consists of four overlapping phases. These include an early phase, late childhood, adolescence and adult.

1.4.1 Early phase

The early phase begins at birth and can continue until 8 years of age. The most important aspect of this phase is the early recognition of the presence of the disorder. The young boys will usually present with delayed walking and may also have difficulty running or performing simple gross motor tasks. Serum creatine kinase (CK) levels are also increased in this phase. This enzyme originates in muscle and escapes into the serum as the muscle degenerates. Grossly elevated levels of CK also occur in BMD. Levels of serum CK decrease as the disease progresses, likely due to the decrease in physical activity of the young boys and the increased levels of fibrosis, reducing available muscle mass from which the enzyme can be released. In this early phase, the pelvis tilts forwards as a result of gluteal maximum weakness and a compensatory lumbar lordosis develops. To maintain balance, the child also tends to walk on his toes. Gowers manoeuvre, a clinical feature of DMD, is frequently manifested at this stage of the disease (Figure 1.1). Due to weakness from the hips and knee extensors, a young boy will climb up his thighs using his hands, pushing down on them to extend the hips and trunk (Figure 1.1).

1.4.2 Late Childhood

The main features of this phase are increasing contractures in the lower extremities and decreasing muscle strength, which usually occurs between the ages of 6 and 13. Gowers manoeuvre is also often seen during this phase and ultimately the ability to walk will be severely affected and lost. Changes in functional status in this phase are decreased exercise tolerance and increased frequency of falling episodes. As the disease progresses,

shortening of the Achilles tendon becomes more marked and the lumbar lordosis more exaggerated.

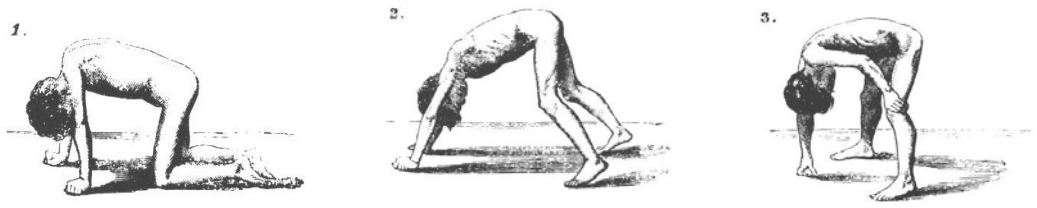

Figure 1.1: Gowers Manoeuvre
The child climbs up his thighs, using his hands when attempting to stand up. Figure from Emery (1993).

1.4.3 Adolescence

This stage occurs from 8-15 years of age, when the patient becomes dependent on a wheelchair for mobility and joint contractures progress rapidly. Unless adequate support is provided in the wheelchair, severe kyphoscoliosis can develop. This curvature of the thoraco-lumbar spine is the most significant deformity to develop in these later stages of the disease (Figure 1.2). Once the curvature has progressed beyond 20-30 degrees continued progression is certain. When the spine is curved to this extent there will be an associated deterioration of cardiac and pulmonary function. There is also a significant loss of skeletal muscle strength at this stage of DMD.

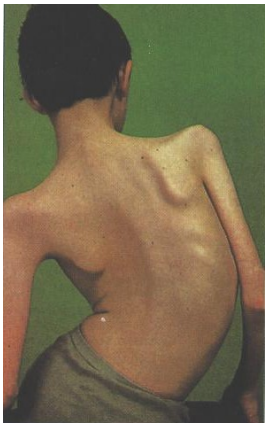

Figure 1.2: DMD patient with extreme kyphoscoliosis
Figure from Forbes and Jackson (1997)

1.4.5 Adulthood

At 15 years of age and older, cardiac manifestations of DMD, in addition to ongoing skeletal muscle pathology, are observed. Heart complications become the main threat to both health and life expectancy due to necrosis and fibrosis of cardiac muscle. As a result, the myocardium begins to deteriorate causing a high risk of heart failure, with nearly 90% of DMD patients exhibiting impaired cardiac function. A decade ago, many DMD boys died of respiratory failure before 20 years of age (McDonald et al. 1995), but improvement in care and ventilation has extended this age by 5-10 years (Eagle et al. 2002). This longer lifespan has in turn increased the presentation of cardiac manifestations and heightened awareness of cardiomyopathy as a contributor to mortality (Eagle et al. 2002), with death due to cardiomyopathy occurring in 20% of cases (Boland et al. 1996; Farah, Evans & Vignos 1980; Finsterer & Stollberger 2003; Hoogerwaard et al. 1999).

1.5 Dystrophin Gene and Dystrophin

1.5.1 Dystrophin Gene

DMD follows an X-linked pattern of inheritance, with two thirds of affected males inheriting the disease from a carrier mother and one third resulting from *de novo* mutations. The dystrophin locus is now known to span 2.6 million bases and 79 exons of the human X chromosome, making it the largest known mammalian gene. The dystrophin gene was first identified in 1987 and localised to band Xp 21 on the human X chromosome (Hoffman, Brown & Kunkel 1987). The 14 kb mRNA encodes 3685 amino acids to create the 427 kDA protein, dystrophin. The enormous size of the dystrophin gene explains the high mutation rate seen in patients (Davies 1997). Errors within the dystrophin gene comprise of deletions and point mutations, with deletions shown to occur in 65% of DMD cases (Emery 2002). In deletions one or more bases in the sequence are deleted, resulting in a shift in the open reading frame. This causes a loss of the normal reading sequence of the gene and halts production of the gene product. A point mutation results from a single substitution of one base with another and these occur in 30% of patients. Such a mutation may also prevent further processing of the gene and hence stop synthesis of the dystrophin protein (Gillis 1996). The remaining 5% of DMD patients have gene duplications (O'Brien & Kunkel 2001).

1.5.2 Dystrophin Protein

Dystrophin is found in skeletal, cardiac and smooth muscle and has been shown to be absent or greatly diminished in muscle from DMD patients (McArdle, Edwards & Jackson 1995). Dystrophin is also found in some neurones in the spinal cord and the

cerebellum, which is thought to contribute to the intellectual retardation seen in some boys with DMD (Tay et al. 1992).

The cytoskeletal protein dystrophin is located on the cytoplasmic side of the plasma membrane (Figure 1.3). The exact role of dystrophin has not yet been fully determined, but it is thought that dystrophin acts either as a structural scaffold that distributes mechanical stress through the sarcolemma (muscle cell membrane) or participates in the regulation of intracellular calcium levels (Niebroj-Dobosz, Fidzianska & Hausmanowa-Petrusewicz 2001).

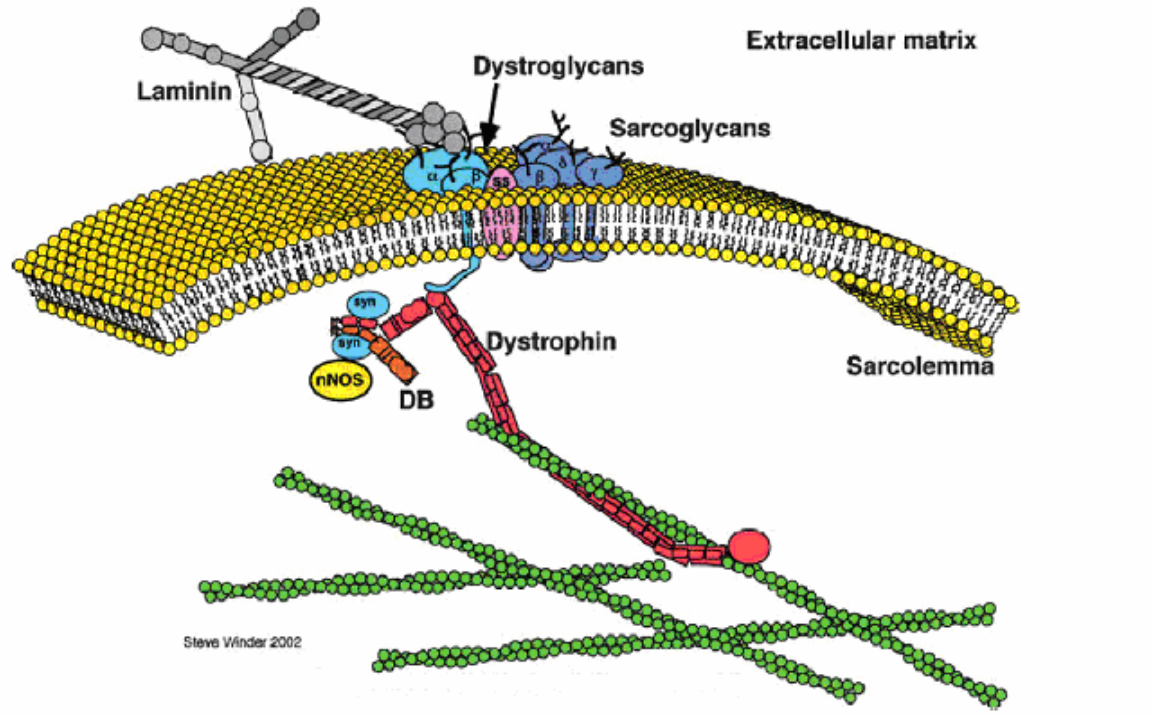

Figure 1.3: The cytoskeletal protein, dystrophin
The location of dystrophin (red) and its association with the actin (green) filaments. Figure adapted from Spence, Chen & Winder (2002).

The 427kDa protein is composed of four distinct structural domains, an N-terminal actin binding domain, a rod shaped domain consisting of spectrin like repeats, a cysteine rich domain and a carboxyl terminal domain. Dystrophin is not inserted directly into the membrane but rather via β-dystroglycan (indicated in light blue in Figure 1.3). A loss of dystrophin completely severs the link between the contractile protein actin and the cell membrane. This leads to a marked reduction in all other dystrophin associated proteins, thus disrupting the link between the subsarcolemmal cytoskeleton and the extracellular matrix. This loss of integrity of the cell membrane of dystrophin-deficient muscle disrupts normal muscle homeostasis and permits the unregulated transit of extracellular calcium into the cytoplasm which increases activation of calcium dependent proteases such as calpains (Spencer, Croall & Tidball 1995). Affected myofibres are more susceptible to inflammation and cell death (Matsumura & Campbell 1993). The presence of muscle satellite cells allows regeneration of new muscle fibres, but the new muscle fibres are also dystrophin deficient and subsequently degenerate. In turn, each cycle of degeneration and regeneration increases the extent of fibrosis within that muscle (Wehling, Spencer & Tidball 2001). This process is also known as the mechanical damage theory, described in Figure 1.4.

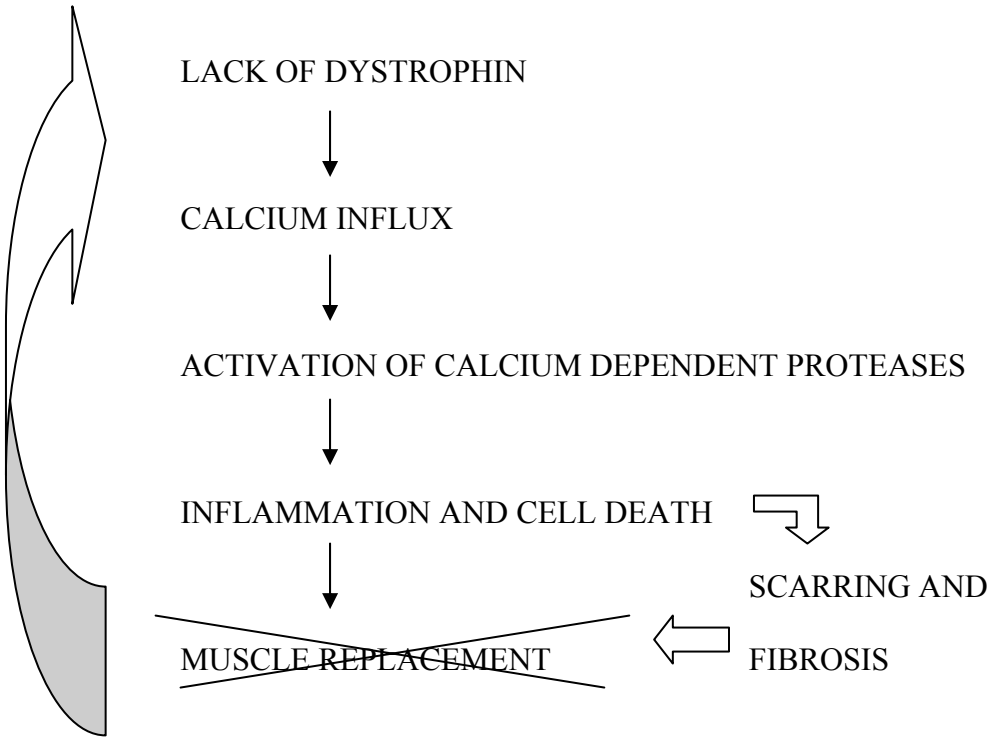

Figure 1.4: The mechanical damage theory
A lack of dystrophin leads to a calcium influx and activation of calcium dependent proteases. This results in inflammation and cell death. In DMD, replaced muscle is also deficient in dystrophin, allowing repetition of this cycle. The inflammation and cell death causes scarring and fibrosis which affects the muscle being replaced. This cycle is continuous and each time it is repeated, it increases the extent of fibrosis within that muscle.

Mutations in the cysteine domain and first half of the carboxy-terminal of the dystrophin protein usually result in severe phenotypes, whereas deletions of the actin end of the end central rod domain can be associated with mild and severe phenotypes. In BMD the nature of the mutations or deletions are such that they allow for synthesis of an abridged, yet partly functional, dystrophin molecule, which may explain the milder phenotype observed for these patients. For example, a loss of the last 200 amino acids of dystrophin

results in a BMD or milder DMD phenotype (Chakkalakal et al. 2005; O'Brien & Kunkel 2001).

1.5.3 Dystrophin Associated Glycoprotein Complex

The dystrophin associated glycoprotein complex (DAGPC) is divided into several sub-groups, the dystroglycans including dystrophin and the laminin alpha-2 chain, the intracellular syntrophins and dystrobrevins and lastly the proteins comprising the transmembrane sarcoglycan-sarcospan subcomplex (Figure 1.5). Deletions or mutations within these sub-groups can lead to different types of muscular dystrophy. A mutation or deletion of dystrophin as mentioned previously, will lead to either DMD or BMD, an alteration in the laminin alpha-2 chain can cause congenital muscular dystrophy (CMD) and mutations in the sarcoglycan-sarcospan subcomplex lead to the various forms of the limb girdle muscular dystrophies (LGMD) (Cox & Kunkel 1997; O'Brien & Kunkel 2001) (Figure 1.5).

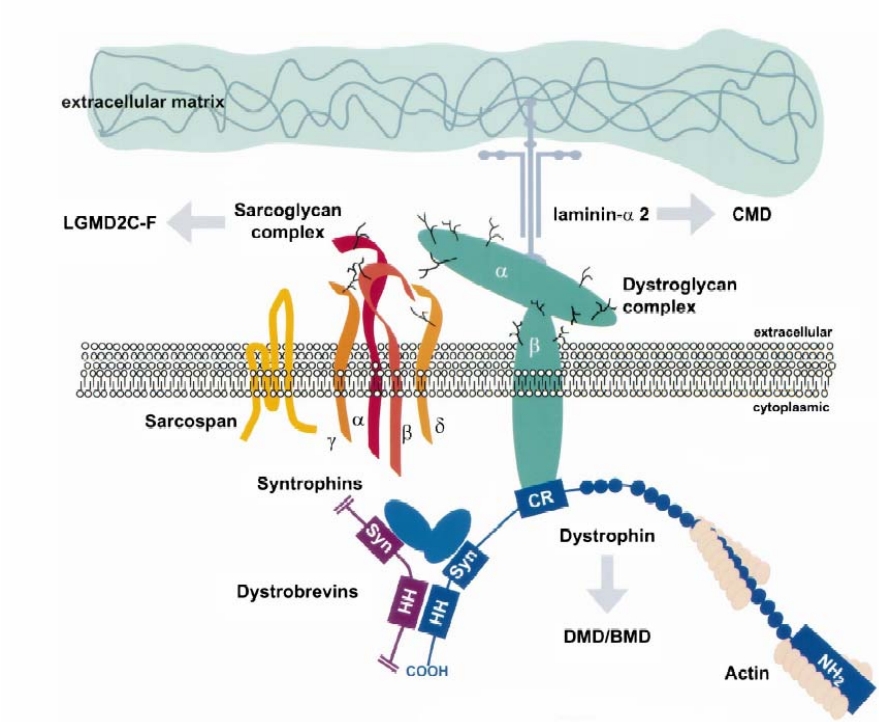

Figure 1.5: The dystrophin associated glycoprotein complex
The dystrophin associated glycoprotein complex and muscular dystrophies that arise due to primary defects in different areas of the complex. Arrows indicate the disorder arising from a dysfunction in that section of the dystrophin glycoprotein complex. DMD = Duchenne Muscular Dystrophy, LGMD2C-F = Limb Girdle Muscular Dystrophy, CMD = Congenital Muscular Dystrophy. Figure adapted from O'Brien & Kunkel (2001).

1.6 Utrophin

A dystrophin-related protein utrophin was discovered on chromosome 6 in 1989 (Love et al. 1989). The utrophin transcript encodes a 400kDa protein that has been found in all tissues and continues to be expressed in DMD patients at elevated levels (Koenig et al. 1989). Utrophin is not only expressed within skeletal, cardiac and smooth muscle cells but is also found within nerves and blood vessels. Utrophin is found in high levels in the lungs and kidneys and is enriched at the neuromuscular junction (NMJ) where it binds to components of the DAPC, including the dystroglycans and syntrophins. Although the role of utrophin has not been determined, it is thought to play an important role in the

structure of the post-synaptic cytoskeleton (Michalak & Opas 1997). Initial examination of the primary sequence and protein structure of utrophin revealed clear similarities to dystrophin (Tinsley, J. M. et al. 1992), thereby creating interest in up-regulation of this protein for potential DMD therapies.

1.7 Animal Models

The discovery and characterisation of the X-linked gene that is defective in DMD and of its protein product has led to the identification of biochemical homologues of this disease in the mouse, dog and cat, amongst other animals. These three main animal models resemble DMD in that they lack dystrophin and that skeletal muscle fibres undergo fibrosis, spontaneous necrosis and regeneration (Partridge 1991). However, there remain limitations in using these various animal models.

1.7.1 Golden Retriever Muscular Dystrophy

The golden retriever muscular dystrophy (*GRMD*) dog shows greatest similarity to DMD of all current animal models. This animal model manifests with muscle weakness, paralleled by a progressive loss of muscle tissue and development of fibrosis. Histopathological investigations of muscles of *GRMD* reveal early fibre necrosis and regeneration associated with endomysial and perimysial fibrosis, resulting in severe myopathy (Valentine et al. 1990). However, due to its high cost, maintenance and ethical issues involving canine research, this DMD model is not frequently used.

1.7.2 Feline X-linked Muscular Dystrophy

The feline X-linked muscular dystrophy (*FXMD*) is another dystrophic model not widely used. The cat has dystrophin deficiency characterised by muscular hypertrophy. The *FXMD* model, however, never loses muscle tissue and therefore maintains its contractile strength. Moderate fibrosis does occur in this model, but there is no fatty infiltration, unlike the *mdx* and *GRMD* animal models (De la Porte, Morin & Koenig 1999). For this reason, the *FXMD* model is limited in DMD research.

1.7.3 Mdx Mouse

The animal model most frequently used in DMD research is the mouse model, C57BL10ScSn *mdx* (*mdx*). The *mdx* mouse was first described by Bulfield et al., (1984) as a spontaneous mutation arising from a colony of C57BL10Sc/Sn mice (C57). This allows for the C57 mice to be used as the comparable control animals in research using *mdx* mice. The genetic defect is a point mutation introducing a premature stop codon at exon 23 in the gene coding for dystrophin (Sicinski et al. 1989) thus resembling the genetic defect seen in boys with DMD. Many subsequent studies have used the *mdx* mouse as a model to examine the potential role of dystrophin in normal muscle and the mechanisms by which the dystrophin deficiency leads to myopathy (McArdle, Edwards & Jackson 1995).

In the *mdx* mouse, skeletal muscles exhibit degeneration and necrosis starting at 2-3 weeks postnatal and persisting throughout the life of the mice, without gross impairment of motor activities in the young animals (Pastoret & Sebille 1995b).

Mdx muscles degenerate following membrane damage, resulting in calcium uptake by the cell, overcontraction of muscle fibres and activation of intracellular proteases (De la Porte, Morin & Koenig 1999). *Mdx* mice exhibit successive cycles of degeneration-regeneration in their skeletal muscle from 3 weeks to approximately 18 months of age. *Mdx* muscle exhibits the pathological loss of muscle fibres and fibrosis characteristic of muscular dystrophy relatively late in the life span of these mice. As in DMD, a combination of necrosis and an inadequacy of muscle fibre regeneration is thought to be responsible for replacement of muscle with connective tissue and fat in later stages of the disease (Zeman et al. 2000). In the *mdx* animal model, significant fibrosis is evident. The lack of dystrophin in *mdx* mice leads to persistent necrosis of muscle fibres (Pagel & Partridge 1999) with the eventual onset of fibrosis, first in the diaphragm (Stedman et al. 1991), and towards the end of the second year, in the limb muscles (Pastoret & Sebille 1995a).

Mdx mice demonstrate tachycardia, decreased heart rate variability and altered autonomic heart rate modulation. The *mdx* mouse also displays abnormal electrocardiograms (ECG) and myocardial lesions, characterised by necrosis, macrophage infiltration and inflammation. These cardiac parameters are consistent with observations of DMD patients (Bridges 1986; Chu et al. 2002). At 8-10 weeks of age cardiomyocytes have a reduced threshold for the development of sarcolemmal injury under mechanical stress and at 12-14 weeks the pathophysiology of the *mdx* myocardium is evident by altered contractile function (Danialou et al. 2001; Sapp, Bobet & Howlett 1996). Because of these similar pathological features between the *mdx* mouse and DMD patients, the *mdx*

mouse has been used extensively for research into understanding the pathogenic mechanisms and exploring better treatment protocols for DMD. Advantages of using the *mdx* mouse include short breeding time, low cost and close pathological resemblance between murine and human diseases.

1.8 Current Treatment of Duchenne Muscular Dystrophy

There are currently a wide range of therapies and treatment options for patients with DMD. Unfortunately, many of these will only treat the symptoms of this disorder, without affecting the underlying cause. There are numerous current research projects aimed at symptomatic improvement and the underlying pathology of DMD.

1.8.1 Physical Therapy

A combination of different therapies play an important role in keeping the body as flexible, upright and mobile as possible. There are three main areas where contractures (loss of elasticity in the joints) are most prevalent: the Achilles tendons, hamstrings, and hip flexors. Exercise and stretching can help postpone or even prevent contractures in boys with DMD. The simplest form of exercise for boys with DMD is swimming. This is a non-weight bearing exercise where the buoyancy of the water makes the exercise easier to perform (Posselt 2005). Throughout their life, braces may be required for support and wheelchairs allow the child to move faster and prevent falling. Kyphoscoliosis is one of the physical symptoms of DMD as mentioned earlier. Surgery is usually recommended for children whose spinal curvature exceeds 25-30 degrees. To

reduce further compromise in their respiratory system, surgery for scoliosis should be performed as early as practical on DMD patients.

1.8.2 Pharmacological Therapies

Pharmacological therapies have attempted to improve the functional and morphological aspects of DMD for decades. Many of these have attempted to prevent degeneration of muscles and delay the onset of the more serious sequelae of DMD (Chakkalakal et al. 2005).

1.8.2.1 Prednisone

Prednisone is a glucocorticoid that slows the rate of muscle degeneration. Prednisone and related drugs such as prednisolone have been shown to be effective in the treatment of DMD (Drachman, Toyka & Myer 1974) and accordingly are the most widely used drugs to treat this disorder. In some cases walking may be prolonged for two or more years, and pulmonary function can also be improved (Brooke et al. 1987; DeSilva et al. 1987). More recently prednisone was found to delay or prevent scoliosis in DMD patients (Yilmaz, Karaduman & Topaloglu 2004). Not only is muscle loss halted by this glucocorticoid, but strength and function also improve dramatically (Fenichel et al. 1991). The benefits of prednisone may also be optimised by initiating treatment before the onset of functional decline in DMD patients (Merlini et al. 2003).

The exact mechanism of action, however, remains unknown, with several modes of action proposed. These include anti-inflammatory actions, where the total T-cell number

and cytotoxic cells were decreased after prednisone treatment (Kissel et al. 1991). A reduction in the concentration of inflammatory cells in *mdx* muscle results in a decrease in muscle degeneration suggesting prednisone also has immunosuppressive effects (Wehling-Henricks, Lee & Tidball 2004). Some of the beneficial effects of prednisone treatment in DMD patients may be due to a reduction of calcium influx and of the size of calcium pools in dystrophic muscle fibres (Metzinger et al. 1995). Prednisone has been shown to enhance the myogenesis of satellite cells and increase dystrophin-related protein expression in *mdx* mouse skeletal muscle cell cultures (Passaquin et al. 1993). The beneficial effects of prednisone on strength in DMD are associated with an increase in muscle mass. This improvement is thought to be mediated by inhibition of muscle proteolysis rather than stimulation of muscle protein synthesis (Kawai et al. 1993; Rifai et al. 1995). There are many different theories on how prednisone improves muscle function. Changes in gene expression, increased protein levels, and neurotransmission have all been suggested as possible modes of action (Fukudome et al. 2000; Rifai et al. 1995). mRNA levels of structural, signalling and immune response genes are altered after steroid treatment, explaining how this steroid-induced gene expression may improve strength (Muntoni et al. 2002). Prednisone treatment affects neuromuscular transmission in isolated *mdx* diaphragm (Fukudome et al. 2000) and increases strength and endurance in *mdx* mice (Hudecki et al. 1993). Prednisone may also increase the activity of a utrophin promoter, thereby affecting the expression of utrophin in muscle (Courdier-Fruh et al. 2002).

Unfortunately prednisone is known to have several significant side effects including weight gain, which can lead to hypertension and the development of lenticular cataracts (Griggs et al. 1993). Growth may also be arrested and bone density decreased, leading to osteoporosis (Bianchi et al. 2003). There are also severe psychological side effects in some patients, such as difficulty concentrating, sleeping, and controlling emotions which may lead to further complications such as depression or aggression. In addition, the long term use of glucocorticoids may impair the body's ability to fight infections and heal wounds. Fortunately, severe side effects can be minimised by non-daily dosing regimes.

1.8.2.2 Deflazacort

Deflazacort is a glucocorticoid that also improves muscle strength and function significantly (Biggar et al. 2001; Campbell & Jacob 2003). It is an oxalazine derivative of prednisone and it appears to have less severe side effects than prednisone (Biggar et al. 2004; Mesa et al. 1991). Thirty percent of boys on long-term daily deflazacort treatment have been shown to develop asymptomatic cataracts (Biggar et al. 2001). Long-term alternate day treatment, however, is not associated with cataracts, but the preservation of muscle function is not as effective as daily deflazacort (Biggar et al. 2004). This drug is not widely available in Australia or in the United States of America. Deflazacort has been shown to improve respiratory and left ventricular function (Silversides et al. 2003) and recently has been shown to stimulate utrophin expression (St-Pierre et al. 2004). Deflazacort increases myogenic repair and myoblast fusion. Treatment with this glucocorticoid increased laminin expression, prevented the progression of cardiomyopathy in *mdx* mice and increased NOS-Imu expression in regenerating muscles

(Anderson, McIntosh & Poettcker 1996; Anderson & Vargas 2003; Anderson, Weber & Vargas 2000; Skrabek & Anderson 2001), all suggestive of improved satellite cell function.

1.8.2.3 Creatine Monohydrate

Creatine monohydrate is a nutritional supplement which improves muscle performance in athletes and healthy subjects. This prompted interest in its potential to limit muscle degeneration or restore muscle function in neuromuscular diseases (Louis et al. 2003). The decrease in intracellular creatine concentration in DMD may contribute to the deterioration of intracellular energy homeostasis and may thus be one of the factors aggravating muscle weakness and degeneration (Felber et al. 2000). In a clinical case report, a 9 year old DMD patient experienced improved muscle performance during creatine supplementation (Escolar et al. 2005). These preliminary observations indicate a potential role for creatine supplementation in the symptomatic therapy of patients with muscle disease. A recent clinical trial by the Cooperative International Neuromuscular Research Group (CINRG) involved 34 DMD patients where 15 patients were administered 5 g/day of creatine, with the remaining 19 receiving a placebo (Escolar et al. 2005). Manual Measure of Muscle Strength (MMT) and Quantitative Measure of Muscle Strength (QMT) were measured before and after the clinical trial. Consistent trends were evident with a reduced deterioration in QMT which suggests a modest improvement of strength over time. Unfortunately, the study was underpowered and no statistical significance was evident. This study concluded that creatine does not improve strength to

the same degree as prednisone or deflazacort (Escolar et al. 2005). In conclusion, this therapy might relieve some clinical symptoms, but will not treat the underlying condition.

1.8.3 Myostatin Blocking agents

Satellite cells are quiescent myogenic precursor cells residing at the interface between the basal lamina and sarcolemma. These cells give rise to myoblasts that partake in the normal development of myofibres. Satellite cells can migrate to sites of muscle injury and fuse with existing myofibres to maintain muscle mass. Myostatin is a member of the TGF-β family that is expressed in muscle and circulates in the blood (McPherron & Lee 1997). It is a negative regulator of skeletal muscle growth with gene mutations leading to increased musculature *in vivo*. To determine the effect of myostatin loss in *mdx* mice, such mice were crossed with myostatin null mutant mice. The diaphragm of these myostatin deficient *mdx* mice showed less fibrosis, suggesting improved muscle regeneration (Wagner et al. 2002). It has been hypothesised that myostatin blockade may offer a strategy for reversing muscle wasting in DMD (Bogdanovich et al. 2005). The mechanism behind the ability of myostatin to decrease muscle growth is unknown, but it has been stated that myostatin negatively regulates satellite cell activation (McCroskery et al. 2003).

1.8.4 Aminoglycosides

1.8.4.1 Gentamicin

Gentamicin is an aminoglycoside antibiotic known to affect bacterial DNA processing pathways. Aminoglycosides such as gentamicin and negamycin may have therapeutic

value for the treatment of DMD because of their ability to induce ribosomes to read through stop codons of nonsense mutations (Howard et al. 2004). Gentamicin and negamycin have induced low levels of dystrophin in *mdx* muscle fibres (Arakawa et al. 2003; Barton-Davis et al. 1999). Subsequent studies have failed to induce dystrophin expression in *mdx* mice (Dunant et al. 2003) and no dystrophin expression has been achieved in human studies of DMD and BMD (Nowak & Davies 2004). The application of this approach to a treatment for DMD is limited as only between 5-15% of DMD cases are caused by premature stop codons in the dystrophin gene (Emery & Muntoni 2003), and due to the nephrotoxicity of aminoglycosides their long term administration is limited.

1.8.4.2 PTC124

PTC124 is an investigational drug for the treatment of genetic defects resulting from nonsense mutations including some cases of DMD. PTC124 allows the cellular machinery to bypass the nonsense mutation, so that translation continues and restores the production of the full-length, functional protein. In *mdx* mice, oral administration of PTC124 resulted in production of dystrophin protein in skeletal muscles, as measured by immunofluorescence. Phase 1 studies have been successfully completed and have provided the basis for the development of a dosing regimen for Phase 2 studies in DMD which are due to begin later this year (PTCTherapeutics 2005).

1.8.5 Utrophin upregulation

Upregulation of utrophin has been proposed as a potential therapy for DMD. Utrophin overexpression along the length of dystrophin deficient muscles may correct dystrophic symptoms. The expression of full length utrophin in muscles from transgenic *mdx* mice can lead to significant improvements in mechanical functions and prevention of dystrophic pathology (Tinsley, J. et al. 1998). If utrophin is able to be safely upregulated using pharmacological means, it could be a potential treatment for DMD. A limitation of this strategy is that upregulation of utrophin does not appear to be effective in cardiomyocytes as utrophin upregulation was unable to prevent the development of life-threatening myocardial dysfunction in two patients with severe dilated cardiomyopathy due to dystrophin gene mutations (Fanin et al. 1999).

1.8.6 Tumour Necrosis Factor alpha Blockade

Tumour Necrosis Factor alpha (TNF-α) is an early and potent inflammatory cytokine that stimulates the inflammatory response. The concentration of this cytokine is increased in muscular dystrophy (Gosselin et al. 2003). In dystrophic muscle TNF-α could exacerbate damage seen in this fragile membrane. Remicade (Infliximab) and Enbrel (Etanercept) are two agents used clinically to block the functional activity of TNF-α. Treatment of *mdx* mice with Remicade (anti-TNF-α antibody) reduces the onset and intensity of necrosis and dystrophic pathology in skeletal muscle (Grounds & Torrisi 2004). Enbrel inhibits the binding of TNF-α to TNF receptors and blocks the acute inflammatory cell response *in vivo* in female C57BL10ScSn mice after whole muscle autografts (Grounds et al. 2005). Elimination of TNF-α in *mdx* mice resulted in significant improvements in

ventilatory function and diaphragm strength (Gosselin et al. 2003). Administration of TNF-α results in negative inotropic effects, therefore inhibition of TNF-α may improve left ventricular dysfunction (Bozkurt et al. 1998). In addition, it has been observed that these drugs can worsen the clinical condition of patients with heart failure (Ziegelstein 2005) which may include DMD patients. The reason why this TNF-α antagonism adversely affects the clinical status in heart failure is not clear (Gupta & Tripathi 2005).

1.8.7 Cell therapies

1.8.7.1 Myoblast transplantation

During the early stages of DMD, new muscle fibres are formed following cycles of degeneration. Eventually myogenic satellite cell supply is exhausted, causing the muscle fibres to be replaced with fat and connective tissue, leading to the characteristic loss of muscle mass and strength observed in DMD. Myoblast transplantation involves injecting or transplanting donor muscle precursor cells (containing dystrophin) into a dystrophin deficient host. This process allows fusion of donor cells with the host tissue, inducing expression of dystrophin (Chakkalakal et al. 2005). Transplantation of donor myoblasts that carry a normal functional copy of the dystrophin gene has the potential to not only repair existing fibres, but also to generate new muscle fibres and replenish the regenerative satellite cell population (Biggar et al. 2002). Early results indicate successful myoblast transfer in *mdx* muscle and primates (Gussoni et al. 1992; Skuk 2004). Unfortunately, clinical trials have given disappointing results (Mendell et al. 1995; Tremblay et al. 1993) and the effectiveness of this technique is hindered by

numerous limitations, including minimal distribution of cells after injection, immune rejection, and poor cell survival.

1.8.7.2 Stem Cell Therapy

Pluripotent stem cells have the potential of developing into muscle cells and are obtained from bone marrow, umbilical cord blood and even early embryos. Stem cells have been shown to proliferate longer than myoblast cells (Nowak & Davies 2004). Bone marrow transplantation has been performed to correct dystrophin deficiency in the *mdx* mouse resulting in dystrophin positive fibres in skeletal and cardiac muscle (Bittner et al. 1999; Ferrari et al. 1998; Gussoni et al. 1999). Bone marrow transplantation from a dystrophin positive donor to a DMD patient was shown to be a viable means by which to deliver these cells to muscle (Gussoni et al. 2002). However, in the above studies only a few fibres became dystrophin positive after transplantation. Mesoangioblasts are vessel associated foetal stem cells that can differentiate into most mesoderm cell types when exposed to certain cytokines. In α-sarcoglycan null mice (a model for limb girdle muscular dystrophy), mesoangioblasts isolated from juvenile dystrophic mice and transfected with a lentiviral vector expressing α-sarcoglycan, diffused from the arterial tree into skeletal muscle where they were incorporated into regenerating fibres (Sampaolesi et al. 2003). After the mesoangioblast injection, the dystrophic phenotype of virtually all downstream muscles was corrected morphologically and functionally to a level similar to that seen in wild type cells. The mice also showed a decrease in Evans Blue dye uptake (Sampaolesi et al. 2003) suggesting a reduction in overall muscle

necrosis. These positive outcomes suggest a promising approach to using stem cells in furthering DMD research.

1.8.8 Molecular Therapy

1.8.8.1 Gene therapy

Gene therapy involves delivering DNA-coding regions for dystrophin directly into the muscle using vectors. These vectors deliver the genetic material to target tissues, such as skeletal and cardiac muscle. This can result in the expression of dystrophin in muscle fibres by the cells using pre-existing cellular machinery to make dystrophin.

1.8.8.2 Plasmid vectors

Mdx mice injected with plasmid vectors (both locally (intramuscular) and systemically) have shown both an expression of dystrophin persisting 6 months, and an increase in peripheral nuclei, indicating greater muscle regeneration (Acsadi et al. 1991; Liang et al. 2004; Zhang et al. 2004). Low dystrophin expression (6%) was observed in DMD patients 3 weeks after an intramuscular injection of a plasmid containing full length human dystrophin (Romero et al. 2004). The disadvantage with the use of plasmid vectors is poor transduction efficiency and repeat administration is necessary to enable integration into the muscle (Chamberlain 2002). These problems are currently being addressed, with experiments using high pressure injections and electroporation (Aihara & Miyazaki 1998; Liu et al. 2001).

1.8.8.3 Viral vectors

1.8.8.3.1 Adenoviruses

Adenoviruses display relatively efficient infection of muscle and have been used to deliver dystrophin mini-genes to *mdx* mice. Unfortunately these early vectors activated cellular and humoral immune responses and were unable to carry the large dystrophin gene (2.4Mb) thus limiting their usefulness (Chamberlain 2002). To improve this technique, viruses were 'gutted', where the vector backbone was eliminated of all viral genes, allowing the full gene to be carried with minimal immune reactions (DelloRusso et al. 2002). Adenovectors do not integrate into the host permanently, so this form of gene therapy requires repeated delivery.

1.8.8.3.2 Adeno-Associated Viruses

Adeno-associated virus (AAV) vectors are identified by their low immune responses after administration, but are unable to carry the full dystrophin gene. Mini and micro dystrophin genes can be carried by these vectors. The use of smaller dystrophin genes will not result in expression of full length dystrophin and may only convert a DMD patient to a BMD phenotype (Chakkalakal et al. 2005). Direct systemic delivery of AAV dystrophin to neonatal and adult *mdx* mice resulted in widespread transduction in skeletal and cardiac muscle 11 days and 10 months respectively after injection (Gregorevic et al. 2004; Yue et al. 2003). It has also been shown that the AAV-mediated microdystrophin expression protects young *mdx* mice from contraction induced injury in extensor digitorum longus (EDL) muscle three months after the initial injection (Liu, M. et al. 2005).

If gene therapy becomes a successful avenue for boys with DMD, treatment would need to start early in life. As stated by Kakulas (1997), lost muscle fibres cannot be replaced, joint contractures and scoliosis cannot be reversed and respiratory complications are permanent, necessitating the earliest onset of therapy to achieve optimum results.

1.8.9 Antisense oligonucleotides

Sometimes as a result of exon skipping mechanism, misreading of dystrophin mutations can be corrected, resulting in the expression of dystrophin positive fibres, known as revertant fibres. These have been noted in *mdx* mice (Wells et al. 2003) and boys with DMD (Fanin et al. 1995). Antisense oligonucleotides (AOs) skip selected exons, thereby excluding mutations and restoring the reading frame to produce a shorter partially functional dystrophin protein. This causes the DMD transcript to be manipulated to that of a BMD patient (Gebski et al. 2005). Antisense induced exon skipping is able to restore functional dystrophin to *mdx* mice (Lu, Q. L. et al. 2003; Mann et al. 2001). AOs target specific sites on the gene, so only the DMD patients that have the particular mutation for which that AO was specifically designed will benefit from the therapy, necessitating customized design. Clinical trials are currently being planned.

1.9 Fibrosis in Dystrophic Muscle

Fibrosis is the excessive and inappropriate deposition of collagenous extracellular matrix. The progressive development of fibrosis affects a variety of mechanisms crucial to the proper function of cardiac or skeletal muscle in diseases like DMD (Morrison et al. 2000). Vascular and extravascular perfusion, critical for the supply of nutrients and

removal of waste products in skeletal muscle, is likely to be compromised by the accumulation of dense, sclerotic scar tissue in the inter-fibre spaces (Morrison et al. 2000). It has been suggested that scar tissue itself may assume a pathogenic role and contribute to the disease progression by interfering with effective muscle regeneration and re-innervation (Lipton 1979).

Collagen is the primary structural protein of all tissues, and its synthesis and degradation is normally maintained under tight control, but may be altered in repair processes such as wound healing. DMD patients have a marked increase of type I and type III collagen in their muscles (Foidart, Foidart & Engel 1981). Eight percent of collagen is composed of hydroxyproline which in turn is derived from the amino acid proline. Hydroxyproline can be digested from a tissue sample and its concentration within the sample can be spectrophotometrically measured, providing an accurate indication of the extent of fibrosis within that muscle sample.

1.10 Molecular Mechanisms of Fibrosis

Muscle fibrosis involves cytokines such as transforming growth factor beta 1 (TGF-β) and growth factors including insulin like growth factor 1 (IGF-1) and TNF-α.

1.10.1 Transforming Growth Factor Beta

TGF-β is a pleiotropic cytokine known to play an important role in inflammation, cell growth, embryonic development and wound repair (Passerini et al. 2002). TGF-β is present in normal tissues as well as in transformed cells. Blood platelets also store

relatively large amounts of TGF-β, suggesting that this factor plays an important role in the normal response to tissue injury (Ignotz & Massague 1986). This growth factor affects the *in vitro* behaviour of most cells involved in muscle regeneration, including satellite cells and fibroblasts. Variations in the amount or localisation of this growth factor may profoundly influence the balance between regeneration of muscle fibres and the development of excessive fibrosis (Murakami et al. 1999). TGF-β induces the accumulation of extracellular matrix in various diseases, such as liver cirrhosis (Milani et al. 1991) and interstitial pneumonitis (chronic pulmonary fibrosis) (Khalil et al. 1989). It has also been found to be expressed at high levels, and associated with fibrosis, in the skeletal muscles of patients with DMD. Further, there is clear evidence that its expression is related to the degree of muscle fibrosis and patient age (Bernasconi et al. 1995).

TGF-β increases collagen synthesis primarily via increased transcription (Mauviel 2005). Other mechanisms leading to TGF-β stimulated increased collagen levels include stabilisation of procollagen mRNA and decreased degradation of collagen via decreased matrix metalloproteases (MMP) activity (Eghbali et al. 1991; Li, Y. Y., McTiernan & Feldman 2000). In contrast, TGF-β also opposes the effects of inflammatory cytokines with regard to both decreasing collagen degradation and increasing collagen synthesis (Siwik & Colucci 2004).

Decorin is a natural antifibrotic agent that inactivates TGF-β thus interfering with collagen metabolism and structure, and reducing muscle fibrosis. It affects the formation

of collagen fibrils *in vitro* through binding of its core protein to types I and II collagen (Zimmerman et al. 2001) and reduces fibrosis in various tissues such as kidney, liver and lung (Giri et al. 1997; Isaka et al. 1996). Prevented muscle fibrosis was also evident, 2 weeks after muscle laceration (Fukushima et al. 2001) Decorin is the only known antifibrotic agent utilised in research for the prevention of skeletal muscle fibrosis.

1.10.2 Tumour Necrosis Factor alpha

Tumour necrosis factor alpha (TNF-α) is an early and potent pro-inflammatory cytokine that stimulates the inflammatory response. This cytokine is elevated in damaged myofibres from both injured normal and myopathic skeletal muscle. The role of TNF-α in inflammation-induced fibrosis appears complex, since available evidence suggests TNF-α regulates collagen synthesis in a tissue specific manner (Theiss et al. 2005). A study of liver injury indicates anti-fibrogenic actions of TNF-α in hepatic stellate cells via inhibition of collagen 1α gene expression (Hernandez et al. 2000). However, increasing evidence indicates TNF-α as a mediator of inflammation induced fibrosis in other systems (Theiss et al. 2005). TNF-α may also increase the breakdown of collagen by increasing MMP activity (Siwik & Colucci 2004).

TNF-α is up regulated in DMD patients (Porreca et al. 1999). It may function as a mediator of the dystrophic pathology through direct toxicity and by enhancing the inflammatory response. TNF-α specifically plays a role in the progressive deterioration of dystrophic diaphragm muscle as indicated in *mdx* mice with a TNF-α deletion (Gosselin et al. 2003; Spencer, Marino & Winckler 2000). Elimination of TNF-α in 10-

12 month old *mdx* mice resulted in significant improvements in ventilatory function and diaphragm strength and alterations in the MHC isoform composition (Gosselin et al. 2003). At 4 weeks of age, *mdx* mice deficient in TNF-α showed increased pathology compared to the TNF-α positive diaphragm and at 8 weeks of age, the pathology was no longer evident. TNF-α knockout mice had significantly less muscle mass than the *mdx* mice with the TNF-α gene, indicating that TNF-α plays an important role in muscle development especially at varying ages (Spencer, Marino & Winckler 2000). As previously mentioned (section 4.6) *mdx* mice treated with Remicade showed reduced skeletal muscle necrosis (Grounds & Torrisi 2004). TNF-α has also been associated with promoting muscle development, postnatal growth and regeneration. For example, an increase in TNF-α expression occurs during the early hours of differentiation and is required for normal differentiation of C2C12 skeletal myoblasts (Li, Y. P. & Schwartz 2001). The above findings show that the role of TNF-α remains contentious, with numerous functions in muscle and it is therefore not feasible to predict beneficial or detrimental effects in muscle of DMD patients at this stage (Tidball & Wehling-Henricks 2004).

1.10.3 Oxidative stress

Oxidative stress appears to be elevated in the failing myocardium and may be an important regulator of the extracellular matrix through effects on MMPs and collagen synthesis (Siwik & Colucci 2004). Abnormal membrane structure results in altered homeostasis of intracellular calcium, resulting in excessive generation of reactive oxygen free radical species (ROS) (Haycock et al. 1996). Actively contracting muscle generates

increased levels of reactive oxygen intermediates (Kobzik et al. 1994). An increased production of ROS through the dystrophin deficiency and subsequent decreased DAGPC signalling results in decreased NO production and oxidative stress (Rando 2002). This higher level of ROS is involved in many disorders affecting cardiac muscle. They react with macromolecules to initiate free radical chain reactions resulting in membrane and cell damage (Ascensao et al. 2005). The absence of dystrophin renders muscle specifically more susceptible to free radical induced injury (Rando et al. 1998). An impaired regulation of blood flow to muscle associated with dystrophin mutations and an increase of muscle cell susceptibility to oxidant stress may produce a muscular dystrophic phenotype (Disatnik, Chamberlain & Rando 2000). Further, ROS have been found to affect fibrosis by regulating cardiac fibroblast collagen synthesis and MMP activity. A study by Siwik and coworkers (2004) demonstrated that oxidative stress may regulate the quantity and quality of the extracellular matrix by decreasing fibrillar collagen synthesis as well as activating MMPs.

1.10.4 Matrix metalloproteinases

Matrix metalloproteinases (MMPs) are a family of proteolytic enzymes which cooperatively degrade all components of the extracellular matrix (ECM). MMPs are regulated by a variety of growth factors, cytokines and matrix fragments (Spinale 2002). The progression of the fibrotic processes in the heart are determined by MMPs, tissue inhibitors of metalloproteinases (TIMPs) and their regulators. Variation of this process can affect the final outcome of fibrosis and therefore myocardial function (Li, Y. Y., McTiernan & Feldman 2000). Remodelling of ECM during skeletal muscle degeneration

and regeneration suggests a tight regulation of matrix-degrading activity. TGF-β induces organ fibrosis by increasing ECM synthesis and may simultaneously inhibit matrix degrading proteases such as MMPs, whereas TNF-α can increase the breakdown of collagen by increasing MMP activity (Li, Y. Y., McTiernan & Feldman 2000; Siwik & Colucci 2004).

1.11 Skeletal Muscle Fibrosis

Skeletal muscle represents the largest tissue mass in the body. It is a composite structure consisting of muscle cells, organised networks of nerves and blood vessels, and an extracellular matrix. This framework is necessary to support the regenerative processes that occur after injury. In general, injured muscle fibres heal very slowly, usually with incomplete functional recovery. Injured muscles can initiate regeneration promptly, but the healing process is often inefficient and hindered by the formation of scar tissue. This formation of scar tissue is also referred to as fibrosis, a prominent feature of DMD (Huard, Li & Fu 2002).

1.11.1 DMD patients

In DMD patients, skeletal muscle biopsies reveal conspicuous myofibre degeneration with fibrosis replacing lost muscle tissue. The proportion of connective tissue in muscle biopsies increases progressively with age in DMD patients and TGF-β levels peak at 2 and 6 years of age. This suggests that TGF-β may stimulate fibrosis in DMD (Bernasconi et al. 1995).

In DMD patients necrotic muscle fibres are partially replaced by regeneration from dormant satellite cells, so that pathology progresses slowly over the first two decades of life. Eventually the process of degeneration dominates and muscle tissue is replaced by fibrous material (Gillis 1996). It is difficult from investigations in humans to determine the role of dystrophin in cardiac and skeletal muscle function; these questions may be addressed using the *mdx* mouse model of DMD (Sapp, Bobet & Howlett 1996).

1.11.2 Mdx Mice

Several studies have highlighted the influence of work-induced injury on muscle deterioration. Functionally induced damage present in normal muscles is reportedly aggravated in dystrophin-deficient muscles. Stretch or eccentric contractions increase sarcolemmal disruption, leading to fibre necrosis (Weller, Karpati & Carpenter 1990). The diaphragm of the *mdx* mouse has been shown to exhibit marked degeneration, fibrosis and functional insufficiency similar to that seen in DMD limb muscles (Stedman et al. 1991), although extensive fibrosis in skeletal muscle was first observed in a proximal hind limb muscle cross-section in a 18 month old *mdx* mouse by Kunkel and Hoffman (1989).

Evidence of extensive fibrosis in the adult *mdx* diaphragm has shown that ageing and work play a role in the development of dystrophic features. This fibrosis also appears to be present in other skeletal muscles and leads to clinical muscle weakness and premature muscle death (Lefaucheur, Pastoret & Sebille 1995). Greater deterioration in the diaphragm is evident compared to limb muscles. This is likely to be due to exercise loading and constant activity of this muscle (Muller et al. 2001). In contrast, there is

evidence that increased workload (induced by tracheal banding) does not accelerate degeneration in the diaphragm of *mdx* mice (Krupnick et al. 2003). The force and stiffness of skeletal muscles from old *mdx* mice also decreases with age and low intensity exercises (Bobet, Mooney & Gordon 1998).

The mechanisms involved in development of muscle fibrosis remain hypothetical in DMD dystrophinopathy. Possible mediators include TGF-β, TNF-α and other inflammatory cytokines. These cytokines may induce an active fibrotic process, reduced breakdown or turnover of collagen or decreased regenerative capacity or induced availability of muscle precursor cells as outlined in sections 1.10.1 – 1.10.4 (Hayes, Lynch & Williams 1993; Hayes & Williams 1998; Lefaucheur, Pastoret & Sebille 1995).

1.12 Effect of Exercise in Dystrophic Muscles

Fibrosis in *mdx* mice progresses with age. The *mdx* diaphragm exhibits fibrosis earlier than other skeletal muscles (Zeman et al. 2000). This finding has led to the conclusion that the absence of dystrophin in this muscle lowers the threshold for work-induced injury, so that the dystrophic pathology appears earlier in the diaphragm compared with other, less active muscles (Stedman et al. 1991; Vilquin et al. 2001; Weller, Karpati & Carpenter 1990).

Exercise has been used extensively to understand the mechanism of muscle degeneration-regeneration. Particularly striking and well studied is the muscle damage induced by eccentric contractions (Brussee, Tardif & Tremblay 1997). Eccentric contractions consist

of the muscle body being lengthened, while its constituted fibres are activated. Downhill running in humans and rodents causes eccentric contractions of certain leg muscles and consequently results in fibre damage (Clarkson & Tremblay 1988). Eccentric exercise may also be encountered naturally in situations such as downward stepping or running, or lowering the arms. Eccentric exercise is known to damage muscle fibres, probably by inducing local microlesions of the fibres (Vilquin et al. 2001).

Normal skeletal muscle fibres appear to be more susceptible to damage by exercise that involves lengthening (eccentric contractions) than by exercise that involves isometric or shortening (concentric) contractions. While reasons for this are not clear, it appears that peak forces developing during lengthening contractions cause mechanical disruption of the muscle fibres. Plasma membrane disruption is an early form of structural damage to muscle fibres of eccentrically exercised muscles (McNeil & Khakee 1992). In DMD patients certain pelvic girdle and proximal leg muscles display severe damage in disease progression. This raises the possibility that lengthening (eccentric) contractions to which these muscles are subjected during physical activity are more likely to damage dystrophin-deficient muscle fibres than concentric contractions (Weller, Karpati & Carpenter 1990). Since the absence of dystrophin is thought to lead to excessive calcium influx and hence muscle weakness, it may be possible that dystrophic muscle is more susceptible to eccentric exercise (Zeman et al. 2000). It has also been found that the cumulative effects of fibre microlesions following chronic exercise could lead to increased muscle wasting, weakness or acceleration of the dystrophic process including fibrosis and degeneration (Brussee et al. 1998). Exercise involving eccentric contractions

can also produce more severe muscle fibre damage in non-respiratory *mdx* muscles (Brussee, Tardif & Tremblay 1997).

Several subsequent studies using eccentric contractions in the dystrophin deficient mouse, have demonstrated elevated creatine kinase (Vilquin et al. 2001), increased intracellular calcium and exacerbation of muscle necrosis than control animals (Kilmer 1998).

1.12.1 Insulin Like Growth Factor 1

Insulin like growth factor 1 (IGF-1) is an endogenous hormone produced by numerous tissues including skeletal muscle. Levels of IGF-1 are increased after injury when formation of new fibres or growth of existing fibres occurs. Although its main function is the induction of muscle differentiation, IGF-1 is known to activate satellite cells (Adams & Haddad 1996) and lead to muscle hypertrophy (Adams & McCue 1998). This growth factor also stimulates protein synthesis (Russell-Jones et al. 1994), indicating that these beneficial effects of IGF-1 may be advantageous in treatment of patients with DMD. IGF-1 delivered systemically can reduce pathology by shifting muscle toward a positive protein balance and by stimulating regeneration (Tidball & Wehling-Henricks 2004). IGF-1 increases the production of collagen fibroblasts, leading to the implication that growth factors are potential stimuli for fibrosis. However, treatment with human recombinant IGF-1 reduced fibrosis and necrosis and improved fatigue resistance of skeletal muscles in *mdx* mice (Gregorevic, Plant & Lynch 2004). The overexpression of

IGF-1 has also been reported to ameliorate the histopathological changes in the *mdx* mouse (Barton et al. 2002).

Left ventricular contractility in rats and mice is increased without significant development of fibrosis as a result of increased IGF-1 and skeletal muscle specific overexpression of IGF-1 has been shown to reduce the sarcolemmal damage and necrosis in young *mdx* myofibres (Cittadini et al. 1996; Shavlakadze et al. 2004; Tanaka et al. 1998). It has been observed that exercise restores IGF-1 action in old C57Bl/6 mice (Willis et al. 1997; Willis et al. 1998) and swimming exercise increases expression of myocardial IGF-1 (Scheinowitz et al. 2003).

1.13 Cardiac Muscle Fibrosis

Mechanisms that are thought to contribute to cardiac fibrosis include inflammation and oxidative stress. There is a close relationship between inflammatory cells and myocardial fibrosis. Inflammatory cells co-localise with myocardial fibroblasts, such that fibrosis may not be a single pathological process, but involves inflammatory responses resulting in the release of cytokines that act on resident cardiac cells (Nicoletti et al. 1996; Nicoletti & Michel 1999).

Fibrosis impairs the re-lengthening of cardiomyocytes during the diastolic relaxation phase of the cardiac cycle (Weber et al. 1989) and thereby results in exaggerated mechanical stiffness (Brilla, Janicki & Weber 1991). Cardiac stiffness may then result in progressive diastolic and systolic dysfunction and ultimately cardiac failure. In addition,

it has been proposed that myocardial stiffness is also determined by characteristics of fibrosis, such as collagen cross-linking (Badenhorst et al. 2003; Norton et al. 1997)

1.13.1 DMD patients

The development of DMD cardiomyopathy may not be limited to myocardial loss of dystrophin, but may also be influenced by extrinsic parameters associated with the disease progression. Cardiac fibrosis is associated with functional and electrical cardiac abnormalities characteristic in DMD patients. Post mortem studies by Globus and Cohen in 1836 showed myocardial fibre atrophy and fibrosis in half of the patients dying with progressive muscular dystrophy (Nigro et al. 1990). The cardiac lesions consist of focal areas of fibrosis and degenerative changes involving the atria, posterobasal and lateral walls of the left ventricle and the conduction system (James 1962; Perloff et al. 1967). Residual viable cardiomyocytes can become encased in connective tissue, compromising their intercellular connections and ability to conduct signals (Fenoglio et al. 1983).

Echocardiography is normal or shows regional wall motion abnormalities in areas of fibrosis in early DMD. With the progression of fibrosis, left ventricular dysfunction and incidence of ventricular arrhythmias increase (de Kermadec et al. 1994; Farah, Evans & Vignos 1980; Melacini et al. 1996). During the final stages of the disease systolic dysfunction may lead to heart failure and sudden death (Finsterer & Stollberger 2003).

1.13.2 Mdx Mice

Left ventricular systolic function is normal in eight week old *mdx* mice, but progresses to a dilated cardiomyopathy at 42 weeks (Quinlan et al. 2004). It has been shown that 8-12 week *mdx* mice do not show an increase in left ventricular stiffness (Wilding et al. 2005). The *mdx* mouse demonstrates myocardial lesions, characterised by necrosis, macrophage infiltration and inflammation similar to those seen in boys with DMD (Bridges 1986). In addition, isolated cardiac preparations from *mdx* mice exhibit profound alterations in contractile properties, which are likely to be due to defective intracellular calcium homeostasis (Alloatti et al. 1995) and vunerability to mechanical stress-induced injury resulting from a loss of sarcolemmal integrity (Danialou et al. 2001). In addition, *mdx* mice are unable to sustain left ventricular function in the isolated working heart model (Danialou et al. 2001).

A dilated cardiomyopathy is evident in older *mdx* mice, with patchy fibrosis affecting all the regions of the left ventricle (Quinlan et al. 2004). The hearts of older *mdx* mice show an accumulation of connective tissue which suggests that fibrosis may be responsible for some features of myopathy (Morrison et al. 2000).

Mdx mice also display functional changes in cardiac receptors that mediate the role of the autonomic nervous system (Lu, S. & Hoey 2000) and have been shown to exhibit abnormal ECGs with a reduced heart rate variability typified by increased sympathetic and decreased parasympathetic activity (Chu et al. 2002).

1.14 Potential to reverse or prevent fibrosis.

Expression of TGF-β in the early stages of DMD may be critical in initiating muscle fibrosis and it is at this stage that antifibrotic treatment could potentially slow progression of this disease.

There are several potential antifibrotic treatments for patients with DMD, which may prevent or reverse fibrosis. These treatments could increase the mobility and muscular functions of boys with DMD, thereby decreasing the suffering endured by these young patients. Two of these potential treatments, l-arginine and pirfenidone will be investigated in this thesis.

1.15 L-arginine and the role of nNOS

L-arginine is a semi-essential amino acid found in large quantities in fish, chicken and beans (Goumas et al. 2001). It is defined as semi-essential due to its requirement for growth and its unique immunostimulatory properties. It can be metabolised to support glucose synthesis or catabolised to produce energy, depending on the needs of the body, (Maher 2000) and is a substrate for nitric oxide (NO). Nitric oxide is involved in the mechanisms of inflammation, tissue repair and fibrosis (Mane et al. 2001).

This endogenous amino acid is also involved in the l-arginine-nitric oxide pathway of blood pressure control. NO produces vasorelaxation of blood vessels, acts as a negative inotropic agent in cardiac muscle and assumes an important place in the pathophysiological response to haemorrhagic hypovolaemia and shock (Todorovic,

Prostran & Vuckovic 2001). L-arginine in humans may cause hypotension and tachycardia as well as insulin, glucagon, prolactin and growth hormone release.

Dystrophin deficient muscles demonstrate large reductions in the expression of the enzyme NOS (nitric oxide synthase). The NOS family of enzymes is responsible for the production of NO from l-arginine (i.e. nNOS converts arginine to NO). There are three major isoforms of NOS, with nNOS being the most prominent form of NOS expressed in skeletal muscle (Nakane et al. 1993). In DMD and *mdx* biopsy samples deficiencies of nNOS have been shown (Gucuyener et al. 2000).

nNOS has well characterised functions in several tissues and is a prominent member of the protein complex that interacts with dystrophin at the muscle cell surface (Brenman et al. 1995), although it does not bind directly to dystrophin itself (Chang et al. 1996). Membrane localisation of nNOS in skeletal muscle is mediated by the dystrophin associated glycoprotein complex (DAGPC) (Rando 2001a). Figure 1.6 shows the dystrophin glycoprotein complex in relation to nNOS.

Dystrophin is involved in specific signalling functions of the sarcolemma that may involve NO. In the absence of dystrophin, the concentration of nNOS at the cell membrane and in the cytoplasm decreases. Without dystrophin, nNOS is not correctly anchored to the sarcolemma, but is misdirected to the cytosol, where it maintains only partial enzymatic activity. Although the mislocalisation of nNOS doesn't contribute to

disease pathogenesis, absence of nNOS from the sarcolemma could conceivably impede nitric oxide (NO) mediated regulation of vasodilation (Crosbie 2001).

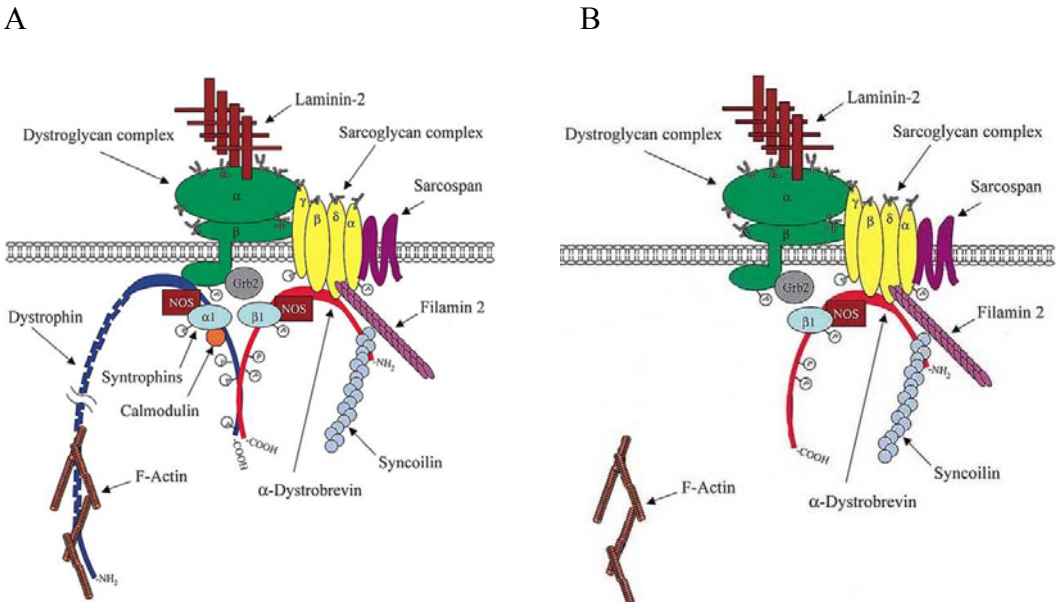

Figure 1.6: Dystrophin glycoprotein complex showing location of nNOS
A) DGP complex showing the localisation of nNOS in normal muscle and B) in dystrophic muscle. Figure adapted from Rando (2001b).

When nNOS is mislocated, muscle contraction may not properly stimulate sufficient levels of NO production to relieve vasoconstriction, resulting in local muscle ischaemia and ultimately skeletal muscle necrosis and fibrosis (Thomas et al. 1998). Data from uninjured muscle suggests that manipulation of NO could potentially prevent or treat other forms of muscle atrophy (Anderson 2000) and, similarly, restoration of normal blood flow to muscle may reduce muscle necrosis and fibrosis in DMD. On this basis l-arginine will be investigated for its potential to restore muscle function and reduce fibrosis.

1.16 Pirfenidone

Pirfenidone (PD) is an orally active small molecule drug that appears to inhibit collagen synthesis, downregulate production of multiple cytokines and block fibroblast proliferation and stimulation in response to cytokines. PD has demonstrated activity in multiple fibrotic conditions and has been studied in numerous phase 2 clinical trials for fibrotic diseases of the lung, kidney and liver (Intermune 2005). A phase III study in patients with Hermansky Pudlak syndrome (a rare autosomal recessive disease characterised by progressive pulmonary fibrosis) is expected to begin in the first half of 2006. In recent clinical trials, PD improved vital capacity and prevented acute exacerbation of idiopathic pulmonary fibrosis, and both reduced incidence of relapses and improved bladder dysfunction in patients with multiple sclerosis (Azuma et al. 2005; Walker, Giri & Margolin 2005).

PD is an antifibrotic agent that inhibits fibroblast growth and collagen synthesis induced by TGF-β. It thus reduces the synthesis of collagen I and III in a dose-dependent manner (Lee, Margolin & Nowak 1998). *In vitro* studies have demonstrated the ability of PD to decrease proliferation of human lung fibroblasts (Giri et al. 2002) and subsequently prevent and reverse lung fibrosis and attenuate pulmonary dysfunction following bleomycin treatment in hamsters by suppressing inflammatory events. In addition it appears to inhibit TGF-β at the transcriptional level in lung tissue from bleomycin treated mice and downregulates lung procollagen 1 overexpression (Iyer, Gurujeyalakshmi & Giri 1999a; Iyer, Hyde & Giri 2000). PD has also been shown to decrease collagen production and deposition in a rat model of hepatic fibrosis (Tada et al. 2001). Miric *et*

al. (2001) have shown the ability of PD to reverse cardiac and renal fibrosis and attenuate the increase in diastolic stiffness of diabetic hearts from streptozotocin-treated rats without normalising cardiac contractility or renal function. Dietary intake of PD reduced collagen accumulation in the remnant kidney with partial nephrectomy and post-obstructive models of kidney fibrosis in rats (Shimizu et al. 1997; Shimizu et al. 1998). More recently, PD has been shown to inhibit local arginase activity through suppression of TGF-β, thereby limiting the development of fibrosis in lung allografts (Liu, H. et al. 2005). PD attenuated the limited fibrotic potential of tacrolimus by reducing pro-fibrotic gene expression in a rat model of tacrolimus-induced nephrotoxicity (Brook et al. 2005a). Further, it reversed the calcineurin inhibitor-induced changes in fibrotic gene expression in the salt-depleted rat model (Brook et al. 2005b). These studies suggest that pirfenidone may be beneficial in the treatment of fibrosis in *mdx* mice as well as DMD patients.

1.17 Aims and Scope of the Study

There has been little research into DMD fibrosis, hence the aim of this thesis was to investigate options to reduce or prevent fibrosis and thereby improve skeletal and cardiac function in the *mdx* mouse model. It is known that DMD patients and *mdx* mice have elevated TGF-β levels and decreased NO levels. Therefore, antifibrotic agents such as PD and l-arginine may be able to correct these levels of TGF-β and NO respectively, decreasing the fibrosis observed in this disease. By running *mdx* mice downhill consistently in an effort to increase fibrosis, the treatment time required to investigate antifibrotic pharmacological agents may be reduced. PD and l-arginine are novel antifibrotics that have not been applied to the DMD disease state or *mdx* mice, adding to

the originality of this project. The aims and scope of each individual project are listed below.

All experiments in this dissertation have undergone extensive optimisation to determine the best conditions for each experiment. Protocols were developed to improve experimental techniques and data acquisition which would lead to the most successful and reproducible experiments (see Appendix).

1.18 Exercise

The aim of this project was to run *mdx* and C57 mice downhill at an angle of 10° for 5 months in an attempt to increase fibrosis and thereby shorten the duration of time required to evaluate pharmacological agents with antifibrotic potential. This project used 7 month old mice that were exercised 4 times per week for 30 minutes. The total exercise period lasted for 5 months, thus ensuring the mice were 12 months old at the cessation of the experiments. At this age, fibrosis is already well established in the *mdx* mouse. Both skeletal and cardiac experiments were performed in these mice.

1.18.1 Cardiac

Cardiac contractility, stiffness and coronary flow were measured using the Langendorff isolated heart technique to determine if exercise had a detrimental effect on the heart. After these experiments, levels of cardiac fibrosis were measured. Methods of measuring fibrosis included the colorimetric hydroxyproline assay to determine collagen content and a histological technique using a collagen specific stain, picrosirius red.

1.18.2 Skeletal

Skeletal muscle contractility was measured using muscles mounted in organ baths to determine how eccentric exercise affected the contractility of the extensor digitorum longus (EDL), soleus (SOL) and diaphragm muscles. The skeletal muscle morphometry and fibrosis of these muscles were also measured. Morphometry of these muscles was determined using haematoxylin and eosin stains and fibrosis was measured using hydroxyproline assays and picrosirius red staining as mentioned earlier. Succinate dehydrogenase levels in the gastrocnemius muscle were also measured.

1.19 Pirfenidone

The antifibrotic action of pirfenidone has been demonstrated in several animal models of fibrosis in different organs including cardiac and skeletal muscle. The aim of this project was to determine if administration of pirfenidone would elicit an antifibrotic action on cardiac and skeletal muscle and improve functional responses in *mdx* mice. Eight month old mice were treated for 7 months, ensuring mice were 15 months old at cessation of treatment. It has been shown that *mdx* mice display the most severe fibrosis at this age (Laws 2005). Different doses of pirfenidone were trialled to determine the dose which produced the optimum antifibrotic potential. Protocols were used to determine if cardiac and skeletal muscle contractility had improved as a result of administration of this antifibrotic agent.

1.20 L-arginine

Deficiency of dystrophin results in lowered nNOS levels in DMD patients and *mdx* mice. The family of nitric oxide synthase (NOS) enzymes utilise l-arginine as the substrate to produce nitric oxide (NO). Nitric oxide plays important roles in fibrosis and can reduce muscle inflammation and muscle membrane lysis (Wehling, Spencer & Tidball 2001). Treatment with l-arginine has been shown to reduce fibrosis and improve muscle function in fibrotic models of mice and rats. The aim of this project was to treat 6 month old *mdx* mice with l-arginine (10 mg/g) via oral gavage daily for 6 months to test if l-arginine administration improved contractility and reduced fibrosis in cardiac and skeletal muscles. Quantitative protocols were used to determine if cardiac and skeletal muscle contractility and the fibrotic state of the muscles had improved as a result of administration of this antifibrotic agent.

1.21 Co-administration of L-arginine/Prednisone

Research has shown that the combination of l-arginine with the glucocorticoid deflazacort resulted in improved tissue integrity in *mdx* skeletal muscle cells, resulting in expression of NOS in dystrophin deficient satellite cells (Anderson & Vargas 2003). This led to the hypothesis that co-administration of l-arginine and prednisone (a similar glucocorticoid to deflazacort) would elicit a similar protective effect on dystrophin deficient cardiac muscle. *Mdx* and C57 mice at 7 months of age were treated with the combinations of l-arginine and prednisone for 7 months, after which the Langendorff isolated heart technique was used to measure cardiac contractility, stiffness and coronary

flow. Hydroxyproline and quantitative measurement of picrosirius red-stained cardiac sections were utilised to determine fibrosis.

1.22 Overview

Fibrosis is known to contribute significantly to the skeletal muscle dysfunction in DMD patients, however cardiac fibrosis leading to cardiomyopathy has not been extensively investigated. It is an area of intense interest as improved ventilatory care has increased the presentation of cardiac manifestations highlighting awareness of cardiomyopathy as a contributor to mortality. Together, the four projects in this thesis provide a unique approach to determine if fibrosis could be increased or prevented, using novel treatments in the *mdx* mouse. These findings would contribute to the ultimate aim to prevent fibrosis and improve cardiac function and therefore improve quality of life in these young patients until a cure is found for this debilitating condition.

CHAPTER 2 : EFFECT OF ECCENTRIC EXERCISE IN *MDX* MICE

2.1 Introduction

Duchenne Muscular Dystrophy (DMD) is a fatal X-linked recessive disease, characterised by lack of the protein dystrophin. Dystrophin is a cytoskeletal protein normally present in skeletal, cardiac and smooth muscle. The exact role of dystrophin has not yet been fully determined, but it is thought to act as a structural scaffold that distributes mechanical stress through the sarcolemma (Emery & Muntoni 2003; Niebroj-Dobosz, Fidzianska & Hausmanowa-Petrusewicz 2001). A loss of dystrophin severs the link between the contractile protein actin and the cell membrane, leading to damaging calcium influx and membrane instability and causing severe cycles of degeneration and regeneration of the muscle. These repeated cycles cause infiltration of adipose tissue and fibrosis. In the heart, fibrosis may lead to changes in contractility and rhythm conduction (Finsterer & Stollberger 2003), while in skeletal muscle, increased fibrosis impairs the regenerative potential of the muscle (Morrison et al. 2000). Thus, strategies to reduce fibrosis would be beneficial in the treatment of DMD.

The *mdx* mouse is a widely used and accepted animal model for DMD due to its similar dystrophin deficiency. Like boys with DMD, the diaphragm is significantly affected, as evidenced by a decrease in force production and increased fibrosis, which is more extensive than that of limb skeletal muscles (Zeman et al. 2000). This finding has led to the conclusion that the absence of dystrophin in the diaphragm lowers the threshold for work-induced injury, allowing the dystrophic pathology to appear earlier in this muscle

compared with other less active muscles (Stedman et al. 1991; Vilquin et al. 2001; Weller, Karpati & Carpenter 1990). This raises the question of whether increased workload, such as exercise, hastens muscle damage and fibrosis.

Exercise has been used extensively to attempt to understand the mechanisms of muscle degeneration-regeneration. Particularly striking and well studied is the muscle damage induced by eccentric contractions (Brussee, Tardif & Tremblay 1997). Eccentric contractions occur when the muscle body is being lengthened while its fibres are contracting. Eccentric exercise may be encountered naturally in situations such as downward stepping or running and is known to damage muscle fibres (Vilquin et al. 2001).

In patients suffering from DMD, leg muscles display severe damage relatively early, possibly because eccentric contractions during physical activity damage dystrophin-deficient muscle fibres more readily (Weller, Karpati & Carpenter 1990; Zeman et al. 2000). Further, evidence suggests that chronic exercise causes increased muscle wasting, weakness and/or acceleration of the dystrophic process with signs of fibrosis and degeneration (Brussee et al. 1998).

In *mdx* mice experiments involving treadmill running conducted by several researchers have shown that *mdx* tissue has a higher propensity to damage (Carter, Abresch & Fowler 2002; Dupont-Versteegden, McCarter & Katz 1994; Hara et al. 2002; Wineinger et al.

1998). However, these have all been short term experiments (3 days – 8 weeks) and to date, no research has been undertaken regarding chronic exercise in older *mdx* mice.

The hypothesis that increased eccentric exercise caused by running older *mdx* mice downhill would increase fibrosis was tested. If proven successful, this will shorten the duration of time required to evaluate drugs with antifibrotic potential.

2.2 Materials and Methods

2.2.1 Animals

Male C57BL/10ScSn mice (control strain) (C57) were purchased from the Animal Resource Centre, Nedlands, WA. Male C57BL10ScSn *mdx* (*mdx*) mice were bred at the University of Southern Queensland Animal House, Toowoomba, QLD. Mice were 7-8 months old at the commencement of experiments. All experimental protocols were conducted with the approval of the University of Southern Queensland Animal Ethics Committee, under the guidelines of the National Health and Medical Research Council of Australia.

2.2.2 Methods

Each strain of mice was randomised into 2 groups: exercise and sedentary (*mdx*-ex (n=12); C57-ex (n=5); *mdx*-s (n=12); C57-s (n=5)). All mice were given free access to feed and were trained for a total of 5 months.

2.2.3 Exercise protocol

All exercise mice ran 4 times per week for up to 30 minutes on a modified treadmill at 17.5 m/minute. The initial exercise regime commenced by running mice at a downward angle of 5° for 2 weeks prior to increasing the angle to 7.5° for 2 weeks. For the remainder of the exercise period mice ran at a downward angle of 10°. All sedentary mice were left to move freely in their cage with no induced exercise.

The *mdx* mice showed avoidance behaviour approximately 10-15 minutes after commencement of running, but would run for several minutes longer when gently stimulated by hand. After a period of recovery (5 minutes) attempts were made to complete the 30 minutes of running, however, this was often not possible. In contrast, the C57 mice showed no avoidance behaviour and did not appear fatigued throughout the exercise period. After it was discovered the *mdx* mice could not maintain the 30 minute running protocol, the exercise period was reduced to a 20 minute time point. Mice were weighed weekly and were exercised until the day prior to the *in vitro* experiments.

2.2.4 Langendorff Experiments

At 12 months of age mice were weighed and anaesthetised with sodium pentobarbital (70 mg/kg) administered intraperitoneally.

A thoracotomy was performed and hearts were excised rapidly into modified Krebs-Henseleit buffer containing (mM): NaCl, 119; $NaHCO_3$, 22; KCl, 4.7; KH_2PO_4, 1.2; $CaCl_2$, 2.5; $MgSO_4$, 1.2; glucose, 11; Na-pyruvate, 1 and EDTA, 0.5 containing 10 mM 2,3-butanedione monoxime (BDM) (temperature 21°C). The BDM was placed into the dissection buffer to limit detrimental actions of calcium during tissue preparation. The aorta was cannulated via the dorsal root and perfused retrogradely at a pressure of 80 mmHg with Krebs-Henseleit perfusion buffer maintained at 37°C and bubbled with carbogen (95%O_2-5%CO_2) to ensure a pH of 7.4. The Krebs-Henseleit buffer used for perfusion of the hearts did not contain BDM.

A small polyethylene apical drain was used to vent the left ventricle preventing an accumulation of fluid in the heart via Thesbian veins. The left atrium was excised and a fluid filled balloon constructed from polyvinyl chloride plastic film was inserted into the left ventricle via the mitral valve for the measurement of left ventricular function. The left ventricular function was recorded via a MLT844 physiological pressure transducer (ADInstruments, Castle Hill, NSW, Australia) linked to a PowerLab recording system (ADInstruments, Castle Hill, NSW, Australia). Coronary flow was regulated via a ML175 STH Pump Controller (ADInstruments, Castle Hill, NSW, Australia).

Data from hearts with a coronary flow greater than 5mL/min were excluded from the experimental analysis. Data was recorded using Chart 4.1.1 software (ADInstruments, Castle Hill, NSW, Australia) to calculate end systolic pressure (ESP), end diastolic pressure (EDP), contraction and relaxation over time (±dP/dt) and heart rate. Fluid temperature was measured via a thermometer at the entry of the aortic cannula and temperature was maintained at 37.3°C. Hearts were paced at 420 bpm via a silver wire embedded into the left ventricle and grounded using an electrode attached to the cannula. The balloon was inflated to an EDP between 0 and 5 mmHg and the heart was then equilibrated for 10 minutes at this pressure. Following this equilibration period, the EDP was measured for 30 seconds at each of the following increments: 0, 5, 10, 15, 20 and 30 mmHg. Myocardial stiffness was defined by the stiffness constant (κ, dimensionless), that is, the slope of the linear relationship between the tangent elastic modulus (E, dyne/cm^2) and stress (σ, dyne/cm^2) as described in detail (Mirsky & Parmley 1973) (See Appendix A2.0). At cessation of the *in vitro* experiments, the right atrium, right ventricle

and the left ventricle plus septum were separated and weighed. The left ventricle plus septum was bisected transversely with the superior portion stored for histology and the remainder snap frozen in liquid nitrogen and stored at -80°C for subsequent hydroxyproline assays.

2.2.5 Skeletal Muscle Contractility

Immediately after the removal of the heart, the following skeletal muscles were dissected free: extensor digitorum longus (EDL) and soleus (SOL) from the left leg and a strip of the diaphragm, these strips were cut consistently from the same region of diaphragm to minimise experimental error. These muscles were placed in ice-cold Krebs-Henseleit solution containing (mM): NaCl, 118; $NaHCO_3$, 25; KCl, 4.7; KH_2PO_4, 1.18; $CaCl_2.2H_2O$, 2.5; $MgSO_4.7H_2O$, 1.16; glucose, 11; bubbled with carbogen, (95%O_2-5%CO_2). The three muscles were tied individually around the tendon at either end with 5.0 silk suture and attached with one end to a fixed peg and the other end attached to a physiological force transducer (TRI 201, Panlab, Spain). All three skeletal muscles were suspended in water-jacketed tissue baths (25°C) containing Krebs-Henseleit buffer bubbled with carbogen. Two parallel platinum electrodes along the length of the muscles provided field stimulation (0.2 ms pulse duration) from a Grass S48 stimulator (West Warwick, RI) with amplified current intensity (EP500B, Audio Assemblies, Campbellfield, Victoria, Australia). Contractile force was recorded via a PowerLab recording system (ADInstruments, Castle Hill, NSW, Australia) and analysed using Chart 4.1.1. Optimal preload (L_o) was defined as the length eliciting maximal single twitch force. Optimum voltage was also determined for each muscle, as was the frequency

eliciting maximal tetanic force ranging from 50-180 Hz. Once determined, the optimum values were used for the remainder of the experiment. Reported data were the average of three individual single-twitch or tetanic stimulations per muscle strip obtained after 25 minutes of equilibration and optimization of conditions. Upon completion of the organ bath experiments, muscle lengths (L_o) and widths were recorded, using a digital micrometer. The muscles were blotted for 3 seconds and weighed. The cross-sectional area and normalization of force was calculated as described previously, where tissue cross-sectional area equals tissue weight divided by length multiplied by 1.06 (density of mammalian muscle) (Lynch et al. 2001). This calculation for cross-sectional area accounts for the differences in thickness between different tissues. (Diaphragm thickness in mm: C57 0.4-0.5, *mdx* 0.8-0.95; SOL thickness C57 0.9, *mdx* 1.51-1.60; EDL thickness C57 1.64-1.70, *mdx* 2.60-2.67). Subsequently, the three skeletal muscles were frozen in liquid nitrogen and stored at -80°C for hydroxyproline assays.

2.2.6 Hydroxyproline Measurements

Hydroxyproline (HP) assays were used as a measure of collagen content. The individual frozen EDL, SOL and diaphragm sections were trimmed of tendons and capsular tissue. All skeletal tissue and a section of the left ventricle were weighed. The tissues were cut into smaller pieces with a scalpel and placed in a sealed tube containing 6 M HCl. The tissues and standards (0, 1, 2, 3, 4, 5, 6 and 7 μM hydroxyproline) were hydrolysed overnight (18 hours) at 107°C. After hydrolysation, the tissues were dried using low heat (50°C) and filtered air under pressure. The dried sample was reconstituted with 500 μL distilled water (dH_2O) and vortexed. A working solution of the buffer stock solution (50

g citric acid.1H_2O, 12 mL glacial acetic acid, 120 g sodium acetate.3H_2O and 34 g sodium hydroxide made up to 1 L with dH_2O water) was made prior to use by taking 500 mL of the stock and adding 100 mL of dH_2O and 150 mL of n-propanol. 250 µL of Chloramine T reagent (1.41 g chloramine T, 10 mL dH_2O water, 10 mL n-propanol and 80 mL buffer working solution) was added to each sample (ensuring the samples and Chloramine T were at room temperature); the oxidation step was then allowed to progress for 20 minutes at room temperature. 250 µL of Ehrlich's reagent (1.664 g dimethylaminobenzaldehyde and 10 mL of a 2:1 n-propanol/perchloric acid solution) was then added and samples were subsequently incubated at 60°C in a shaking water bath for 20 minutes to allow the chromophore to develop. The tubes were then cooled under tap water before the absorbance was read at 550 nm. Using a standard curve, the µg hydroxyproline content was measured, assuming that 12.5% of collagen is hydroxyproline. Values are expressed as µg HP/mg of wet tissue weight.

2.2.7 Histology

The superior ventricular, EDL, SOL and diaphragm sections were fixed in Telly's fixative (70% ethanol, 37% formaldehyde and glacial acetic acid) for 3 days, modified Bouin's solution (saturated picric acid, 37% formaldehyde and glacial acetic acid) for 1 day and 70% ethanol before the muscles were embedded in paraffin wax. Sections of 10 µm thickness were cut and placed on Polysine glass slides and stained using the collagen selective stain, 0.1% wt/vol picrosirius red solution (Sirius Red F3B, Chroma Dyes, in saturated picric acid). Slides were left in 0.2% phosphomolybdic acid for 5 minutes, then washed, stained in picrosirius red for 90 minutes and placed in 1 mM HCl for 2 minutes.

The slides were then placed in 70% ethanol for 30 seconds and coverslipped using Depex.

Stained muscle sections were viewed blinded to the strain and treatment of mouse using a Nikon Eclipse E600 epifluorescence microscope and 20X magnification. Images were captured with a cooled CCD digital camera (Micropublisher 5.0, QImaging, Canada), with the percentage collagen quantified using AnalySIS software (Soft Imaging System, GmbH, Münster, Germany). To determine the average percentage collagen of each left ventricle and skeletal muscle section, five regions (for left ventricle) and two regions (for skeletal muscle) were viewed per muscle sample and the final percentage of collagen was calculated from the average of these five or two regions respectively.

To determine cell diameter and central nucleation of the skeletal muscles, 5 μm sections were cut and placed on Polysine glass slides and stained using haematoxylin and eosin. These slides were analysed under brightfield using the same software as described previously. Due to the smaller size of these muscles, only 2 regions (counting 100 cells per region) were viewed per skeletal muscle sample with the mean cell diameter and central nucleation calculated from the averages obtained from these two regions. To reduce experimental errors such as the orientation of the sectioning angle, the minimal 'Feret's diameter' was measured which allows for reliable measure of muscle fibre cross-sectional size and reliably discriminates between dystrophic and normal phenotypes (Briguet et al. 2004).

2.2.8 Succinate Dehydrogenase Assay

The gastrocnemius muscle was also dissected free and frozen in liquid nitrogen before storage at -80°C. The frozen gastrocnemius was weighed and the muscle was teased and sliced into small pieces using a scalpel blade. The tissue was homogenised with an ice cold mortar and pestle in the presence of a phosphate/sodium succinate buffer until there was no visible evidence of tissue. A small amount of homogenate (0.02 mL) was placed in a 4 mL glass cuvette with 0.1 mL of 0.5 M sodium succinate and incubated for 2 minutes at 25°C. 0.1 mL Sodium cyanide (NaCN) (0.01 M in 0.17 M phosphate buffer) and 2.8 mL Cytochrome C salt solution (1 mL 0.0001 M horse heart cytochrome C in 0.17 M phosphate buffer combined with 3 mL dH_2O and 0.4 mL of $AlCl_3/CaCl_3$) were then added to the cuvette and mixed well. The absorbance was read at 550 nm every 30 seconds for 3 minutes and the SDH content was calculated from using the mathematical equation below. This protocol was adapted from Cooperstein, Lazarow and Kurfess (1950), where the constant value, 19.6, is the slope of the line which measures the drop in concentration of oxidised Cytochrome C. Values were expressed as μg SDH/g of tissue.

Calculations:

$$\frac{\text{Optical Density (OD)/ minute}}{19.6} \times \text{dilution factor} = \mu\text{M/g/minute}$$

$$\text{OD/minute} = \frac{\text{reading at 3 mins} - \text{reading at time zero}}{3}$$

2.2.9 Statistical Analysis

Data is presented as mean ± standard error of the mean (SEM), comparisons were made using the unpaired Student's t-test; $P<0.05$ was considered statistically significant.

2.3 Results

2.3.1 Cardiac function

Sedentary *mdx* mice revealed an increase in +dP/dt or cardiac contractility compared to the sedentary C57 mice (Figure 2.1 (A) (P<0.05)). Exercise did not affect cardiac function in *mdx*-ex mice in relation to *mdx*-s, whereas C57-ex mice had an increased +dP/dt (Figure 2.1 (A); P<0.01) and developed pressure compared to C57-s (Figure 2.1 (B) P<0.05) respectively. Exercise improved force production with higher end systolic pressure in *mdx*-ex and C57-ex relative to their respective sedentary control strain. The end systolic pressure of *mdx*-s was higher than C57-s (Figure 2.1 (C); P<0.01). There were no differences in diastolic stiffness between any of the groups.

2.3.2 Cardiac Collagen Measurements

Mdx-s had a higher left ventricular hydroxyproline content than C57-s mice (P<0.01) with similar findings evident in the exercised groups (P<0.05). Surprisingly, C57-ex had a 49% increase in the level of hydroxyproline in the left ventricle compared to C57-s mice (P<0.05) (Table 2.1), there was no increase in hydroxyproline content in *mdx*-ex and *mdx*-s mice.

Analysis of picrosirius red-stained left ventricular sections provided complementary results to the hydroxyproline results described above with *mdx* mice having higher collagen content than C57-s mice regardless of whether they were exercised or sedentary (Figure 2.2; Table 2.2).

A

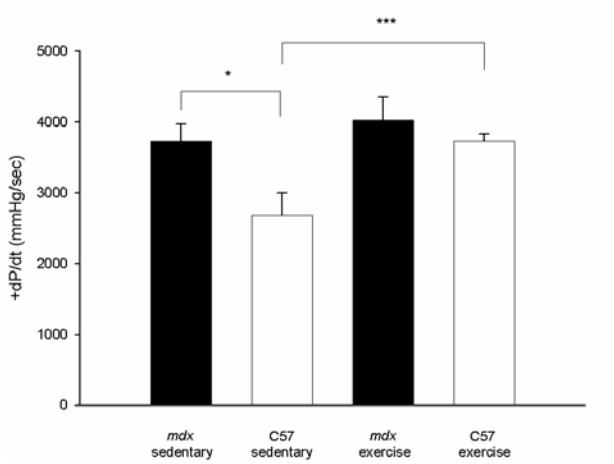

B

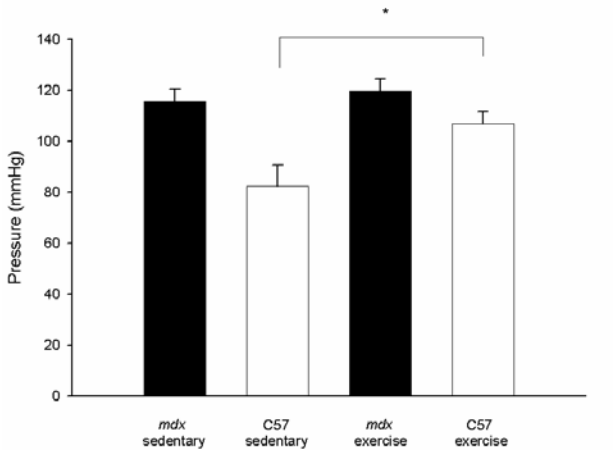

C

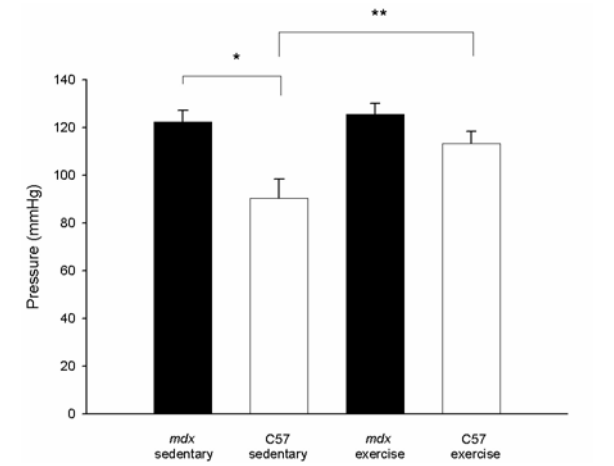

Figure 2.1: Cardiac function of sedentary and exercise *mdx* and C57 mice
Rate of pressure development (+dP/dt) (A), left ventricular developed pressure (B) and end systolic pressure (C) from isolated hearts of control *mdx* and C57 mice and exercised *mdx* and C57 mice. Exercise did not affect cardiac function in *mdx* mice, but increased cardiac function in C57 mice. $^{*}P<0.05$; $^{**}P<0.01$; $^{***}P<0.001$.

	C57	*mdx*
Sedentary	31.48±1.89	31.11±1.07
Exercise	33.53±0.72	31.83±0.91

Table 2.1: Cardiac stiffness of sedentary and exercise *mdx* and C57 mice
There was not difference in diastolic stiffness between any of the mice

	C57	*mdx*
Sedentary	2.15±0.28	5.09±0.89
Exercise	3.21±0.26	4.55±0.47

Table 2.2: Left ventricular hydroxyproline content of sedentary and exercise *mdx* and C57 mice
Exercise increased HP levels in C57 mice, but did not affect HP levels in *mdx* mice

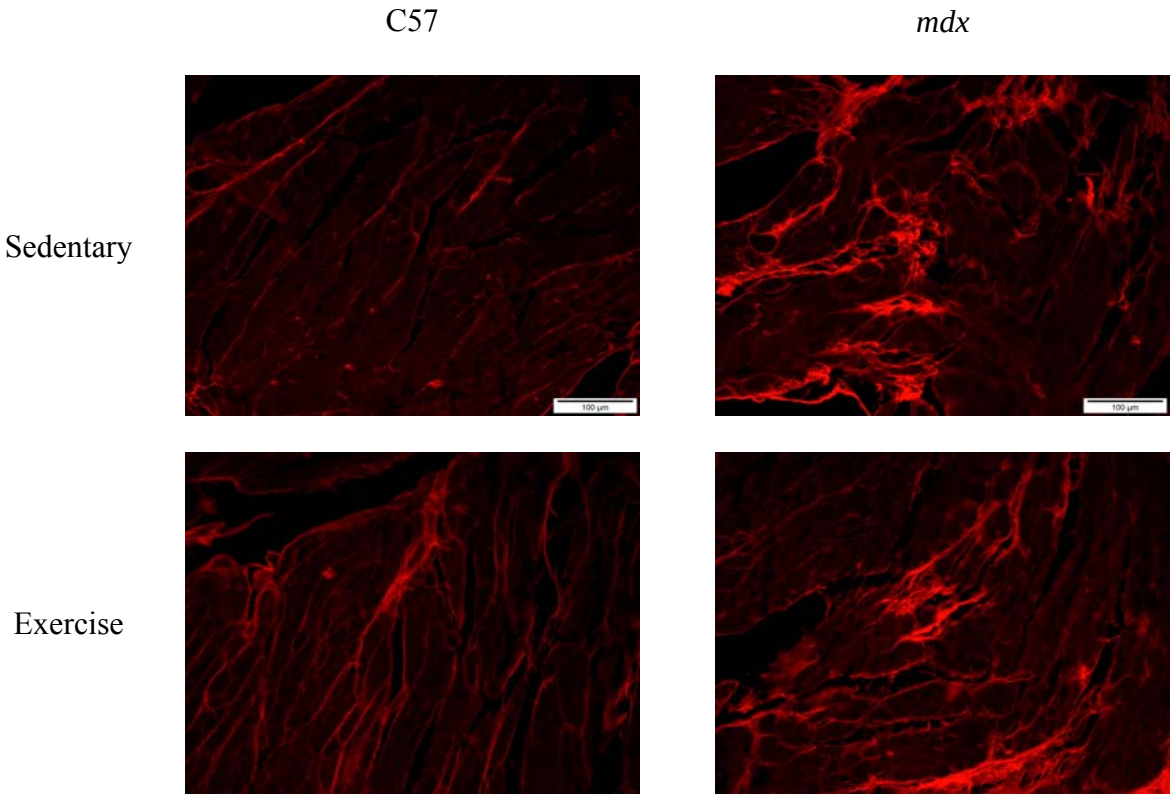

Figure 2.2: Picrosirius red left ventricular sections of sedentary and exercise mice
Magnification: X20. Areas stained red indicate presence of collagen.
Mdx mice have a higher collagen content than C57 mice. Exercise increased collagen content in the C57 mice but did not affect these levels in *mdx* mice.

	C57	*mdx*
Sedentary	4.48±0.61	11.37±1.25*
Exercise	6.32±1.70	11.10±1.33^{+}

Table 2.3: Quantitative left ventricular PSR data
Mdx mice have a higher collagen % area than C57 mice. Exercise did not affect the levels of collagen. $^{**}P<0.01$; $^{+}P<0.05$

2.3.3 Skeletal Muscle Function

Mdx-s mice had a significantly lower specific force production (sPo and sPt) compared to C57-s mice in all three skeletal muscles tested (Figure 2.3 and 2.4; $P<0.01$). Five months of chronic eccentric exercise influenced the contractile force of the SOL in C57 mice, causing a trend for a lower specific twitch force in C57-ex compared to C57-s mice (Figure 2.3 (A) $P<0.06$). In contrast, eccentric exercise did not impair the strength of the *mdx* SOL, indicating that eccentric exercise resulted in a detrimental effect only in the C57 mice.

The exercise protocol did not affect the EDL muscles of either strain, again indicating that exercise did not contribute to a reduction in contractility (Figure 2.3 (B) and 2.4 (B)).

Chronic exercise in *mdx* and C57 mice did not cause any change in diaphragm twitch compared to sedentary mice (Figure 2.3 (C)). The tetanic contractions of the diaphragm of C57-ex mice improved, however this was not significant (Figure 2.4 (C)). This slight increase indicates a minor benefit to this respiratory muscle in the control mice. This improvement was not evident in the tetanic contractions of the *mdx*-ex mice.

A

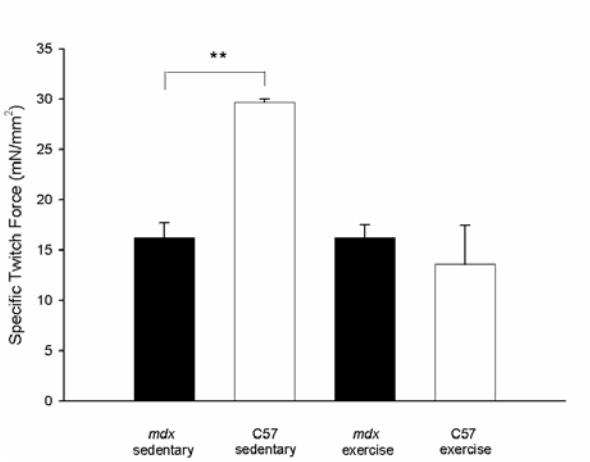

B

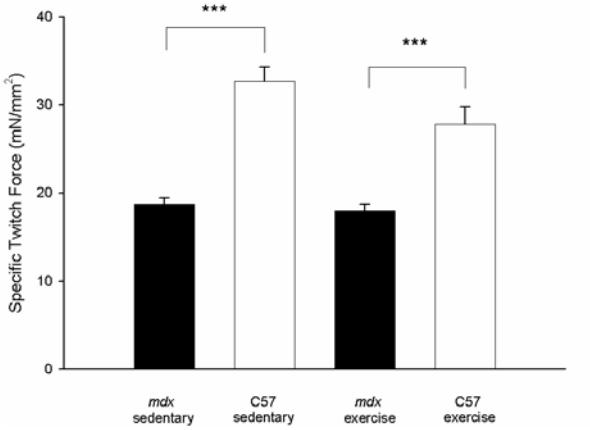

C

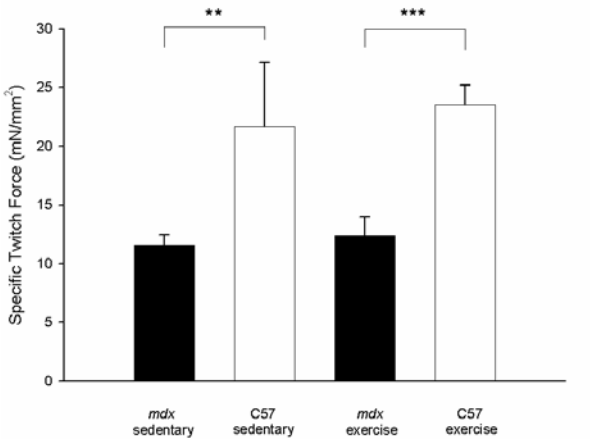

Figure 2.3: Specific twitch contractions of sedentary and exercise *mdx* and C57 mice SOL (A), EDL (B) and diaphragm (C).
Mdx-s have lower twitch contractions than C57-s. Exercise did not affect force production in any of the three muscles in *mdx* mice. However, force production of the SOL in C57 mice was decreased. $^{*}P<0.05$; $^{**}P<0.01$; $^{***}P<0.001$.

A

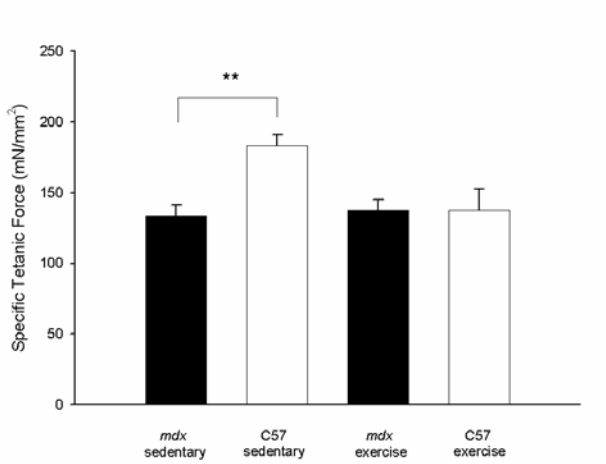

B

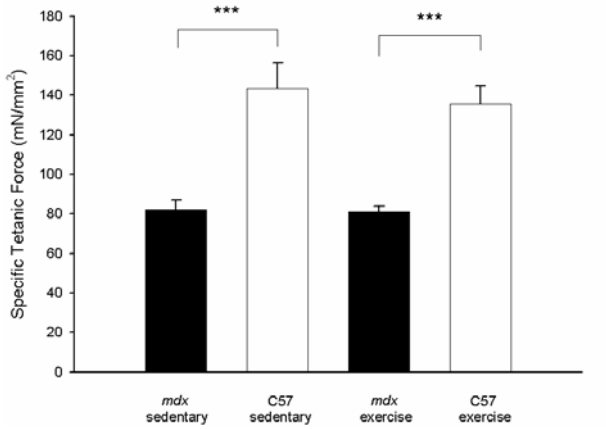

C

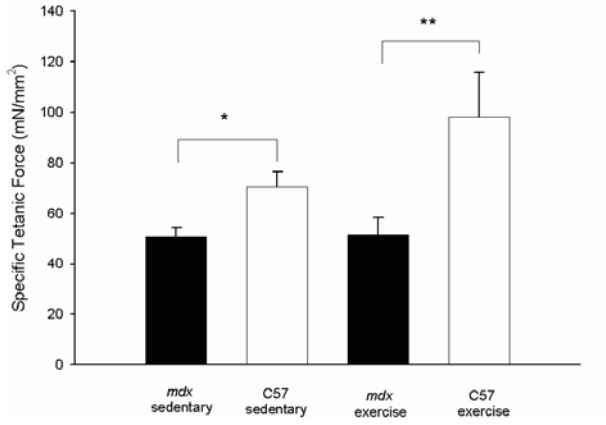

Figure 2.4: Specific tetanus contractions of sedentary and exercise *mdx* and C57 mice SOL (A), EDL (B) and diaphragm (C).
Mdx-s have lower tetanic contractions than C57-s. Exercise did not affect force production in any of the three muscles in *mdx* mice, and non-significantly increased force production of the diaphragm in C57 mice. $^{*}P<0.05$; $^{**}P<0.01$; $^{***}P<0.001$.

2.3.4 Skeletal Muscle Collagen Measurements

The hydroxyproline content of EDL and SOL muscles were not different between *mdx*-s and C57-s and exercise did not affect hydroxyproline levels in these two muscles. In contrast, the diaphragm from *mdx*-s contained in excess of a two-fold increase in hydroxyproline levels compared to C57-s, but again exercise did not alter these ratios (Figure 2.5).

Using the more focal method of collagen content analysis picrosirius red-stained muscle sections, it was revealed *mdx*-s EDL, SOL and diaphragm muscles all contained more collagen than C57-s mice ($P<0.01$), but again exercise did not cause a difference in collagen content in any of the three skeletal muscles (Figure 2.6; Table 2.3).

In the hydroxyproline assays, a small section of the muscle is used in each experiment. If the section that is taken from one end of the muscle is not representative of the change in the overall muscle, then a difference may not be detected. In contrast, in histological analyses, a 10 micron section of the whole muscle cross-section is viewed, thereby allowing the muscle to be examined more fully, rather than just a small portion of the muscle.

2.3.5 Muscle Morphology

EDL, SOL and diaphragm myocytes from C57 mice exhibited a lower percentage of central nucleation compared to the *mdx*-s mice ($P<0.001$). Exercise did not alter this difference in *mdx* and C57 mice. The cell diameter was greater in the EDL of *mdx*-s

mice compared to *mdx*-ex and the C57-s ($P<0.05$) and remained unchanged in the SOL and diaphragm of the other exercise and sedentary groups. The minimum diameter of the diaphragm in *mdx*-s mice was greater than in the C57-s mice ($P<0.01$) (Figure 2.7; Table 2.3).

2.3.6 Succinate Dehydrogenase Assays

Stress placed on exercised muscle brings about an adaptive increase in the enzymes in the mitochondrial electron transport chain, thereby increasing SDH levels (Holloszy 1967). It is highly probable that C57-s mice are more active than *mdx*-s mice as the SDH levels measured in the gastrocnemius were higher although this did not quite reach significance ($P<0.08$) (Figure 2.8). Exercise did not cause an increase in SDH levels in either *mdx* or C57 mice.

A

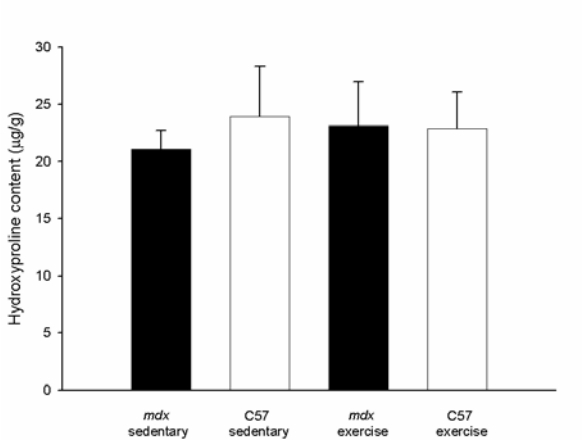

B

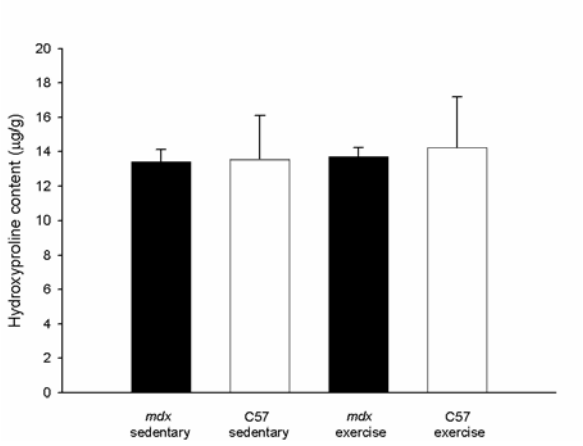

C

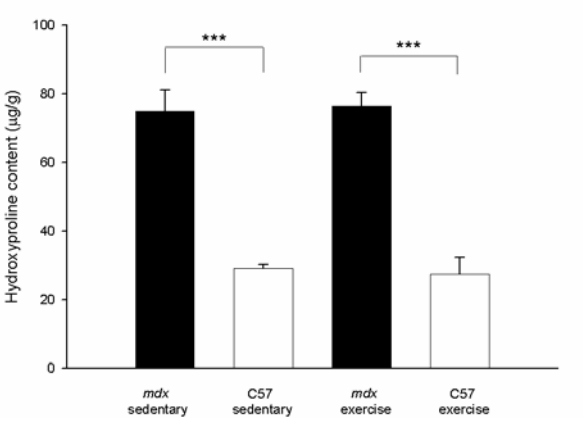

Figure 2.5: Skeletal muscle hydroxyproline content of sedentary and exercise mice Hydroxyproline content of SOL (A) and EDL (B) muscles were not different in *mdx*-s and C57-s. Exercise did not affect HP levels. The diaphragm (C) from *mdx*-s increased HP levels compared to C57-s, exercise did not affect these HP levels. $^{***}P<0.001$.

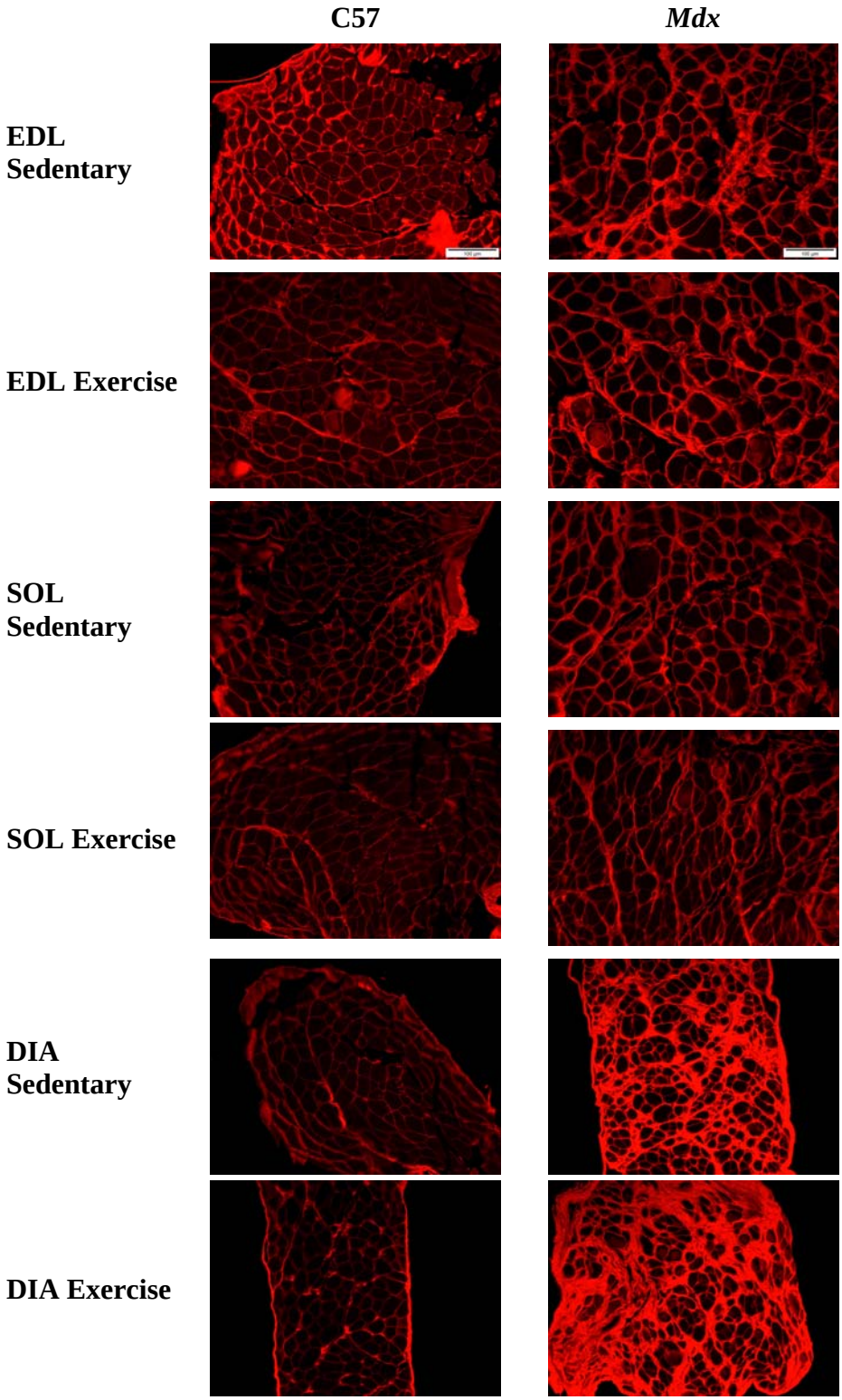

Figure 2.6: Skeletal muscle sections of sedentary and exercise mice (PSR)
Magnification: X20. Areas stained red indicate presence of collagen. *Mdx*-s EDL, SOL and diaphragm muscles all contained more collagen than C57-s mice, exercise did not cause a difference in collagen content in any of the three skeletal muscles

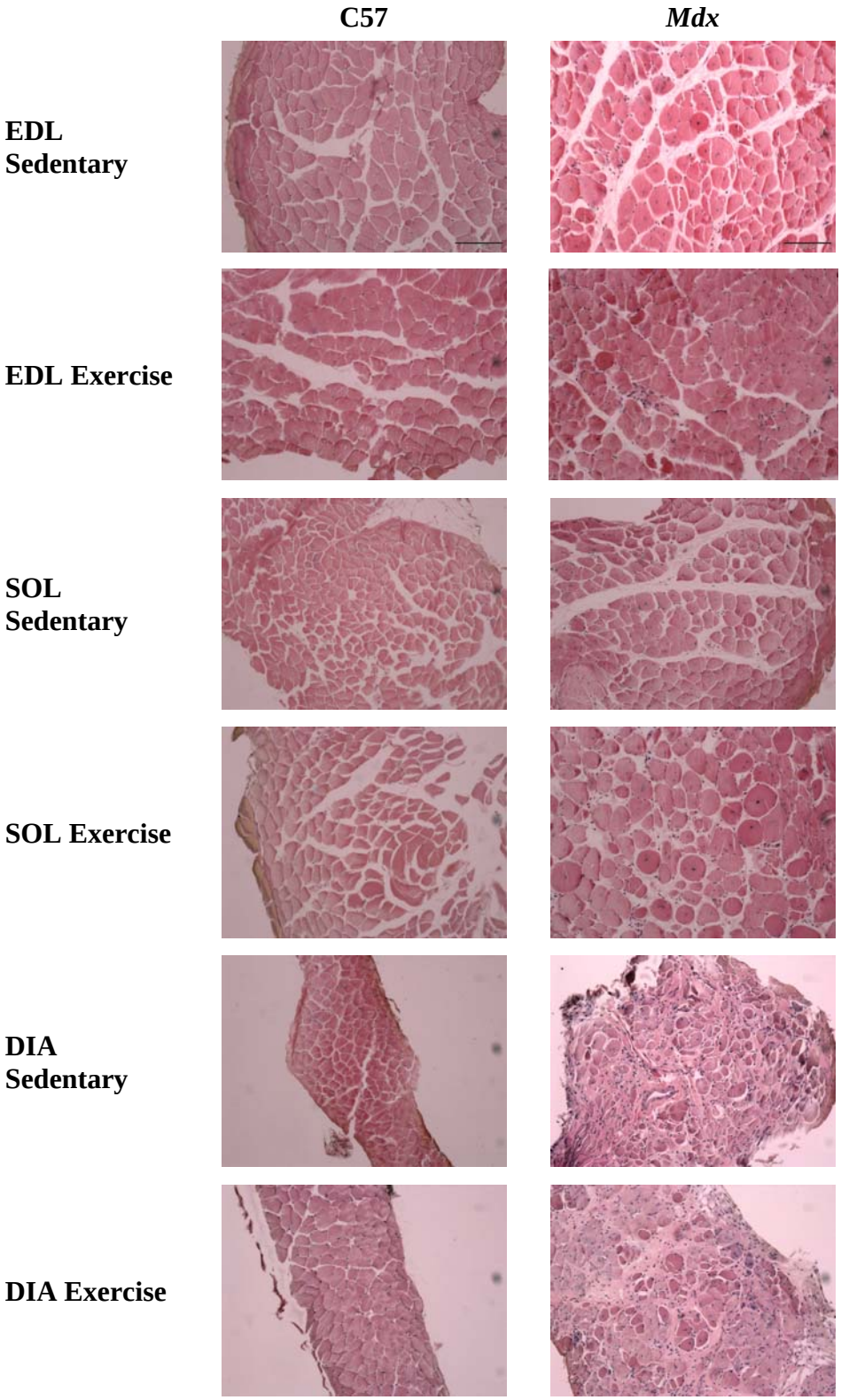

Figure 2.7: Skeletal muscle sections of sedentary and exercise *mdx* and C57 mice (H&E) Magnification: X20. C57 myocytes exhibit less central nucleation in all three muscles than *mdx*-s, exercise didn't alter this. Cell diameter is greater in *mdx*-s EDL compared to *mdx*-ex and C57-s and unchanged in SOL and diaphragm. *mdx*-s diaphragm minimum diameter is greater than C57-s

Mouse	PSR (% area)	Average Cell Diameter (μm)	Percentage Central Nucleation (%)
EDL			
mdx-s	21.03±1.26**	33.33±0.99^{+}	59.34±3.27***
mdx-ex	20.44±1.07**	29.08±0.75	51.92±5.81***
C57-s	3.11±0.10	26.89±3.40	2.06±1.08
C57-ex	4.07±0.51	26.48±1.41	4.90±3.79
SOL			
mdx-s	26.29±1.43**	28.65±0.85	67.27±3.29***
mdx-ex	23.52±2.24**	27.56±1.47	64.22±3.62***
C57-s	11.61±0.10	27.12±2.73	1.0±0.76
C57-ex	7.37±1.17	27.34±1.17	1.36±0.90
DIA			
mdx-s	62.15±3.20**	20.79±0.96	39.02±3.02***
mdx-ex	56.49±4.74**	20.09±8.20	31.47±3.41***
C57-s	13.35±10.90	23.28±1.39	6.67±0.93
C57-ex	20.97±6.72	20.87±1.39	3.91±1.78

Table 2.4: Quantitative histological data of skeletal muscles in sedentary and exercise mice Skeletal muscles from *mdx*-s mice all contained more collagen than C57-s mice, exercise did not alter these levels. C57-s skeletal myocytes display a lower percentage central nucleation compared to *mdx*-s mice. Exercise did not affect this percentage in either strain. The *mdx*-ex mice had a greater cell diameter compared with *mdx*-s. $^{***}P<0.001$; $^{**}P<0.01$ (*mdx* vs. C57) $^{+}P<0.05$ (*mdx*-s vs. *mdx*-ex)

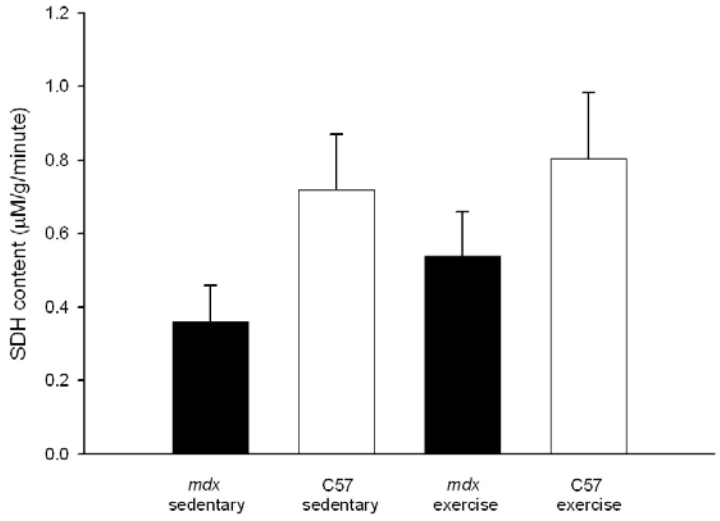

Figure 2.8: Succinate Dehydrogenase levels of sedentary and exercise *mdx* and C57 mice Exercise in the *mdx* and C57 mice increased the Succinate Dehydrogenase levels in the gastrocnemius muscle, but not to a significant level. $P<0.08$

2.4 Discussion

2.4.1 Overview

In this study, we examined the effects of chronic eccentric exercise on cardiac and skeletal muscle function in *mdx* and C57 mice. It has been reported that eccentric exercise is damaging to boys with DMD (Carpenter & Karpati 1979) and *mdx* mice (De Luca, A. et al. 2003; Vilquin et al. 1998). The eccentric exercise protocol has been used in *mdx* mice to mimic the limb muscle dystrophy seen in DMD (De Luca, A. et al. 2003; Granchelli, Pollina & Hudecki 2000; Hudecki et al. 1993). In exercised *mdx* mice, fibre necrosis might occur earlier and more drastically than in non-exercised mice based on the fact that *mdx* muscles are more vulnerable to exercise (Brussee, Tardif & Tremblay 1997; De Luca, A. et al. 2003; Granchelli, Pollina & Hudecki 2000; Vilquin et al. 1998).

2.4.2 Cardiac Structure and Function

Exercise has been shown to be detrimental to the *mdx* heart with physical exercise accelerating the dystrophic process through activation of intracellular signalling molecules (Nakamura et al. 2002). In contrast, IGF-1 increases cardiac output and contractility (with a slight increase in ESP) when given to normal human subjects (Donath et al. 1996) and swimming exercise increases expression of myocardial IGF-1 as a result of increasing left ventricular wall stress, thereby triggering the expression of the IGF-1 gene (Scheinowitz et al. 2003). IGF-1 alone increases left ventricular +dP/dt in rats, without significant development of fibrosis, (Cittadini et al. 1996) and in mice treated with a combination of IGF-1 and growth hormone, left ventricular contractility is enhanced as evidenced by augmented +dP/dt, again, without affecting collagen content

(Tanaka et al. 1998). In the current study, there was an increase in +dP/dt in both the *mdx*-ex and C57-ex mice compared to the *mdx*-s and C57-s mice, although this increase was significant only in the C57 mice.

The developed pressure and end systolic pressure were both improved as a result of exercise in the C57 mice, unfortunately this was not evident in the *mdx* mice. It may be assumed that by increasing left ventricular wall stress as a result of exercise, expression of the IGF-1 gene was triggered (Scheinowitz et al. 2003) (especially in C57 mice, which underwent the exercise protocol without difficulty), leading to an improvement of cardiac function as has been shown by a number of studies and an increase in end systolic pressure, which has been found by Donath *et al*. (1996).

Endurance exercise may accelerate collagen synthesis in the subepicardium of the left ventricle of canines as shown by an increase in left ventricular hydroxyproline (Childers et al. 2002), however similar findings have not been evident in mice or rats. Endurance training did not increase left ventricular weight or hydroxyproline concentration in mice (Kainulainen et al. 1983). Similarly in rats, total collagen content in the left ventricle was not altered in exercise trained rats compared with control rats in and neither was mRNA of collagen I and III affected by exercise (Burgess et al. 1996; Jin et al. 2000). Furthermore, myocardial collagen concentration, the ratio of cardiac collagen types I and III and the solubility of myocardial collagen were not altered in exercised rats in comparison to their sedentary controls (Woodiwiss, Oosthuyse & Norton 1998). These findings may explain the lack of change in mice from this study. The *mdx* mice in the

current study did not complete an endurance running protocol, which may have further reduced the likelihood of an increase in fibrosis. The slight but nonsignificant increase in picrosirius red staining of the LV of C57-ex mice may be as a result of the completion of the full 30 minute exercise protocol.

The histological appearance of *mdx* hearts has been found to be largely normal in the absence of experimental manipulations that impose an abnormally high level of mechanical stress on the heart (Danialou et al. 2001). Further, *mdx* cardiomyocytes may suffer micro-disruptions of the sarcolemma that are quickly resealed and hence non-lethal for the cell (Danialou et al. 2001). The inability to complete an exercise protocol in the current study may have been a protective mechanism to minimise the extent of such mechanical stress on the heart, which may explain the lack of histological difference.

2.4.3 Skeletal Muscle Structure and Function

Exercise (especially non-weight bearing such as swimming) is beneficial for boys with DMD (Posselt 2005) and *mdx* mice (Hayes, Lynch & Williams 1993; Hayes & Williams 1998). Weight bearing exercise has also been shown to improve the skeletal muscle function of *mdx* mice after voluntary wheel running (Dupont-Versteegden, McCarter & Katz 1994; Wineinger et al. 1998) and research has indicated that dystrophic muscle may not be more susceptible to damage induced by eccentric exercise than control muscle (Sacco et al. 1992).

The lack of extensive muscle fibre loss and lack of improvement in the respiratory muscle following exercise in the *mdx*-ex mice (unlike the increase in diaphragm tetanus seen in C57-ex) may simply be due to insufficient intensity (steepness of decline) or duration of exercise. Another possibility for a lack of detrimental effect is that muscles such as the diaphragm which increase in strength with exercise (as seen in C57 tetanus diaphragm contractions) are more resistant to activity-induced damage (Zeman et al. 2000). The inspiratory workload is increased due to the exercise period, but this did not hasten degeneration in the *mdx* diaphragm. There is evidence that increased respiratory workload (induced by tracheal banding) does not accelerate degeneration in the *mdx* diaphragm (Krupnick et al. 2003), which could explain the results in the current study.

Hind limb muscles were effectively repaired despite repetitive bouts of exercise and it was shown that *mdx* mice have a large capacity for muscle repair after work-induced fibre necrosis (Okano et al. 2005). It has been suggested that the *mdx* diaphragm undergoes degeneration due to an ineffective regenerative response rather than higher work-related damage and under certain physiological circumstances the *mdx* diaphragm can upregulate myofibre regeneration to meet physiological demands (Krupnick et al. 2003). It could be assumed that the *mdx*-ex mice had an effective repair mechanism which did not allow for a difference in contractile force after the eccentric exercise period. However, central nucleation was not increased in any of the three muscles after chronic exercise, suggesting there was little increase in regeneration of the muscles. Therefore, this mechanism may not be the reason for the expected impaired force production in exercised mice.

Histologically, *mdx* muscle shows many similarities to damaged normal muscle, containing both degenerating and regenerating fibres after lengthening contractions (Brussee, Tardif & Tremblay 1997). In *mdx* mice, the presence of central nuclei has been used as a marker that the fibre has been regenerated by proliferation and fusion of muscle precursor cells (Schmalbruch, 1986). All *mdx* mice in the current study had a significant increase in central nucleation in the skeletal muscle cells of the three muscles. Eccentric exercise did not affect the central nucleation percentage when comparing the exercise and sedentary groups. C57 mice did not display a high percentage of central nucleation and similarly, *mdx* mice exhibited no significant difference between exercised and sedentary mice, indicating no difference in regeneration. *Mdx* mice have a peak active degeneration-regeneration period which starts at 3 weeks and continues up to 2-3 months. Necrosis diminishes at 3-6 months and our exercise protocol started at the end of this period.

The analysis of collagen content by picrosirius red and hydroxyproline analysis indicated there were no detrimental effects of exercise on the skeletal muscles of either *mdx* or C57-ex mice. It can therefore be concluded that eccentric exercise does not result in a change of collagen or fibrosis in the skeletal muscles of either mouse strain.

Okano found that *mdx* mice are more vulnerable to exercise, however fibre necrosis was shown to be repaired as effectively as in control mice. Necrotic fibres or connective tissue proliferation were not altered in the *mdx* muscles of this study. Similarly, the

picrosirius red slide analysis in the current study showed no change in connective tissue proliferation (fibrosis).

In a study by Weller (1990), the vast majority of muscle fibre segments from old *mdx* mice were shown to have suffered at least one cycle of necrosis and then regenerated. These regenerated *mdx* muscle fibres were relatively resistant to further necrosis *in vivo*, even though they were still dystrophin deficient. Therefore, this acceleration of degeneration-regeneration may be an adaptation of the *mdx* mice to cope with exercise (Okano et al. 2005). In addition, this may be why a deleterious effect of eccentric exercise was not evident in the *mdx* mice of this study. Furthermore, in contrast to the dystrophin negative fibres in DMD, it has been suggested that dystrophin negative *mdx* fibres can recover from the destabilizing effects of dystrophin deficiency, as a result of their shorter lengths (Head, Williams & Stephenson 1992).

Various cytokines and growth factors, such as TGF-β, IGF-1 and TNF-α, are increased (upregulated) in the active stage of DMD and in *mdx* mice (Bernasconi et al. 1995; De Luca, A. et al. 1999; Spencer, Marino & Winckler 2000). This upregulation becomes less evident as the disease progresses (Okano et al. 2005). IGF-1 plays a critical role in muscle regeneration. It promotes the proliferation and differentiation of satellite cells in the muscle, enabling them to fuse to existing muscle fibres and repair damaged regions (Allen & Rankin 1990; Barton et al. 2002; Doumit, Cook & Merkel 1993).

In *mdx* mice administered with recombinant human IGF-1 for 8 weeks, specific force output and resistance to fatigue of diaphragm, EDL and SOL muscles was increased (Gregorevic et al. 2002; 2004). Exercise restores IGF 1 action in old mice (Willis et al. 1997; Willis et al. 1998) and IGF-1 overexpression in *mdx* mice reduces the severity of dystrophy and prevents fibrosis in addition to promoting functional hypertrophy (Barton et al. 2002). Skeletal muscle specific overexpression of IGF-1 reduces the sarcolemmal damage and necrosis in young *mdx* myofibres (Shavlakadze et al. 2004).

The results in the current study suggest that perhaps due to the chronic exercise training regime, levels of IGF-1 could have increased in the mice, which may lead to increased satellite cell proliferation, thereby increasing fibre size (as seen in average cell diameter of *mdx*-ex vs. *mdx*-s EDL and higher maximum diameters in *mdx*-ex vs. *mdx*-s SOL) and causing no detrimental effects to the skeletal muscles of the *mdx* mice.

Okano however, found that IGF-1 was downregulated by exercise in *mdx* mice, suggesting that the population of early regenerating fibres (which produce IGF-1) was decreased at the time of sacrifice. The age of the mice in this study however was 42 days, compared with 15 months in the current study. When using these mice at the younger age, the loss of viability observed with eccentric contractions may only be occurring in fibres which are already compromised by the underlying degenerative process (McArdle, Edwards & Jackson 1995).

Endurance downhill running in mice conferred protection to recruited skeletal muscles (SOL and EDL) against the effects of an acute bout of repeated eccentric contractions due to intracellular calcium levels and force production values being similar to sedentary control mice (Lynch, Fary & Williams 1997). This may indicate a further reason why no difference was seen in our mice. Calcium sequestration by the sarcoplasmic reticulum from fast twitch muscles is depressed after training. Immediately after running, decrease in SR function occurred in both plantaris and SOL muscles (more pronounced in SOL) (Inashima et al. 2003).

Chronic aerobic exercise training increases SDH activity in human muscle fibres (Chilibeck et al. 1998) and training significantly elevates SDH activity in rats (Hammeren et al. 1992). Research has found contradictory data stating that aerobic exercise training produced no effect on SDH activity in heart and skeletal muscles of mice and that the effect of exercise on SDH depends on the mammal considered (Soares, Folmer & Rocha 2003) which may explain the lack of difference in this study.

2.4.4 Study Limitations

The *mdx* mice in this project showed an adverse behaviour to the running protocol, which has also been encountered by previous researchers (Brussee, Tardif & Tremblay 1997; De Luca, A. et al. 2005; De Luca, A. et al. 2003; Vilquin et al. 1998). This was regarded as a strain idiosyncrasy rather than poor experimental protocol.

Many studies have been conducted to investigate the effect of eccentric exercise in *mdx* mice with most researchers using mice of 3-8 weeks of age. Mice at this young age undergo acute cycles of degeneration-regeneration and eccentric exercise in this time period of the *mdx* life has been shown to be detrimental (Carter, Abresch & Fowler 2002; Hara et al. 2002; Vilquin et al. 1998; Weller, Karpati & Carpenter 1990). In the current study, mice were 12 months old at cessation of the exercise period, thereby allowing age-related differences to impact on the effect of chronic exercise in older mice.

A hindrance when comparing studies involving exercise is that all researchers conduct their experiments very differently. Sacco *et al*. (1992) points out that many projects completed the experiments a matter of hours after the initial exercise period. It is known that the main deleterious effects and fibre necrosis occur several days after exercise (McArdle, Edwards & Jackson 1995).

Mdx muscles have been shown to respond to exercise in the same way as C57 muscles. Twelve days after cessation of the exercise both strains showed a similar loss of force and a similar time course of both degeneration and recovery (Sacco et al. 1992). A chronic protocol such as 5 months in the current study may have a similar effect on the skeletal muscles, with both the *mdx* and C57 mice responding in a similar way (disregarding the obvious reduction of the force of contraction between the species). It has been mentioned that a universal problem with all of the experiments about stability of membrane is the age of the mice studied (McArdle, Edwards & Jackson 1995).

2.4.5 Study Outcomes

Chronic exercise in older *mdx* mice did not exacerbate the dystrophic pathology of *mdx* heart, EDL, SOL or diaphragm muscles. It appears from the above experiments that moderate exercise at the later stage of the *mdx* mouse is not detrimental and suggests that fibrosis is not worsened by eccentric contractions.

CHAPTER 3 : THE EFFECT OF LONG TERM ADMINISTRATION OF PIRFENIDONE ON CARDIAC AND SKELETAL MUSCLE FUNCTION IN *MDX* MICE

3.1 Introduction

Deficiency of dystrophin, due to a mutation in the dystrophin gene on the X-chromosome, is the primary cause of Duchenne Muscular Dystrophy (DMD). This neuromuscular disorder affects approximately 1 in 3500 live male births. Dystrophin deficiency affects all muscle types causing repeated cycles of myocyte degeneration and consequently leading to increased deposition of collagenous extracellular matrix or fibrosis (Chen et al. 2005; Ionasescu & Ionasescu 1982). Such fibrosis in skeletal muscle impairs contractile activity and contributes to contractures (Morrison et al. 2000) whereas in the heart, in addition to impairing contractility, fibrosis may interfere with impulse conduction and thus rhythm (Finsterer & Stollberger 2003). The precise mechanisms causing fibrosis are unknown, although inflammatory cytokines such as TGF-β have been implicated.

TGF-β is a pleiotropic cytokine that plays an important role in inflammation, cell growth and wound and tissue repair (Passerini et al. 2002). This cytokine has also been found to be expressed at high levels in the skeletal muscles of patients with DMD with evidence that its level of expression is related to the degree of muscle fibrosis (Bernasconi et al. 1995). Similarly, in the dystrophin deficient *mdx* mouse, fibrosis in the diaphragm is associated with increased TGF-β transcript (Gosselin et al. 2004).

Pirfenidone is an orally active antifibrotic drug that inhibits TGF-β–induced fibroblast growth and collagen synthesis in a range of tissues and disease models. For example, pirfenidone effectively reduced pulmonary fibrosis in the bleomycin hamster model (Iyer, Gurujeyalakshmi & Giri 1999b), glomerulosclerosis in the FGS/Kist mouse model of renal fibrosis, collagen accumulation in post-obstructive models of kidney fibrosis in rats (Shimizu et al. 1997; Shimizu et al. 1998) and hepatic fibrosis in the male Wistar King A rats treated with dimethylnitrosamine (DMN) to induce fibrosis (Tada et al. 2001). Likewise in streptozotocin-induced diabetic rats, pirfenidone reversed cardiac and renal fibrosis, without normalising cardiac contractility or renal function (Miric et al. 2001).

As the antifibrotic action of pirfenidone has been demonstrated in several animal models of fibrosis in different organs including cardiac, lung, kidney and liver, the hypothesis that administration of pirfenidone would elicit an antifibrotic action on cardiac and skeletal muscle and improve functional responses in *mdx* mice, a model which displays extensive skeletal and cardiac fibrosis later in life was tested.

3.2 Materials and Methods

3.2.1 Animals

Male C57BL10ScSn mice (control strain) (C57) were purchased from the Animal Resource Centre, Nedlands, WA. Male C57BL10ScSn *mdx* (*mdx*) mice were bred at the University of Southern Queensland Animal House, Toowoomba, QLD. Cardiac and skeletal muscle fibrosis in the *mdx* mouse is severe at approximately 15 months of age (Laws 2005; Laws & Hoey 2004) thus it was investigated if this extensive fibrosis could be prevented by administration of pirfenidone for the preceding 7 months. Accordingly mice were 8 months old at the commencement of experiments. All experimental protocols were conducted with the approval of the University of Southern Queensland Animal Ethics Committee, under the guidelines of the National Health and Medical Research Council of Australia.

3.2.2 Mouse groups

Mdx mice were randomised into four groups, with nine mice per group. Three groups of *mdx* mice were treated with pirfenidone (Intermune, Brisbane, CA) in their drinking water at the following doses, 0.4, 0.8 and 1.2 g/100 mL. A further group of *mdx* and C57 mice received untreated drinking water and were designated *mdx* and C57 controls. This treatment regime allowed assessment of the drug-induced benefit relative to the untreated *mdx* and untreated healthy C57 mice. All animals were given free access to feed. All mice were treated for a total of 7 months.

3.2.3 Langendorff Experiments

Mice at 15 months of age were weighed and anaesthetised with pentobarbitone sodium (Nembutal, Boehringer Ingelheim) at 70 mg/kg administered intraperitoneally. A thoracotomy was performed and hearts were rapidly excised into modified Krebs-Henseleit buffer containing (mM): NaCl, 119; $NaHCO_3$, 22; KCl, 4.7; KH_2PO_4, 1.2; $CaCl_2$, 2.5; $MgSO_4$, 1.2; glucose, 11; Na-pyruvate, 1 and EDTA, 0.5 containing 10 mM 2,3-butanedione monoxime (temperature 21°C). The BDM was placed into the dissection buffer to limit detrimental actions of calcium during tissue preparation. The aorta was cannulated via the dorsal root and perfused retrogradely at a pressure of 80 mmHg with Krebs-Henseleit perfusion buffer maintained at 37°C and bubbled with carbogen ($95\%O_2$-$5\%CO_2$) to ensure a pH of 7.4. The Krebs-Henseleit buffer used for perfusion of the hearts did not contain BDM.

A small polyethylene apical drain was used to vent the left ventricle preventing an accumulation of fluid in this chamber via Thesbian veins. The left atrium was excised and a fluid filled balloon constructed from polyvinyl chloride plastic film was inserted into the left ventricle via the mitral valve for the measurement of left ventricular function. The left ventricular function was recorded via a MLT844 physiological pressure transducer (ADInstruments, Castle Hill, NSW, Australia) linked to a PowerLab recording system (ADInstruments, Castle Hill, NSW, Australia). Coronary flow was regulated via a ML175 STH Pump Controller (ADInstruments, Castle Hill, NSW, Australia).

Data from hearts with a coronary flow greater than 5 mL/min were excluded from the experimental analysis. Data was recorded using Chart 4.1.1 software (ADInstruments, Castle Hill, NSW, Australia) to calculate end systolic pressure (ESP) and end diastolic pressure (EDP), developed pressure and relaxation over time (±dP/dt) and heart rate. Fluid temperature was measured via a thermometer at the entry of the aortic cannula, and temperatures were maintained at 37.3°C. Hearts were paced at 420 bpm via a silver wire embedded into the left ventricle and grounded using an electrode attached to the cannula. The balloon was inflated to an EDP between 0 and 5 mmHg and the heart was then equilibrated for 10 minutes at this pressure. Following this equilibration period, the EDP was measured for 30 seconds at each of the following increments: 0, 5, 10, 15, 20 and 30mmHg. Myocardial stiffness was defined by the stiffness constant (κ, dimensionless), that is, the slope of the linear relationship between the tangent elastic modulus (E, dyne/cm^2) and stress (σ, dyne/cm^2) as described in detail (Mirsky & Parmley 1973) (See Appendix A2.0). At cessation of the *in vitro* experiments, the right atrium, right ventricle and the left ventricle plus septum were separated and weighed. The left ventricle plus septum was bisected transversely with the superior portion stored for histology. Half of the remaining tissue was snap frozen in liquid nitrogen and stored at -80°C for subsequent hydroxyproline assays and the other half was stored in RNA*later*™ (Ambion, Canada) to determine TGF-β RNA expression .

3.2.4 Skeletal Muscle Contractility

Immediately after the removal of the heart, the following skeletal muscles were dissected: extensor digitorum longus (EDL) and soleus (SOL) from the left leg and a strip of the

diaphragm, these strips were cut consistently from the same region of diaphragm to minimise experimental error. These muscles were placed in ice-cold Krebs-Henseleit solution containing (mM): NaCl, 118; $NaHCO_3$, 25; KCl, 4.7; KH_2PO_4, 1.18; $CaCl_2.2H_2O$, 2.5; $MgSO_4.7H_2O$, 1.16; glucose, 11; bubbled with carbogen, (95%O_2-5%CO_2). The three muscles were tied individually around the tendon at either end with 5.0 silk suture with one end attached to a fixed peg and the other end attached to a physiological force transducer (TRI 201, Panlab, Spain). All three skeletal muscles were suspended in water-jacketed tissue baths (25°C) containing Krebs-Henseleit buffer bubbled with carbogen. Two parallel platinum electrodes along the length of the muscles provided field stimulation (0.2 ms pulse duration) from a Grass S48 stimulator (West Warwick, RI) with amplified current intensity (EP500B, Audio Assemblies, Campbellfield, Victoria, Australia). Contractile force was recorded via the force transducer connected to a PowerLab recording system (ADInstruments, Castle Hill, NSW, Australia) and analysed using Chart 4.1.1. Optimal preload (L_o) was defined as the length eliciting maximal single twitch force. Optimum voltage was also determined for each muscle, as was the frequency eliciting maximal tetanic force ranging from 50-180Hz. The optimum values were used for the remainder of the experiment. Reported data were the average of three individual single-twitch or tetanic stimulations per muscle strip after 25 minutes of equilibration and optimization of conditions. Upon completion of the functional skeletal muscle experiments, muscle lengths (L_o) and muscle width were recorded, using a digital micrometer. The muscles were blotted for 3 seconds and weighed. The cross-sectional area and normalization of force were calculated as described previously, where tissue cross sectional area equals tissue weight divided by

length multiplied by 1.06 (density of mammalian muscle) (Lynch et al. 2001). This calculation for cross-sectional area accounts for the differences in thickness between different tissues. (Diaphragm thickness in mm: C57 0.4, *mdx* 0.7; SOL thickness C57 0.83, *mdx* 1.39; EDL thickness C57 1.53, *mdx* 2.00-2.45). Subsequently, the three skeletal muscles were frozen in liquid nitrogen and stored at -80°C for hydroxyproline assays.

3.2.5 Hydroxyproline Measurements

Hydroxyproline (HP) assays were used as a measure of collagen content. The individual frozen EDL, SOL and diaphragm sections were trimmed of tendons and capsular tissue. All skeletal tissue and a section of the left ventricle were weighed. The tissues were cut into smaller pieces with a scalpel and placed in a sealed tube containing 6 M HCl. The tissues and standards (0, 1, 2, 3, 4, 5, 6 and 7 μM hydroxyproline) were hydrolysed overnight (18 hours) at 107°C. After hydrolysation, the tissues were dried using low heat (50°C) and filtered air under pressure. The dried sample was reconstituted with 500 μL distilled water (dH_2O) and vortexed. A working solution of the buffer stock solution (50 g citric acid.$1H_2O$, 12 mL glacial acetic acid, 120 g sodium acetate.$3H_2O$ and 34 g sodium hydroxide made up to 1 L with dH_2O) was made prior to use by taking 500 mL of the stock and adding 100 mL of dH_2O and 150 mL of n-propanol. 250 μL of Chloramine T reagent (1.41 g chloramine T, 10 mL dH_2O water, 10 mL n-propanol and 80 mL buffer working solution) was added to each sample (ensuring the samples and Chloramine T were at room temperature); the oxidation step was then allowed to progress for 20 minutes at room temperature. 250 μL of Ehrlich's reagent (1.664 g

dimethylaminobenzaldehyde and 10 mL of a 2:1 n-propanol/perchloric acid solution) was then added and samples were subsequently incubated at 60°C in a shaking water bath for 20 minutes to allow the chromophore to develop. The tubes were then cooled under tap water before the absorbance was read at 550 nm. Using a standard curve, the μg hydroxyproline content was measured, assuming that 12.5% of collagen is hydroxyproline. Values are expressed as μg HP/mg of wet tissue weight.

3.2.6 Histology

The superior ventricular, EDL, SOL and diaphragm segments were fixed in Telly's fixative (70% ethanol, 37% formaldehyde and glacial acetic acid) for 3 days, modified Bouin's solution (saturated picric acid, 37% formaldehyde and glacial acetic acid) for 1 day and 70% ethanol before the muscles were embedded in paraffin wax. Sections of 10 μm thickness were cut and placed on Polysine glass slides and stained using the collagen selective stain, 0.1% wt/vol picrosirius red solution (Sirius Red F3B, Chroma Dyes, in saturated picric acid). Slides were left in 0.2% phosphomolybdic acid for 5 minutes, then washed, stained in picrosirius red for 90 minutes and then placed in 1 mM HCl for 2 minutes. Slides were then placed in 70% ethanol for 30 seconds and coverslipped using Depex.

Stained muscle sections were viewed blinded to the strain of mouse using a Nikon Eclipse E600 epifluorescence microscope and 20X magnification. Images were captured with a cooled CCD digital camera (Micropublisher 5.0, QImaging, Canada), with the percentage collagen quantified using AnalySIS software (Soft Imaging System, GmbH,

Münster, Germany). To determine the average percentage collagen of each left ventricle and skeletal muscle section, five regions (for left ventricle) and two regions (for skeletal muscle) were viewed per muscle sample and the final percentage of collagen was calculated from the average of these five or two regions. Picrosirius red-stained cardiac sections were viewed under polarised light to determine the ratio of type I and type III collagen with colour separation achieved using AnalySIS. Again 5 left ventricular regions were viewed and averaged.

Skeletal muscle sections of 5 μm thickness were cut and placed on Polysine glass slides and stained using haematoxylin and eosin stain to determine cell diameter and central nucleation. These slides were analysed using the same software as mentioned earlier. Again due to the smaller size of these muscles, only 2 regions were viewed per muscle sample (counting 100 cells per region). The cell diameter and central nucleation was calculated from the average of the cells in these two regions. To prevent experimental errors such as the orientation of the sectioning angle, the minimal 'Feret's diameter' was measured which allows for reliable measure of muscle fibre cross-sectional size and reliably discriminates between dystrophic and normal phenotypes (Briguet et al. 2004).

3.2.7 RNA Analysis

3.2.7.1 RNA Extractions

RNA later treated frozen samples were sectioned with a cryostat at 6μm thickness and total RNA extracted with an RNAqueous Kit (Ambion, Austin, Texas). All samples were

DNase treated with Turbo DNA-free^{TM} (Ambion, Austin, Texas) prior to RT-PCR. The resulting RNA was screened for genomic DNA contamination by PCR using primers specific for mouse β-actin. If a product was produced then genomic DNA was present as RNA cannot be amplified. RNA was quantified using Quant-it^{TM} Ribogreen^{R} RNA Assay Kit (Molecular Probes, Invitrogen, Oregon, USA). RNA samples were stored at -80^{o}C.

3.2.7.2 Relative Reverse-Transcriptase PCR

Relative RT-PCR was carried out with 100pg of total RNA as the starting material for 26 cycles of amplification in the Titan One-Tube RT-PCR system (Roche Molecular Biochemicals, Mannheim, Germany).

TGF-β was amplified with the following forward and reverse primers:

TGF-β 1446F 5'-TGAGTGGCTGTCTTTTGACG-3',

TGF-β 1738R 5'-TCTCTGTGGAGCTGAAGCAA-3'.

β-actin was co-amplified as an internal control using the following forward and reverse primers:

β-actin F561 5'-CACACTGTGCCCATCTACGA-3',

β-actin R688 5'-GTGGTGGTGAAGCTGTAG-3'.

To determine specificity, all sequences were compared with Genbank using the program Blast available at the National Center for Biotechnology Information website

(www.ncbi.nlm.nih.gov). Primers were synthesized by GeneWorks Pty Ltd. TGF-β and β -actin primers were used at a concentration of 10μM and 20μM respectively. Optimal magnesium chloride concentration was 1.0mM with all other reaction components added as per manufacturer's instructions of the Titan One-Tube RT-PCR system. Multiplex reactions were carried out on a ThermoHybaid PCR Express (Integrated Sciences, UK). A first cycle of 48^{o}C for 30 minutes was undertaken for cDNA synthesis. An initial denaturation step of 94^{o}C for 2 minutes was performed, followed by a touch-down PCR protocol as described below: 30 seconds at 94^{o}C, 1 minute at 62^{o}C, 2 minutes at 72^{o}C for 2 cycles; 30 seconds at 94^{o}C, 1 minute at 60^{o}C and 2 minutes at 72^{o}C for 2 cycles; 30 seconds at 94^{o}C, 1 minute at 58^{o}C and 2 minutes at 72^{o}C for 2 cycles; 30 seconds at 94^{o}C, 1 minute at 56^{o}C and 2 minutes at 72^{o}C for 20 cycles. A final extension was performed at 72^{o}C for 5 minutes. Cycling parameters were optimized to ensure exponential phase amplification of TGF-β and β-actin. PCR products were run on a 2% agarose gel in TAE buffer and visualised with ethidium bromide. A PCR DNA ladder (NEB) was run on each gel to confirm the expected molecular weight of the amplification product. Results were analysed using Scion Image Software Beta 4.0.2 (www.scioncorp.com) and TGF-β product normalized by comparison to the β-actin internal control product.

3.2.8 Statistical Analysis

Data is presented as mean ± SEM, comparisons were made using the unpaired Student's t-test and ANOVA. $P<0.05$ was considered statistically significant. Differences between

groups were determined post hoc using Tukeys HSD test if variances were shown to be equal or Games-Howell post hoc test if variance was unequal.

3.3 Results

3.3.1 Cardiac Muscle

Mdx mice showed impaired cardiac function relative to age-sex matched C57 mice. This impairment was evidenced by a reduction of 26% in left ventricular developed pressure (P<0.001: Fig 3.1), 29% in +dP/dt (P<0.01: Fig 3.2 (A) and 21% in –dP/dt (P<0.01: Fig 3.2 (B)).

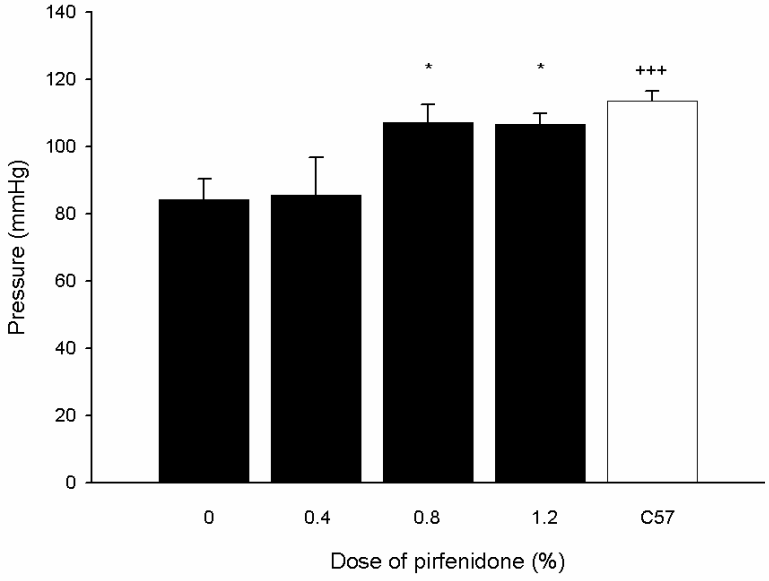

Figure 3.1: Cardiac function of control and pirfenidone treated mice
Left ventricular developed pressure from isolated hearts of control *mdx* and C57 mice and the pirfenidone treated *mdx* mice.
Untreated *mdx* and *mdx* treated with the 0.4% dose had a lower developed pressure than C57 mice. *Mdx* mice treated with 0.8 and 1.2% doses of pirfenidone increased developed pressures to a level commensurate with that measured in hearts from C57 mice.
$^{+++}$ P<0.001; C57 vs. *mdx* control; *P<0.05; (pirfenidone treated *mdx* vs. control *mdx*).

A

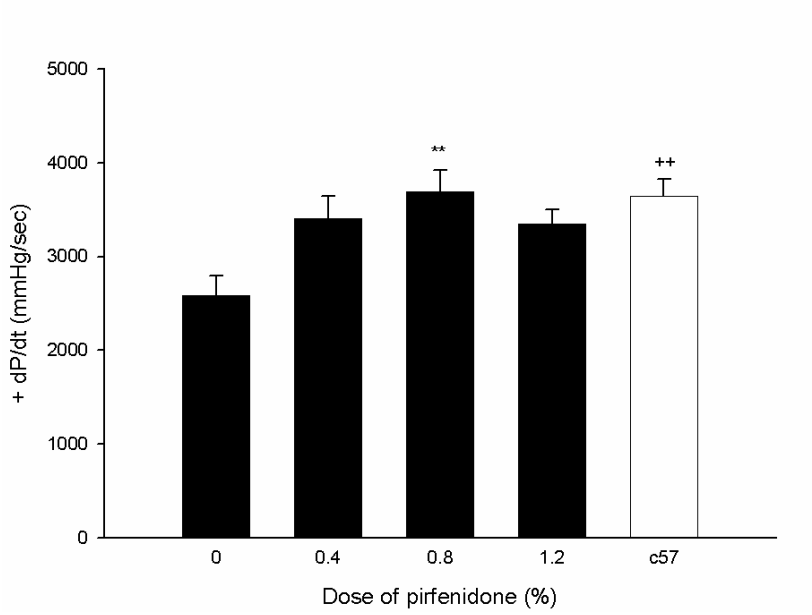

B

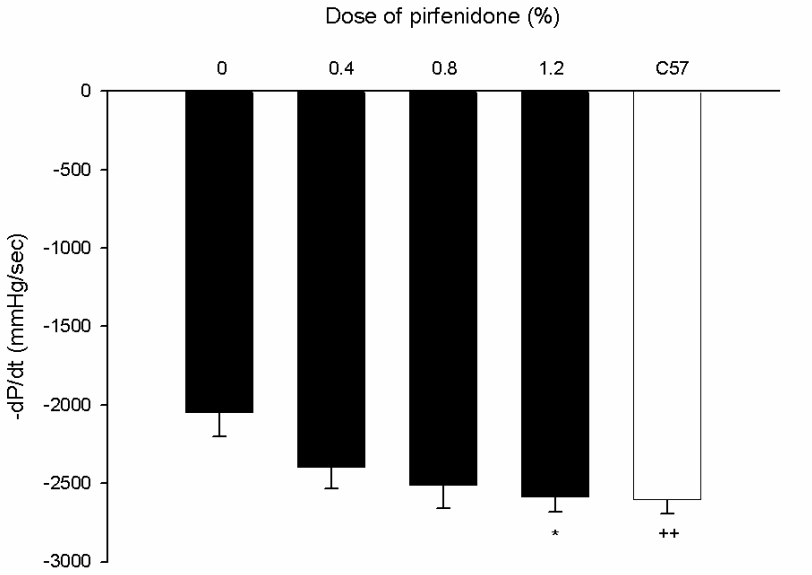

Figure 3.2: Cardiac function of control and pirfenidone treated mice
Rate of pressure development (+dP/dt) (A) and rate of relaxation (-dP/dt) (B) from isolated hearts of control *mdx* and C57 mice and the pirfenidone treated *mdx* mice. +dP/dt was improved in the 0.8% pirfenidone dose treated *mdx*, -dP/dt was improved with the 1.2% dose and non-significantly improved in the 0.8% dose versus untreated *mdx*, resulting in values similar to those measured in hearts from C57 mice. $^{++}P<0.01$; C57 vs. *mdx* control; $^{*}P<0.05$; $^{**}P<0.01$; pirfenidone treated *mdx* vs. control *mdx*.

To counter this, pirfenidone treatment caused a significant improvement in cardiac contractility with both 0.8% and 1.2% treatment groups causing increased developed pressure in *mdx* to a level commensurate with that measured in hearts from C57 mice. Similarly, +dP/dt was improved in pirfenidone treated *mdx* with this reaching significance ($P<0.01$) in mice treated with 0.8% pirfenidone, but narrowly missing significance in mice treated with 0.4% ($P<0.07$) and 1.2% ($P<0.08$). Associated with this, -dP/dt was also improved with 1.2% ($P<0.05$) and 0.8% concentrations ($P<0.06$) versus untreated *mdx*, resulting in values similar to those measured in hearts from C57 mice. There were no significant differences in coronary flow (Figure 3.3) or diastolic stiffness (Table 3.1) between the untreated *mdx* and C57 mice or between hearts from untreated and pirfenidone treated *mdx* mice.

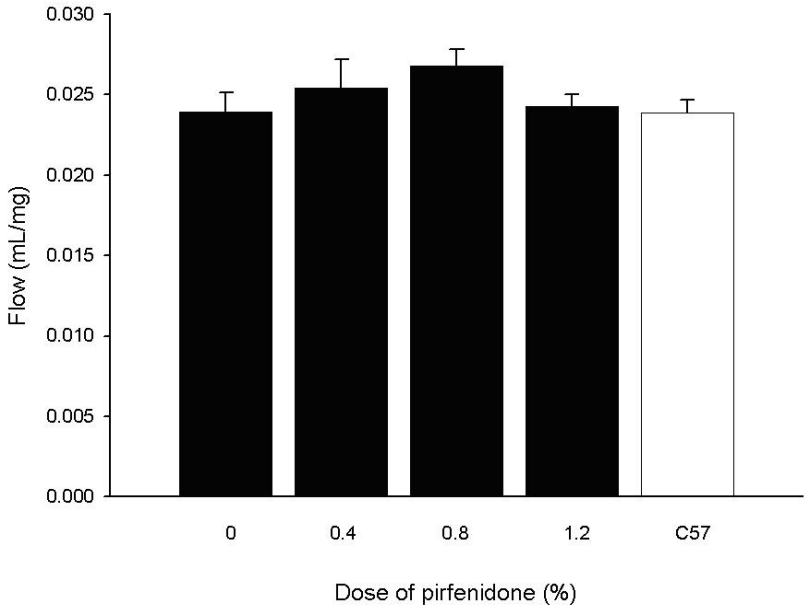

Figure 3.3: Coronary flow from control and pirfenidone treated mice
Coronary flow from isolated hearts of control *mdx* and C57 mice and the pirfenidone treated *mdx* mice. There was no difference in coronary flow between the mice.

	C57	*Mdx* 0	0.4	0.8	1.2
Stiffness	32.56±1.29	30.80±2.3	31.34±2.69	33.11±2.13	29.77±2.44

Table 3.1: Stiffness values of control and pirfenidone treated mice
Pirfenidone treatment did not alter cardiac stiffness parameters

To determine if changes in contractility and stiffness were related to reduced fibrosis, cardiac collagen content was measured. Hydroxyproline content was increased in the left ventricles of untreated *mdx* mice compared to C57 control mice ($P<0.01$) and pirfenidone treatment did not reduce hydroxyproline content (Figure 3.4).

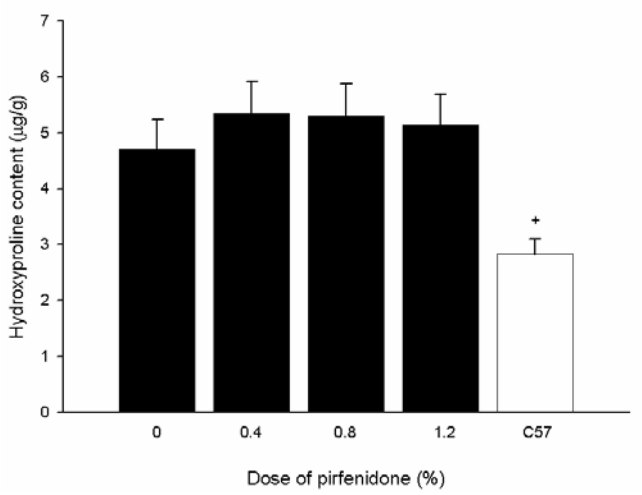

Figure 3.4: Cardiac hydroxyproline content of control and pirfenidone treated mice
Left ventricular hydroxyproline content from hearts of control *mdx* and C57 mice and the pirfenidone treated *mdx* mice. Control and treated *mdx* mice had higher hydroxyproline content than C57 mice. $^{+}P<0.05$; C57 vs. *mdx* control.

These findings were reinforced by analysis of picrosirius red-stained left ventricular sections viewed under polarised light which showed that total collagen was increased in *mdx* mice ($P<0.05$), but unaltered by pirfenidone treatment (Figure 3.5; Table 3.2). The ratio of type I:III collagen was measured, but again no difference was evident between treated *mdx* and untreated *mdx* nor was a ratio difference evident between *mdx* and C57s (Table 3.3).

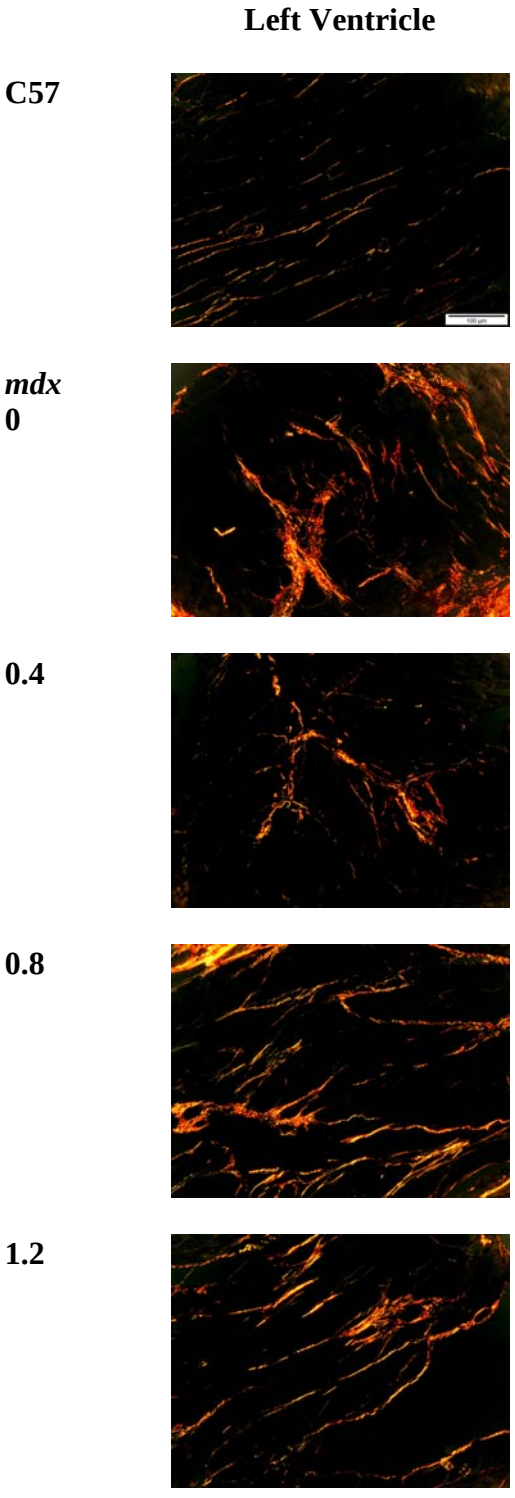

Figure 3.5: Left ventricular sections of control and pirfenidone treated mice (polarised) Viewed under polarised light, magnification: X20. Areas stained red/yellow indicate presence of collagen I and areas stained green indicate presence of collagen III.
Total collagen was higher in untreated *mdx* mice and unaltered by pirfenidone treatment.

	C57	*Mdx* 0	0.4	0.8	1.2
Total Collagen	7.75±1.58	12.54±3.93*	13.07±1.95*	10.19±1.84*	10.19±1.84*

Table 3.2: Total collagen in *mdx* and C57 mice cardiac muscle
Total collagen is increased in *mdx* mice compared to C57 mice, pirfenidone treatment did not affect these levels. *P<0.05 (vs. C57 mice)

	C57	*Mdx* 0	0.4	0.8	1.2
RatioI:III	2.15±0.14	2.06±0.045	2.30±0.09	2.20±0.1	2.2±0.04

Table 3.3: Ratio of type I:III collagen in *mdx* and C57 mice
There was no difference in collagen I:III ratio in control *mdx* and C57 or treated *mdx* mice

3.3.2 RNA Analysis

The RNA values of TGF-β in untreated *mdx* were not different to the TGF-β RNA values in C57 mice. The higher doses of pirfenidone (0.8 and 1.2%) decreased the TGF-β RNA levels significantly (P<0.01) compared to both the C57 and untreated *mdx* mice. The lowest dose of pirfenidone (0.4%) did not decrease these RNA levels (Figure 3.6).

A

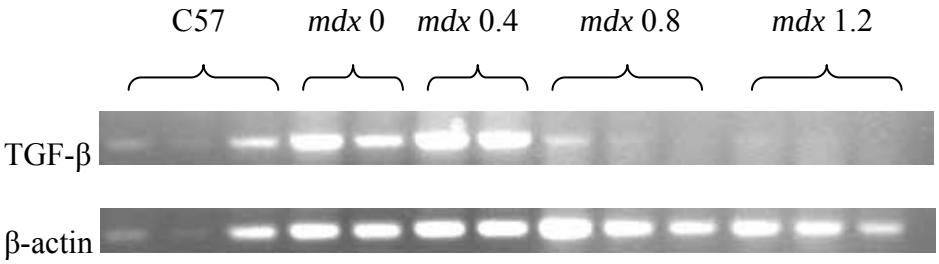

B

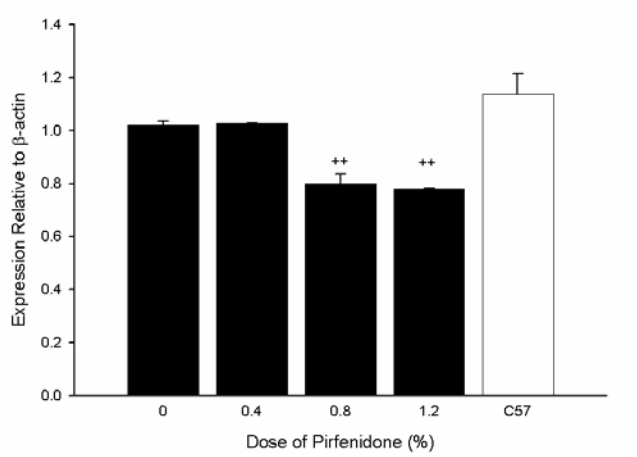

Figure 3.6: Relative RT-PCR analysis of TGF-β relative to that of β-actin
Relative RT-PCR gel of TGF-β (293 bp) and β-actin (127 bp) (A)
TGF-β expression relative to that of β-actin (B). Standard error bars represent the variation of 3 relative RT-PCR experiments.

3.3.3 Skeletal Muscle

Untreated *mdx* mice had significantly lower twitch force production in EDL, SOL and diaphragm when compared to C57 mice ($P<0.01$; Figure 3.7) with tetanic forces showing similar quantitative changes ($P<0.01$; Figure 3.8). Pirfenidone did not increase force production in EDL, SOL or diaphragm muscles.

3.3.4 Skeletal Muscle Structural Changes

Hydroxyproline content was elevated significantly in the EDL, SOL and diaphragm muscles from untreated *mdx* compared to C57 mice ($P<0.0001$; Figure 3.9). Pirfenidone treatment did not impact on fibrosis measured by HP. Evaluation of picrosirius red-stained muscle sections revealed similar quantitative changes for all three muscles (Figure 3.10; Table 3.4).

C57 mice exhibited significantly less central nucleation when compared to *mdx* mice ($P<0.0001$) in all three muscles (Table 3.4). There were no differences in the average or minimum myocyte diameters between *mdx* and C57 mice for all three muscles, but *mdx* myocytes had significantly larger maximum myocyte diameters for all three muscle types ($P<0.05$) compared to C57 myocyte diameters. Pirfenidone did not affect any of these parameters. Examples of H&E stained sections are shown in Figure 3.11.

A

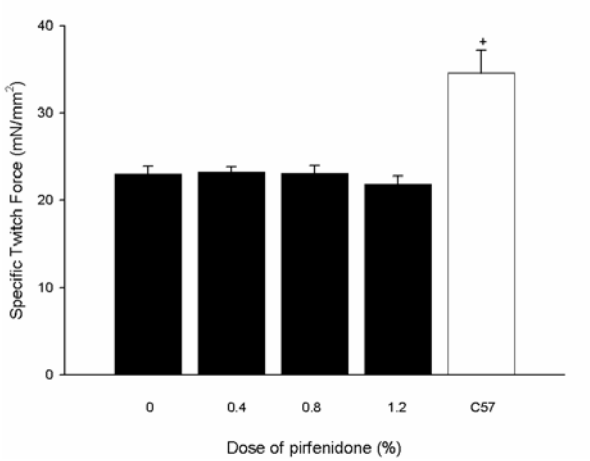

B

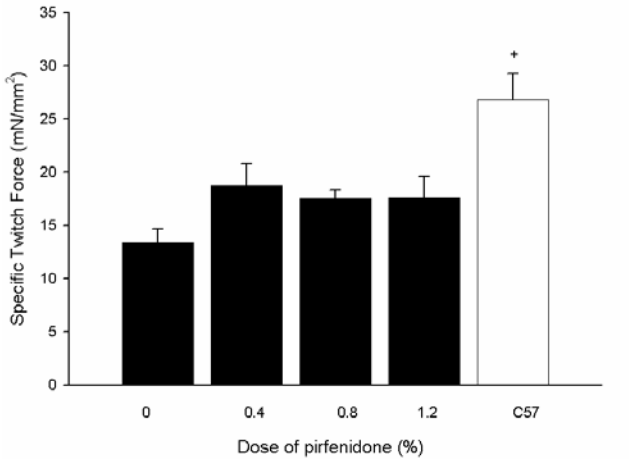

C

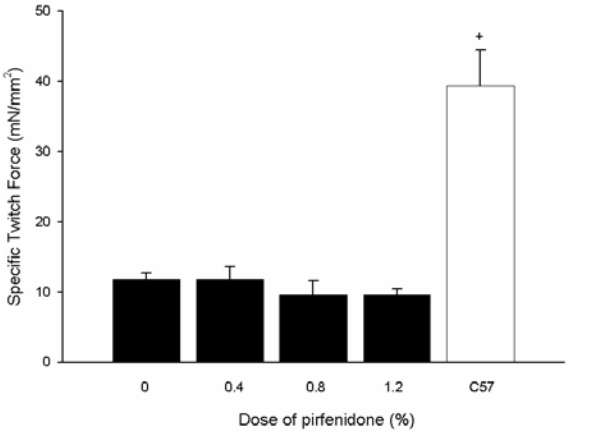

Figure 3.7: Skeletal muscles contraction of control and pirfenidone treated mice Specific twitch contractions of control and pirfenidone treated *mdx* and control C57 mice EDL (A), SOL (B) and diaphragm (C). Untreated and pirfenidone treated *mdx* mice had significantly lower twitch force production in EDL, SOL and diaphragm compared to C57 mice. $^{+}P<0.05$; C57 vs. *mdx* control.

A

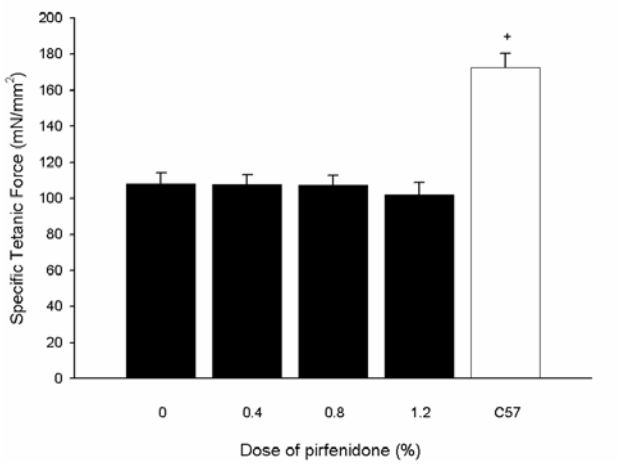

B

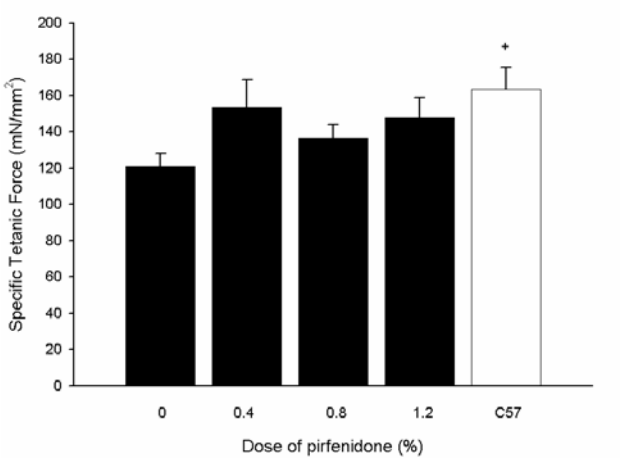

C

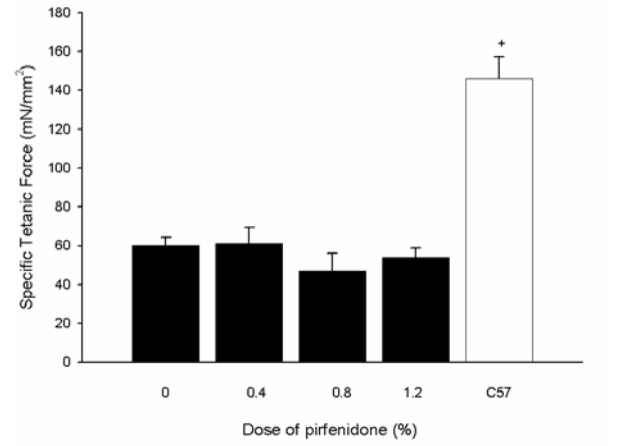

Figure 3.8: Skeletal muscle contractions of control and pirfenidone treated mice Specific tetanic contractions of control and pirfenidone treated *mdx* and control C57 mice EDL (A), SOL (B) and diaphragm (C). Untreated and pirfenidone treated *mdx* mice had significantly lower tetanus force production in EDL, SOL and diaphragm compared to C57 mice. $^{+}P<0.05$; C57 vs. *mdx* control.

A

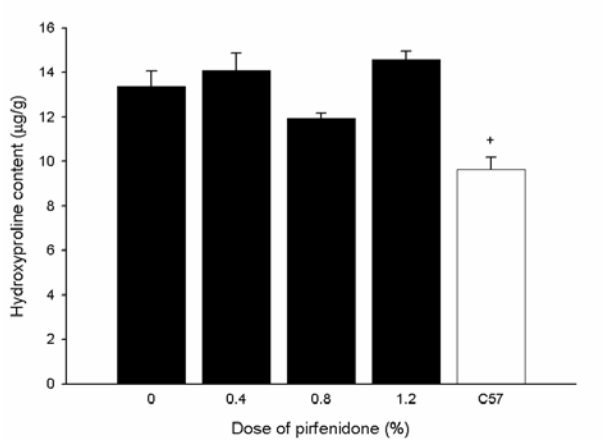

B

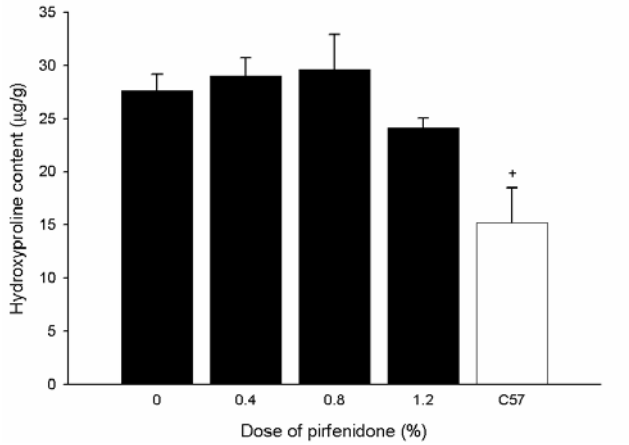

C

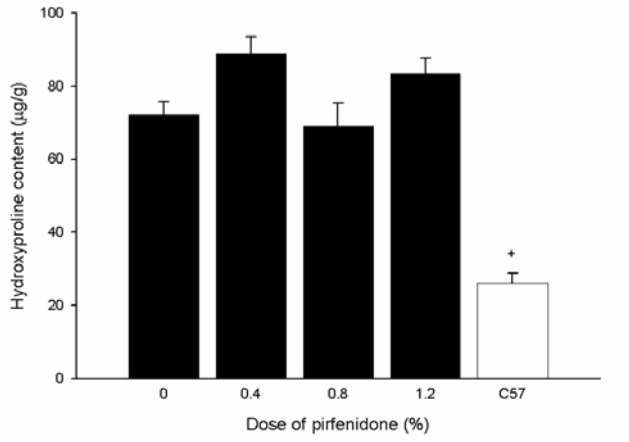

Figure 3.9: Skeletal muscle hydroxyproline content
Hydroxyproline content was elevated in the EDL (A), SOL (B) and diaphragm (C) muscles of untreated *mdx* compared to C57 mice. Pirfenidone treatment did not alter these levels. $^{+}P<0.05$; C57 vs. *mdx* control.

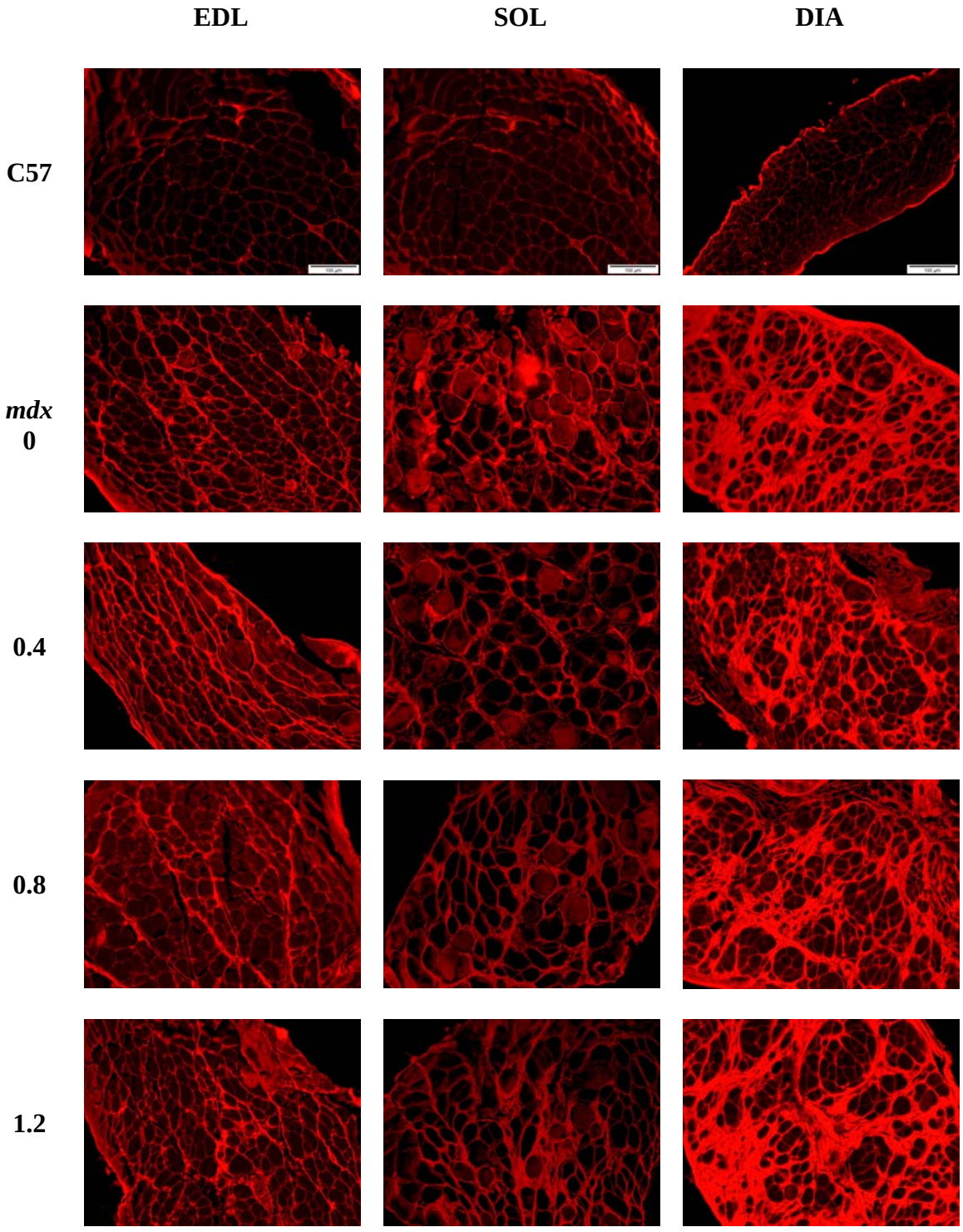

Figure 3.10: Skeletal muscle sections of control and pirfenidone treated mice (PSR)
Skeletal muscle sections of control C57, *mdx* mice and pirfenidone treated *mdx* mice stained with picrosirius red, magnification: X20. Areas stained red indicate presence of collagen. Control *mdx* mice have increased levels of fibrosis compared with C57 mice. Pirfenidone treatment did not decrease this fibrosis

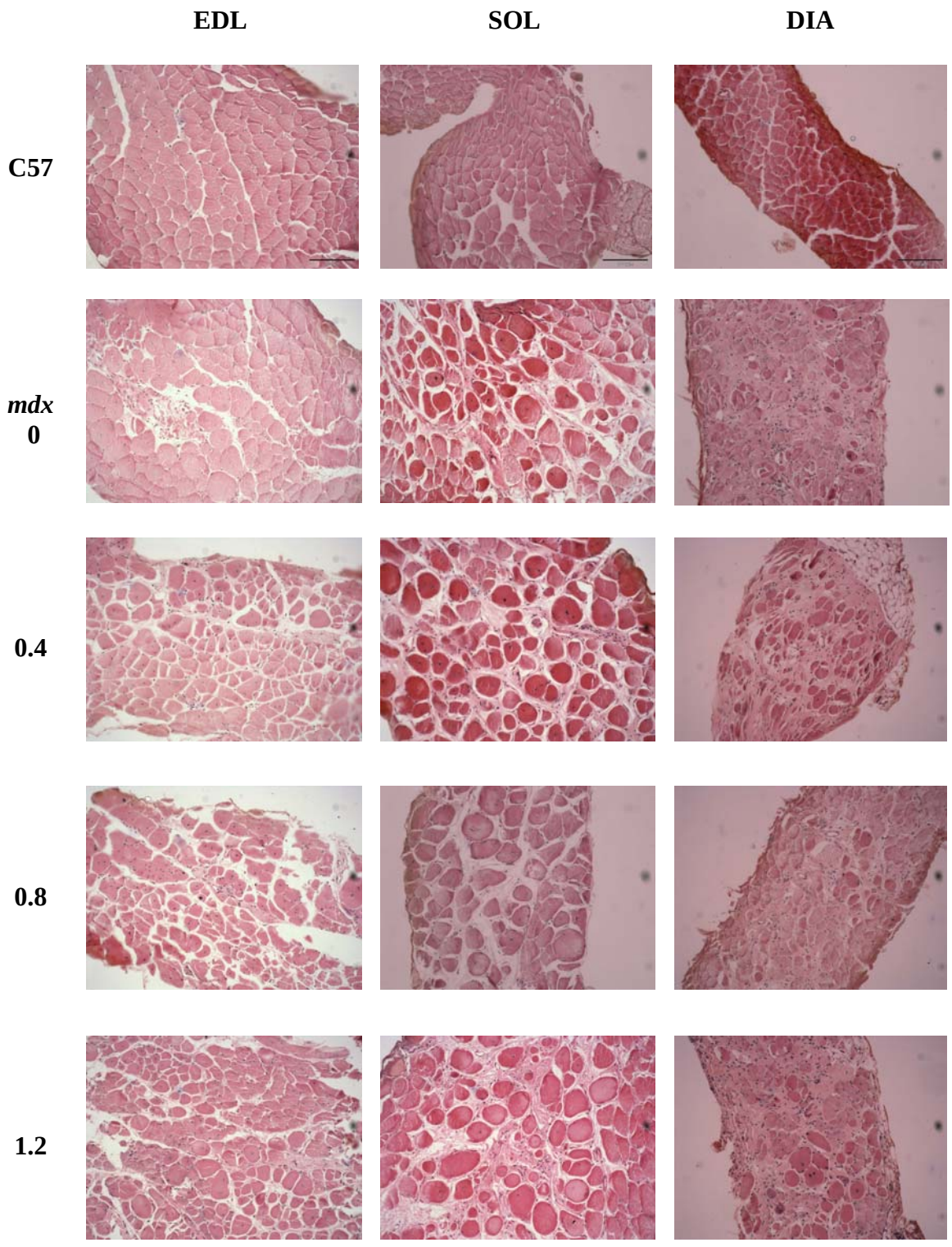

Figure 3.11: Skeletal muscle sections of control and pirfenidone treated mice (H&E) Magnification: X20 C57 mice exhibited significantly less central nucleation when compared to *mdx* mice in all three muscles. *Mdx* myocytes had larger maximum myocyte diameters for all three muscle types.

Mouse	PSR (% area)	Average Cell Diameter (μm)	Percentage Central Nucleation (%)
EDL			
mdx-0	29.79±5.92**	21.73±0.24	62.17±4.08***
mdx-0.4	27.47±2.71**	22.22±0.37	62.63±3.65***
mdx-0.8	20.84±0.87**	21.66±1.57	60.25±10.02***
mdx-1.2	32.62±3.5**	25.20±1.68	66.35±6.57***
C57	12.97±2.99	23.80±1.66	3.79±2.09
SOL			
mdx-0	39.22±3.50**	29.75±0.42	49.53±3.36***
mdx-0.4	36.97±2.11**	27.79±1.75	54.38±3.22***
mdx-0.8	32.17±5.06**	29.63±1.21	59.11±2.68***
mdx-1.2	31.70±3.44**	29.27±1.22	58.12±4.31***
C57	16.89±2.29**	22.43±1.95	1.33±0.50
DIA			
mdx-0	56.98±2.33**	19.68±0.87	34.61±1.73***
mdx-0.4	44.65±1.90**	19.27±0.53	32.43±2.55***
mdx-0.8	52.31±2.44**	19.68±0.80	28.26±3.43***
mdx-1.2	48.72±5.38**	18.11±0.53	29.69±2.13***
C57	13.74±4.17	18.79±1.02	6.10±2.11

Table 3.4: Quantitative histological data of skeletal muscles of control and pirfenidone treated mice
Skeletal muscles from *mdx* mice contained more collagen than C57 mice, pirfenidone treatment did not alter these levels. C57-s skeletal myocytes display a lower percentage central nucleation compared to *mdx*-s mice. Exercise did not affect this percentage in either strain. The *mdx*-ex mice had a greater cell diameter compared with *mdx*-s.
$^{***}P<0.001$ (vs. C57 mice); $^{**}P<0.01$ (vs. C57)

3.4 Discussion

3.4.1 Overview

The aged *mdx* mouse exhibits several cardiomyopathic features similar to those observed in DMD cardiomyopathy. This study shows evidence of reduced ventricular contractility and rate of pressure development and relaxation in the *mdx* heart which corresponds to these cardiac features in boys with DMD where there is clear evidence of reduced systolic and diastolic function (Brockmeier et al. 1998). The *mdx* ventricles also exhibit significantly elevated collagen content evident by picrosirius red staining as reported previously (Quinlan et al. 2004). Using hydroxyproline assays, this increase in collagen has been verified and a lack of difference in cardiac collagen subtypes between *mdx* and C57 was evident. Interestingly, despite the increased cardiac collagen, there is no difference in diastolic stiffness. This was unexpected, although a similar finding was reported in younger *mdx* (Wilding et al. 2005). The lack of increased stiffness in older *mdx* mice suggests low levels of crosslinking or other compensatory changes in the *mdx* to allay the effects of the increased collagen (Badenhorst et al. 2003; Bronzwaer & Paulus 2005).

3.4.2 Cardiac Structure and Function

This is the first study investigating the effect of pirfenidone in *mdx* mice and the first long term study with pirfenidone in experimental animals. The results show that pirfenidone reduced TGF-β mRNA levels associated with a marked improvement in cardiac function without a reduction of ventricular collagen content. Evidence of improved cardiac function included increased ventricular developed pressure, +dP/dt and -dP/dt.

Importantly, these functional parameters improved to values that were not significantly different to values measured in C57 mice.

While treatment with pirfenidone has reproducibly shown antifibrotic effects in a range of acutely induced fibrosis in tissues including lungs, liver, kidneys and heart, no antifibrotic effect was evident in this study. The lack of anti-fibrotic effects in this study was not due to an insufficient dosage as 0.8 and 1.2% both caused a significant reduction in TGF-β expression. Many animal studies investigating the action of pirfenidone have utilised rats or hamsters in their research, however because mice have a higher metabolic rate, allometric scaling was utilized. Therefore, in our study mice received a range of doses from 0.4 to 1.2% in water (equating to approximately 0.4-1.2 g/kg) in contrast to previous studies in rats and hamsters that utilised pirfenidone at a dose of 0.4 to 0.5 % in food (equating to approximately 0.3-0.7 g/kg).

It can be hypothesised that the lack of antifibrotic effect is due to either: 1) impairment of collagen degradation rather than the increased collagen synthesis causing increased fibrosis in *mdx* hearts; or 2) advanced establishment of profibrotic pathways in the *mdx* hearts by 8 months of age which was when pirfenidone treatment commenced.

Recent data obtained from diaphragms of *mdx* mice shows extensive and progressive development of fibrosis from early in life with increased procollagen 1 mRNA evident from 6 weeks of age. However, by 12 weeks of age, no difference in procollagen 1 mRNA was evident between *mdx* and C57 diaphragms, suggesting reduced degradation

rather than increased fibrosis is the basis of increased collagen content (Gosselin et al. 2004). This in turn would reduce the likelihood of antifibrotic benefits of pirfenidone, especially in mice 15 months of age.

The *mdx* mouse undergoes an acute inflammatory response early in life with increased expression of cytokines including TNF-α and TGF-β which may lay the foundation for increased fibrosis early in life. For example, TGF-β expression is elevated at 6 and 9 weeks of age, but not at 12 weeks (Gosselin et al. 2004), suggesting profibrotic pathways are initiated early. Treating mice older than 6 to 9 weeks with pirfenidone, which acts to inhibit TGF-β expression, would thus be unlikely to be effective. Further support for the need to intervene early in the inflammatory process, is that treatment of hamsters with pirfenidone for 3 days before amiodarone-induction of pulmonary fibrosis, prevented subsequent fibrosis when measured at its peak 21 days later. In contrast, delaying pirfenidone treatment until 7 days post-amiodarone treatment did not protect against fibrosis developing. This lack of anti-fibrotic effect occurred despite the capacity of pirfenidone to reduce TGF-β mRNA, although to a lesser extent than the reduction that was measured with pirfenidone administration prior to amiodarone-induction of pulmonary fibrosis (Card et al. 2003).

The current study shows that long term treatment causes a clear improvement in cardiac function, in contrast to previous studies. Acute rat models of cardiovascular diseases (DOCA-salt and STZ-diabetes) did not show improved cardiac contractility after two weeks of pirfenidone treatment at doses that were effective at preventing increased

fibrosis and diastolic stiffness (Miric et al. 2001; Mirkovic et al. 2002). These differences may be due to species differences or duration of treatment.

Recent studies have shown that pirfenidone also modifies numerous other cytokines, including inhibition of TNF-α, interferon-γ and interleukin-6, while enhancing synthesis of the anti-inflammatory cytokine interleukin-10 in mouse and rat models of endotoxic shock (Kaibori et al. 2004; Nakazato et al. 2002). Pirfenidone may also scavenge reactive oxygen species (Giri et al. 1999). The inhibition of interleukin-6 can inhibit the upregulation of iNOS, an enzyme that has been shown to be elevated seven-fold in *mdx* mice at 12 months of age (Bia et al. 1999). Thus, the basis of the improved cardiac function may be prevention of the iNOS upregulation, as it has been well established that high levels of NO produced by iNOS can be detrimental to the heart (Drexler 1999; Paulus et al. 1997). *Mdx* tissues are also known to exhibit high levels of reactive oxygen species which are detrimental (Rando et al. 1998). Pirfenidone's capacity to scavenge reactive oxygen species and lower levels of H_2O_2, OH^- and O_2^- may be the basis of improved cardiac function. As it is increasingly recognised that cardiomyopathy is a complex neurohumoral disorder involving many inflammatory cytokines, it is unlikely that inhibition of a single cytokine will be useful in the treatment of cardiomyopathy (Fonarow 2001). In light of this, pirfenidone's action to inhibit a range of inflammatory cytokines appears to have potential.

3.4.3 Skeletal Muscle Structure and Function

Pirfenidone treatment in skeletal muscle has not been investigated previously. When administered to *mdx* mice, pirfenidone treatment did not result in a functional improvement in any of the three skeletal muscles investigated. The absence of a specific antifibrotic action of pirfenidone may explain the lack of effect on skeletal muscle contractile function. Pirfenidone did not prevent muscle degeneration and regeneration as no changes in central nucleation were observed in mice treated with pirfenidone.

3.4.4 Outcomes of the Study

In conclusion, long term treatment with pirfenidone improves cardiac function in *mdx* mice, but does not prevent fibrosis when treatment is commenced later in the lifespan. Pirfenidone treatment did not affect skeletal muscle structure or function. This finding indicates that TGF-β and the inflammatory processes may have different actions within different muscle types at varying ages of the life of a mouse. It is also possible that Pirfenidone may also act through different predominant mechanisms between the two muscle types investigated, hence allowing improvement in cardiac but not skeletal muscle.

The higher pirfenidone doses (0.8 and 1.2%) decreased TGF-β RNA expression and these same doses demonstrated an increase in cardiac function, indicating that these dosages improved cardiac function associated with the decrease in TGF-β. It appears that the administration of pirfenidone at 0.8% is the most beneficial which indicates that 0.8% is the optimum dose for *mdx* mice to produce the most cardiac improvement. Further

studies should investigate the actions of pirfenidone during the acute inflammatory stage of the disease to determine if earlier administration will inhibit upregulation of inflammatory or profibrotic cytokines to both improve function and prevent fibrosis.

CHAPTER 4 : EFFECT OF L-ARGININE ON *MDX* CARDIAC AND SKELETAL MUSCLE

4.1 Introduction

Duchenne Muscular Dystrophy (DMD), an inherited neuromuscular disorder occurring in approximately 1 in 3500 live male births, is caused by lack of the membrane bound protein, dystrophin. Dystrophin deficiency affects all muscle types causing repeated cycles of myocyte degeneration and consequently leading to increased deposition of collagenous extracellular matrix or fibrosis (Chen et al. 2005; Ionasescu & Ionasescu 1982). Such fibrosis in skeletal muscle impairs contractile activity and contributes to contractures (Morrison et al. 2000) whereas in the heart, in addition to impairing contractility, fibrosis may interfere with impulse conduction and thus cause arrhythmias (Finsterer & Stollberger 2003).

The membrane bound neuronal nitric oxide synthase (nNOS) is normally co-localised with dystrophin. The deficiency of dystrophin thus results in lowered nNOS levels in DMD patients (Brenman et al. 1995) as well as the *mdx* mouse (Bia et al. 1999). The family of nitric oxide synthase (NOS) enzymes utilise l-arginine, a semi-essential amino acid obtained mainly from dietary sources such as fish, chicken and beans, as the substrate to produce nitric oxide (NO). Nitric oxide plays important roles in inflammation, tissue repair and fibrosis, as well as vascular control (Mane et al. 2001; Palmer, Ashton & Moncada 1988). In dystrophin deficient muscles, NOS inhibition increases the severity of dystrophy and hastens muscle degeneration (Anderson & Vargas

2003). It has been proposed that the reduction of nNOS may impede NO-mediated regulation of vasodilation (Crosbie 2001). If muscle fibres express sufficient levels of nNOS, elevated l-arginine concentrations could augment NO synthesis and improve muscle function (Chazalette et al. 2005). This may also improve blood flow to muscle, potentially reducing the muscle necrosis and fibrosis characteristic of DMD.

Mice were treated with l-arginine (5 mg/g) via oral gavage daily for 6 months to assess the cardiac contractility and skeletal muscle function. This study tests the hypothesis that l-arginine supplementation improves cardiac and skeletal muscle function in the dystrophin deficient *mdx* mouse. It is the first study to investigate chronic administration of l-arginine in *mdx* and C57 mice and is the first study to examine the action of l-arginine in both cardiac and skeletal muscle concurrently.

4.2 Materials and Methods

4.2.1 Animals

Male C57BL/10ScSn mice (control strain) (C57) were purchased from the Animal Resource Centre, Nedlands, WA. Male C57BL10ScSn *mdx* (*mdx*) mice were bred at the University of Southern Queensland Animal House, Toowoomba, QLD. Mice were 6 months old at the commencement of experiments. All experimental protocols were conducted with the approval of the University of Southern Queensland Animal Ethics Committee, under the guidelines of the National Health and Medical Research Council of Australia.

4.2.2 Methods

Mdx mice were randomised into two groups, with eight mice per group. One group of *mdx* mice was treated daily for 6 months with l-arginine (*mdx*-larg) in water via oral gavage (5mg/g body weight). This is equivalent to consuming drinking water containing 5% l-arginine. The control *mdx* group (*mdx*-c) and C57 group (C57) received an equivalent volume of water via oral gavage and were used as controls. This treatment regime allowed assessment of the drug-induced benefit relative to both the untreated *mdx* and untreated C57 mice. All animals were given free access to feed. Mice were treated for a total of 6 months.

4.2.3 Langendorff Experiments

12 month old mice were weighed and anaesthetised with pentobarbitone sodium (Nembutal, Boehringer Ingelheim) at 70 mg/kg administered intraperitoneally. A thoracotomy was performed and hearts were rapidly excised into modified Krebs-Henseleit buffer containing (mM): NaCl, 119; $NaHCO_3$, 22; KCl, 4.7; KH_2PO_4, 1.2; $CaCl_2$, 2.5; $MgSO_4$, 1.2; glucose, 11; Na-pyruvate, 1 and EDTA, 0.5 containing 10 mM 2,3-butanedione monoxime (temperature 21°C). The BDM was placed into the dissection buffer to limit detrimental actions of calcium during tissue preparation. The aorta was cannulated via the dorsal root and perfused retrogradely at a pressure of 80 mmHg with Krebs-Henseleit perfusion buffer maintained at 37°C and bubbled with carbogen ($95\%O_2$-$5\%CO_2$) to ensure a pH of 7.4. The Krebs-Henseleit buffer used for perfusion of the hearts did not contain BDM.

A small polyethylene apical drain was used to vent the left ventricle preventing an accumulation of fluid in the heart via Thesbian veins. The left atrium was excised and a fluid filled balloon constructed from polyvinyl chloride plastic film was inserted into the left ventricle via the mitral valve for the measurement of left ventricular function. The left ventricular function was recorded via a MLT844 physiological pressure transducer (ADInstruments, Castle Hill, NSW, Australia) linked to a PowerLab recording system (ADInstruments, Castle Hill, NSW, Australia). Coronary flow was regulated via a ML175 STH Pump Controller (ADInstruments, Castle Hill, NSW, Australia).

Data from hearts with a coronary flow greater than 5 mL/min were excluded from the experimental analysis. Data was recorded using Chart 4.1.1 software (ADInstruments, Castle Hill, NSW, Australia) to calculate end systolic pressure (ESP) and end diastolic pressure (EDP), developed pressure and relaxation over time (±dP/dt) and heart rate. Fluid temperature was measured via a thermometer at the entry of the aortic cannula, and temperatures were maintained at 37.3°C. Hearts were paced at 420 bpm via a silver wire embedded into the left ventricle and grounded using an electrode attached to the cannula. The balloon was inflated to an EDP between 0 and 5 mmHg and the heart was then equilibrated for 10 minutes at this pressure. Following this equilibration period, the EDP was measured for 30 seconds at each of the following increments: 0, 5, 10, 15, 20 and 30 mmHg. Myocardial stiffness was defined by the stiffness constant (κ, dimensionless), that is, the slope of the linear relationship between the tangent elastic modulus (E, dyne/cm^2) and stress (σ, dyne/cm^2) as described in detail (Mirsky & Parmley 1973) (See Appendix 2A). At cessation of the *in vitro* experiments, the right atrium, right ventricle and left ventricle plus septum were separated and weighed. The left ventricle plus septum was bisected transversely with the superior portion stored for histology and the remainder snap frozen in liquid nitrogen and stored at -80°C for subsequent hydroxyproline assays.

4.2.4 Skeletal Muscle Contractility

Immediately after the removal of the heart, the following skeletal muscles were dissected: extensor digitorum longus (EDL) and soleus (SOL) from the left leg and a strip of the diaphragm, these strips were cut consistently from the same region of diaphragm to

minimise experimental error. These muscles were placed in ice-cold Krebs-Henseleit solution containing (mM): NaCl, 118; $NaHCO_3$, 25; KCl, 4.7; KH_2PO_4, 1.18; $CaCl_2.2H_2O$, 2.5; $MgSO_4.7H_2O$, 1.16; glucose, 11; bubbled with carbogen, (95%O_2-5%CO_2). The three muscles were individually tied around their tendon at either end with 5.0 silk suture and with one end attached to a fixed peg and the other end attached to a physiological force transducer (TRI 201, Panlab, Spain). All three skeletal muscles were suspended in water-jacketed tissue baths (25°C) containing Krebs-Henseleit buffer bubbled with carbogen. Two parallel platinum electrodes along the length of the muscles provided field stimulation (0.2 ms pulse duration) from a Grass S48 stimulator (West Warwick, RI) with amplified current intensity (EP500B, Audio Assemblies, Campbellfield, Victoria, Australia). Contractile force was recorded via the force transducer connected to a PowerLab recording system (ADInstruments, Castle Hill, NSW, Australia) and analysed using Chart 4.1.1. Optimal preload (L_o) was defined as the length eliciting maximal single twitch force. Optimum voltage was also determined for each muscle, as was the frequency eliciting maximal tetanic force ranging from 50-180 Hz. The optimum values were used for the remainder of the experiment. Reported data were the average of three individual single-twitch or tetanic stimulations per muscle strip after 25 minutes of equilibration and optimization of conditions. Upon completion of the functional skeletal muscle experiments, muscle lengths (L_o) and widths were recorded, using a digital micrometer. The muscles were blotted for 3 seconds and weighed. The cross-sectional area and normalization of force was calculated as previously described, where tissue CSA equals tissue weight divided by length multiplied by 1.06 (density of mammalian muscle) (Lynch et al. 2001). This calculation for cross-sectional area

accounts for the differences in thickness between different tissues. (Diaphragm thickness in mm: C57 0.66, *mdx* 1.25-1.37; SOL thickness C57 0.77, *mdx* 1.22-1.33; EDL thickness C57 1.5, *mdx* 2.06-2.17). Subsequently, the three skeletal muscles were frozen in liquid nitrogen and stored at -80°C for hydroxyproline assays.

4.2.5 Hydroxyproline Measurements

Hydroxyproline (HP) assays were used as a measure of collagen content. The individual frozen EDL, SOL and diaphragm sections were trimmed of tendons and capsular tissue. All skeletal tissue and a section of the left ventricle were weighed. The tissues were cut into smaller pieces with a scalpel and placed in a sealed tube containing 6 M HCl. The tissues and standards (0, 1, 2, 3, 4, 5, 6 and 7 μM hydroxyproline) were hydrolysed overnight (18 hours) at 107°C. After hydrolysation, the tissues were dried using low heat (50°C) and filtered air under pressure. The dried sample was reconstituted with 500 μL distilled water (dH_2O) and vortexed. A working solution of the buffer stock solution (50 g citric acid.$1H_2O$, 12 mL glacial acetic acid, 120 g sodium acetate.$3H_2O$ and 34 g sodium hydroxide made up to 1 L with dH_2O) was made prior to use by taking 500 mL of the stock and adding 100 mL of dH_2O and 150 mL of n-propanol. 250 μL of Chloramine T reagent (1.41 g chloramine T, 10 mL dH_2O water, 10 mL n-propanol and 80 mL buffer working solution) was added to each sample (ensuring the samples and Chloramine T were at room temperature); the oxidation step was then allowed to progress for 20 minutes at room temperature. 250 μL of Ehrlich's reagent (1.664 g dimethylaminobenzaldehyde and 10 mL of a 2:1 n-propanol/perchloric acid solution) was then added and samples were subsequently incubated at 60°C in a shaking water bath for

20 minutes to allow the chromophore to develop. The tubes were then cooled under tap water before the absorbance was read at 550 nm. Using a standard curve, the μg hydroxyproline content was measured, assuming that 12.5% of collagen is hydroxyproline. Values are expressed as μg HP/mg of wet tissue weight.

4.2.6 Histology

The superior ventricular, EDL, SOL and diaphragm sections were fixed in Telly's fixative (70% ethanol, 37% formaldehyde and glacial acetic acid) for 3 days, Modified Bouin's solution (saturated picric acid, 37% formaldehyde and glacial acetic acid) for 1 day and 70% ethanol before the muscles were embedded in paraffin wax. Sections of 10 μm thickness were cut and placed on Polysine glass slides and stained using the collagen selective stain, 0.1% wt/vol picrosirius red solution (Sirius Red F3B, Chroma Dyes, in saturated picric acid). Slides were left in 0.2% phosphomolybdic acid for 5 minutes, then washed, stained in picrosirius red for 90 minutes and in placed in 1 mM HCl for 2 minutes. The slides were then placed in 70% ethanol for 30 seconds and coverslipped using Depex.

Stained muscle sections were viewed blinded to the strain of mouse using a Nikon Eclipse E600 epifluorescence microscope and 20X magnification. Images were captured with a cooled CCD digital camera (Micropublisher 5.0, QImaging, Canada), with the percentage collagen quantified using AnalySIS software (Soft Imaging System, GmbH, Münster, Germany). To determine the average percentage collagen of each left ventricle and skeletal muscle section, five regions (for left ventricle) and two regions (for skeletal

muscle) were viewed per muscle sample and the final percentage of collagen was calculated from the average of these five or two regions.

To determine cell diameter and central nucleation of the skeletal muscles, 5 μm sections were cut and placed on Polysine glass slides and stained using haematoxylin and eosin. These slides were analysed under brightfield using the same software as described earlier. Again due to the smaller size of these muscles, only 2 regions were viewed per muscle (counting 100 cells per region). The cell diameter and central nucleation was calculated from the average of the cells in these two regions. To prevent experimental errors such as the orientation of the sectioning angle, the minimal 'Feret's diameter' was measured which allows for reliable measure of muscle fibre cross-sectional size and reliably discriminates between dystrophic and normal phenotypes (Briguet et al. 2004).

4.2.7 Statistical Analysis

Data is presented as mean ± SEM. Comparisons were made using the unpaired Student's t-test; $P<0.05$ was considered statistically significant.

4.3 Results

4.3.1 Morphometry

The untreated *mdx* and C57 mice gained weight during the 6 month treatment period (2 g and 1.6 g respectively), whereas treatment with l-arginine caused *mdx* mice to lose weight (1.5 g) throughout the treatment period. The left ventricle of the untreated *mdx* mice weighed more than the left ventricle of the *mdx*-larg mice and C57 mice ($P<0.001$), which reflected the same change in the weight of the whole hearts ($P<0.001$). When this heart weight was normalised to body weight however, the significance was lost.

4.3.2 Cardiac Muscle

Mdx mice had an impaired cardiac function relative to age and sex matched C57 mice. This impairment was evidenced by a reduction of 15% and 25% in left ventricular developed pressure ($P<0.05$: Figure 4.1 (A)), and +dP/dt ($P<0.05$: Fig 4.1 (B)) respectively. In contrast, l-arginine treatment caused a non-significant improvement in cardiac contractility ($P<0.06$) with increased developed pressure in *mdx* mice to a level commensurate with that of C57 mouse hearts. Diastolic stiffness was also decreased by 26% in *mdx*-larg mice compared with *mdx*-c mice ($P<0.04$) (Figure 4.0 (C)). Coronary flow normalised to heart weight revealed a non-significant improvement in *mdx* treated with l-arginine compared with untreated *mdx* and a significant improvement in C57 mice compared with *mdx* treated mice ($P<0.06$ and $P<0.01$ respectively) (Figure 4.2).

A

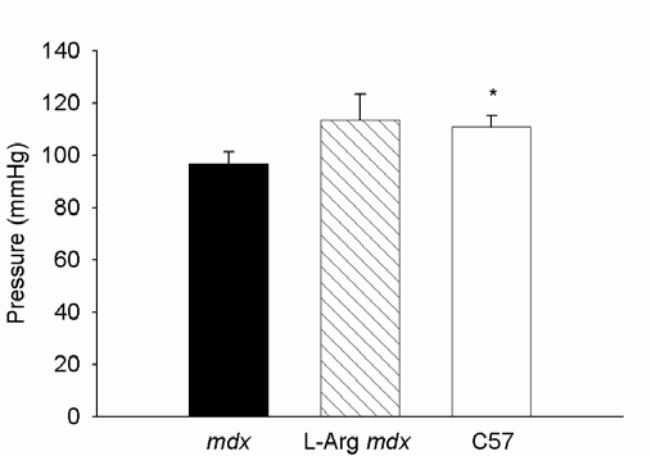

B

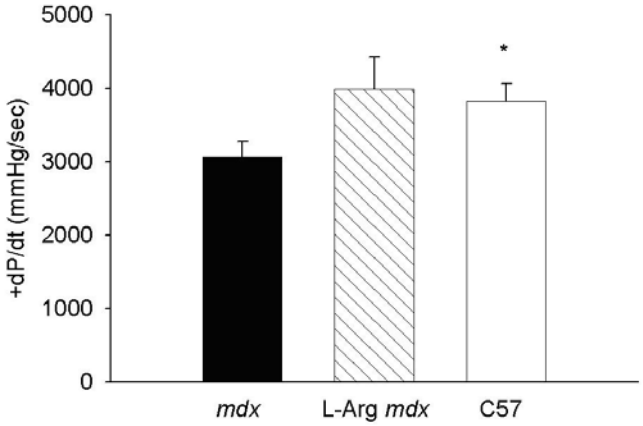

C

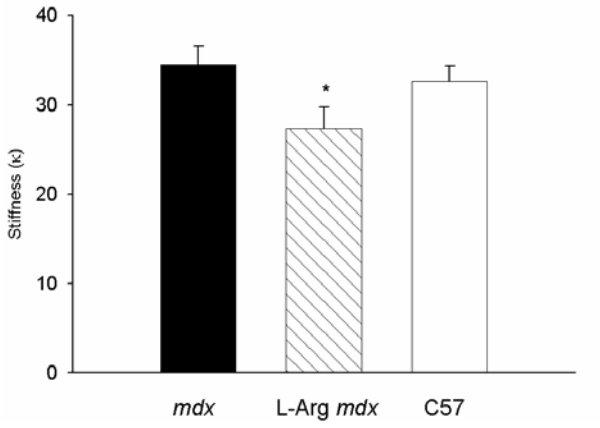

Figure 4.1: Cardiac function of control and l-arginine treated mice
Left ventricular developed pressure (A); Rate of pressure development (+dP/dt) (B) and stiffness (C) from isolated hearts of control *mdx*-c, *mdx*-larg and C57 mice. *Mdx*-c had impaired cardiac function compared to C57 mice. L-arginine improved in cardiac contractility and caused a decrease in stiffness. **P*<0.05 relative to *mdx*.

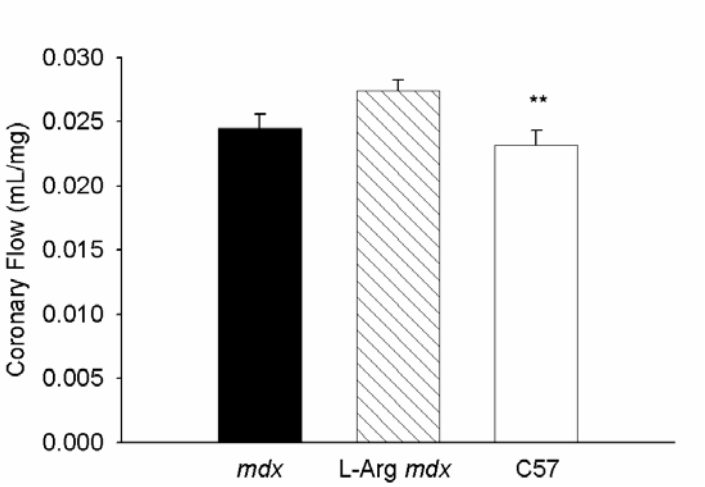

Figure 4.2: Coronary flow of control and l-arginine treated mice
Coronary flow of isolated hearts of *mdx*-c, *mdx*-larg and C57 mice. L-arginine administration improved coronary flow in *mdx* mice. ***P*<0.01; *mdx*-c vs. C57 control.

To determine if changes in contractility and stiffness were due to reduced fibrosis, cardiac collagen content was measured. The C57 mice had a lower hydroxyproline content compared to both *mdx* groups and l-arginine treatment did not change hydroxyproline content in the *mdx* mice (Table 4.1). Picrosirius red-stained left ventricular sections showed that l-arginine treatment caused a reduction in total collagen content compared with the *mdx*-c mice (*P*<0.01) (Figure 4.3). This level was, however, still higher than the level of collagen in the C57 mice, although not significantly (*P*=0.09).

Mouse	Left Ventricular Hydroxyproline Content (µg/g)	Left Ventricular PSR (% Area)
C57-control	1.93±0.22	7.31±2.22
mdx-control	3.62±0.35**	20.18±1.62^{++}
mdx-larg	4.48±0.35**	12.61±1.92

Table 4.1: Left ventricular hydroxyproline and collagen content of control and l-arginine treated mice
Hydroxyproline content was significantly elevated in the muscles from *mdx*-c compared to C57 mice. L-arginine treatment did not affect this difference in hydroxyproline.
**P*<0.001; ****P*<0.001 (vs. C57 mice); $^{++}$P<0.01 (vs. *mdx*-larg)

C57

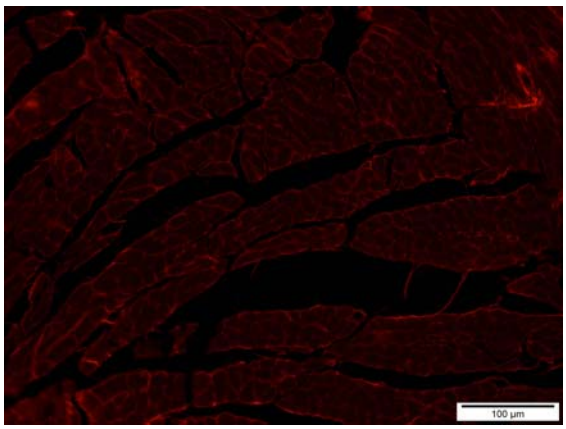

mdx

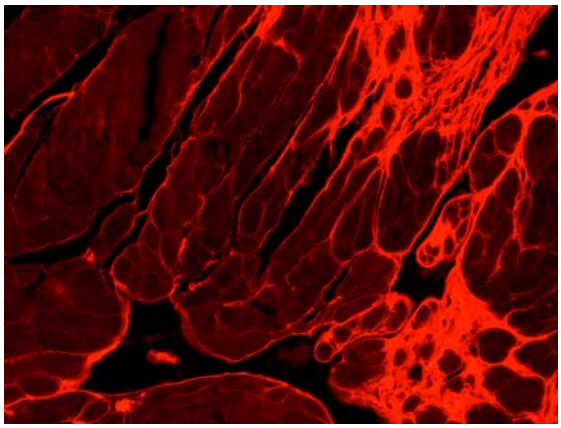

mdx
l-arginine

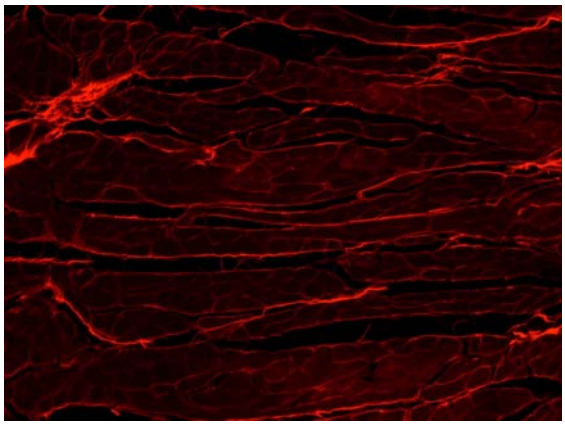

Figure 4.3: Left ventricular sections of control and l-arginine treated mice (PSR)
Left ventricular cardiac sections of treated and untreated *mdx* and C57 mice stained with picrosirius red, magnification: X20. Areas stained red indicate presence of collagen. L-arginine treatment caused a reduction in total collagen content compared with the *mdx*-c mice. Collagen content in cardiac sections of both *mdx* groups were still elevated compared to C57 mice.

4.3.3 Skeletal Muscle

Untreated *mdx* mice had significantly lower twitch force production in EDL and diaphragm muscles when compared to C57 mice (Figure 4.4 (A); $P<0.001$). Similarly, EDL tetanic forces showed similar quantitative changes (Figure 4.5 (A); $P<0.01$), but this difference in tetanic force was not observed in the diaphragm. In comparison, SOL muscles showed no difference in force production between any of the three groups. L-arginine treatment did not increase force production in any of the three skeletal muscles examined.

The twitch:tetanus ratio was higher in the SOL muscles of C57 mice versus *mdx*-c ($P<0.01$), but not in diaphragm or EDL. L-arginine treatment did not change the twitch:tetanus ratio in the *mdx* mice in any of the three muscles after treatment.

4.3.4 Skeletal Muscle Structural Changes

Hydroxyproline content was significantly elevated in the diaphragm and SOL in muscles from untreated *mdx* compared to C57 mice ($P<0.001$ and $P<0.01$ respectively) (Figure 4.6) and l-arginine treatment did not alleviate this difference in hydroxyproline. The EDL muscle showed no differences in hydroxyproline content in any of the mouse groups.

A

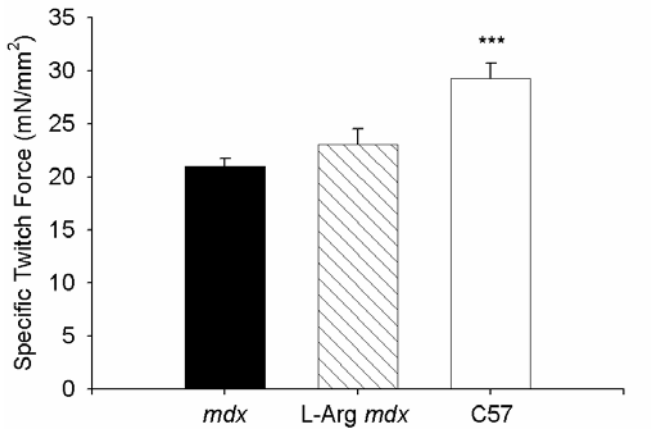

B

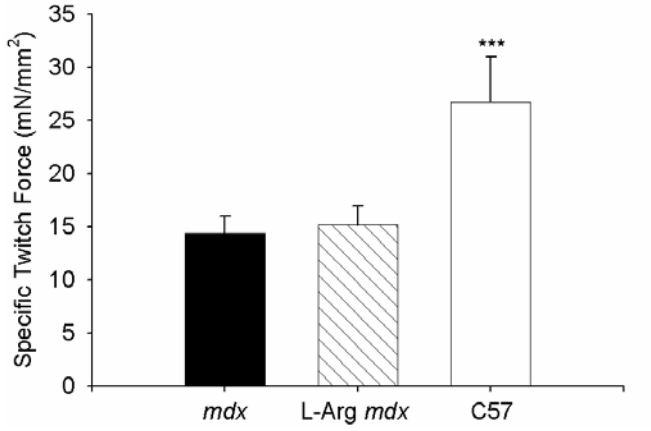

C

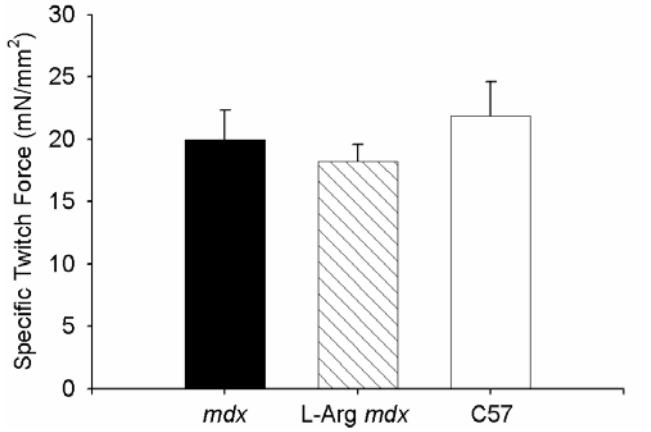

Figure 4.4: Skeletal muscle contractions of control and l-arginine treated mice
Specific twitch contractions of EDL (A), diaphragm (B) and SOL (C). C57 mice had higher force production than *mdx* mice in EDL and diaphragm muscles, but showed no difference in SOL muscles. L-arginine did not affect the contractility in any of the groups. $^{*}P<0.001$; C57 vs. *mdx*-c.

A

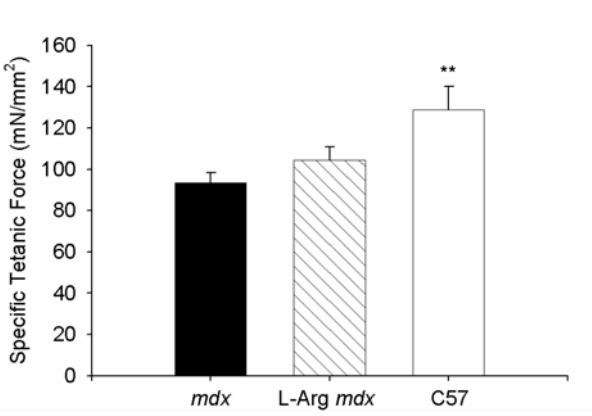

B

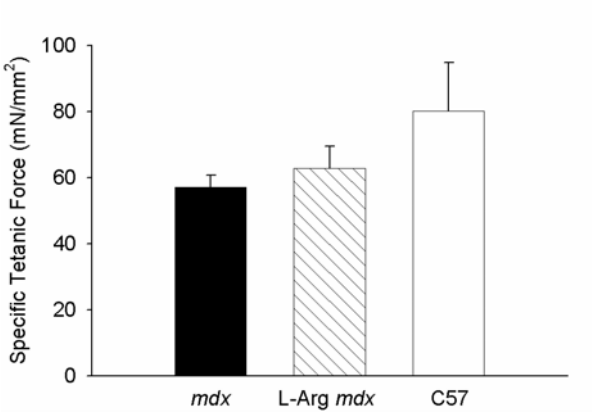

C

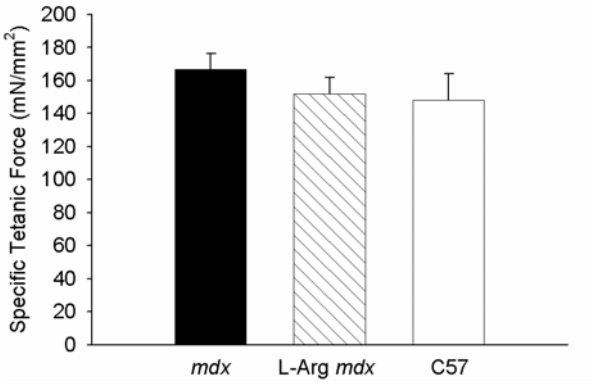

Figure 4.5: Skeletal muscle contractions of control and l-arginine treated mice
Specific tetanus contractions of EDL (A), diaphragm (B) and SOL (C). C57 mice had a higher force production in the EDL muscles only, with no difference in diaphragm or SOL compared with untreated *mdx*. L-arginine did not affect contractility in any of the three muscles. $^{*}P<0.01$; C57 vs. *mdx*-c.

A

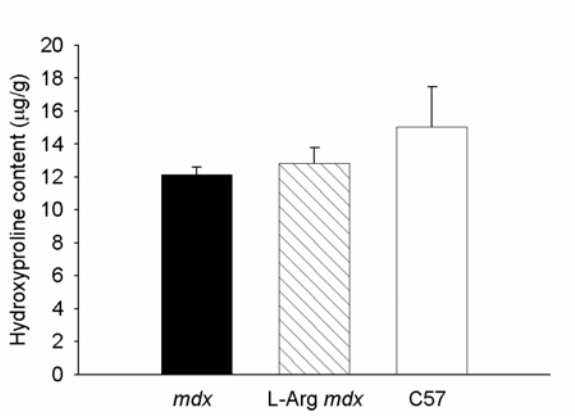

B

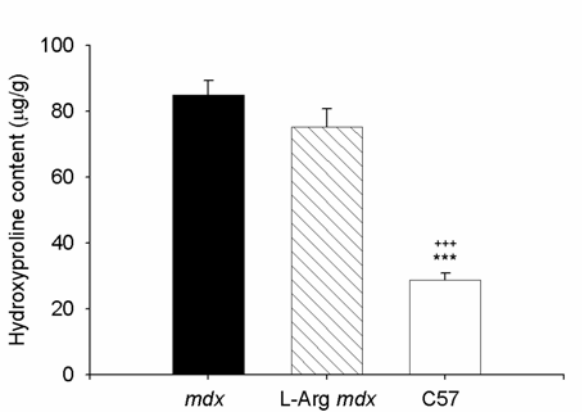

C

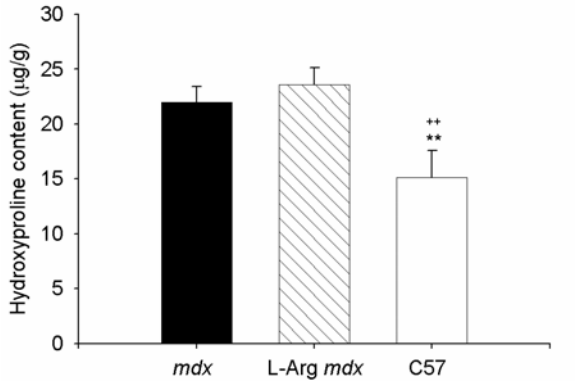

Figure 4.6: Hydroxyproline content of control and l-arginine treated mice
Hydroxyproline content was significantly elevated in the diaphragm (B) and SOL (C) muscles from *mdx*-c compared to C57 mice and l-arginine treatment did not affect this difference in hydroxyproline. The EDL (A) muscles showed no differences in hydroxyproline content in any of the mouse groups.
$^{**}P<0.01$; $^{***}P<0.001$; C57 vs. *mdx*-c; $^{++}P<0.01$; $^{+++}P<0.001$; C57 vs. *mdx*-larg.

Evaluation of picrosirius red-stained muscle sections revealed increased collagen content in all three *mdx* skeletal muscles compared to the C57 mice. L-arginine treatment did not decrease these levels of skeletal muscle collagen ($P<0.01$) (Figure 4.7; Table 4.2).

C57 mice exhibited significantly less central nucleation when compared to *mdx* dystrophic mice ($P<0.0001$) with no differences in myocyte diameters between *mdx* and C57 mice for all three muscles (Figure 4.8). L-arginine treatment did not affect any of these parameters.

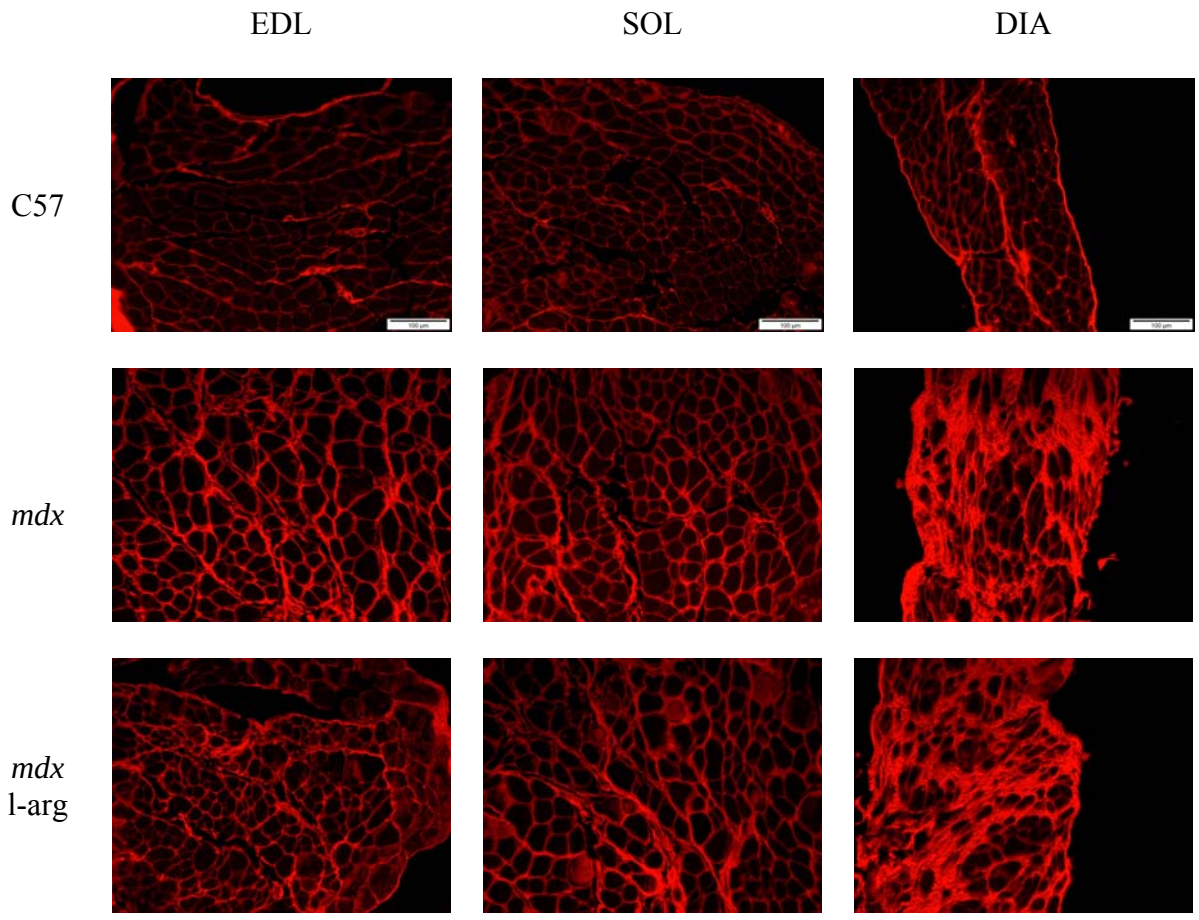

Figure 4.7: Skeletal muscle sections of control and l-arginine treated mice (PSR)
Skeletal muscle sections of treated and untreated *mdx* and untreated C57 mice stained with picrosirius red, magnification: X20. Areas stained red indicate presence of collagen Increased collagen content is evident in all three *mdx* skeletal muscles compared to the C57 mice. L-arginine treatment did not affect these levels of skeletal muscle collagen

Mouse	PSR EDL	PSR SOL	PSR DIA
C57-control	9.26±3.29	15.25±2.14	30.76±7.8
***mdx*-control**	25.17±1.07**	26.71±2.78**	68.48±2.63**
***mdx*-larg**	24.32±2.23**	25.24±3.63**	61.10±6.66**

Table 4.2: Total percentage area of collagen in *mdx* and C57 mice
Total collagen is increased in *mdx* mice compared to C57 mice, l-arginine treatment did not affect these levels. ** $P<0.01$ (vs. C57 mice)

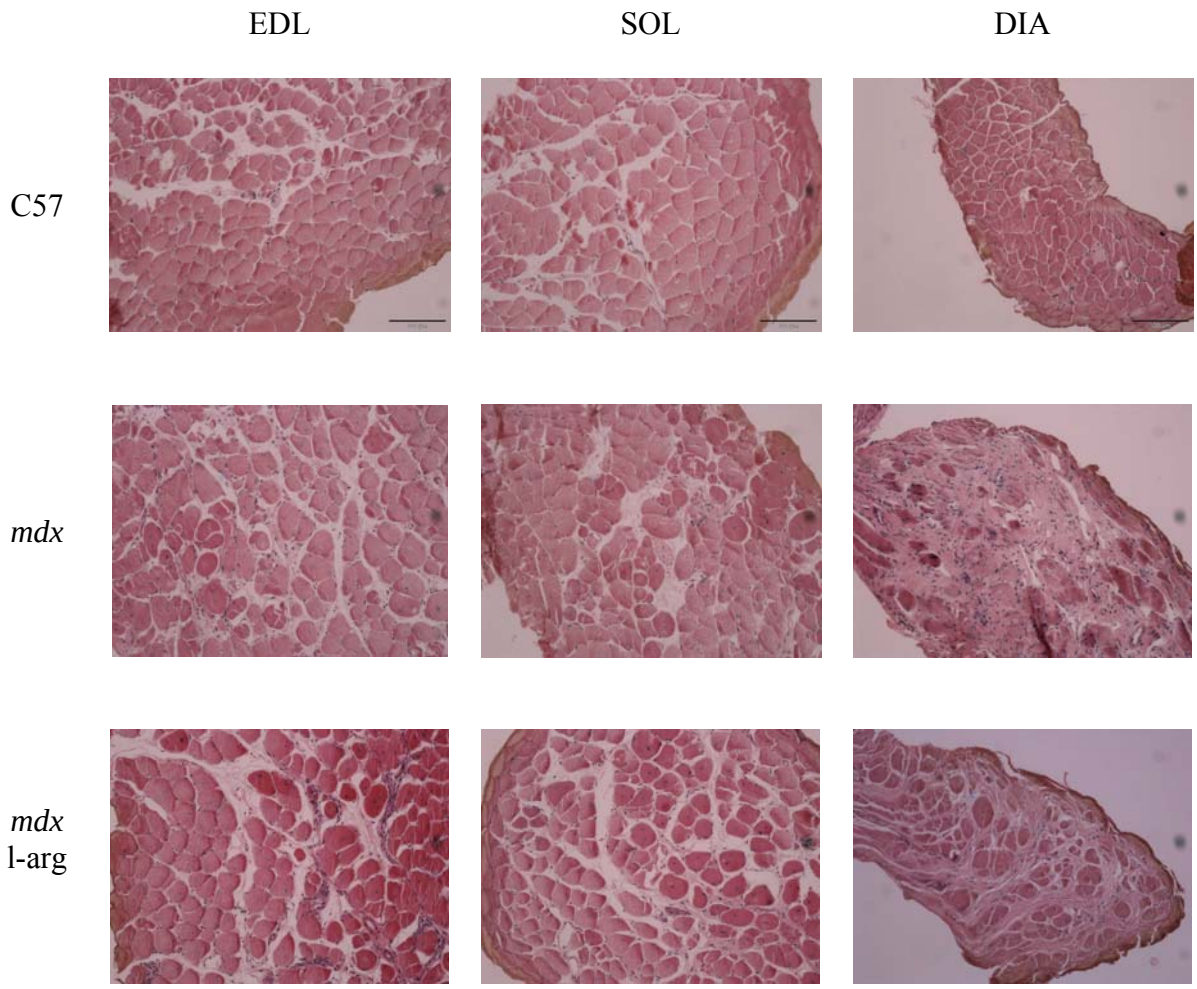

Figure 4.8: Skeletal muscle sections of control and l-arginine treated mice (H&E)
Skeletal muscle sections of treated and untreated *mdx* and untreated C57 mice stained with haematoxylin and eosin, magnification: X20. C57 mice exhibited significantly less central nucleation when compared to *mdx* dystrophic mice. L-arginine treatment did not affect this parameter.

4.4 Discussion

L-arginine has been reported to improve cardiac structure and function in various models of cardiac dysfunction, including the DOCA-salt hypertensive rat, the ageing spontaneously hypertensive rat and diabetic (db/db) mice (Fenning et al. 2005; Khaidar et al. 1994; Susic, Varagic & Frohlich 2001). The deficiency of nNOS and consequential lowered production of NO indicated that the substrate of NOS, l-arginine, may be beneficial in dystrophic cardiac muscle.

4.4.1 Cardiac Structure and Function

L-arginine supplementation causes an elevation of NO as reported in previous studies (Susic, Francischetti & Frohlich 1999), resulting in coronary vasodilation and increased coronary flow. Likewise, this study showed that l-arginine treatment of the *mdx* mice improved coronary flow by 12%. This may be of particular benefit in dystrophic tissues where the deficiency of nNOS modulates vascular tone (Sander et al. 2000). Therefore, it has been suggested that increased NO production by myocytes may diffuse to nearby arterioles to facilitate vasodilation (Thomas et al. 1998).

L-arginine caused a significant improvement in cardiac contractility in *mdx* isolated hearts. Nitric oxide is an important regulator of intracellular calcium handling, through alteration of L-type calcium channel inactivation, sarcoplasmic reticular (SR) calcium load and force frequency responses (Ashley et al. 2002; Khan et al. 2003; Sears et al. 2003). Mice deficient in nNOS have a depressed force frequency response, both *in vivo* and in isolated myocytes, accompanied by a decrease in calcium release (Khan et al.

2003). In the heart, NO inhibits L-type calcium channels (Abi-Gerges, Fischmeister & Mery 2001) but stimulates SR calcium release (Xu et al. 1998). The elevation of NO caused by l-arginine supplementation may have caused stimulation of SR calcium release via ryanodine receptors to facilitate the improved contractility (Xu et al. 1998). nNOS influences the frequency-mediated rise in cardiac contractility and calcium cycling in a manner different to other NOS isoforms. Spatial confinement of different NOS isoforms allows NO signals to have independent effects on cardiac function (Barouch et al. 2002).

The l-arginine/NO system plays an integral role in the pathogenesis of diastolic dysfunction (Fenning et al. 2005). Diastolic stiffness was found to be decreased in *mdx* mice treated with l-arginine with this decrease likely due to the antifibrotic effect of l-arginine. It has been shown that compounds that release nitric oxide, such as bradykinin, decrease cardiac fibroblast function to decrease collagen expression. This is likely to occur by increasing intracellular cGMP concentrations (Kim et al. 1999). Therefore, nitric oxide may inhibit local collagen production in the heart and blood vessels.

Although the hydroxyproline content of the l-arginine treated mice was unchanged in this study, when analysing the picrosirius red slides, the l-arginine treated mice had decreased collagen content compared to the untreated *mdx* mice. The hydroxyproline assays appear to be a less accurate measurement compared to the more visual histological method.

In the hydroxyproline assays, a small section of part of the muscle is used in the experiment. If the section that is cut is in a small area which has not got increased levels

of collagen, there will be no increase in hydroxyproline levels. In the histological analysis, a 10 micron section of the whole muscle is viewed, thereby allowing the muscle to be examined fully, rather than just a small section of the muscle like that used in the hydroxyproline assays. This could also account for differences in hydroxyproline levels in the same muscle types between groups of mice especially throughout the projects/studies undertaken in this thesis.

The picrosirius red-stained left ventricular sections revealed a decrease in fibrosis as a result of l-arginine treatment, indicating that l-arginine ameliorated this pathological feature in the *mdx* heart. Nitric oxide produced by l-arginine decreases inflammation and muscle damage (Nguyen & Tidball 2003; Wehling, Spencer & Tidball 2001). Although fibrosis was not prevented in skeletal muscle, cardiac muscle showed reduced interstitial collagen. This may be due to the prevention of inflammation by l-arginine.

4.4.2 Skeletal Muscle Structure and Function

L-arginine administration has been shown to be beneficial in skeletal muscle function of *mdx* mice. Studies have indicated improvement in myocytes after l-arginine treatment due to increases in utrophin expression (Chaubourt et al. 1999; Segalat et al. 2005; Voisin et al. 2005). Utrophin is a structural protein which may be capable of performing the same cellular functions as dystrophin (Blake et al. 2002; Tinsley, J. et al. 1998). Although many studies have found utrophin upregulation minimises the skeletal dystrophic condition, it is thought that the levels may not be sufficient for full correction

and are not predicted to protect completely against contractile damage (Barton et al. 2005; Chazalette et al. 2005).

Studies have reported improvements in the eccentric contractile function of the EDL and isometric contractions of the diaphragm in *mdx* mice treated with l-arginine (Barton et al. 2005; Voisin et al. 2005). L-arginine, however, showed no functional improvement in the three skeletal muscles used in this study. In an acute study using young mice by Barton *et al*. (2005) a similar result was evident, with EDL isometric twitch and maximum tetanic contractile forces not resulting in a functional improvement after l-arginine treatment. Contractile differences may have been evident in the current study if eccentric contractions were measured. A higher level of regeneration in the three skeletal muscles may have lead to a greater resistance to necrosis, affecting the rate of further fibrosis and leading to no differences in force production as a result of l-arginine administration.

In the recent study by Barton *et al*. (2005), SERCA levels and the twitch:tetanus ratios were also measured and both indicated no difference as a result of l-arginine treatment. In the current study, l-arginine did not change the twitch:tetanus ratio, but there was a strain difference between the ratio in the soleus and diaphragm contractions in accordance to the data presented by Barton *et al*. (2005), concluding that the ryanodine receptor is affected in the *mdx* mice and l-arginine treatment did not change this.

L-arginine has been shown to activate satellite cells in cultures (Anderson & Pilipowicz 2002; Chaubourt et al. 1999) and *in vivo* (Anderson & Pilipowicz 2002; Anderson & Vargas 2003; Chaubourt et al. 2002). A NOS inhibitor, L-NAME (NG-nitro-l-arginine-methyl-ester), inhibits satellite cells (Anderson 2000), thereby demonstrating that l-arginine activates satellite cells through a NO pathway. In the current study, however, central nucleation was not altered after l-arginine administration. The lack of functional improvement as a result of l-arginine administration may indicate that this amino acid did not cause satellite cell activation. L-arginine can influence satellite cell activation in a dose dependent manner, however at high concentrations its effects are diminished, with *in vitro* concentrations above 1 mM satellite cells are no longer activated (Anderson & Pilipowicz 2002). It may be that the 5% dose utilised for 6 months deactivated or failed to activate satellite cells, resulting in a lack of improvement in contractility. In *mdx* mice treated with l-arginine for 6 weeks, fibres with central nucleation were also unchanged, indicating that reduction of necrosis was not normalised by regeneration of myofibres (Voisin et al. 2005).

Less myonecrosis was observed in the gastrocnemius and diaphragm muscles of *mdx* mice after short term l-arginine treatment as indicated by a decreased Evan's blue uptake (Barton et al. 2005; Voisin et al. 2005). Although l-arginine has been shown to prevent fibrosis in skeletal muscles previously (Voisin et al. 2005), the current study indicates that chronic l-arginine treatment had no antifibrotic action in those skeletal muscles examined. The lack of antifibrotic action of l-arginine is likely to be the basis for lack of improvement of skeletal muscle function.

It has been suggested that age is an explanation for the differences observed in skeletal muscle function in l-arginine treated mice. It remains an open question as to the effect of age on the NO-satellite cell pathway (Barton et al. 2005). It is possible that through inhibition of satellite cell activation, l-arginine administration could explain the effect of the body weight loss in the l-arginine treated *mdx* mice.

Molsidomine is a drug used in the treatment of coronary disease. It is metabolised in the liver and the resulting metabolite is the NO donor, 3-morpholinosydnonimine (SIN-1). This drug, when given to mice, results in utrophin upregulation and a decrease in necrosis in the diaphragm, soleus and gastrocnemius muscles, similar to the outcomes observed in *mdx* mice treated with l-arginine (Voisin et al. 2005). It may be of interest to see if the improvement in cardiac structure and function seen in the current study as a result of l-arginine could be mimicked in future studies using molsidomine.

In conclusion, the results indicate that a 5% dose of l-arginine improved coronary flow, reduced cardiac fibrosis and improved cardiac contractility, whilst reducing diastolic stiffness without altering skeletal muscle structure and function. L-arginine treatment caused a reduction in body weight of the *mdx* mice. Future experiments should involve l-arginine administration at lower doses in younger *mdx* mice to examine the potential of this NOS substrate to ameliorate cardiac and skeletal muscle dysfunction in DMD.

CHAPTER 5 : EFFECT OF CO-ADMINISTRATION OF L-ARGININE AND PREDNISONE IN *MDX* MICE

5.1 Introduction

Duchenne Muscular Dystrophy (DMD), an inherited neuromuscular disorder occurring in approximately 1 in 3500 live male births, is caused by lack of the membrane bound protein, dystrophin. Initially DMD was considered a skeletal myopathy manifesting as impaired mobility and respiratory dysfunction, however, improved care has prolonged life expectancy significantly. This longer lifespan has in turn increased the presentation of cardiac manifestations and heightened awareness of cardiomyopathy as a contributor to mortality (Eagle et al. 2002). Studies have shown that 90% of DMD patients have impaired cardiac function, with death due to cardiomyopathy occurring in 20% of cases (Boland et al. 1996; Farah, Evans & Vignos 1980; Finsterer & Stollberger 2003; Hoogerwaard et al. 1999). While the pathogenesis of cardiomyopathy arising from dystrophin deficiency has not been fully elucidated, the pathology has been well described. Of note is the development of cardiac fibrosis located particularly in the left ventricle, which may be a contributor to altered contractility as well as conduction and rhythm disturbances (Perloff & Marelli 1992; Perloff et al. 1967).

The only pharmacological treatment shown to be effective in improving the symptoms and prognosis of DMD are the corticosteroids such as prednisone and deflazacort. These have been shown to maintain muscle strength and function and slow disease progression (Drachman, Toyka & Myer 1974; Wong & Christopher 2002). More recently,

deflazacort has been demonstrated to be cardioprotective in DMD patients although the mechanism for this has not yet been reported (Silversides et al. 2003).

The membrane bound neuronal Nitric Oxide Synthase (nNOS) is normally co-localised with dystrophin, thus the deficiency of dystrophin results in lowered levels of nNOS in DMD patients (Brenman et al. 1995) and *mdx* mouse (Bia et al. 1999). The family of nitric oxide synthase (NOS) enzymes utilise L-arginine, a semi-essential amino acid obtained mainly from dietary sources such as fish, chicken and beans, as the substrate to produce nitric oxide (NO). Nitric oxide plays important roles in inflammation, tissue repair and fibrosis as well as vascular function (Mane et al. 2001; Palmer, Ashton & Moncada 1988). In dystrophin deficient muscles NOS inhibition increases the severity of dystrophy and hastens muscle degeneration (Anderson & Vargas 2003). It has been proposed that the reduction of nNOS may impede NO mediated regulation of vasodilation (Crosbie 2001). If muscle fibres express sufficient levels of nNOS, elevated l-arginine concentrations could augment NO synthesis and improve sarcolemmal integrity (Chazalette et al. 2005). This may improve blood flow to muscle, potentially reducing muscle necrosis and subsequent fibrosis in DMD.

The combination of l-arginine and deflazacort has been shown to improve tissue integrity in *mdx* skeletal muscle cells, resulting in expression of NOS in dystrophin deficient satellite cells (Anderson & Vargas 2003). This study found NOS manipulation affected the extent of skeletal muscle inflammation and regeneration in deflazacort-treated *mdx*

and co-administration of l-arginine significantly augmented the benefits of deflazacort treatment in the *mdx* diaphragm.

This current study tested the hypothesis that co-administration of l-arginine and prednisone could elicit a similar protective effect on cardiac muscle structure and function in *mdx* mice. The corticosteroid prednisone was chosen as it is more widely available for clinical use than deflazacort and has similar structure and function.

This study tested the hypothesis that the co-administration of l-arginine and prednisone would improve cardiac function and reduce cardiac fibrosis in the dystrophin deficient *mdx* mouse.

5.2 Materials and Methods

5.2.1 Animals

Male C57BL/10ScSn mice (control strain) (C57) were purchased from the Animal Resource Centre, Nedlands, WA. Male C57BL10ScSn-*mdx* (*mdx*) mice were bred at the University of Southern Queensland Animal House, Toowoomba, QLD. Mice were 7 months old at the commencement of experiments. All experimental protocols were conducted with the approval of the University of Southern Queensland Animal Ethics Committee, under the guidelines of the National Health and Medical Research Council of Australia.

5.2.2 Methods

Mice were randomised into eight groups, with 10 mice per group as described below: C57-sham and *mdx*-sham received daily subcutaneous (s.c.) injections of vehicle only (sesame oil); C57-l-arg and *mdx*-l-arg consumed drinking water containing 10% l-arginine and received daily s.c. injections of vehicle; C57-pred and *mdx*-pred were administered prednisone (1.5 mg/kg/day s.c., 5 days per week); and C57-pred/l-arg and *mdx*-pred/l-arg consumed drinking water containing 10% l-arginine and administered prednisone (1.5 mg/kg/day s.c., 5 days per week). All animals were given free access to feed and untreated water, with the exception of the groups receiving l-arginine medicated water. All mice were treated for a total of 7 months.

5.2.3 Langendorff Experiments

Mice at 14 months of age were anaesthetised with 50 mg/kg sodium pentobarbitone administered intraperitoneally. A thoracotomy was performed and hearts were rapidly excised into modified Krebs-Henseleit buffer containing (mM): NaCl, 119; $NaHCO_3$, 22; KCl, 4.7; KH_2PO_4, 1.2; $CaCl_2$, 2.5; $MgSO_4$, 1.2; glucose, 11; Na-pyruvate, 1 and EDTA, 0.5 containing 10 mM 2,3-butanedione monoxime (temperature 21°C). The BDM was placed into the dissection buffer to limit detrimental actions of calcium during tissue preparation. The aorta was cannulated via the dorsal root and perfused retrogradely at a pressure of 80 mmHg with Krebs-Henseleit perfusion buffer maintained at 37°C and bubbled with carbogen (95%O_2-5%CO_2) to ensure a pH of 7.4. The Krebs-Henseleit buffer used for perfusion of the hearts did not contain BDM. The perfusion fluid was filtered via an in-line Sterivex-HV filter cartridge (0.45 μm, Millipore, Bedford, MA, USA).

A small polyethylene apical drain was used to vent the left ventricle preventing an accumulation of fluid in the heart via Thesbian veins. The left atrium was excised and a fluid filled balloon constructed from polyvinyl chloride plastic film was inserted into the left ventricle via the mitral valve for the measurement of left ventricular function. Left ventricular function was recorded via a physiological pressure transducer (UFI, Model 1050BP, Morro Bay, CA, USA) linked to a PowerLab recording system (ADInstruments, Castle Hill, NSW, Australia). Coronary flow was monitored via a Doppler flow probe located in the aortic perfusion line and connected to a TS410 flow meter (Transonics, Ithaca, New York, USA).

Data from hearts with a coronary flow greater than 5 mL/min were excluded from the experimental analysis. Data was recorded using Chart 5 software (ADInstruments, Castle Hill, NSW, Australia) to calculate end systolic pressure (ESP) and end diastolic pressure (EDP), developed pressure and relaxation over time (±dP/dt) and heart rate. Fluid temperature was measured via a thermometer at the entry of the aortic cannula, and temperatures were maintained at 37.3°C. Hearts were paced at 420 bpm via a Grass S48 stimulator (West Warwick, RI, USA) and a silver wire embedded into the left ventricle and grounded using an electrode attached to the cannula. The balloon was inflated to an EDP between 0 and 5 mmHg and the heart was then equilibrated for 10 minutes at this pressure. Following this equilibration period, the EDP was measured for 30 seconds at each of the following increments: 0, 5, 10, 15, 20 and 30mmHg. Myocardial stiffness was defined by the stiffness constant (κ, dimensionless), that is, the slope of the linear relationship between the tangent elastic modulus (E, dyne/cm^2) and stress (σ, dyne/cm^2) as described in detail (Mirsky & Parmley 1973) (See Appendix A2.0).

At cessation of the *in vitro* experiments, the right atrium, right ventricle and left ventricle plus septum were separated and weighed. The left ventricle plus septum was bisected transversely with the superior portion stored for histology and the remainder snap frozen in liquid nitrogen and stored at -80°C for subsequent hydroxyproline assays.

5.2.4 Hydroxyproline Measurements

Hydroxyproline (HP) assays were used as a measure of collagen content. The section of the left ventricle was weighed and cut into smaller pieces with a scalpel and placed in a

sealed tube containing 6 M HCl. The tissues and standards (0, 1, 2, 3, 4, 5, 6 and 7 μM hydroxyproline) were hydrolysed overnight (18 hours) at 107°C. After hydrolysation, the tissues were dried using low heat (50°C) and filtered air under pressure. The dried sample was reconstituted with 500 μL distilled water (dH_2O) and vortexed. A working solution of the buffer stock solution (50 g citric acid.$1H_2O$, 12 mL glacial acetic acid, 120 g sodium acetate.$3H_2O$ and 34 g sodium hydroxide made up to 1 L with dH_2O) was made prior to use by taking 500 mL of the stock and adding 100 mL dH_2O and 150 mL of n-propanol. 250 μL of Chloramine T reagent (1.41 g chloramine T, 10 mL dH_2O, 10 mL n-propanol and 80 mL buffer working solution) was added to each sample (ensuring the samples and Chloramine T were at room temperature); the oxidation step was then allowed to progress for 20 minutes at room temperature. 250 μL of Ehrlich's reagent (1.664 g dimethylaminobenzaldehyde and 10 mL of a 2:1 n-propanol/perchloric acid solution) was then added, and samples were subsequently incubated at 60°C in a shaking water bath for 20 minutes to allow the chromophore to develop. The tubes were then cooled under tap water before the absorbance was read at 550 nm. Using a standard curve, the μg hydroxyproline content was measured, assuming that 12.5% of collagen is hydroxyproline. Values are expressed as μg HP/mg of wet tissue weight.

5.2.5 Histology

The superior ventricular section was fixed in Telly's fixative (70% ethanol, 37% formaldehyde and glacial acetic acid) for 3 days, modified Bouin's solution (saturated picric acid, 37% formaldehyde and glacial acetic acid) for 1 day and 70% ethanol before embedding in paraffin wax. Sections of 10 μm thickness were cut and placed on Polysine

glass slides and stained using the collagen selective stain, 0.1% wt/vol picrosirius red solution (Sirius Red F3B, Chroma Dyes, in saturated picric acid). Slides were left in 0.2% phosphomolybdic acid for 5 minutes, then washed, stained in picrosirius red for 90 minutes and in placed in 1 mM HCl for 2 minutes, the slides were then placed in 70% ethanol for 30 seconds and coverslipped using Depex.

Stained left ventricular sections were viewed blinded to the strain of mouse using a Nikon Eclipse E600 epifluorescence microscope and 20X magnification. Images were captured with a cooled CCD digital camera (Micropublisher 5.0, QImaging, Canada), with the percentage collagen quantified using AnalySIS software (Soft Imaging System, GmbH, Münster, Germany). To determine the average percentage collagen of each left ventricle section, five regions were viewed per left ventricle and the final percentage of collagen was calculated from the average of these five regions.

Picrosirius red-stained sections were also viewed under polarised light to determine the ratio of type I and type III collagen with colour separation achieved using AnalySIS. Again 5 left ventricular regions per sample were viewed; and averaged.

5.2.6 Statistical Analysis

Data is presented as Mean ± SEM. Comparisons were made using the unpaired Student's *t*-test, with $P<0.05$ considered statistically significant.

5.3 Results

5.3.1 Morphometry

At 14 months of age the *mdx*-sham mice weighed significantly less than their age matched C57-sham ($P<0.001$), and this difference was maintained across all 3 treatment groups when comparing *mdx* and C57 mice (Figure 5.1). Prednisone treatment did not alter the body weights of *mdx* and C57, whereas l-arginine induced weight loss with pred/l-arg mice having similar final weights to the l-arginine treated mice (22% weight loss in *mdx* and 10% weight loss in C57; $P<0.05$) (Figure 5.1).

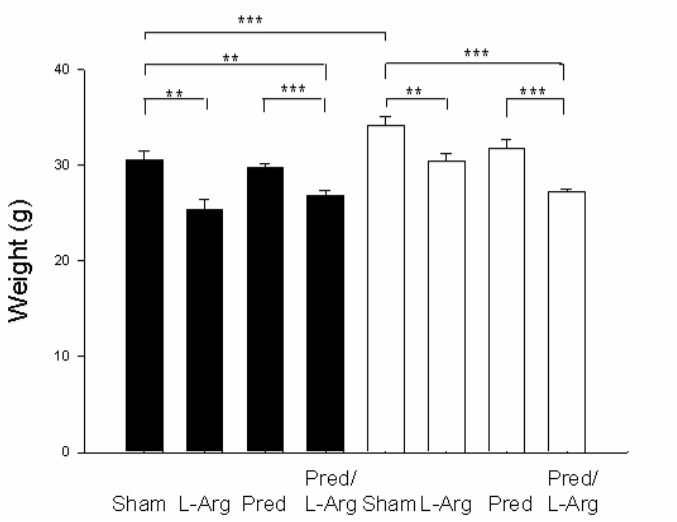

Figure 5.1: Final body weight of treated and untreated *mdx* and C57 mice
Mdx-sham mice weighed significantly less than their age matched C57-sham, this difference was maintained across all 3 treatment groups. Prednisone treatment did not alter the body weights of *mdx* and C57, whereas l-arginine treatment alone caused a significant loss of body weight in both strains that was not prevented by co-administration of prednisone. $^{**}P<0.05$, $^{***}P<0.001$ (■=*mdx*; □=C57)

Parallel trends between heart weights and body weights were observed. (P<0.001). The hearts of *mdx* treated with l-arginine (*mdx*-l-arg and *mdx*-pred/l-arg) weighed significantly less than the *mdx*-sham and *mdx*-pred (Figure 5.2). Similar differences were evident between C57 groups, reflecting effects of treatment rather then an effect of strain (Figure 5.2).

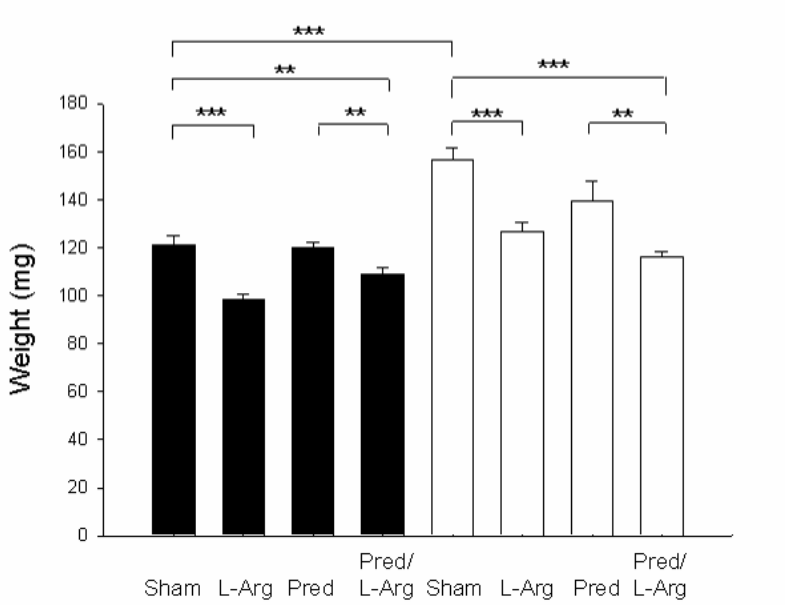

Figure 5.2: Final heart weight of treated and untreated *mdx* and C57 mice
Mdx sham hearts weighed less than C57 sham hearts. Hearts of *mdx* groups treated with l-arginine weighed significantly less than the *mdx*-sham and *mdx*-pred hearts, a difference mimicked in the C57 mice groups. $^{*}P$<0.01; $^{**}P$<0.05, $^{***}P$<0.001 (■=*mdx*; □=C57).

When heart weights were normalised for body weight, *mdx* hearts remained smaller than the C57 hearts, however, the effect of l-arginine on heart weight was eliminated. In contrast, the C57 groups showed a reduced normalised heart weight in response to treatment with l-arginine alone and combined prednisone/l-arginine treatment (Figure 5.3).

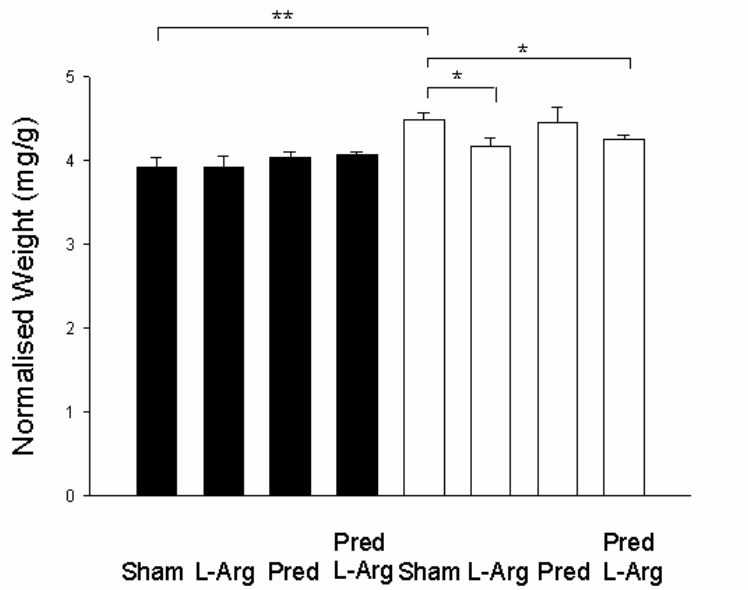

Figure 5.3: Normalised heart weight of treated and untreated *mdx* and C57 mice
Mdx hearts remained smaller than the C57 hearts when normalised for body weight and the effect of l-arginine on heart weight was eliminated. The C57 groups showed a reduced normalised heart weight in response to treatment with l-arginine alone and co-administration with prednisone. $^{*}P<0.01$; $^{**}P<0.05$ (■=*mdx*; □=C57).

5.3.2 Cardiac Function

The combined treatment with prednisone and l-arginine resulted in a significant improvement in contractility (+dP/dt) in both *mdx* and C57 mice (Figure 5.4 (A)). A similar improvement in relaxation (-dP/dt) was also evident in C57 mice treated with the combined prednisone and l-arginine, however, this effect was not observed in *mdx* (Figure 5.4 (B)).

When coronary flow was normalised to heart weight there were higher flow rates in sham *mdx* compared with sham C57 mice. L-arginine treatment alone or in combination with prednisone caused a significant improvement in coronary flow in the range of 15% to 25% in both *mdx* and C57 mice ($P<0.05$) (Figure 5.5).

A

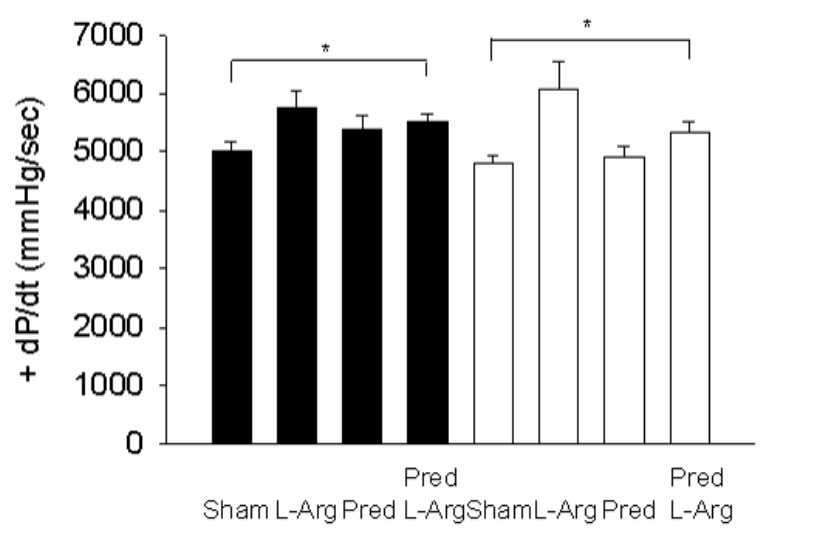

B

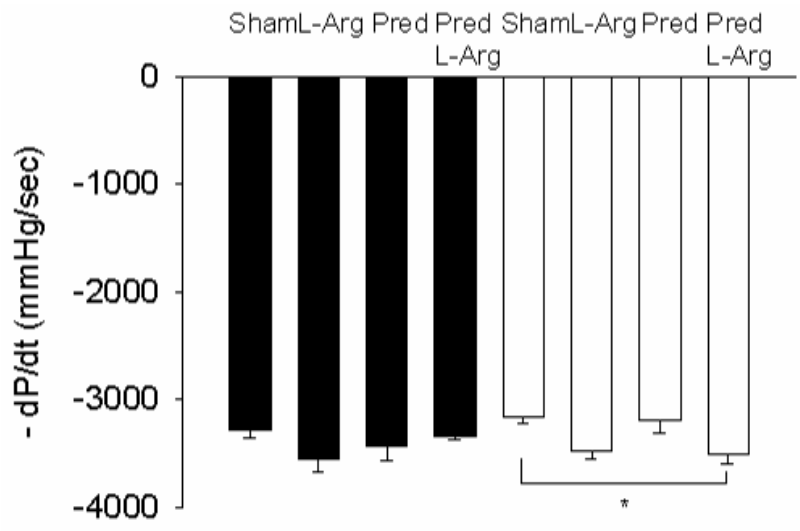

Figure 5.4: Cardiac function of untreated and treated *mdx* and C57 mice
Rate of pressure development (A) and rate of cardiac relaxation (B) from isolated hearts of untreated and treated *mdx* and C57 mice. The combined treatment with prednisone and l-arginine resulted in a significant improvement in +dP/dt in both *mdx* and C57 mice. A similar improvement in -dP/dt was also evident in C57 mice treated with the combined prednisone and l-arginine, an effect was not observed in *mdx*. $^{*}P<0.01$ (■=*mdx*; □=C57).

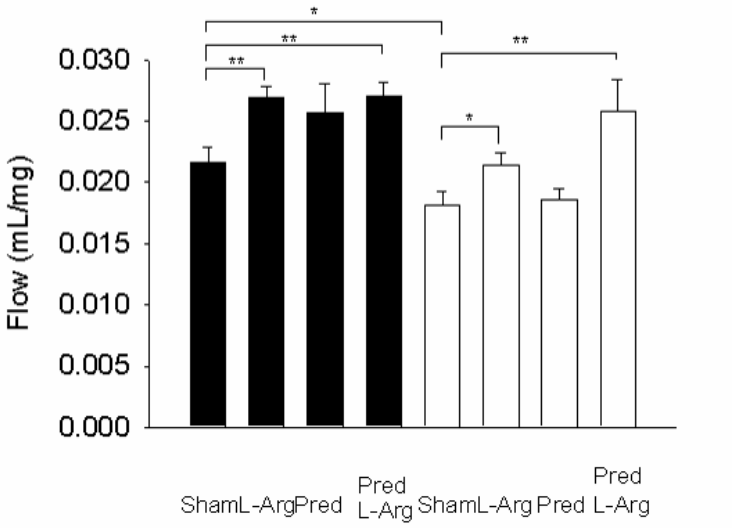

Figure 5.5: Coronary flow of treated and control *mdx* and C57 mice
When coronary flow was normalised to heart weight sham *mdx* had a higher flow rates compared with sham C57 mice. L-arginine treatment alone or co-administered with prednisone caused an improvement in coronary flow. $^{*}P<0.01$; $^{**}P<0.05$ (■=*mdx*; □=C57).

Diastolic stiffness was decreased by 12% ($P<0.001$) and 16% ($P<0.01$) in the *mdx* and C57 mice respectively that had been treated with the combination of prednisone/l-arginine. There was a trend for a decrease in stiffness in the *mdx* group treated with l-arginine alone, however, because of the variability between mice, the standard error was too large to conclude a significant positive effect (Figure 5.6).

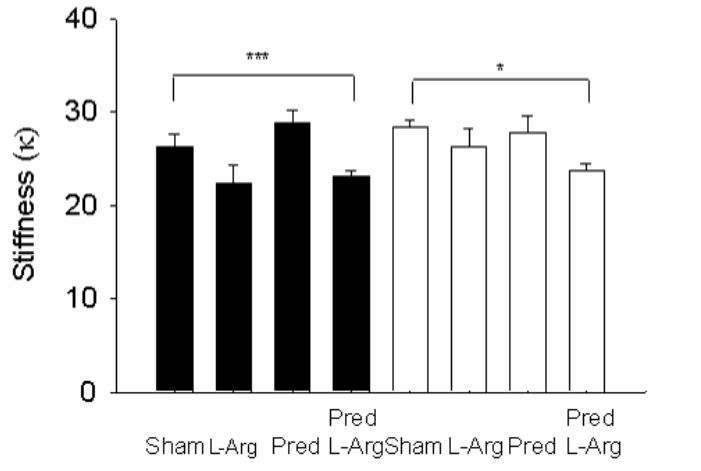

Figure 5.6: Cardiac stiffness of treated and control *mdx* and C57 mice
Diastolic stiffness was decreased in the *mdx* and C57 mice respectively that had been treated with the combination of prednisone/l-arginine. $^{*}P<0.01$; $^{***}P<0.001$(■=*mdx*; □=C57).

5.3.3 Collagen

Previous studies have shown the hearts of old *mdx* mice contain a higher content of hydroxyproline than C57 mice, a finding that was reinforced by this study (Table 5.1). Analysis of picrosirius red-stained ventricular sections showed parallel changes to those obtained from HP assays with representative photomicrographs shown in Fig 5.7. The hearts of both strains of mice treated with l-arginine showed an increase in collagen relative to sham treated mice but this increase was prevented by co-administration of prednisone.

	Sham	**L-arginine**	**Prednisone**	**Pred/L-arginine**
C57	$2.3 \pm 0.09^{***}$	$3.0 \pm 0.3^{***\dagger}$	$2.4 \pm 0.07^{***}$	$2.4 \pm 0.06^{***}$
mdx	5.08 ± 0.7	$7.3 \pm 0.6^{+}$	6.1 ± 0.2	5.4 ± 0.7

Table 5.1: Hydroxyproline content of treated and control C57 and *mdx* mice
Mdx mice contain a higher content of hydroxyproline than C57 mice. Hearts of both strains of mice treated with l-arginine showed an increase in collagen relative to sham treated mice but this increase was prevented by co-administration of prednisone.
$^{***}P<0.001$ (*mdx* sham vs. C57 sham); $^{+}P<0.05$ (*mdx* sham vs. *mdx* l-arginine); $^{\dagger}P<0.05$ (C57 sham vs. C57 l-arginine).

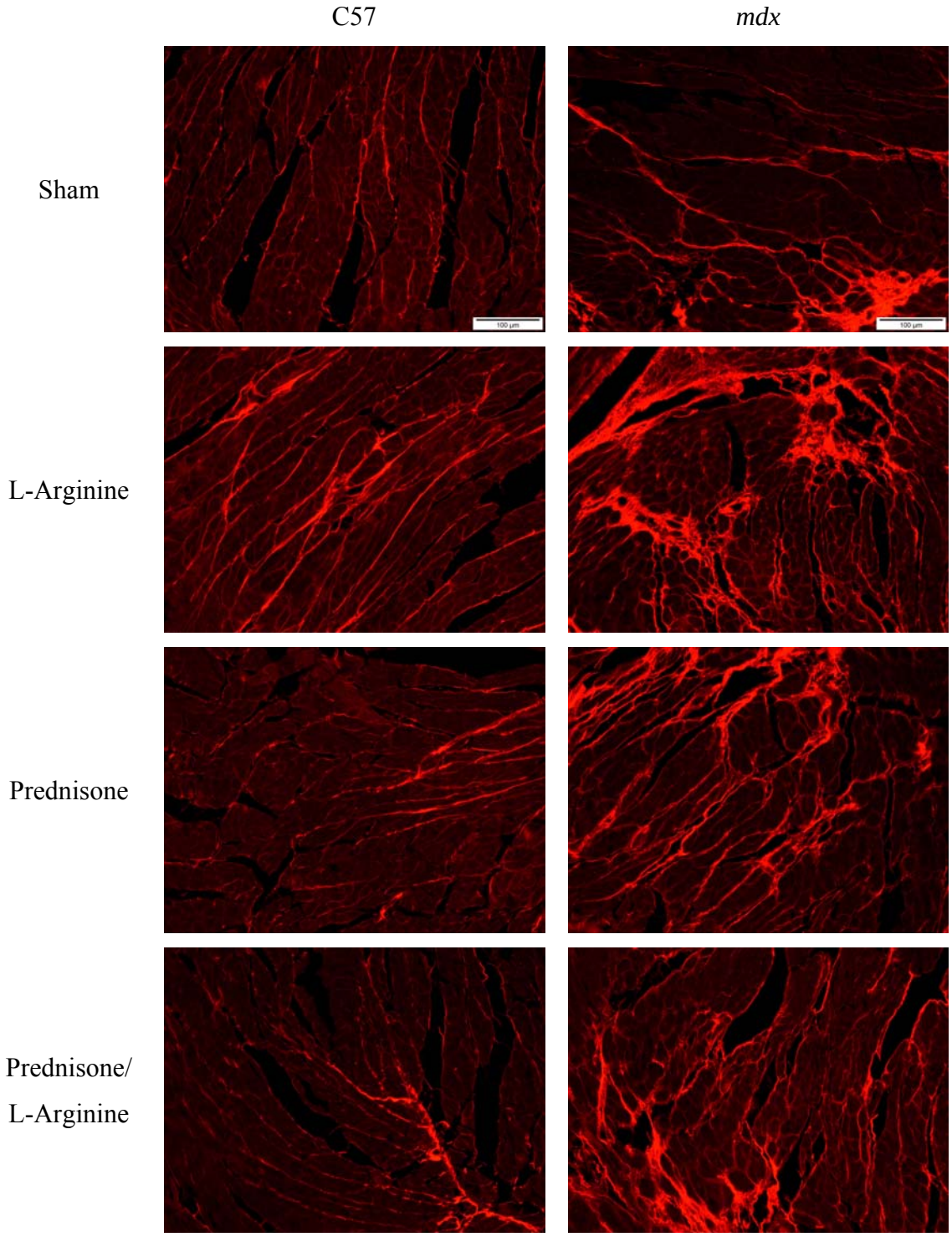

Figure 5.7: Left ventricular sections of treated and control *mdx* and C57 mice (PSR**)** Magnification: X20. Areas stained red indicate presence of collagen.
Mdx mice contain a higher collagen content than C57 mice The hearts of both strains of mice treated with l-arginine showed an increase in collagen relative to sham treated mice but this increase was prevented by co-administration of prednisone

Given the change in stiffness from hearts of mice treated with the combination of prednisone and l-arginine, the ratio of type I:III collagen was measured (Figure 5.8; Table 5.2). No differences in ratios were observed between any of the groups.

	Sham	**L-arginine**	**Prednisone**	**Pred/L-arginine**
C57	1.93±0.10	2.11±0.20	1.72±0.09	1.69±0.15
mdx	1.98±0.61	2.04±0.19	2.08±0.10	1.90±0.19

Table 5.2: Ratio of type I:III collagen in treated and control C57 and *mdx* mice
There was no difference in collagen I:III ratio in control and treated C57 and *mdx* mice

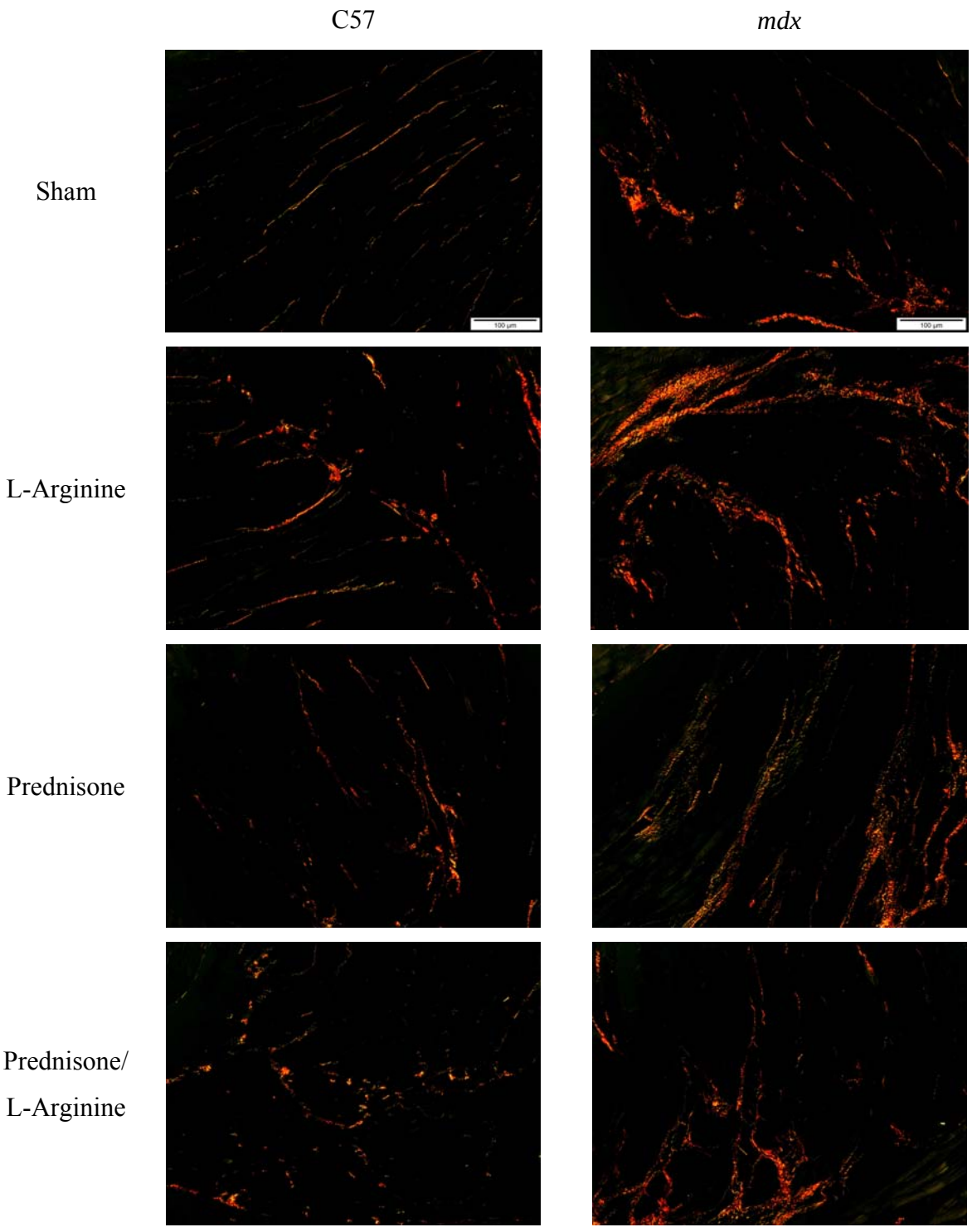

Figure 5.8: Left ventricular sections of treated and control *mdx* and C57 mice (polarised) Magnification: X20. Areas stained red/yellow indicate presence of collagen 1 and areas stained green indicate presence of collagen 3, no differences in ratios were observed between any of the groups

5.4 Discussion

L-arginine has been reported to improve cardiac structure and/or function in various models of cardiac dysfunction including the DOCA-salt hypertensive rat, aging spontaneously hypertensive rat and diabetic (db/db) mice (Fenning et al. 2005; Khaidar et al. 1994; Susic, Varagic & Frohlich 2001). The deficiency of nNOS and consequential lowered production of NO indicated that the substrate of NOS, l-arginine, may be beneficial in dystrophic cardiac muscle. The data presented in this current study showed parallel changes in both nNOS deficient *mdx* mice as well as control C57 mice, suggesting that the benefits of l-arginine were independent of nNOS deficiency.

The most prominent effect of l-arginine alone or in combination with prednisone was a marked improvement in coronary flow (*mdx*; 15%, C57; 25%). Nitric oxide levels play a major role in maintaining coronary flow (Amrani et al. 1992). The elevation of NO caused by l-arginine supplementation, as reported in previous studies (Susic, Francischetti & Frohlich 1999), may result in coronary vasodilation and increased coronary flow. This may be of particular benefit in dystrophic tissues where the deficiency of nNOS modulates vascular tone (Sander et al. 2000) therefore it has been suggested that increased levels of NO produced by myocytes may diffuse to nearby arterioles to facilitate vasodilation (Smith et al. 1996). Many studies show a beneficial effect of l-arginine on endothelium in conditions associated with a reduced NO synthesis, demonstrating that NOS is also regulated in vascular smooth muscle cells which could

indicate that the increased levels of NO could be produced by the smooth muscle cells (Cylwik, Mogielnicki & Buczko 2005)

The combination of l-arginine and prednisone also caused a significant improvement in cardiac contractility in both *mdx* and C57 isolated hearts and l-arginine treatment alone demonstrated a trend towards an improvement. Nitric oxide is an important regulator of intracellular calcium handling, influencing inactivation of L-type calcium channels, lusitropy, sarcoplasmic reticular (SR) calcium load and force frequency responses (Ashley et al. 2002; Khan et al. 2003; Sears et al. 2003). The elevation of NO caused by l-arginine supplementation may have caused stimulation of SR calcium release via the ryanodine receptor to facilitate the improved contractility (Xu et al. 1998).

Changes in diastolic stiffness are not solely due to altered interstitial collagen content or properties such as subtype ratios or crosslinking (Bronzwaer & Paulus 2005). In this current study, reduced stiffness was evident in mice treated with 10% l-arginine in drinking water despite an increase in collagen and no change in type I:III ratio. Other factors contributing to stiffness include phosphorylation of cytoskeletal proteins such as titin (Fukuda et al. 2005) or low grade diastolic cross-bridge cycling such as that caused by defective diastolic calcium removal from the cytosol (Bronzwaer & Paulus 2005). The elevation of NO via l-arginine enhanced myocardial relaxation and reduced diastolic tone in isolated perfused hearts via a NO/cGMP mediated pathway (Zieman et al. 2001). The precise action through which NO mediates this positive lusitropic effect is as yet unclear, but this may explain the basis of the reduced diastolic stiffness.

In contrast to previous studies where l-arginine has been reported to lower collagen deposition, we report here that 10% l-arginine causes a significant increase in collagen deposition in both *mdx* and C57 mice. This was due to the higher level of l-arginine utilised in this study. Preliminary studies using a range of concentrations suggested 10% l-arginine treated mice showed the largest improvement in cardiac function over a 10 day treatment period (data not shown) at a lifestage when the *mdx* mouse shows an acute and severe muscle breakdown (Partridge 1991). The basis for the increase of collagen is unclear, but we suggest that it may be due to excess l-arginine being catalysed by arginase to ornithine and subsequently hydroxyproline, a major component of collagen (Liu, H. et al. 2005). Other reports showing anti-fibrotic effects with l-arginine utilise lower doses ranging from 0.12% to 5%. Prednisone, which has been shown to reduce collagen content in *mdx* diaphragms (Hartel et al. 2001), was able to effectively ameliorate the deleterious effects of l-arginine on cardiac collagen deposition. This antifibrotic benefit of prednisone on cardiac muscle offers encouragement as corticosteroids remain the mainstay of therapy for DMD.

Finally, l-arginine caused a significant reduction in heart and body weights in *mdx* and C57, an effect not ameliorated by prednisone. L-arginine can influence satellite cell activation in a dose dependent manner, however at high concentrations its effects diminish. At *in vitro* concentrations above 1 mM, satellite cells are no longer activated (Anderson & Pilipowicz 2002). While this effect of l-arginine on satellite cells could potentially explain the effect on whole body weight, as a large percentage of body weight consists of skeletal muscle, alternate mechanisms may exist for cardiac muscle. In

conditions of extreme hyperarginaemia one of the classical symptoms is a reduced growth rate, although the basis of this is not clear (Crombez & Cederbaum 2005).

In conclusion, the combination of 10% l-arginine and prednisone improved coronary flow and cardiac contractility while reducing diastolic stiffness. L-arginine alone improved cardiac contractility non-significantly and improved coronary flow but also increased cardiac collagen and reduced body weight. It is highly probable that these latter two effects were mediated by an excess of l-arginine. Future experiments should involve dose-ranging studies of l-arginine with prednisone to further examine their potential to ameliorate cardiac dysfunction in DMD.

CHAPTER 6 : CONCLUSIONS AND FUTURE DIRECTIONS

Duchenne Muscular Dystrophy was initially considered to be a skeletal myopathy involving muscle wasting, fibrosis and contractures that lead to impaired mobility, respiratory dysfunction and kyphoscoliosis. In the last decade with ventilatory assistance and improved care, life expectancy of DMD patients has prolonged significantly. This increased lifespan has therefore increased the presentation of cardiac manifestations and heightened awareness of cardiomyopathy as a contributor to mortality in this neuromuscular disease (Eagle et al. 2002).

The development of cardiac fibrosis, particularly in the left ventricle, is an important facet of cardiomyopathy in patients with DMD, contributing to altered contractility as well as conduction and rhythm disturbances (Perloff & Marelli 1992; Perloff et al. 1967). The aim of this thesis was to investigate different novel pharmacological therapies in an attempt to improve function and reduce the fibrosis observed in skeletal and cardiac muscle in *mdx* mice as a model of DMD.

The pathways involved in fibrosis development and progression are complex and multifactorial, and therefore potential antifibrotic strategies may involve widely differing mechanisms as outlined by Figure 6.1.

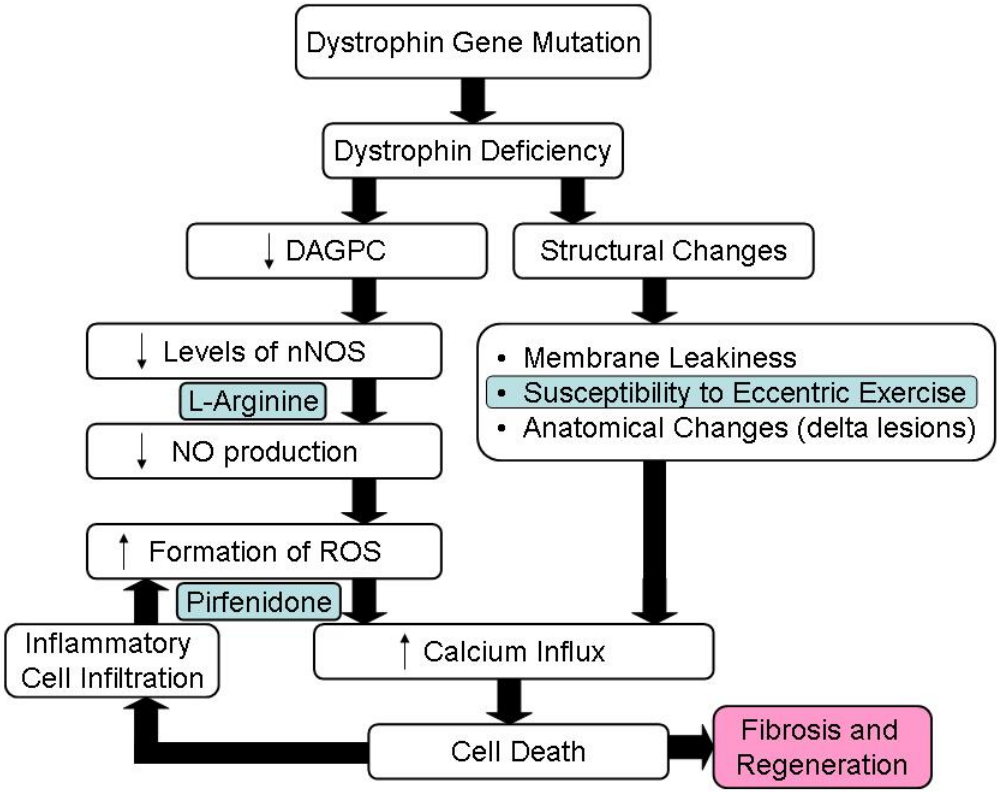

Figure 6.1: Potential fibrotic pathways
Pathways which can alter fibrosis. Blue areas were targeted to influence the fibrotic process.

6.1 Exercise

Muscle weakness is one of the major symptoms of DMD and the only treatment demonstrated to slow the progression of this weakness is prednisone, albeit with significant side-effects. To counteract the progression of weakness in normal muscle, exercise training is desirable. Unfortunately, exercise training, especially resistive exercise, is thought to be harmful for the DMD patient (Ansved 2003). In DMD patients, lower limb muscles display damage relatively early, as a result of eccentric contractions during physical activity (Weller, Karpati & Carpenter 1990; Zeman et al. 2000).

According to Brussee et al., (1998) chronic eccentric exercise also causes increased muscle wasting, weakness and acceleration of the dystrophic process with signs of fibrosis and degeneration. Similarly, it is reported that eccentric exercise can induce fibrosis at a faster rate in ageing *mdx* mice (De Luca, A. et al. 2003; De Luca, A et al. 2002; Vilquin et al. 1998).

In this study it was observed that downhill running did not exacerbate the dystrophic condition of cardiac or skeletal muscle in older *mdx* mice as the pathology of these muscles was unchanged with exercise. It appeared that moderate exercise in the later stages of the lifespan of the *mdx* mouse is not detrimental and the fibrotic condition of the muscles in these mice is not worsened by eccentric contractions in skeletal muscles. These results argue against the workload hypothesis that muscle damage increases due to eccentric exercise. This finding supports the study of Krupnick *et al*. (2003), who noted that increased workload as a result of tracheal banding in *mdx* mice was not detrimental to the diaphragm.

Although chronic eccentric exercise did not exacerbate the muscle pathology of the *mdx* mouse, extrapolating data from animal studies to humans requires caution. There are obvious differences in biomechanics and in phenotypic expression between humans and the *mdx* mouse (Ansved 2003). The advantage of working with the *mdx* mouse however, encourages further mechanistic experiments involving eccentric exercise to be undertaken.

Future experiments could investigate the effect of eccentric exercise on cardiac and skeletal muscle structure and function in younger mice using short term exercise periods. Such experiments should also involve biochemical experiments to examine the levels of IGF-1 and inflammatory cytokines, as the latter have a major influence on fibrosis and function.

The outcomes of this study demonstrated that eccentric exercise is not a significant contributor to the development of fibrosis in older *mdx* and C57 mice. Instead, it was hypothesised that development of fibrosis might be influenced to a greater extent by cytokines, as will be discussed below.

6.2 Pirfenidone

The structural changes as a result of dystrophin deficiency lead to an influx of calcium which contributes to cell death. Cell death results in inflammatory cell infiltration that involves the inflammatory cytokine TGF-β which plays a key role in fibrosis. An orally active anti-fibrotic drug that inhibits TGF-β–induced fibroblast growth and collagen synthesis in a range of tissues and disease models, such as pirfenidone, may be beneficial.

To determine the effect of the TGF-β antagonist, *mdx* mice were administered pirfenidone in water at three different doses. It was hypothesised that administration of pirfenidone would elicit an anti-fibrotic action on cardiac and skeletal muscle and improve functional responses in *mdx* mice. This study demonstrated that pirfenidone caused a marked improvement in cardiac function without a reduction of ventricular

collagen content despite lowering TGF-β mRNA levels as described in Chapter 3. Another aspect of this study was to investigate the effect of pirfenidone treatment in EDL, SOL and diaphragm muscles. This study showed that the administration of pirfenidone to older *mdx* mice, did not cause a functional improvement in any of the three skeletal muscles investigated, nor did pirfenidone prevent skeletal muscle degeneration and regeneration.

It may be hypothesised that the TGF- β fibrotic pathways are already established by six months of age, thereby impairing the ability of pirfenidone to prevent fibrosis. Despite this, pirfenidone could still improve cardiac function, which is a novel and important finding. This suggests that administration of pirfenidone to young *mdx* before the profibrotic pathways are established may have the two-fold benefit of preventing fibrosis and improving cardiac function. Further molecular biological experiments to determine protein expression of TGF-β, downstream regulators (Smad) and other cytokines may address the mechanisms of action in more detail.

6.3 L-arginine

Dystrophin deficiency decreases the DAGPC leading to decreased levels of nNOS. nNOS deficiency results in a reduction of NO (Brenman et al. 1995). This is similar to NOS inhibition, which increases the severity of dystrophy and hastens muscle degeneration (Anderson & Vargas 2003) and is likely to affect subsequent pathways in

fibrosis. Since NOS utilises l-arginine as the substrate to produce NO, it is feasible that l-arginine administration may inhibit another component within the fibrosis pathway.

In this study, a 5% dose of l-arginine improved coronary flow, cardiac structure and contractility, decreased diastolic stiffness and reduced cardiac collagen without altering skeletal muscle structure and function, although a slight reduction in body weight was observed. It is likely that the 5% dose of l-arginine increased NO production to prevent cardiac fibrosis through a decrease in the inflammatory pathways and collagen expression. Other possible effects facilitated by l-arginine administration include vasodilation, subsequently increasing the coronary flow and stimulating SR calcium release via the ryanodine receptor to improve cardiac contractility.

Future experiments could involve administration of the NO donor 3-morpholinosydnonimine (SIN-1). SIN-1 is metabolised in the liver following administration of the drug molsidomine. Voisin et al., (2005) showed that administration of molsidomine in *mdx* mice resulted in decreased necrosis of the diaphragm, soleus and gastrocnemius muscles. This was similar to the outcomes observed in *mdx* mice treated with l-arginine in the same study. Therefore, a logical progression of the l-arginine study would be to see if the l-arginine-induced improvement in cardiac structure and function from the current study can be mimicked with the drug molsidomine. This would provide evidence that l-arginine produces its effects in a NO-dependent mechanism. This would be preferable to co-administration with the NOS inhibitor NG-nitro-l-arginine-methyl-

ester (L-NAME) which causes detrimental cardiovascular effects and would confound interpretation of cardiovascular responses.

6.4 Combined Prednisone and L-arginine

The combination of l-arginine and the glucocorticoid, deflazacort, has been shown to improve tissue integrity in *mdx* skeletal muscle cells, presumably by upregulation of NOS expression in dystrophin-deficient satellite cells (Anderson & Vargas 2003). The combination of these two pharmacological agents caused a decrease in skeletal muscle inflammation and regeneration. Prednisone (another glucocorticoid) has several proposed modes of action, which include reducing inflammatory cell infiltration and calcium influx. It was hypothesised that the combination of prednisone and l-arginine would result in a similar protective effect on cardiac muscle structure and function in *mdx* mice.

The combination of 10% l-arginine with the glucocorticoid, prednisone, improved coronary flow and cardiac contractility whilst reducing diastolic stiffness. L-arginine alone improved coronary flow, but also increased cardiac collagen, an anomaly that is most likely due to the high dosage of l-arginine administered. This suggests that l-arginine, although considered safe, can have potentially detrimental effects when a high dose is administered. Fortunately, this undesirable side effect was partially prevented when the high dose of L-arginine was co-administered with prednisone.

These results are important as many parents currently administer l-arginine to their children with DMD, even though an effective dose has not been established clinically. The current findings show that high doses of l-arginine may increase the risk of fibrosis, although prednisone reduces this risk. The other important finding from this study was that even if treatment with l-arginine is not commenced until later stage in life, marked improvements in cardiac muscle function may still be achievable.

Future experiments should involve dose-ranging studies of l-arginine with prednisone to further examine their potential to ameliorate cardiac dysfunction in *mdx* mice. In previous studies, altered NO levels and activities of nNOS, iNOS and eNOS have been reported in *mdx* cardiomyocytes (Bia et al. 1999; Heydemann et al. 2004). To confirm or clarify changes in NOS isoforms and their role in the dystrophic heart with l-arginine treatment, the levels of these isoforms should be investigated in future experiments. Finally, the impact of l-arginine on cardiac collagen crosslinking should be investigated using cyanogen bromide digestion.

6.5 Summary

In the experiments described in this dissertation, pharmacologically-induced improvements in cardiac structure and function were obtained. The mechanisms underlying these improvements were investigated and described.

This thesis has indicated for the first time that it is possible to improve cardiac function in *mdx* mice and this is achievable through two different pathways. It is possible that

fibrosis may be reduced through inhibiting TGF-β, preventing inflammation and decreasing collagen production. These different treatments at varying ages may benefit young or older DMD patients. Although pirfenidone did not prevent fibrosis, this study indicates that treatment early in life may have greater potential. Treatment with l-arginine can begin later in life, as it decreases fibrosis and improves cardiac function at a later age in the *mdx* mouse. These results demonstrate that it may be possible for the two antifibrotic agents, working by different mechanisms, to improve cardiac function and prevent fibrosis. However, as shown in Figure 6.1, both l-arginine and pirfenidone may also prevent the formation of ROS. It is therefore feasible that pirfenidone and l-arginine could act synergistically to reduce fibrosis by both decreasing ROS formation.

The data discussed in this dissertation points to a separation of collagen content from functional outcomes. The treatments given to *mdx* and C57 mice could act to improve function through mechanisms independent of collagen alterations such as prevention of inflammation (Wehling-Henricks et al. 2005).

The experiments conducted and reported in this thesis demonstrate novel treatments that involve the fibrotic pathway, neither of which have been reported to date, to prevent this debilitating side effect of DMD. The dystrophic condition can be improved through inhibiting inflammatory cell infiltration and through increasing NO levels with or without co-administration of prednisone. Future experiments to further elucidate the fibrotic pathway should also address other areas shown in figure 6.1 and further research to

optimise these results are necessary to guide future pharmacological antifibrotic therapies.

Muscle fibrosis severely impacts on the quality of life of DMD patients, leading to contractures and worsening immobility. Fibrosis also affects the heart, causing rhythm disturbances and impaired contractility highlighting the need for safe and effective antifibrotic treatments. It is anticipated that the findings of this thesis may benefit future research investigating fibrosis and function in *mdx* mice and potentially in DMD patients.

REFERENCES

Abi-Gerges, N, Fischmeister, R & Mery, PF 2001, 'G protein-mediated inhibitory effect of a nitric oxide donor on the L-type Ca2+ current in rat ventricular myocytes', *J Physiol*, vol. 531, no. Pt 1, pp. 117-30.

Acsadi, G, Dickson, G, Love, DR, Jani, A, Walsh, FS, Gurusinghe, A, Wolff, JA & Davies, KE 1991, 'Human dystrophin expression in *mdx* mice after intramuscular injection of DNA constructs', *Nature*, vol. 352, no. 6338, pp. 815-8.

Adams, GR & Haddad, F 1996, 'The relationships among IGF-1, DNA content, and protein accumulation during skeletal muscle hypertrophy', *J Appl Physiol*, vol. 81, no. 6, pp. 2509-16.

Adams, GR & McCue, SA 1998, 'Localized infusion of IGF-I results in skeletal muscle hypertrophy in rats', *J Appl Physiol*, vol. 84, no. 5, pp. 1716-22.

Aihara, H & Miyazaki, J 1998, 'Gene transfer into muscle by electroporation in vivo', *Nat Biotechnol*, vol. 16, no. 9, pp. 867-70.

Allen, RE & Rankin, LL 1990, 'Regulation of satellite cells during skeletal muscle growth and development', *Proc Soc Exp Biol Med*, vol. 194, no. 2, pp. 81-6.

Alloatti, G, Gallo, MP, Penna, C & Levi, RC 1995, 'Properties of cardiac cells from dystrophic mouse', *J Mol Cell Cardiol*, vol. 27, no. 8, pp. 1775-9.

Amrani, M, O'Shea, J, Allen, NJ, Harding, SE, Jayakumar, J, Pepper, JR, Moncada, S & Yacoub, MH 1992, 'Role of basal release of nitric oxide on coronary flow and mechanical performance of the isolated rat heart', *J Physiol*, vol. 456, pp. 681-7.

Anderson, JE 2000, 'A role for nitric oxide in muscle repair: nitric oxide-mediated activation of muscle satellite cells', *Mol Biol Cell*, vol. 11, no. 5, pp. 1859-74.

Anderson, JE & Pilipowicz, O 2002, 'Activation of muscle satellite cells in single-fiber cultures', *Nitric Oxide*, vol. 7, no. 1, pp. 36-41.

Anderson, JE & Vargas, C 2003, 'Correlated NOS-Imu and myf5 expression by satellite cells in *mdx* mouse muscle regeneration during NOS manipulation and deflazacort treatment', *Neuromuscul Disord*, vol. 13, no. 5, pp. 388-96.

Anderson, JE, McIntosh, LM & Poettcker, R 1996, 'Deflazacort but not prednisone improves both muscle repair and fiber growth in diaphragm and limb muscle in vivo in the *mdx* dystrophic mouse', *Muscle Nerve*, vol. 19, no. 12, pp. 1576-85.

Anderson, JE, Weber, M & Vargas, C 2000, 'Deflazacort increases laminin expression and myogenic repair, and induces early persistent functional gain in *mdx* mouse muscular dystrophy', *Cell Transplant*, vol. 9, no. 4, pp. 551-64.

Ansved, T 2003, 'Muscular dystrophies: influence of physical conditioning on the disease evolution', *Curr Opin Clin Nutr Metab Care*, vol. 6, no. 4, pp. 435-9.

Arakawa, M, Shiozuka, M, Nakayama, Y, Hara, T, Hamada, M, Kondo, S, Ikeda, D, Takahashi, Y, Sawa, R, Nonomura, Y, Sheykholeslami, K, Kondo, K, Kaga, K, Kitamura, T, Suzuki-Miyagoe, Y, Takeda, S & Matsuda, R 2003, 'Negamycin restores dystrophin expression in skeletal and cardiac muscles of *mdx* mice', *J Biochem (Tokyo)*, vol. 134, no. 5, pp. 751-8.

Ascensao, AA, Magalhaes, JF, Soares, JM, Ferreira, RM, Neuparth, MJ, Appell, HJ & Duarte, JA 2005, 'Cardiac mitochondrial respiratory function and oxidative stress: the role of exercise', *Int J Sports Med*, vol. 26, no. 4, pp. 258-67.

Ashley, EA, Sears, CE, Bryant, SM, Watkins, HC & Casadei, B 2002, 'Cardiac nitric oxide synthase 1 regulates basal and beta-adrenergic contractility in murine ventricular myocytes', *Circulation*, vol. 105, no. 25, pp. 3011-6.

Azuma, A, Nukiwa, T, Tsuboi, E, Suga, M, Abe, S, Nakata, K, Taguchi, Y, Nagai, S, Itoh, H, Ohi, M, Sato, A & Kudoh, S 2005, 'Double-blind, placebo-controlled trial of pirfenidone in patients with idiopathic pulmonary fibrosis', *Am J Respir Crit Care Med*, vol. 171, no. 9, pp. 1040-7.

Badenhorst, D, Maseko, M, Tsotetsi, OJ, Naidoo, A, Brooksbank, R, Norton, GR & Woodiwiss, AJ 2003, 'Cross-linking influences the impact of quantitative changes in myocardial collagen on cardiac stiffness and remodelling in hypertension in rats', *Cardiovasc Res*, vol. 57, no. 3, pp. 632-41.

Barouch, LA, Harrison, RW, Skaf, MW, Rosas, GO, Cappola, TP, Kobeissi, ZA, Hobai, IA, Lemmon, CA, Burnett, AL, O'Rourke, B, Rodriguez, ER, Huang, PL, Lima, JA, Berkowitz, DE & Hare, JM 2002, 'Nitric oxide regulates the heart by spatial confinement of nitric oxide synthase isoforms', *Nature*, vol. 416, no. 6878, pp. 337-9.

Barton, ER, Morris, L, Musaro, A, Rosenthal, N & Sweeney, HL 2002, 'Muscle-specific expression of insulin-like growth factor I counters muscle decline in *mdx* mice', *J Cell Biol*, vol. 157, no. 1, pp. 137-48.

Barton, ER, Morris, L, Kawana, M, Bish, LT & Toursel, T 2005, 'Systemic administration of L-arginine benefits *mdx* skeletal muscle function', *Muscle Nerve*.

Barton-Davis, ER, Cordier, L, Shoturma, DI, Leland, SE & Sweeney, HL 1999, 'Aminoglycoside antibiotics restore dystrophin function to skeletal muscles of *mdx* mice', *J Clin Invest*, vol. 104, no. 4, pp. 375-81.

Bernasconi, P, Torchiana, E, Confalonieri, P, Brugnoni, R, Barresi, R, Mora, M, Cornelio, F, Morandi, L & Mantegazza, R 1995, 'Expression of transforming

growth factor-beta 1 in dystrophic patient muscles correlates with fibrosis. Pathogenetic role of a fibrogenic cytokine', *J Clin Invest*, vol. 96, no. 2, pp. 1137-44.

Bia, BL, Cassidy, PJ, Young, ME, Rafael, JA, Leighton, B, Davies, KE, Radda, GK & Clarke, K 1999, 'Decreased myocardial nNOS, increased iNOS and abnormal ECGs in mouse models of Duchenne muscular dystrophy', *J Mol Cell Cardiol*, vol. 31, no. 10, pp. 1857-62.

Bianchi, ML, Mazzanti, A, Galbiati, E, Saraifoger, S, Dubini, A, Cornelio, F & Morandi, L 2003, 'Bone mineral density and bone metabolism in Duchenne muscular dystrophy', *Osteoporos Int*, vol. 14, no. 9, pp. 761-7.

Biggar, WD, Gingras, M, Fehlings, DL, Harris, VA & Steele, CA 2001, 'Deflazacort treatment of Duchenne muscular dystrophy', *J Pediatr*, vol. 138, no. 1, pp. 45-50.

Biggar, WD, Klamut, HJ, Demacio, PC, Stevens, DJ & Ray, PN 2002, 'Duchenne muscular dystrophy: current knowledge, treatment, and future prospects', *Clin Orthop Relat Res*, no. 401, pp. 88-106.

Biggar, WD, Politano, L, Harris, VA, Passamano, L, Vajsar, J, Alman, B, Palladino, A, Comi, LI & Nigro, G 2004, 'Deflazacort in Duchenne muscular dystrophy: a comparison of two different protocols', *Neuromuscul Disord*, vol. 14, no. 8-9, pp. 476-82.

Bittner, RE, Schofer, C, Weipoltshammer, K, Ivanova, S, Streubel, B, Hauser, E, Freilinger, M, Hoger, H, Elbe-Burger, A & Wachtler, F 1999, 'Recruitment of bone-marrow-derived cells by skeletal and cardiac muscle in adult dystrophic *mdx* mice', *Anat Embryol (Berl)*, vol. 199, no. 5, pp. 391-6.

Blake, DJ, Weir, A, Newey, SE & Davies, KE 2002, 'Function and genetics of dystrophin and dystrophin-related proteins in muscle', *Physiol Rev*, vol. 82, no. 2, pp. 291-329.

Bobet, J, Mooney, RF & Gordon, T 1998, 'Force and stiffness of old dystrophic (*mdx*) mouse skeletal muscles', *Muscle Nerve*, vol. 21, no. 4, pp. 536-9.

Bogdanovich, S, Perkins, KJ, Krag, TO, Whittemore, LA & Khurana, TS 2005, 'Myostatin propeptide-mediated amelioration of dystrophic pathophysiology', *Faseb J*, vol. 19, no. 6, pp. 543-9.

Boland, BJ, Silbert, PL, Groover, RV, Wollan, PC & Silverstein, MD 1996, 'Skeletal, cardiac, and smooth muscle failure in Duchenne muscular dystrophy', *Pediatr Neurol*, vol. 14, no. 1, pp. 7-12.

Bozkurt, B, Kribbs, SB, Clubb, FJ, Jr., Michael, LH, Didenko, VV, Hornsby, PJ, Seta, Y, Oral, H, Spinale, FG & Mann, DL 1998, 'Pathophysiologically relevant concentrations of tumor necrosis factor-alpha promote progressive left ventricular dysfunction and remodeling in rats', *Circulation*, vol. 97, no. 14, pp. 1382-91.

Brenman, JE, Chao, DS, Xia, H, Aldape, K & Bredt, DS 1995, 'Nitric oxide synthase complexed with dystrophin and absent from skeletal muscle sarcolemma in Duchenne muscular dystrophy', *Cell*, vol. 82, no. 5, pp. 743-52.

Bridges, LR 1986, 'The association of cardiac muscle necrosis and inflammation with the degenerative and persistent myopathy of *MDX* mice', *J Neurol Sci*, vol. 72, no. 2-3, pp. 147-57.

Briguet, A, Courdier-Fruh, I, Foster, M, Meier, T & Magyar, JP 2004, 'Histological parameters for the quantitative assessment of muscular dystrophy in the *mdx*-mouse', *Neuromuscul Disord*, vol. 14, no. 10, pp. 675-82.

Brilla, CG, Janicki, JS & Weber, KT 1991, 'Impaired diastolic function and coronary reserve in genetic hypertension. Role of interstitial fibrosis and medial thickening of intramyocardial coronary arteries', *Circ Res*, vol. 69, no. 1, pp. 107-15.

Brockmeier, K, Schmitz, L, von Moers, A, Koch, H, Vogel, M & Bein, G 1998, 'X-chromosomal (p21) muscular dystrophy and left ventricular diastolic and systolic function', *Pediatr Cardiol*, vol. 19, no. 2, pp. 139-44.

Bronzwaer, JG & Paulus, WJ 2005, 'Matrix, cytoskeleton, or myofilaments: which one to blame for diastolic left ventricular dysfunction?' *Prog Cardiovasc Dis*, vol. 47, no. 4, pp. 276-84.

Brook, NR, Waller, JR, Bicknell, GR & Nicholson, ML 2005a, 'The experimental agent pirfenidone reduces pro-fibrotic gene expression in a model of tacrolimus-induced nephrotoxicity', *J Surg Res*, vol. 125, no. 2, pp. 137-43.

---- 2005b, 'The novel antifibrotic agent pirfenidone attenuates the profibrotic environment generated by calcineurin inhibitors in the rat salt-depletion model', *Transplant Proc*, vol. 37, no. 1, pp. 130-3.

Brooke, MH, Fenichel, GM, Griggs, RC, Mendell, JR, Moxley, RT, 3rd, Miller, JP, Kaiser, KK, Florence, JM, Pandya, S, Signore, L & et al. 1987, 'Clinical investigation of Duchenne muscular dystrophy. Interesting results in a trial of prednisone', *Arch Neurol*, vol. 44, no. 8, pp. 812-7.

Brussee, V, Tardif, F & Tremblay, JP 1997, 'Muscle fibers of *mdx* mice are more vulnerable to exercise than those of normal mice', *Neuromuscul Disord*, vol. 7, no. 8, pp. 487-92.

Brussee, V, Merly, F, Tardif, F & Tremblay, JP 1998, 'Normal myoblast implantation in *MDX* mice prevents muscle damage by exercise', *Biochem Biophys Res Commun*, vol. 250, no. 2, pp. 321-7.

Bulfield, G, Siller, WG, Wight, PA & Moore, KJ 1984, 'X chromosome-linked muscular dystrophy (*mdx*) in the mouse', *Proc Natl Acad Sci U S A*, vol. 81, no. 4, pp. 1189-92.

Burgess, ML, Buggy, J, Price, RL, Abel, FL, Terracio, L, Samarel, AM & Borg, TK 1996, 'Exercise- and hypertension-induced collagen changes are related to left ventricular function in rat hearts', *Am J Physiol*, vol. 270, no. 1 Pt 2, pp. H151-9.

Bushby, KM, Thambyayah, M & Gardner-Medwin, D 1991, 'Prevalence and incidence of Becker muscular dystrophy', *Lancet*, vol. 337, no. 8748, pp. 1022-4.

Campbell, C & Jacob, P 2003, 'Deflazacort for the treatment of Duchenne Dystrophy: a systematic review', *BMC Neurol*, vol. 3, no. 1, p. 7.

Card, JW, Racz, WJ, Brien, JF, Margolin, SB & Massey, TE 2003, 'Differential effects of pirfenidone on acute pulmonary injury and ensuing fibrosis in the hamster model of amiodarone-induced pulmonary toxicity', *Toxicol Sci*, vol. 75, no. 1, pp. 169-80.

Carpenter, S & Karpati, G 1979, 'Duchenne muscular dystrophy: plasma membrane loss initiates muscle cell necrosis unless it is repaired', *Brain*, vol. 102, no. 1, pp. 147-61.

Carter, GT, Abresch, RT & Fowler, WM, Jr. 2002, 'Adaptations to exercise training and contraction-induced muscle injury in animal models of muscular dystrophy', *Am J Phys Med Rehabil*, vol. 81, no. 11 Suppl, pp. S151-61.

Chakkalakal, JV, Thompson, J, Parks, RJ & Jasmin, BJ 2005, 'Molecular, cellular, and pharmacological therapies for Duchenne/Becker muscular dystrophies', *Faseb J*, vol. 19, no. 8, pp. 880-91.

Chamberlain, JS 2002, 'Gene therapy of muscular dystrophy', *Hum Mol Genet*, vol. 11, no. 20, pp. 2355-62.

Chang, WJ, Iannaccone, ST, Lau, KS, Masters, BS, McCabe, TJ, McMillan, K, Padre, RC, Spencer, MJ, Tidball, JG & Stull, JT 1996, 'Neuronal nitric oxide synthase

and dystrophin-deficient muscular dystrophy', *Proc Natl Acad Sci U S A*, vol. 93, no. 17, pp. 9142-7.

Chaubourt, E, Fossier, P, Baux, G, Leprince, C, Israel, M & De La Porte, S 1999, 'Nitric oxide and l-arginine cause an accumulation of utrophin at the sarcolemma: a possible compensation for dystrophin loss in Duchenne muscular dystrophy', *Neurobiol Dis*, vol. 6, no. 6, pp. 499-507.

Chaubourt, E, Voisin, V, Fossier, P, Baux, G, Israel, M & De La Porte, S 2002, 'Muscular nitric oxide synthase (muNOS) and utrophin', *J Physiol Paris*, vol. 96, no. 1-2, pp. 43-52.

Chazalette, D, Hnia, K, Rivier, F, Hugon, G & Mornet, D 2005, 'alpha7B integrin changes in *mdx* mouse muscles after L-arginine administration', *FEBS Lett*, vol. 579, no. 5, pp. 1079-84.

Chen, YW, Nagaraju, K, Bakay, M, McIntyre, O, Rawat, R, Shi, R & Hoffman, EP 2005, 'Early onset of inflammation and later involvement of TGF{beta} in Duchenne muscular dystrophy', *Neurology*.

Childers, MK, Okamura, CS, Bogan, DJ, Bogan, JR, Petroski, GF, McDonald, K & Kornegay, JN 2002, 'Eccentric contraction injury in dystrophic canine muscle', *Arch Phys Med Rehabil*, vol. 83, no. 11, pp. 1572-8.

Chilibeck, PD, Bell, GJ, Socha, T & Martin, T 1998, 'The effect of aerobic exercise training on the distribution of succinate dehydrogenase activity throughout muscle fibres', *Can J Appl Physiol*, vol. 23, no. 1, pp. 74-86.

Chu, V, Otero, J, Lopez, O, Sullivan, M, Morgan, J, Amende, I & Hampton, T 2002, 'Electrocardiographic findings in *mdx* mice: a cardiac phenotype of Duchenne muscular dystrophy.' *Muscle Nerve*, vol. 26, no. 4, pp. 513-9.

Cittadini, A, Stromer, H, Katz, SE, Clark, R, Moses, AC, Morgan, JP & Douglas, PS 1996, 'Differential cardiac effects of growth hormone and insulin-like growth factor-1 in the rat. A combined in vivo and in vitro evaluation', *Circulation*, vol. 93, no. 4, pp. 800-9.

Clarkson, PM & Tremblay, I 1988, 'Exercise-induced muscle damage, repair, and adaptation in humans', *J Appl Physiol*, vol. 65, no. 1, pp. 1-6.

Cooperstein, SJ, Lazarow, A & Kurfess, NJ 1950, 'A microspectrophotometric method for the determination of succinic dehydrogenase', *J Biol Chem*, vol. 186, no. 1, pp. 129-39.

Courdier-Fruh, I, Barman, L, Briguet, A & Meier, T 2002, 'Glucocorticoid-mediated regulation of utrophin levels in human muscle fibers', *Neuromuscul Disord*, vol. 12 Suppl 1, pp. S95-104.

Cox, GF & Kunkel, LM 1997, 'Dystrophies and heart disease', *Curr Opin Cardiol*, vol. 12, no. 3, pp. 329-43.

Crombez, EA & Cederbaum, SD 2005, 'Hyperargininemia due to liver arginase deficiency', *Mol Genet Metab*, vol. 84, no. 3, pp. 243-51.

Crosbie, RH 2001, 'NO vascular control in Duchenne muscular dystrophy', *Nat Med*, vol. 7, no. 1, pp. 27-9.

Cylwik, D, Mogielnicki, A & Buczko, W 2005, 'L-arginine and cardiovascular system', *Pharmacol Rep*, vol. 57, no. 1, pp. 14-22.

Danialou, G, Comtois, AS, Dudley, R, Karpati, G, Vincent, G, Des Rosiers, C & Petrof, BJ 2001, 'Dystrophin-deficient cardiomyocytes are abnormally vulnerable to mechanical stress-induced contractile failure and injury', *Faseb J*, vol. 15, no. 9, pp. 1655-7.

Davies, KE 1997, 'Challenges in Duchenne muscular dystrophy', *Neuromuscul Disord*, vol. 7, no. 8, pp. 482-6.

de Kermadec, JM, Becane, HM, Chenard, A, Tertrain, F & Weiss, Y 1994, 'Prevalence of left ventricular systolic dysfunction in Duchenne muscular dystrophy: an echocardiographic study', *Am Heart J*, vol. 127, no. 3, pp. 618-23.

De la Porte, S, Morin, S & Koenig, J 1999, 'Characteristics of skeletal muscle in *mdx* mutant mice', *Int Rev Cytol*, vol. 191, pp. 99-148.

De Luca, A, Pierno, S, Liantonio, A & Conte Camerino, D 2002, 'Pre-clinical trials in Duchenne dystrophy: what animal models can tell us about potential drug effectiveness.' *Neuromuscul Disord*, vol. 12 Suppl 1, pp. S142-6.

De Luca, A, Pierno, S, Camerino, C, Cocchi, D & Camerino, DC 1999, 'Higher content of insulin-like growth factor-I in dystrophic *mdx* mouse: potential role in the spontaneous regeneration through an electrophysiological investigation of muscle function', *Neuromuscul Disord*, vol. 9, no. 1, pp. 11-8.

De Luca, A, Pierno, S, Liantonio, A, Cetrone, M, Camerino, C, Fraysse, B, Mirabella, M, Servidei, S, Ruegg, UT & Conte Camerino, D 2003, 'Enhanced dystrophic progression in *mdx* mice by exercise and beneficial effects of taurine and insulin-like growth factor-1', *J Pharmacol Exp Ther*, vol. 304, no. 1, pp. 453-63.

De Luca, A, Nico, B, Liantonio, A, Didonna, MP, Fraysse, B, Pierno, S, Burdi, R, Mangieri, D, Rolland, JF, Camerino, C, Zallone, A, Confalonieri, P, Andreetta, F, Arnoldi, E, Courdier-Fruh, I, Magyar, JP, Frigeri, A, Pisoni, M, Svelto, M & Conte Camerino, D 2005, 'A multidisciplinary evaluation of the effectiveness of cyclosporine a in dystrophic *mdx* mice', *Am J Pathol*, vol. 166, no. 2, pp. 477-89.

DelloRusso, C, Scott, JM, Hartigan-O'Connor, D, Salvatori, G, Barjot, C, Robinson, AS, Crawford, RW, Brooks, SV & Chamberlain, JS 2002, 'Functional correction of adult *mdx* mouse muscle using gutted adenoviral vectors expressing full-length dystrophin', *Proc Natl Acad Sci U S A*, vol. 99, no. 20, pp. 12979-84.

DeSilva, S, Drachman, DB, Mellits, D & Kuncl, RW 1987, 'Prednisone treatment in Duchenne muscular dystrophy. Long-term benefit', *Arch Neurol*, vol. 44, no. 8, pp. 818-22.

Disatnik, MH, Chamberlain, JS & Rando, TA 2000, 'Dystrophin mutations predict cellular susceptibility to oxidative stress', *Muscle Nerve*, vol. 23, no. 5, pp. 784-92.

Donath, MY, Jenni, R, Brunner, HP, Anrig, M, Kohli, S, Glatz, Y & Froesch, ER 1996, 'Cardiovascular and metabolic effects of insulin-like growth factor I at rest and during exercise in humans', *J Clin Endocrinol Metab*, vol. 81, no. 11, pp. 4089-94.

Doumit, ME, Cook, DR & Merkel, RA 1993, 'Fibroblast growth factor, epidermal growth factor, insulin-like growth factors, and platelet-derived growth factor-BB stimulate proliferation of clonally derived porcine myogenic satellite cells', *J Cell Physiol*, vol. 157, no. 2, pp. 326-32.

Drachman, DB, Toyka, KV & Myer, E 1974, 'Prednisone in Duchenne muscular dystrophy', *Lancet*, vol. 2, no. 7894, pp. 1409-12.

Drexler, H 1999, 'Nitric oxide synthases in the failing human heart: a doubled-edged sword?' *Circulation*, vol. 99, no. 23, pp. 2972-5.

Dunant, P, Walter, MC, Karpati, G & Lochmuller, H 2003, 'Gentamicin fails to increase dystrophin expression in dystrophin-deficient muscle', *Muscle Nerve*, vol. 27, no. 5, pp. 624-7.

Dupont-Versteegden, EE, McCarter, RJ & Katz, MS 1994, 'Voluntary exercise decreases progression of muscular dystrophy in diaphragm of *mdx* mice', *J Appl Physiol*, vol. 77, no. 4, pp. 1736-41.

Eagle, M, Baudouin, SV, Chandler, C, Giddings, DR, Bullock, R & Bushby, K 2002, 'Survival in Duchenne muscular dystrophy: improvements in life expectancy since 1967 and the impact of home nocturnal ventilation', *Neuromuscul Disord*, vol. 12, no. 10, pp. 926-9.

Eghbali, M, Tomek, R, Sukhatme, VP, Woods, C & Bhambi, B 1991, 'Differential effects of transforming growth factor-beta 1 and phorbol myristate acetate on cardiac fibroblasts. Regulation of fibrillar collagen mRNAs and expression of early transcription factors', *Circ Res*, vol. 69, no. 2, pp. 483-90.

Emery, AE 1993, *Duchenne Muscular Dystrophy*, 2nd edn, Oxford Monographs on Medical Genetics, Oxford University Press, Oxford.

---- 2002, 'Muscular dystrophy into the new millennium', *Neuromuscul Disord*, vol. 12, no. 4, pp. 343-9.

Emery, AE & Muntoni, F 2003, *Duchenne Muscular Dystrophy*, 3 edn, Oxford University Press, Oxford.

Escolar, DM, Buyse, G, Henricson, E, Leshner, R, Florence, J, Mayhew, J, Tesi-Rocha, C, Gorni, K, Pasquali, L, Patel, KM, McCarter, R, Huang, J, Mayhew, T, Bertorini, T, Carlo, J, Connolly, AM, Clemens, PR, Goemans, N, Iannaccone, ST, Igarashi, M, Nevo, Y, Pestronk, A, Subramony, SH, Vedanarayanan, VV & Wessel, H 2005, 'CINRG randomized controlled trial of creatine and glutamine in Duchenne muscular dystrophy', *Ann Neurol*, vol. 58, no. 1, pp. 151-5.

Fanin, M, Melacini, P, Angelini, C & Danieli, GA 1999, 'Could utrophin rescue the myocardium of patients with dystrophin gene mutations?' *J Mol Cell Cardiol*, vol. 31, no. 8, pp. 1501-8.

Fanin, M, Danieli, GA, Cadaldini, M, Miorin, M, Vitiello, L & Angelini, C 1995, 'Dystrophin-positive fibers in Duchenne dystrophy: origin and correlation to clinical course', *Muscle Nerve*, vol. 18, no. 10, pp. 1115-20.

Farah, MG, Evans, EB & Vignos, PJ, Jr. 1980, 'Echocardiographic evaluation of left ventricular function in Duchenne's muscular dystrophy', *Am J Med*, vol. 69, no. 2, pp. 248-54.

Felber, S, Skladal, D, Wyss, M, Kremser, C, Koller, A & Sperl, W 2000, 'Oral creatine supplementation in Duchenne muscular dystrophy: a clinical and 31P magnetic resonance spectroscopy study', *Neurol Res*, vol. 22, no. 2, pp. 145-50.

Fenichel, GM, Florence, JM, Pestronk, A, Mendell, JR, Moxley, RT, 3rd, Griggs, RC, Brooke, MH, Miller, JP, Robison, J, King, W & et al. 1991, 'Long-term benefit from prednisone therapy in Duchenne muscular dystrophy', *Neurology*, vol. 41, no. 12, pp. 1874-7.

Fenning, A, Harrison, G, Rose'meyer, R, Hoey, A & Brown, L 2005, 'L-arginine attenuates cardiovascular impairment in DOCA-salt hypertensive rats', *Am J Physiol Heart Circ Physiol*.

Fenoglio, JJ, Jr., Pham, TD, Harken, AH, Horowitz, LN, Josephson, ME & Wit, AL 1983, 'Recurrent sustained ventricular tachycardia: structure and ultrastructure of subendocardial regions in which tachycardia originates', *Circulation*, vol. 68, no. 3, pp. 518-33.

Ferrari, G, Cusella-De Angelis, G, Coletta, M, Paolucci, E, Stornaiuolo, A, Cossu, G & Mavilio, F 1998, 'Muscle regeneration by bone marrow-derived myogenic progenitors', *Science*, vol. 279, no. 5356, pp. 1528-30.

Finsterer, J & Stollberger, C 2003, 'The heart in human dystrophinopathies', *Cardiology*, vol. 99, no. 1, pp. 1-19.

Foidart, M, Foidart, JM & Engel, WK 1981, 'Collagen localization in normal and fibrotic human skeletal muscle', *Arch Neurol*, vol. 38, no. 3, pp. 152-7.

Fonarow, GC 2001, 'Pathogenesis and treatment of cardiomyopathy', *Adv Intern Med*, vol. 47, pp. 1-45.

Forbes, CD & Jackson, WF 1997, *Color Atlas and Text of Clinical Medicine*, 2nd edn, Mosby-Wolfe, London.

Fukuda, N, Wu, Y, Nair, P & Granzier, HL 2005, 'Phosphorylation of titin modulates passive stiffness of cardiac muscle in a titin isoform-dependent manner', *J Gen Physiol*, vol. 125, no. 3, pp. 257-71.

Fukudome, T, Shibuya, N, Yoshimura, T & Eguchi, K 2000, 'Short-term effects of prednisolone on neuromuscular transmission in the isolated *mdx* mouse diaphragm', *Tohoku J Exp Med*, vol. 192, no. 3, pp. 211-7.

Fukushima, K, Badlani, N, Usas, A, Riano, F, Fu, F & Huard, J 2001, 'The use of an antifibrosis agent to improve muscle recovery after laceration', *Am J Sports Med*, vol. 29, no. 4, pp. 394-402.

Gebski, BL, Errington, SJ, Johnsen, RD, Fletcher, S & Wilton, SD 2005, 'Terminal antisense oligonucleotide modifications can enhance induced exon skipping', *Neuromuscul Disord*, vol. 15, no. 9-10, pp. 622-9.

Gillis, JM 1996, 'The *mdx* mouse: why diaphragm?' *Muscle Nerve*, vol. 19, no. 9, p. 1230.

Giri, SN, Leonard, S, Shi, X, Margolin, SB & Vallyathan, V 1999, 'Effects of pirfenidone on the generation of reactive oxygen species in vitro', *J Environ Pathol Toxicol Oncol*, vol. 18, no. 3, pp. 169-77.

Giri, SN, Hyde, DM, Braun, RK, Gaarde, W, Harper, JR & Pierschbacher, MD 1997, 'Antifibrotic effect of decorin in a bleomycin hamster model of lung fibrosis', *Biochem Pharmacol*, vol. 54, no. 11, pp. 1205-16.

Giri, SN, Wang, Q, Xie, Y, Lango, J, Morin, D, Margolin, SB & Buckpitt, AR 2002, 'Pharmacokinetics and metabolism of a novel antifibrotic drug pirfenidone, in mice following intravenous administration', *Biopharm Drug Dispos*, vol. 23, no. 5, pp. 203-11.

Gosselin, LE, Barkley, JE, Spencer, MJ, McCormick, KM & Farkas, GA 2003, 'Ventilatory dysfunction in *mdx* mice: impact of tumor necrosis factor-alpha deletion', *Muscle Nerve*, vol. 28, no. 3, pp. 336-43.

Gosselin, LE, Williams, JE, Deering, M, Brazeau, D, Koury, S & Martinez, DA 2004, 'Localization and early time course of TGF-beta 1 mRNA expression in dystrophic muscle', *Muscle Nerve*, vol. 30, no. 5, pp. 645-53.

Goumas, G, Tentolouris, C, Tousoulis, D, Stefanadis, C & Toutouzas, P 2001, 'Therapeutic modification of the L-arginine-eNOS pathway in cardiovascular diseases', *Atherosclerosis*, vol. 154, no. 2, pp. 255-67.

Granchelli, JA, Pollina, C & Hudecki, MS 2000, 'Pre-clinical screening of drugs using the *mdx* mouse', *Neuromuscul Disord*, vol. 10, no. 4-5, pp. 235-9.

Gregorevic, P, Plant, DR & Lynch, GS 2004, 'Administration of insulin-like growth factor-I improves fatigue resistance of skeletal muscles from dystrophic *mdx* mice', *Muscle Nerve*, vol. 30, no. 3, pp. 295-304.

Gregorevic, P, Plant, DR, Leeding, KS, Bach, LA & Lynch, GS 2002, 'Improved contractile function of the *mdx* dystrophic mouse diaphragm muscle after insulin-like growth factor-I administration', *Am J Pathol*, vol. 161, no. 6, pp. 2263-72.

Gregorevic, P, Blankinship, MJ, Allen, JM, Crawford, RW, Meuse, L, Miller, DG, Russell, DW & Chamberlain, JS 2004, 'Systemic delivery of genes to striated muscles using adeno-associated viral vectors', *Nat Med*, vol. 10, no. 8, pp. 828-34.

Griggs, RC, Moxley, RT, 3rd, Mendell, JR, Fenichel, GM, Brooke, MH, Pestronk, A, Miller, JP, Cwik, VA, Pandya, S, Robison, J & et al. 1993, 'Duchenne dystrophy: randomized, controlled trial of prednisone (18 months) and azathioprine (12 months)', *Neurology*, vol. 43, no. 3 Pt 1, pp. 520-7.

Grounds, MD & Torrisi, J 2004, 'Anti-TNFalpha (Remicade) therapy protects dystrophic skeletal muscle from necrosis', *Faseb J*, vol. 18, no. 6, pp. 676-82.

Grounds, MD, Davies, M, Torrisi, J, Shavlakadze, T, White, J & Hodgetts, S 2005, 'Silencing TNFalpha activity by using Remicade or Enbrel blocks inflammation in whole muscle grafts: an in vivo bioassay to assess the efficacy of anti-cytokine drugs in mice', *Cell Tissue Res*, vol. 320, no. 3, pp. 509-15.

Gucuyener, K, Ergenekon, E, Erbas, D, Pinarli, G & Serdaroglu, A 2000, 'The serum nitric oxide levels in patients with Duchenne muscular dystrophy', *Brain Dev*, vol. 22, no. 3, pp. 181-3.

Gupta, S & Tripathi, CD 2005, 'Current status of TNF blocking therapy in heart failure', *Indian J Med Sci*, vol. 59, no. 8, pp. 363-6.

Gussoni, E, Pavlath, GK, Lanctot, AM, Sharma, KR, Miller, RG, Steinman, L & Blau, HM 1992, 'Normal dystrophin transcripts detected in Duchenne muscular dystrophy patients after myoblast transplantation', *Nature*, vol. 356, no. 6368, pp. 435-8.

Gussoni, E, Soneoka, Y, Strickland, CD, Buzney, EA, Khan, MK, Flint, AF, Kunkel, LM & Mulligan, RC 1999, 'Dystrophin expression in the *mdx* mouse restored by stem cell transplantation', *Nature*, vol. 401, no. 6751, pp. 390-4.

Gussoni, E, Bennett, RR, Muskiewicz, KR, Meyerrose, T, Nolta, JA, Gilgoff, I, Stein, J, Chan, YM, Lidov, HG, Bonnemann, CG, Von Moers, A, Morris, GE, Den Dunnen, JT, Chamberlain, JS, Kunkel, LM & Weinberg, K 2002, 'Long-term persistence of donor nuclei in a Duchenne muscular dystrophy patient receiving bone marrow transplantation', *J Clin Invest*, vol. 110, no. 6, pp. 807-14.

Hammeren, J, Powers, S, Lawler, J, Criswell, D, Martin, D, Lowenthal, D & Pollock, M 1992, 'Exercise training-induced alterations in skeletal muscle oxidative and antioxidant enzyme activity in senescent rats', *Int J Sports Med*, vol. 13, no. 5, pp. 412-6.

Hara, H, Nolan, PM, Scott, MO, Bucan, M, Wakayama, Y & Fischbeck, KH 2002, 'Running endurance abnormality in *mdx* mice', *Muscle Nerve*, vol. 25, no. 2, pp. 207-11.

Hartel, JV, Granchelli, JA, Hudecki, MS, Pollina, CM & Gosselin, LE 2001, 'Impact of prednisone on TGF-beta1 and collagen in diaphragm muscle from *mdx* mice', *Muscle Nerve*, vol. 24, no. 3, pp. 428-32.

Haycock, JW, Jones, P, Harris, JB & Mantle, D 1996, 'Differential susceptibility of human skeletal muscle proteins to free radical induced oxidative damage: a histochemical, immunocytochemical and electron microscopical study in vitro', *Acta Neuropathol (Berl)*, vol. 92, no. 4, pp. 331-40.

Hayes, A & Williams, DA 1998, 'Contractile function and low-intensity exercise effects of old dystrophic (*mdx*) mice', *Am J Physiol*, vol. 274, no. 4 Pt 1, pp. C1138-44.

Hayes, A, Lynch, GS & Williams, DA 1993, 'The effects of endurance exercise on dystrophic *mdx* mice. I. Contractile and histochemical properties of intact muscles', *Proc R Soc Lond B Biol Sci*, vol. 253, no. 1336, pp. 19-25.

Head, SI, Williams, DA & Stephenson, DG 1992, 'Abnormalities in structure and function of limb skeletal muscle fibres of dystrophic *mdx* mice', *Proc Biol Sci*, vol. 248, no. 1322, pp. 163-9.

Hernandez, I, de la Torre, P, Rey-Campos, J, Garcia, I, Sanchez, JA, Munoz, R, Rippe, RA, Munoz-Yague, T & Solis-Herruzo, JA 2000, 'Collagen alpha1(I) gene contains an element responsive to tumor necrosis factor-alpha located in the 5' untranslated region of its first exon', *DNA Cell Biol*, vol. 19, no. 6, pp. 341-52.

Heydemann, A, Huber, JM, Kakkar, R, Wheeler, MT & McNally, EM 2004, 'Functional nitric oxide synthase mislocalization in cardiomyopathy', *J Mol Cell Cardiol*, vol. 36, no. 2, pp. 213-23.

Hoffman, EP, Brown, RH, Jr. & Kunkel, LM 1987, 'Dystrophin: the protein product of the Duchenne muscular dystrophy locus', *Cell*, vol. 51, no. 6, pp. 919-28.

Holloszy, JO 1967, 'Biochemical adaptations in muscle. Effects of exercise on mitochondrial oxygen uptake and respiratory enzyme activity in skeletal muscle', *J Biol Chem*, vol. 242, no. 9, pp. 2278-82.

Hoogerwaard, EM, van der Wouw, PA, Wilde, AA, Bakker, E, Ippel, PF, Oosterwijk, JC, Majoor-Krakauer, DF, van Essen, AJ, Leschot, NJ & de Visser, M 1999, 'Cardiac involvement in carriers of Duchenne and Becker muscular dystrophy', *Neuromuscul Disord*, vol. 9, no. 5, pp. 347-51.

Howard, MT, Anderson, CB, Fass, U, Khatri, S, Gesteland, RF, Atkins, JF & Flanigan, KM 2004, 'Readthrough of dystrophin stop codon mutations induced by aminoglycosides', *Ann Neurol*, vol. 55, no. 3, pp. 422-6.

Huard, J, Li, Y & Fu, FH 2002, 'Muscle injuries and repair: current trends in research', *J Bone Joint Surg Am*, vol. 84-A, no. 5, pp. 822-32.

Hudecki, MS, Pollina, CM, Granchelli, JA, Daly, MK, Byrnes, T, Wang, JC & Hsiao, JC 1993, 'Strength and endurance in the therapeutic evaluation of prednisolone-treated *MDX* mice', *Res Commun Chem Pathol Pharmacol*, vol. 79, no. 1, pp. 45-60.

Ignotz, RA & Massague, J 1986, 'Transforming growth factor-beta stimulates the expression of fibronectin and collagen and their incorporation into the extracellular matrix', *J Biol Chem*, vol. 261, no. 9, pp. 4337-45.

Inashima, S, Matsunaga, S, Yasuda, T & Wada, M 2003, 'Effect of endurance training and acute exercise on sarcoplasmic reticulum function in rat fast- and slow-twitch skeletal muscles', *Eur J Appl Physiol*, vol. 89, no. 2, pp. 142-9.

Intermune 2005, *Pirfenidone*, Intermune, viewed 20 March 2003 2003, <http://www.intermune.com/wt/itmn/pirfenidone>.

Ionasescu, V & Ionasescu, R 1982, 'Increased collagen synthesis by Duchenne myogenic clones', *J Neurol Sci*, vol. 54, no. 1, pp. 79-87.

Isaka, Y, Brees, D, Ikegaya, K, Kaneda, Y, Imai, E, Noble, N & Border, W 1996, 'Gene therapy by skeletal muscle expression of decorin prevents fibrotic disease in rat kidney.' *Nat Med*, vol. 2, no. 4, pp. 418-23.

Iyer, SN, Gurujeyalakshmi, G & Giri, SN 1999a, 'Effects of pirfenidone on procollagen gene expression at the transcriptional level in bleomycin hamster model of lung fibrosis', *J Pharmacol Exp Ther*, vol. 289, no. 1, pp. 211-8.

---- 1999b, 'Effects of pirfenidone on transforming growth factor-beta gene expression at the transcriptional level in bleomycin hamster model of lung fibrosis', *J Pharmacol Exp Ther*, vol. 291, no. 1, pp. 367-73.

Iyer, SN, Hyde, DM & Giri, SN 2000, 'Anti-inflammatory effect of pirfenidone in the bleomycin-hamster model of lung inflammation', *Inflammation*, vol. 24, no. 5, pp. 477-91.

James, TN 1962, 'Observations on the cardiovascular involvement, including the cardiac conduction system, in progressive muscular dystrophy', *Am Heart J*, vol. 63, pp. 48-56.

Jin, H, Yang, R, Li, W, Lu, H, Ryan, AM, Ogasawara, AK, Van Peborgh, J & Paoni, NF 2000, 'Effects of exercise training on cardiac function, gene expression, and apoptosis in rats', *Am J Physiol Heart Circ Physiol*, vol. 279, no. 6, pp. H2994-3002.

Kaibori, M, Yanagida, H, Yokoigawa, N, Hijikawa, T, Kwon, AH, Okumura, T & Kamiyama, Y 2004, 'Effects of pirfenidone on endotoxin-induced liver injury after partial hepatectomy in rats', *Transplant Proc*, vol. 36, no. 7, pp. 1975-6.

Kainulainen, H, Takala, T, Myllyla, R, Hassinen, I & Vihko, V 1983, 'Increased prolyl 4-hydroxylase activity in the myocardium of endurance-trained mice', *Experientia*, vol. 39, no. 10, pp. 1094-5.

Kakulas, BA 1997, 'Problems and potential for gene therapy in Duchenne muscular dystrophy', *Neuromuscul Disord*, vol. 7, no. 5, pp. 319-24.

Kawai, H, Adachi, K, Nishida, Y, Inui, T, Kimura, C & Saito, S 1993, 'Decrease in urinary excretion of 3-methylhistidine by patients with Duchenne muscular dystrophy during glucocorticoid treatment', *J Neurol*, vol. 240, no. 3, pp. 181-6.

Khaidar, A, Marx, M, Lubec, B & Lubec, G 1994, 'L-arginine reduces heart collagen accumulation in the diabetic db/db mouse', *Circulation*, vol. 90, no. 1, pp. 479-83.

Khalil, N, Bereznay, O, Sporn, M & Greenberg, AH 1989, 'Macrophage production of transforming growth factor beta and fibroblast collagen synthesis in chronic pulmonary inflammation', *J Exp Med*, vol. 170, no. 3, pp. 727-37.

Khan, SA, Skaf, MW, Harrison, RW, Lee, K, Minhas, KM, Kumar, A, Fradley, M, Shoukas, AA, Berkowitz, DE & Hare, JM 2003, 'Nitric oxide regulation of myocardial contractility and calcium cycling: independent impact of neuronal and endothelial nitric oxide synthases', *Circ Res*, vol. 92, no. 12, pp. 1322-9.

Kilmer, DD 1998, 'The role of exercise in neuromuscular disease', *Phys Med Rehabil Clin N Am*, vol. 9, no. 1, pp. 115-25, vi.

Kim, NN, Villegas, S, Summerour, SR & Villarreal, FJ 1999, 'Regulation of cardiac fibroblast extracellular matrix production by bradykinin and nitric oxide', *J Mol Cell Cardiol*, vol. 31, no. 2, pp. 457-66.

Kissel, JT, Burrow, KL, Rammohan, KW & Mendell, JR 1991, 'Mononuclear cell analysis of muscle biopsies in prednisone-treated and untreated Duchenne muscular dystrophy. CIDD Study Group', *Neurology*, vol. 41, no. 5, pp. 667-72.

Kobzik, L, Reid, MB, Bredt, DS & Stamler, JS 1994, 'Nitric oxide in skeletal muscle', *Nature*, vol. 372, no. 6506, pp. 546-8.

Koenig, M, Beggs, AH, Moyer, M, Scherpf, S, Heindrich, K, Bettecken, T, Meng, G, Muller, CR, Lindlof, M, Kaariainen, H & et al. 1989, 'The molecular basis for Duchenne versus Becker muscular dystrophy: correlation of severity with type of deletion', *Am J Hum Genet*, vol. 45, no. 4, pp. 498-506.

Krupnick, AS, Zhu, J, Nguyen, T, Kreisel, D, Balsara, KR, Lankford, EB, Clark, CC, Levine, S, Stedman, HH & Shrager, JB 2003, 'Inspiratory loading does not accelerate dystrophy in *mdx* mouse diaphragm: implications for regenerative therapy', *J Appl Physiol*, vol. 94, no. 2, pp. 411-9.

Kunkel, LM & Hoffman, EP 1989, 'Duchenne/Becker muscular dystrophy: a short overview of the gene, the protein, and current diagnostics', *Br Med Bull*, vol. 45, no. 3, pp. 630-43.

Laws, N 2005, 'Characterisation and strategic treatment of dystrophic muscle', Doctoral thesis, University of Southern Queensland.

Laws, N & Hoey, A 2004, 'Progression of kyphosis in *mdx* mice', *J Appl Physiol*, vol. 97, no. 5, pp. 1970-7.

Lee, BS, Margolin, SB & Nowak, RA 1998, 'Pirfenidone: a novel pharmacological agent that inhibits leiomyoma cell proliferation and collagen production', *J Clin Endocrinol Metab*, vol. 83, no. 1, pp. 219-23.

Lefaucheur, JP, Pastoret, C & Sebille, A 1995, 'Phenotype of dystrophinopathy in old *mdx* mice', *Anat Rec*, vol. 242, no. 1, pp. 70-6.

Li, YP & Schwartz, RJ 2001, 'TNF-alpha regulates early differentiation of C2C12 myoblasts in an autocrine fashion', *Faseb J*, vol. 15, no. 8, pp. 1413-5.

Li, YY, McTiernan, CF & Feldman, AM 2000, 'Interplay of matrix metalloproteinases, tissue inhibitors of metalloproteinases and their regulators in cardiac matrix remodeling', *Cardiovasc Res*, vol. 46, no. 2, pp. 214-24.

Liang, KW, Nishikawa, M, Liu, F, Sun, B, Ye, Q & Huang, L 2004, 'Restoration of dystrophin expression in *mdx* mice by intravascular injection of naked DNA containing full-length dystrophin cDNA', *Gene Ther*, vol. 11, no. 11, pp. 901-8.

Lipton, BH 1979, 'Skeletal muscle regeneration in muscular dystrophy', in A Mauro (ed.), *Muscle Regeneration*, Raven Press, New York, pp. 31-40.

Liu, F, Nishikawa, M, Clemens, PR & Huang, L 2001, 'Transfer of full-length Dmd to the diaphragm muscle of Dmd(*mdx*/*mdx*) mice through systemic administration of plasmid DNA', *Mol Ther*, vol. 4, no. 1, pp. 45-51.

Liu, H, Drew, P, Gaugler, AC, Cheng, Y & Visner, GA 2005, 'Pirfenidone inhibits lung allograft fibrosis through L-arginine-arginase pathway', *Am J Transplant*, vol. 5, no. 6, pp. 1256-63.

Liu, M, Yue, Y, Harper, SQ, Grange, RW, Chamberlain, JS & Duan, D 2005, 'Adeno-associated virus-mediated microdystrophin expression protects young *mdx* muscle from contraction-induced injury', *Mol Ther*, vol. 11, no. 2, pp. 245-56.

Louis, M, Lebacq, J, Poortmans, JR, Belpaire-Dethiou, MC, Devogelaer, JP, Van Hecke, P, Goubel, F & Francaux, M 2003, 'Beneficial effects of creatine supplementation in dystrophic patients', *Muscle Nerve*, vol. 27, no. 5, pp. 604-10.

Love, DR, Hill, DF, Dickson, G, Spurr, NK, Byth, BC, Marsden, RF, Walsh, FS, Edwards, YH & Davies, KE 1989, 'An autosomal transcript in skeletal muscle with homology to dystrophin', *Nature*, vol. 339, no. 6219, pp. 55-8.

Lu, QL, Mann, CJ, Lou, F, Bou-Gharios, G, Morris, GE, Xue, SA, Fletcher, S, Partridge, TA & Wilton, SD 2003, 'Functional amounts of dystrophin produced by skipping the mutated exon in the *mdx* dystrophic mouse', *Nat Med*, vol. 9, no. 8, pp. 1009-14.

Lu, S & Hoey, A 2000, 'Changes in function of cardiac receptors mediating the effects of the autonomic nervous system in the muscular dystrophy (*MDX*) mouse', *J Mol Cell Cardiol*, vol. 32, no. 1, pp. 143-52.

Lynch, GS, Fary, CJ & Williams, DA 1997, 'Quantitative measurement of resting skeletal muscle [Ca2+]i following acute and long-term downhill running exercise in mice', *Cell Calcium*, vol. 22, no. 5, pp. 373-83.

Lynch, GS, Hinkle, RT, Chamberlain, JS, Brooks, SV & Faulkner, JA 2001, 'Force and power output of fast and slow skeletal muscles from *mdx* mice 6-28 months old', *J Physiol*, vol. 535, no. Pt 2, pp. 591-600.

Maher, TJ 2000, *L-Arginine, Continuing Education Module*, Massachusetts College of Pharmacy and Health Sciences, Massachusetts, February 2000.

Mane, J, Fernandez-Banares, F, Ojanguren, I, Castella, E, Bertran, X, Bartoli, R, Alvarez, M & Gassull, MA 2001, 'Effect of L-arginine on the course of experimental colitis', *Clin Nutr*, vol. 20, no. 5, pp. 415-22.

Mann, CJ, Honeyman, K, Cheng, AJ, Ly, T, Lloyd, F, Fletcher, S, Morgan, JE, Partridge, TA & Wilton, SD 2001, 'Antisense-induced exon skipping and synthesis of dystrophin in the *mdx* mouse', *Proc Natl Acad Sci U S A*, vol. 98, no. 1, pp. 42-7.

Matsumura, K & Campbell, KP 1993, 'Deficiency of dystrophin-associated proteins: a common mechanism leading to muscle cell necrosis in severe childhood muscular dystrophies', *Neuromuscul Disord*, vol. 3, no. 2, pp. 109-18.

Mauviel, A 2005, 'Transforming growth factor-beta: a key mediator of fibrosis', *Methods Mol Med*, vol. 117, pp. 69-80.

McArdle, A, Edwards, RH & Jackson, MJ 1995, 'How does dystrophin deficiency lead to muscle degeneration?--evidence from the *mdx* mouse', *Neuromuscul Disord*, vol. 5, no. 6, pp. 445-56.

McCroskery, S, Thomas, M, Maxwell, L, Sharma, M & Kambadur, R 2003, 'Myostatin negatively regulates satellite cell activation and self-renewal', *J Cell Biol*, vol. 162, no. 6, pp. 1135-47.

McDonald, CM, Abresch, RT, Carter, GT, Fowler, WM, Jr., Johnson, ER, Kilmer, DD & Sigford, BJ 1995, 'Profiles of neuromuscular diseases. Duchenne muscular dystrophy', *Am J Phys Med Rehabil*, vol. 74, no. 5 Suppl, pp. S70-92.

McNeil, PL & Khakee, R 1992, 'Disruptions of muscle fiber plasma membranes. Role in exercise-induced damage', *Am J Pathol*, vol. 140, no. 5, pp. 1097-109.

McPherron, AC & Lee, SJ 1997, 'Double muscling in cattle due to mutations in the myostatin gene', *Proc Natl Acad Sci U S A*, vol. 94, no. 23, pp. 12457-61.

Melacini, P, Vianello, A, Villanova, C, Fanin, M, Miorin, M, Angelini, C & Dalla Volta, S 1996, 'Cardiac and respiratory involvement in advanced stage Duchenne muscular dystrophy', *Neuromuscul Disord*, vol. 6, no. 5, pp. 367-76.

Mendell, JR, Kissel, JT, Amato, AA, King, W, Signore, L, Prior, TW, Sahenk, Z, Benson, S, McAndrew, PE, Rice, R & et al. 1995, 'Myoblast transfer in the treatment of Duchenne's muscular dystrophy', *N Engl J Med*, vol. 333, no. 13, pp. 832-8.

Merlini, L, Cicognani, A, Malaspina, E, Gennari, M, Gnudi, S, Talim, B & Franzoni, E 2003, 'Early prednisone treatment in Duchenne muscular dystrophy', *Muscle Nerve*, vol. 27, no. 2, pp. 222-7.

Mesa, LE, Dubrovsky, AL, Corderi, J, Marco, P & Flores, D 1991, 'Steroids in Duchenne muscular dystrophy--deflazacort trial', *Neuromuscul Disord*, vol. 1, no. 4, pp. 261-6.

Metzinger, L, Passaquin, AC, Leijendekker, WJ, Poindron, P & Ruegg, UT 1995, 'Modulation by prednisolone of calcium handling in skeletal muscle cells', *Br J Pharmacol*, vol. 116, no. 7, pp. 2811-6.

Michalak, M & Opas, M 1997, 'Functions of dystrophin and dystrophin associated proteins', *Curr Opin Neurol*, vol. 10, no. 5, pp. 436-42.

Milani, S, Herbst, H, Schuppan, D, Stein, H & Surrenti, C 1991, 'Transforming growth factors beta 1 and beta 2 are differentially expressed in fibrotic liver disease', *Am J Pathol*, vol. 139, no. 6, pp. 1221-9.

Miric, G, Dallemagne, C, Endre, Z, Margolin, S, Taylor, SM & Brown, L 2001, 'Reversal of cardiac and renal fibrosis by pirfenidone and spironolactone in streptozotocin-diabetic rats', *Br J Pharmacol*, vol. 133, no. 5, pp. 687-94.

Mirkovic, S, Seymour, AM, Fenning, A, Strachan, A, Margolin, SB, Taylor, SM & Brown, L 2002, 'Attenuation of cardiac fibrosis by pirfenidone and amiloride in DOCA-salt hypertensive rats', *Br J Pharmacol*, vol. 135, no. 4, pp. 961-8.

Mirsky, I & Parmley, WW 1973, 'Assessment of passive elastic stiffness for isolated eart muscle and the intact heart', *Circ Res*, vol. 33, no. 2, pp. 233-43.

Morrison, J, Lu, QL, Pastoret, C, Partridge, T & Bou-Gharios, G 2000, 'T-cell-dependent fibrosis in the *mdx* dystrophic mouse', *Lab Invest*, vol. 80, no. 6, pp. 881-91.

Muller, J, Vayssiere, N, Royuela, M, Leger, ME, Muller, A, Bacou, F, Pons, F, Hugon, G & Mornet, D 2001, 'Comparative evolution of muscular dystrophy in diaphragm, gastrocnemius and masseter muscles from old male *mdx* mice', *J Muscle Res Cell Motil*, vol. 22, no. 2, pp. 133-9.

Muntoni, F, Fisher, I, Morgan, JE & Abraham, D 2002, 'Steroids in Duchenne muscular dystrophy: from clinical trials to genomic research', *Neuromuscul Disord*, vol. 12 Suppl 1, pp. S162-5.

Murakami, N, McLennan, IS, Nonaka, I, Koishi, K, Baker, C & Hammond-Tooke, G 1999, 'Transforming growth factor-beta2 is elevated in skeletal muscle disorders', *Muscle Nerve*, vol. 22, no. 7, pp. 889-98.

Nakamura, A, Yoshida, K, Takeda, S, Dohi, N & Ikeda, S 2002, 'Progression of dystrophic features and activation of mitogen-activated protein kinases and calcineurin by physical exercise, in hearts of *mdx* mice', *FEBS Lett*, vol. 520, no. 1-3, pp. 18-24.

Nakane, M, Schmidt, HH, Pollock, JS, Forstermann, U & Murad, F 1993, 'Cloned human brain nitric oxide synthase is highly expressed in skeletal muscle', *FEBS Lett*, vol. 316, no. 2, pp. 175-80.

Nakazato, H, Oku, H, Yamane, S, Tsuruta, Y & Suzuki, R 2002, 'A novel anti-fibrotic agent pirfenidone suppresses tumor necrosis factor-alpha at the translational level', *Eur J Pharmacol*, vol. 446, no. 1-3, pp. 177-85.

Nguyen, HX & Tidball, JG 2003, 'Expression of a muscle-specific, nitric oxide synthase transgene prevents muscle membrane injury and reduces muscle inflammation during modified muscle use in mice', *J Physiol*, vol. 550, no. Pt 2, pp. 347-56.

Nicoletti, A & Michel, JB 1999, 'Cardiac fibrosis and inflammation: interaction with hemodynamic and hormonal factors', *Cardiovasc Res*, vol. 41, no. 3, pp. 532-43.

Nicoletti, A, Heudes, D, Mandet, C, Hinglais, N, Bariety, J & Michel, JB 1996, 'Inflammatory cells and myocardial fibrosis: spatial and temporal distribution in renovascular hypertensive rats', *Cardiovasc Res*, vol. 32, no. 6, pp. 1096-107.

Niebroj-Dobosz, I, Fidzianska, A & Hausmanowa-Petrusewicz, I 2001, 'Controversies about the function of dystrophin in muscle', *Folia Neuropathol*, vol. 39, no. 4, pp. 253-8.

Nigro, G, Comi, LI, Politano, L & Bain, RJ 1990, 'The incidence and evolution of cardiomyopathy in Duchenne muscular dystrophy', *Int J Cardiol*, vol. 26, no. 3, pp. 271-7.

Norton, GR, Tsotetsi, J, Trifunovic, B, Hartford, C, Candy, GP & Woodiwiss, AJ 1997, 'Myocardial stiffness is attributed to alterations in cross-linked collagen rather than total collagen or phenotypes in spontaneously hypertensive rats', *Circulation*, vol. 96, no. 6, pp. 1991-8.

Nowak, KJ & Davies, KE 2004, 'Duchenne muscular dystrophy and dystrophin: pathogenesis and opportunities for treatment', *EMBO Rep*, vol. 5, no. 9, pp. 872-6.

O'Brien, KF & Kunkel, LM 2001, 'Dystrophin and muscular dystrophy: past, present, and future', *Mol Genet Metab*, vol. 74, no. 1-2, pp. 75-88.

Okano, T, Yoshida, K, Nakamura, A, Sasazawa, F, Oide, T, Takeda, S & Ikeda, S 2005, 'Chronic exercise accelerates the degeneration-regeneration cycle and

downregulates insulin-like growth factor-1 in muscle of *mdx* mice', *Muscle Nerve*, vol. 32, no. 2, pp. 191-9.

Pagel, CN & Partridge, TA 1999, 'Covert persistence of *mdx* mouse myopathy is revealed by acute and chronic effects of irradiation', *J Neurol Sci*, vol. 164, no. 2, pp. 103-16.

Palmer, RM, Ashton, DS & Moncada, S 1988, 'Vascular endothelial cells synthesize nitric oxide from L-arginine', *Nature*, vol. 333, no. 6174, pp. 664-6.

Partridge, T 1991, 'Animal models of muscular dystrophy--what can they teach us?' *Neuropathol Appl Neurobiol*, vol. 17, no. 5, pp. 353-63.

Passaquin, AC, Metzinger, L, Leger, JJ, Warter, JM & Poindron, P 1993, 'Prednisolone enhances myogenesis and dystrophin-related protein in skeletal muscle cell cultures from *mdx* mouse', *J Neurosci Res*, vol. 35, no. 4, pp. 363-72.

Passerini, L, Bernasconi, P, Baggi, F, Confalonieri, P, Cozzi, F, Cornelio, F & Mantegazza, R 2002, 'Fibrogenic cytokines and extent of fibrosis in muscle of dogs with X-linked golden retriever muscular dystrophy', *Neuromuscul Disord*, vol. 12, no. 9, pp. 828-35.

Pastoret, C & Sebille, A 1995a, '*mdx* mice show progressive weakness and muscle deterioration with age', *J Neurol Sci*, vol. 129, no. 2, pp. 97-105.

---- 1995b, 'Age-related differences in regeneration of dystrophic (*mdx*) and normal muscle in the mouse', *Muscle Nerve*, vol. 18, no. 10, pp. 1147-54.

Paulus, WJ, Kastner, S, Pujadas, P, Shah, AM, Drexler, H & Vanderheyden, M 1997, 'Left ventricular contractile effects of inducible nitric oxide synthase in the human allograft', *Circulation*, vol. 96, no. 10, pp. 3436-42.

Perloff, JK & Marelli, A 1992, 'Neurological and psychosocial disorders in adults with congenital heart disease', *Heart Dis Stroke*, vol. 1, no. 4, pp. 218-24.

Perloff, JK, Roberts, WC, de Leon, AC, Jr. & O'Doherty, D 1967, 'The distinctive electrocardiogram of Duchenne's progressive muscular dystrophy. An electrocardiographic-pathologic correlative study', *Am J Med*, vol. 42, no. 2, pp. 179-88.

Porreca, E, Guglielmi, MD, Uncini, A, Di Gregorio, P, Angelini, A, Di Febbo, C, Pierdomenico, SD, Baccante, G & Cuccurullo, F 1999, 'Haemostatic abnormalities, cardiac involvement and serum tumor necrosis factor levels in X-linked dystrophic patients', *Thromb Haemost*, vol. 81, no. 4, pp. 543-6.

Posselt, H 2005, Brisbane.

PTCTherapeutics 2005, *PTC124*, viewed September 22 2005, <http://www.ptcbio.com/discovery1-gen.html>.

Quinlan, JG, Hahn, HS, Wong, BL, Lorenz, JN, Wenisch, AS & Levin, LS 2004, 'Evolution of the *mdx* mouse cardiomyopathy: physiological and morphological findings', *Neuromuscul Disord*, vol. 14, no. 8-9, pp. 491-6.

Rando, TA 2001a, 'Role of nitric oxide in the pathogenesis of muscular dystrophies: a "two hit" hypothesis of the cause of muscle necrosis', *Microsc Res Tech*, vol. 55, no. 4, pp. 223-35.

---- 2001b, 'The dystrophin-glycoprotein complex, cellular signaling, and the regulation of cell survival in the muscular dystrophies', *Muscle Nerve*, vol. 24, no. 12, pp. 1575-94.

---- 2002, 'Oxidative stress and the pathogenesis of muscular dystrophies', *Am J Phys Med Rehabil*, vol. 81, no. 11 Suppl, pp. S175-86.

Rando, TA, Disatnik, MH, Yu, Y & Franco, A 1998, 'Muscle cells from *mdx* mice have an increased susceptibility to oxidative stress', *Neuromuscul Disord*, vol. 8, no. 1, pp. 14-21.

Rifai, Z, Welle, S, Moxley, RT, 3rd, Lorenson, M & Griggs, RC 1995, 'Effect of prednisone on protein metabolism in Duchenne dystrophy', *Am J Physiol*, vol. 268, no. 1 Pt 1, pp. E67-74.

Romero, NB, Braun, S, Benveniste, O, Leturcq, F, Hogrel, JY, Morris, GE, Barois, A, Eymard, B, Payan, C, Ortega, V, Boch, AL, Lejean, L, Thioudellet, C, Mourot, B, Escot, C, Choquel, A, Recan, D, Kaplan, JC, Dickson, G, Klatzmann, D, Molinier-Frenckel, V, Guillet, JG, Squiban, P, Herson, S & Fardeau, M 2004, 'Phase I study of dystrophin plasmid-based gene therapy in Duchenne/Becker muscular dystrophy', *Hum Gene Ther*, vol. 15, no. 11, pp. 1065-76.

Russell-Jones, DL, Umpleby, AM, Hennessy, TR, Bowes, SB, Shojaee-Moradie, F, Hopkins, KD, Jackson, NC, Kelly, JM, Jones, RH & Sonksen, PH 1994, 'Use of a leucine clamp to demonstrate that IGF-I actively stimulates protein synthesis in normal humans', *Am J Physiol*, vol. 267, no. 4 Pt 1, pp. E591-8.

Sacco, P, Jones, DA, Dick, JR & Vrbova, G 1992, 'Contractile properties and susceptibility to exercise-induced damage of normal and *mdx* mouse tibialis anterior muscle', *Clin Sci (Lond)*, vol. 82, no. 2, pp. 227-36.

Sampaolesi, M, Torrente, Y, Innocenzi, A, Tonlorenzi, R, D'Antona, G, Pellegrino, MA, Barresi, R, Bresolin, N, De Angelis, MG, Campbell, KP, Bottinelli, R & Cossu, G 2003, 'Cell therapy of alpha-sarcoglycan null dystrophic mice through intra-arterial delivery of mesoangioblasts', *Science*, vol. 301, no. 5632, pp. 487-92.

Sander, M, Chavoshan, B, Harris, SA, Iannaccone, ST, Stull, JT, Thomas, GD & Victor, RG 2000, 'Functional muscle ischemia in neuronal nitric oxide synthase-deficient skeletal muscle of children with Duchenne muscular dystrophy', *Proc Natl Acad Sci U S A*, vol. 97, no. 25, pp. 13818-23.

Sapp, JL, Bobet, J & Howlett, SE 1996, 'Contractile properties of myocardium are altered in dystrophin-deficient *mdx* mice', *J Neurol Sci*, vol. 142, no. 1-2, pp. 17-24.

Scheinowitz, M, Kessler-Icekson, G, Freimann, S, Zimmermann, R, Schaper, W, Golomb, E, Savion, N & Eldar, M 2003, 'Short- and long-term swimming exercise training increases myocardial insulin-like growth factor-I gene expression', *Growth Horm IGF Res*, vol. 13, no. 1, pp. 19-25.

Sears, CE, Bryant, SM, Ashley, EA, Lygate, CA, Rakovic, S, Wallis, HL, Neubauer, S, Terrar, DA & Casadei, B 2003, 'Cardiac neuronal nitric oxide synthase isoform regulates myocardial contraction and calcium handling', *Circ Res*, vol. 92, no. 5, pp. e52-9.

Segalat, L, Grisoni, K, Archer, J, Vargas, C, Bertrand, A & Anderson, JE 2005, 'CAPON expression in skeletal muscle is regulated by position, repair, NOS activity, and dystrophy', *Exp Cell Res*, vol. 302, no. 2, pp. 170-9.

Shavlakadze, T, White, J, Hoh, JF, Rosenthal, N & Grounds, MD 2004, 'Targeted expression of insulin-like growth factor-I reduces early myofiber necrosis in dystrophic *mdx* mice', *Mol Ther*, vol. 10, no. 5, pp. 829-43.

Shimizu, T, Kuroda, T, Hata, S, Fukagawa, M, Margolin, SB & Kurokawa, K 1998, 'Pirfenidone improves renal function and fibrosis in the post-obstructed kidney', *Kidney Int*, vol. 54, no. 1, pp. 99-109.

Shimizu, T, Fukagawa, M, Kuroda, T, Hata, S, Iwasaki, Y, Nemoto, M, Shirai, K, Yamauchi, S, Margolin, SB, Shimizu, F & Kurokawa, K 1997, 'Pirfenidone prevents collagen accumulation in the remnant kidney in rats with partial nephrectomy', *Kidney Int Suppl*, vol. 63, pp. S239-43.

Sicinski, P, Geng, Y, Ryder-Cook, AS, Barnard, EA, Darlison, MG & Barnard, PJ 1989, 'The molecular basis of muscular dystrophy in the *mdx* mouse: a point mutation', *Science*, vol. 244, no. 4912, pp. 1578-80.

Silversides, CK, Webb, GD, Harris, VA & Biggar, DW 2003, 'Effects of deflazacort on left ventricular function in patients with Duchenne muscular dystrophy', *Am J Cardiol*, vol. 91, no. 6, pp. 769-72.

Siwik, DA & Colucci, WS 2004, 'Regulation of matrix metalloproteinases by cytokines and reactive oxygen/nitrogen species in the myocardium', *Heart Fail Rev*, vol. 9, no. 1, pp. 43-51.

Skrabek, RQ & Anderson, JE 2001, 'Metabolic shifts and myocyte hypertrophy in deflazacort treatment of *mdx* mouse cardiomyopathy', *Muscle Nerve*, vol. 24, no. 2, pp. 192-202.

Skuk, D 2004, 'Myoblast transplantation for inherited myopathies: a clinical approach', *Expert Opin Biol Ther*, vol. 4, no. 12, pp. 1871-85.

Smith, TW, Balligand, JL, Kaye, DM, Wiviott, SD, Simmons, WW, Han, X, Michel, T, Singh, K & Kelly, RA 1996, 'The role of the NO pathway in the control of cardiac function', *J Card Fail*, vol. 2, no. 4 Suppl, pp. S141-7.

Soares, JC, Folmer, V & Rocha, JB 2003, 'Influence of dietary selenium supplementation and exercise on thiol-containing enzymes in mice', *Nutrition*, vol. 19, no. 7-8, pp. 627-32.

Spence, HJ, Chen, YJ & Winder, SJ 2002, 'Muscular dystrophies, the cytoskeleton and cell adhesion', *Bioessays*, vol. 24, no. 6, pp. 542-52.

Spencer, MJ, Croall, DE & Tidball, JG 1995, 'Calpains are activated in necrotic fibers from *mdx* dystrophic mice', *J Biol Chem*, vol. 270, no. 18, pp. 10909-14.

Spencer, MJ, Marino, MW & Winckler, WM 2000, 'Altered pathological progression of diaphragm and quadriceps muscle in TNF-deficient, dystrophin-deficient mice', *Neuromuscul Disord*, vol. 10, no. 8, pp. 612-9.

Spinale, FG 2002, 'Matrix metalloproteinases: regulation and dysregulation in the failing heart', *Circ Res*, vol. 90, no. 5, pp. 520-30.

Stedman, HH, Sweeney, HL, Shrager, JB, Maguire, HC, Panettieri, RA, Petrof, B, Narusawa, M, Leferovich, JM, Sladky, JT & Kelly, AM 1991, 'The *mdx* mouse diaphragm reproduces the degenerative changes of Duchenne muscular dystrophy', *Nature*, vol. 352, no. 6335, pp. 536-9.

St-Pierre, SJ, Chakkalakal, JV, Kolodziejczyk, SM, Knudson, JC, Jasmin, BJ & Megeney, LA 2004, 'Glucocorticoid treatment alleviates dystrophic myofiber pathology by activation of the calcineurin/NF-AT pathway', *Faseb J*, vol. 18, no. 15, pp. 1937-9.

Susic, D, Francischetti, A & Frohlich, ED 1999, 'Prolonged L-arginine on cardiovascular mass and myocardial hemodynamics and collagen in aged spontaneously hypertensive rats and normal rats', *Hypertension*, vol. 33, no. 1 Pt 2, pp. 451-5.

Susic, D, Varagic, J & Frohlich, ED 2001, 'Isolated systolic hypertension in elderly WKY is reversed with L-arginine and ACE inhibition', *Hypertension*, vol. 38, no. 6, pp. 1422-6.

Tada, S, Nakamuta, M, Enjoji, M, Sugimoto, R, Iwamoto, H, Kato, M, Nakashima, Y & Nawata, H 2001, 'Pirfenidone inhibits dimethylnitrosamine-induced hepatic fibrosis in rats', *Clin Exp Pharmacol Physiol*, vol. 28, no. 7, pp. 522-7.

Tanaka, N, Ryoke, T, Hongo, M, Mao, L, Rockman, HA, Clark, RG & Ross, J, Jr. 1998, 'Effects of growth hormone and IGF-I on cardiac hypertrophy and gene expression in mice', *Am J Physiol*, vol. 275, no. 2 Pt 2, pp. H393-9.

Tay, JS, Lai, PS, Low, PS, Lee, WL & Gan, GC 1992, 'Pathogenesis of Duchenne muscular dystrophy: the calcium hypothesis revisited', *J Paediatr Child Health*, vol. 28, no. 4, pp. 291-3.

Theiss, AL, Simmons, JG, Jobin, C & Lund, PK 2005, 'Tumor necrosis factor alpha increases collagen accumulation and proliferation in intestinal myofibroblasts via TNF receptor 2', *J Biol Chem*.

Thomas, GD, Sander, M, Lau, KS, Huang, PL, Stull, JT & Victor, RG 1998, 'Impaired metabolic modulation of alpha-adrenergic vasoconstriction in dystrophin-deficient skeletal muscle', *Proc Natl Acad Sci U S A*, vol. 95, no. 25, pp. 15090-5.

Tidball, JG & Wehling-Henricks, M 2004, 'Evolving therapeutic strategies for Duchenne muscular dystrophy: targeting downstream events', *Pediatr Res*, vol. 56, no. 6, pp. 831-41.

Tinsley, J, Deconinck, N, Fisher, R, Kahn, D, Phelps, S, Gillis, JM & Davies, K 1998, 'Expression of full-length utrophin prevents muscular dystrophy in *mdx* mice', *Nat Med*, vol. 4, no. 12, pp. 1441-4.

Tinsley, JM, Blake, DJ, Roche, A, Fairbrother, U, Riss, J, Byth, BC, Knight, AE, Kendrick-Jones, J, Suthers, GK, Love, DR & et al. 1992, 'Primary structure of dystrophin-related protein', *Nature*, vol. 360, no. 6404, pp. 591-3.

Todorovic, Z, Prostran, M & Vuckovic, S 2001, 'The influence of L-arginine on heart rate and tissue oxygen extraction in haemorrhaged rabbits', *Pharmacol Res*, vol. 43, no. 4, pp. 321-7.

Tremblay, JP, Malouin, F, Roy, R, Huard, J, Bouchard, JP, Satoh, A & Richards, CL 1993, 'Results of a triple blind clinical study of myoblast transplantations without immunosuppressive treatment in young boys with Duchenne muscular dystrophy', *Cell Transplant*, vol. 2, no. 2, pp. 99-112.

Valentine, BA, Cooper, BJ, Cummings, JF & de Lahunta, A 1990, 'Canine X-linked muscular dystrophy: morphologic lesions', *J Neurol Sci*, vol. 97, no. 1, pp. 1-23.

Vilquin, JT, Brussee, V, Asselin, I, Kinoshita, I, Gingras, M & Tremblay, JP 1998, 'Evidence of *mdx* mouse skeletal muscle fragility in vivo by eccentric running exercise', *Muscle Nerve*, vol. 21, no. 5, pp. 567-76.

Vilquin, JT, Kennel, PF, Paturneau-Jouas, M, Chapdelaine, P, Boissel, N, Delaere, P, Tremblay, JP, Scherman, D, Fiszman, MY & Schwartz, K 2001, 'Electrotransfer of naked DNA in the skeletal muscles of animal models of muscular dystrophies', *Gene Ther*, vol. 8, no. 14, pp. 1097-107.

Voisin, V, Sebrie, C, Matecki, S, Yu, H, Gillet, B, Ramonatxo, M, Israel, M & De la Porte, S 2005, 'L-arginine improves dystrophic phenotype in *mdx* mice', *Neurobiol Dis*, vol. 20, no. 1, pp. 123-30.

Wagner, KR, McPherron, AC, Winik, N & Lee, SJ 2002, 'Loss of myostatin attenuates severity of muscular dystrophy in *mdx* mice', *Ann Neurol*, vol. 52, no. 6, pp. 832-6.

Walker, JE, Giri, SN & Margolin, SB 2005, 'A double-blind, randomized, controlled study of oral pirfenidone for treatment of secondary progressive multiple sclerosis', *Mult Scler*, vol. 11, no. 2, pp. 149-58.

Weber, KT, Pick, R, Jalil, JE, Janicki, JS & Carroll, EP 1989, 'Patterns of myocardial fibrosis', *J Mol Cell Cardiol*, vol. 21 Suppl 5, pp. 121-31.

Wehling, M, Spencer, MJ & Tidball, JG 2001, 'A nitric oxide synthase transgene ameliorates muscular dystrophy in *mdx* mice', *J Cell Biol*, vol. 155, no. 1, pp. 123-31.

Wehling-Henricks, M, Lee, JJ & Tidball, JG 2004, 'Prednisolone decreases cellular adhesion molecules required for inflammatory cell infiltration in dystrophin-deficient skeletal muscle', *Neuromuscul Disord*, vol. 14, no. 8-9, pp. 483-90.

Wehling-Henricks, M, Jordan, MC, Roos, KP, Deng, B & Tidball, JG 2005, 'Cardiomyopathy in dystrophin-deficient hearts is prevented by expression of a neuronal nitric oxide synthase transgene in the myocardium', *Hum Mol Genet*, vol. 14, no. 14, pp. 1921-33.

Weller, B, Karpati, G & Carpenter, S 1990, 'Dystrophin-deficient *mdx* muscle fibers are preferentially vulnerable to necrosis induced by experimental lengthening contractions', *J Neurol Sci*, vol. 100, no. 1-2, pp. 9-13.

Wells, KE, Fletcher, S, Mann, CJ, Wilton, SD & Wells, DJ 2003, 'Enhanced in vivo delivery of antisense oligonucleotides to restore dystrophin expression in adult *mdx* mouse muscle', *FEBS Lett*, vol. 552, no. 2-3, pp. 145-9.

Wilding, JR, Schneider, JE, Sang, AE, Davies, KE, Neubauer, S & Clarke, K 2005, 'Dystrophin- and MLP-deficient mouse hearts: marked differences in morphology and function, but similar accumulation of cytoskeletal proteins', *Faseb J*, vol. 19, no. 1, pp. 79-81.

Willis, PE, Chadan, S, Baracos, V & Parkhouse, WS 1997, 'Acute exercise attenuates age-associated resistance to insulin-like growth factor I', *Am J Physiol*, vol. 272, no. 3 Pt 1, pp. E397-404.

Willis, PE, Chadan, SG, Baracos, V & Parkhouse, WS 1998, 'Restoration of insulin-like growth factor I action in skeletal muscle of old mice', *Am J Physiol*, vol. 275, no. 3 Pt 1, pp. E525-30.

Wineinger, MA, Abresch, RT, Walsh, SA & Carter, GT 1998, 'Effects of aging and voluntary exercise on the function of dystrophic muscle from *mdx* mice', *Am J Phys Med Rehabil*, vol. 77, no. 1, pp. 20-7.

Wong, BL & Christopher, C 2002, 'Corticosteroids in Duchenne muscular dystrophy: a reappraisal', *J Child Neurol*, vol. 17, no. 3, pp. 183-90.

Woodiwiss, AJ, Oosthuyse, T & Norton, GR 1998, 'Reduced cardiac stiffness following exercise is associated with preserved myocardial collagen characteristics in the rat', *Eur J Appl Physiol Occup Physiol*, vol. 78, no. 2, pp. 148-54.

Xu, L, Eu, JP, Meissner, G & Stamler, JS 1998, 'Activation of the cardiac calcium release channel (ryanodine receptor) by poly-S-nitrosylation', *Science*, vol. 279, no. 5348, pp. 234-7.

Yilmaz, O, Karaduman, A & Topaloglu, H 2004, 'Prednisolone therapy in Duchenne muscular dystrophy prolongs ambulation and prevents scoliosis', *Eur J Neurol*, vol. 11, no. 8, pp. 541-4.

Yue, Y, Li, Z, Harper, SQ, Davisson, RL, Chamberlain, JS & Duan, D 2003, 'Microdystrophin gene therapy of cardiomyopathy restores dystrophin-glycoprotein complex and improves sarcolemma integrity in the *mdx* mouse heart', *Circulation*, vol. 108, no. 13, pp. 1626-32.

Zeman, RJ, Peng, H, Danon, MJ & Etlinger, JD 2000, 'Clenbuterol reduces degeneration of exercised or aged dystrophic (*mdx*) muscle', *Muscle Nerve*, vol. 23, no. 4, pp. 521-8.

Zhang, G, Ludtke, JJ, Thioudellet, C, Kleinpeter, P, Antoniou, M, Herweijer, H, Braun, S & Wolff, JA 2004, 'Intraarterial delivery of naked plasmid DNA expressing full-length mouse dystrophin in the *mdx* mouse model of duchenne muscular dystrophy', *Hum Gene Ther*, vol. 15, no. 8, pp. 770-82.

Ziegelstein, RC 2005, 'Prescribing antitumor necrosis factor drugs to patients with heart failure', *Arch Intern Med*, vol. 165, no. 1, pp. 118-9.

Zieman, SJ, Gerstenblith, G, Lakatta, EG, Rosas, GO, Vandegaer, K, Ricker, KM & Hare, JM 2001, 'Upregulation of the nitric oxide-cGMP pathway in aged myocardium: physiological response to l-arginine', *Circ Res*, vol. 88, no. 1, pp. 97-102.

Zimmerman, SD, Thomas, DP, Velleman, SG, Li, X, Hansen, TR & McCormick, RJ 2001, 'Time course of collagen and decorin changes in rat cardiac and skeletal muscle post-MI', *Am J Physiol Heart Circ Physiol*, vol. 281, no. 4, pp. H1816-22.

APPENDIX

A1: Optimising Skeletal Muscle Contractility Experiments

A1.1 Introduction

Before the commencement of skeletal muscle experiments, preliminary experiments were conducted to determine the optimum environmental conditions and protocols for the forthcoming experiments. Initially, skeletal muscle organ bath experiments were performed using muscles from euthanased mice. The dissected muscles were placed in ice-cold Krebs-Henseleit solution and were tied between platinum electrodes using cotton thread to tie the muscle. The experimental protocol did not utilise an amplifier and used a protocol where, after the twitch and tetanus experiments, the muscles were exposed to fatigue to determine the strength of the contraction after fatigue and to determine the time to relaxation.

To determine the optimum conditions for future skeletal muscle experiments, the variables mentioned above were individually examined to determine the most favourable to achieve optimal contractile results.

A1.2 Methods

C57BL10ScSn *mdx* (*mdx*) mice were bred at the University of Southern Queensland Animal House, Toowoomba, QLD. Mice were 3 months old at the commencement of experiments. Mice were euthanased with pentobarbitone sodium (Nembutal, Boehringer Ingelheim) at 70 mg/kg administered intraperitoneally. Various experiments were

performed, each with a different variable tested. Each tested variable utilised 4 mice. This n number was considered to be acceptable for experiments of this scale.

A1.2.1 Left Leg verus Right Leg

The following skeletal muscles were dissected from both legs: extensor digitorum longus (EDL) and soleus (SOL). Both the left and right leg muscles were kept separate immediately after dissection, with both legs kept in chilled Krebs-Henseleit solution containing (mM): NaCl, 118; $NaHCO_3$, 25; KCl, 4.7; KH_2PO_4, 1.18; $CaCl_2.2H_2O$, 2.5; $MgSO_4.7H_2O$, 1.16; glucose, 11; bubbled with carbogen, ($95\%O_2$-$5\%CO_2$), until the muscles were tied. The muscles were individually tied around the tendon at either end with cotton thread and with one end attached to a fixed peg and the other end attached to a physiological force transducer (TRI 201, Panlab, Spain). All skeletal muscles were suspended in water-jacketed tissue baths (25°C) containing Krebs-Henseleit buffer bubbled with carbogen. Two parallel platinum electrodes along the length of the muscles provided field stimulation (0.2 ms pulse duration) from a Grass S48 stimulator (West Warwick, RI). Contractile force was recorded via the force transducer connected to a PowerLab recording system (ADInstruments, Castle Hill, NSW, Australia) and analysed using Chart 4.0.

A1.2.2 Chilled versus Frozen Krebs

After euthanasia, the left leg EDL and SOL were kept in chilled Krebs-Henseleit solution and the right leg EDL and SOL were kept on a frozen slush of Krebs-Henseleit solution

until the muscles were tied. The same protocol (A1.2.1) was used for the remainder of the experiment.

A1.2.3 Euthanased versus Anaesthetised

The mice were either euthanased or anaesthetised with Ketamine (100mg/mL) and Xylazine (20mg/mL) before removal of the EDL or SOL muscles. The same experimental protocol (A1.2.1) was utilised, with the anaesthetised mouse being carefully monitored and topped up with anaesthetic until all muscles had been removed.

A1.2.4 Cotton Thread versus Silk Suture

The muscles were tied using either cotton thread or 5.0 silk suture before attaching them to the electrodes. The same experimental protocol (A1.2.1) was utilised. It was to be determined which thread (cotton or silk suture) resulted in a greater response when the muscles were stimulated.

A1.2.5 Platinum versus Steel Electrodes

The muscles were dissected as mentioned above and were placed between either platinum or steel electrodes. The muscles were stimulated to determine which type of electrode produced the highest force when stimulating the muscles.

A1.2.6 Amplifier

After these experiments, an amplifier (EP500B, Audio Assemblies, Campbellfield, Victoria, Australia) was trialled to observe the effects of increasing amplitudes during

muscle stimulations. The muscles underwent a protocol where the current, frequency and duration were optimised.

It was known that the optimal preload (L_o) is defined as the length eliciting maximal single twitch force. Optimum voltage, amplitude and the frequency were to be established for each muscle before every experiment . The optimum values obtained from this were to be used for the remainder of the experiment. Reported data would be the average of three individual single-twitch or tetanic stimulations per muscle strip after 25 minutes of equilibration and optimization of conditions.

A1.3 Results

A1.3.1 Left Leg versus Right Leg

Both the left and right EDL and SOL of the mice were tested and it was found that there was no difference in the contractile force in these muscles from either right or left legs. Mice do not appear to have a preference of dexterity.

A1.3.2 Chilled versus Frozen Krebs

Using Krebs stored in the fridge (chilled) or Krebs stored in the freezer (ice-cold) did not cause a variation in force.

A1.3.3 Euthanased versus Anaesthetised

The muscle from the euthanased mice had higher forces of contraction, but the muscles from the anaesthetised mice increased in time to peak force faster than the euthanased mice.

A1.3.4 Cotton Tread versus Silk Suture

Silk suture provided a greater force of contraction than cotton thread. Using suture also eliminated slippage on the tendon.

A1.3.4 Platinum versus Steel Electrodes

The different electrodes did not contribute to a difference in force of contraction.

A1.3.6 Amplifier

A tetanic contraction is a sustained muscle contraction where the muscle is stimulated to twitch rapidly. If there is not enough time for the muscle to relax between these twitches, the twitches summate and a sustained, fused muscle contraction is generated. Initially, both the EDL and SOL muscles were stimulated at a tetanic duration of 1000ms stimulus. After these experiments, it was found that the EDL tetanus fused at a duration of 250ms, whereas the SOL fused at 1000ms duration.

When comparing different amplitudes, it was found that contractions at 7A and 5A produced similar forces.

A force frequency curve was generated by stimulating the muscle at different frequencies to determine which frequency caused the highest force of contraction (Figure A1.1 (A) and (B)).

A

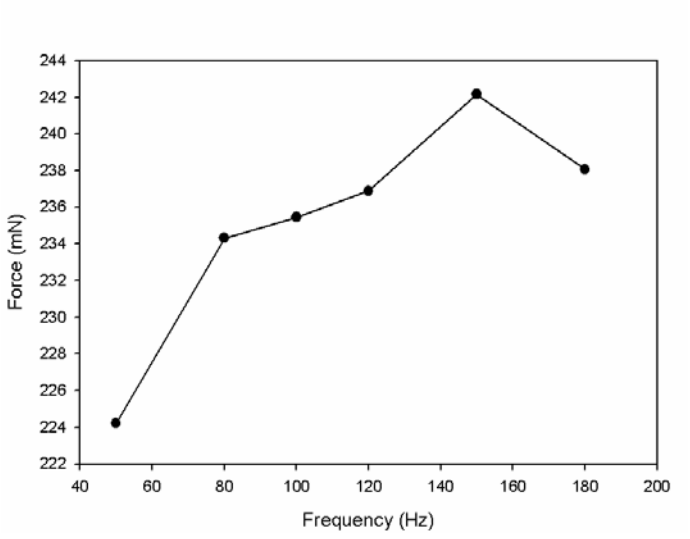

B

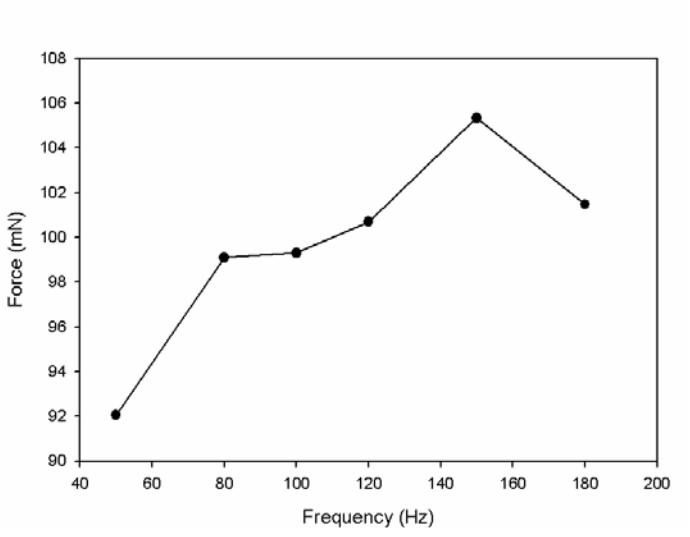

Figure A 1.1: Examples EDL (A) and SOL (B) force frequency curves

A1.4 Discussion

In experiments prior to this protocol re-examination, the left leg was usually used in skeletal muscle organ bath experiments. Due to the conclusion that there is no difference in the right or left leg contractions, it was decided the left leg would continue to be used, although the right leg could also be used confidently, without risk of a difference in dexterity. If the skeletal muscle from the left leg was damaged or not contracting effectively, it was possible to try the same muscle type from the other leg

When dissecting the EDL and SOL of a euthanased mouse, it is a relatively simple and uncomplicated dissection. The leg is able to be manipulated into the correct position to identify, isolate and tie the muscle. In an anaesthetised mouse however, it is very difficult and challenging to tie the muscle successfully and tightly. It is an awkward dissection, which may damage the muscle and subsequently decrease the force observed when comparing the contractions with those from the euthanased mouse.

Many of the previous skeletal muscle experiments used platinum electrodes to provide stimulation to the muscle. For this reason it was decided to continue to use these electrodes, rather than converting to the steel electrodes as there was no difference in contractile force when using either of the electrodes.

Throughout the experiments, it was found that the silk suture provided better results than the cotton thread used to tie the muscles. The suture is much stronger than the cotton

thread. It reduced slippage and provided a better anchor for the muscle, resulting in increased contractile responses of the muscle.

Previous skeletal muscle experiments in the lab used frozen Krebs-Henseleit slush to store the muscle in after dissection and before tying the muscle. There were no differences in contractile force when comparing the muscles stored in frozen or chilled Krebs. It was decided that the muscles would be placed in chilled Krebs rather than frozen Krebs due to the simplicity of using the chilled Krebs (thus also preventing the risk of calcium overload due to rapid cooling contracture (RCC) when the *mdx* muscle is exposed to ice-cold temperatures.

It was decided that due to the EDL fusing at 250ms, this duration would be adopted for the skeletal muscle protocol to reduce the stress put on this muscle and to minimise the damage a 1000ms duration may cause. Similarly to reduce the stress on skeletal muscle, an amplitude of 5A would be implemented rather than the higher 7A which could potentially be detrimental to the muscle for the duration of the experiment. Figure A1.2 shows a typical EDL (A) and SOL (B) contraction.

A

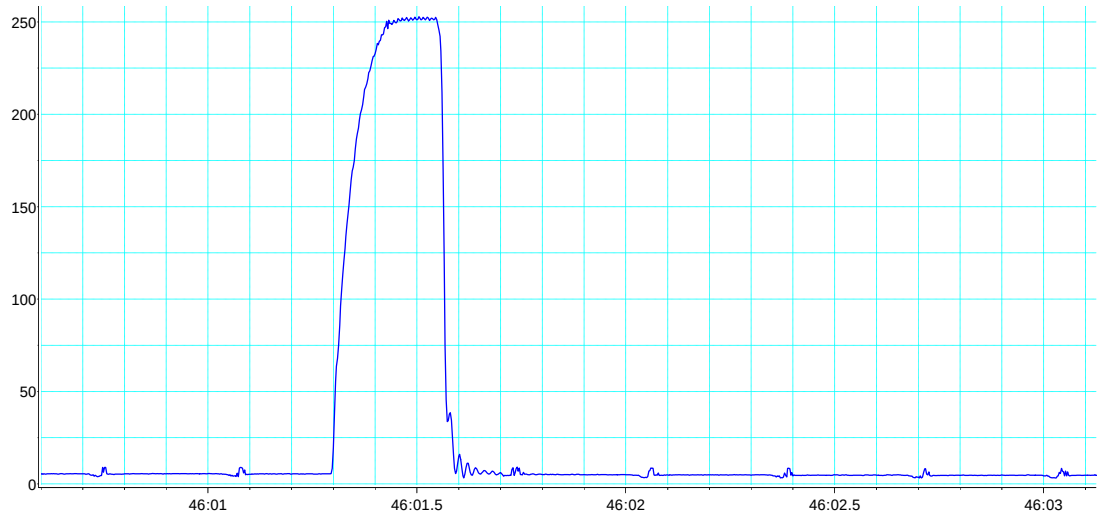

B

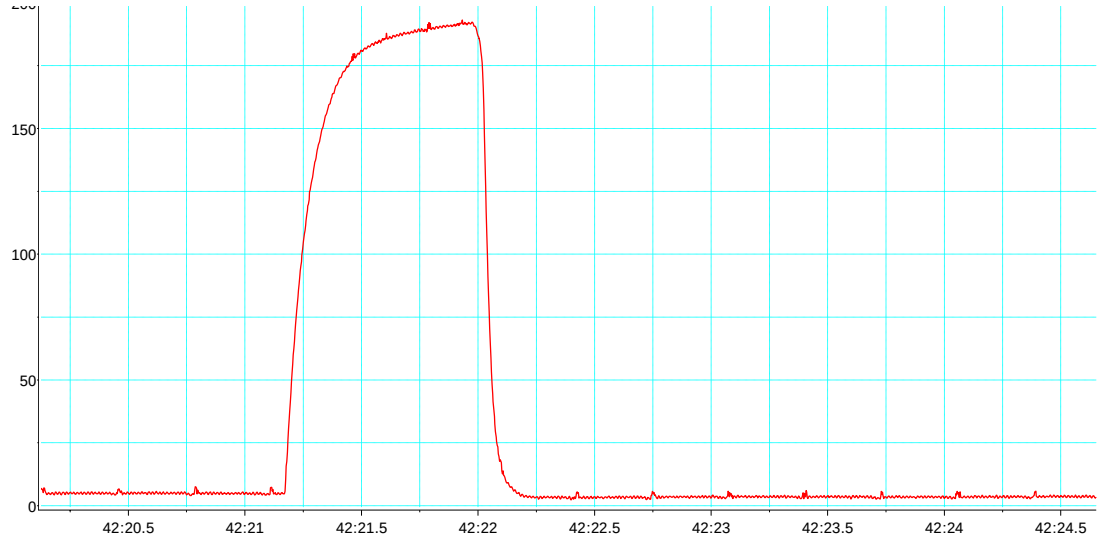

Figure A 1.2: Typical EDL (A) and SOL (B) contractions

A1.5 Conclusions

The final skeletal muscle organ bath protocol (Figure A1.3) was adopted as follows.

Mice are to be euthanased, with the muscle placed in chilled Krebs and tied with suture onto a fixed peg placed between platinum electrodes. Optimum preload was determined

using 1 V, 5 A on Grass S48 stimulator (West Warwick, RI) and the muscle was stimulated to twitch at preloads of 5, 7 and 10 mN. The preload which produced the greatest twitch was set as the optimal preload. The muscle was set at this preload for the remainder of the experiment.

The current continued to be provided at 5 A and the voltage was altered to determine which voltage provided the muscle with the greatest contraction. The stimulator began at 0.4 V and increased by 0.1 V each time up to 1.2V. The optimum voltage was determined and remained constant for the remainder of the experiment. Frequencies were established with the EDL and SOL set at 250 ms and 1000 ms duration respectively. The EDL was stimulated at the following frequencies 10, 30, 50, 80, 100, 120, 150 and 180 Hz. The SOL was stimulated at 10, 20, 30, 50, 80, 100, 120 and 150 Hz. The optimum frequency was the frequency eliciting maximal tetanic force and force frequency curves were created.

Pulse width of 0.2 ms, single twitch
3 minute intervals between twitches
EDL, SOL & DIA dissected from chilled leg

1. Determine optimum preload using 1V, 5A on Ebony amplifier

	10 mN	7 mN	5 mN	3 mN
EDL				
SOL				
DIA				

2. Amp setting 5A stimulator on

	0.4 V	0.5 V	0.6 V	0.7 V	0.8 V	0.9 V	1 V	1.1 V	1.2 V	1.5 V
EDL										
SOL										
DIA										

3. Use optimum settings to conduct 3 single twitches with 3 minute intervals

	1	2	3	**Mean**
EDL				
SOL				
DIA				

4. Use optimum setting to conduct tetanic contractions and measure at various frequencies with 3 minute intervals

EDL at 250 duration
SOL at 1000 duration
DIA at 200 duration

	(13) 50 Hz	(20) 80 Hz	(25) 100 Hz	(30) 120 Hz	(38) 150 Hz	(45) 180 Hz
EDL 1						
EDL 2 at opt. Freq						
EDL 3 at opt. Freq						
Mean						

	50 Hz	80 Hz	100 Hz	120 Hz	150 Hz	180 Hz
SOL 1						
SOL 2 at opt. Freq						
SOL 3 at opt. Freq						
Mean						

Figure A 1.3: Final skeletal muscle experiment protocol and data sheet.

A 2.0: Optimising Langendorff Technique

A2.1 Introduction

Langendorff isolated heart procedures have been well developed and established in many labs. This technique however, had not previously been used in this lab and as such had to be adjusted to suit the *mdx* mouse. The Langendorff isolated heart procedure has been performed extensively using mice in ischaemia reperfusion and cell isolation experiments. This technique is widely used in rats and guinea pigs to determine cardiac function, but also to measure the stiffness of the heart.

To establish this technique in the laboratory at the University of Southern Queensland, several visits to the University of Queensland (St Lucia) and Griffith University (Gold Coast) were necessary. The Langendorff technique at Griffith University used mouse hearts, especially in ischaemia reperfusion experiments without stiffness calculations. At the University of Queensland, the Langendorff technique used rat hearts to calculate cardiac function and stiffness. The technique to be used at the University of Southern Queensland involved a combination of these two methods, using mouse hearts to calculate cardiac function and stiffness. The equipment was acquired from Radnoti and ADInstruments and was independently established. This technique was to be optimised to suit the delicate hearts of *mdx* mice.

The variables to be optimised included optimum perfusion pressure and left ventricular pressure. The effect of increasing balloon volume on the heart was also investigated to determine if high volumes would cause detrimental effects. Contractions against a

workload cause detriment in dystrophic muscles (eg. eccentric exercise); this has not been investigated in detail in dystrophic hearts.

A2.2 Methods

A2.2.1 Animals

Male C57BL/10ScSn mice (control strain) (C57) were purchased from the Animal Resource Centre, Nedlands, WA. Male C57BL10ScSn *mdx* (*mdx*) mice were bred at the University of Southern Queensland Animal House, Toowoomba, QLD. Mice were 12 weeks old at the commencement of experiments. All experimental protocols were conducted with the approval of the University of Southern Queensland Animal Ethics Committee, under the guidelines of the National Health and Medical Research Council of Australia. For both variables tested, both *mdx* (n=10) and C57 (n=10) mice were used.

A2.2.2 Methods

Mice were weighed and anaesthetised with sodium pentobarbital (70mg/kg) administered intraperitoneally. A thoracotomy was performed and hearts were rapidly excised into modified Krebs-Henseleit buffer containing (mM): NaCl, 119; $NaHCO_3$, 22; KCl, 4.7; KH_2PO_4, 1.2; $CaCl_2$, 2.5; $MgSO_4$, 1.2; glucose, 11; Na-pyruvate, 1 and EDTA, 0.5. A small volume of Krebs was frozen and the heart was placed on the ice to isolate the aorta. The aorta was cannulated via the dorsal root and perfused retrogradely at a pressure of 80 mmHg with Krebs-Henseleit perfusion buffer maintained at 37°C and bubbled with carbogen (95%O_2-5%CO_2) to ensure a pH of 7.4. The perfusion fluid was filtered via an in-line Sterivex-HV filter cartridge (0.45 μm, Millipore, Bedford, MA, USA). A small

polyethylene apical drain was used to vent the left ventricle preventing an accumulation of fluid in the heart via Thesbian veins. The left atrium was excised and a fluid filled balloon constructed from polyvinyl chloride plastic film was inserted into the left ventricle via the mitral valve for the measurement of left ventricular function. Left ventricular function was recorded via a physiological pressure transducer (UFI, Model 1050BP, Morro Bay, CA, USA) linked to a PowerLab recording system (ADInstruments, Castle Hill, NSW, Australia). Coronary flow was monitored via a Doppler flow probe located in the aortic perfusion line and connected to a TS410 flow meter (Transonics, Ithaca, New York, USA). Data from hearts with a coronary flow greater than 5 mL/min were excluded from the experiment. Data was recorded using Chart 5.0 software (ADInstruments, Castle Hill, NSW, Australia) to calculate end systolic pressure (ESP), end diastolic pressure (EDP), contraction and relaxation over time (±dP/dt) and heart rate. Fluid temperature was measured via a thermometer at the entry of the aortic cannula and temperature was maintained at 37.3°C. Hearts were paced at 420 bpm via a silver wire embedded into the left ventricle and grounded using an electrode attached to the cannula. The balloon was inflated to an EDP between 0 and 5 mmHg and the heart was then equilibrated for 10 minutes at this pressure. Following this equilibration period, the developed and systolic pressures were measured for 30 seconds at each of the following EDP increments: 0, 5, 10, 15, 20 and 30 mmHg.

In order to determine myocardial diastolic stiffness, the stress (σ, dyne/cm2) and the tangent elastic modulus (E, dyne/cm2) of the mid-wall at the equator of the left ventricle must first be calculated. This is achieved by assuming the ventricle is of spherical geometry and that the mid-wall equatorial region is representative of the remaining myocardium:

$$\sigma = \frac{VP}{W}\left(1 + \frac{4(V+W)}{[V^{1/3} + (V+W)^{1/3}]^3}\right)$$

$$E = 3\left\{\frac{VP}{W} - \sigma + \frac{\left(\frac{\sigma}{V} + \frac{(W\sigma - VP)}{W(V+W)} + \frac{\sigma.dP}{P.dV}\right) \times \left(V^{1/3} + (V+W)^{1/3}\right)}{\left(V^{-2/3} + (V+W)^{-2/3}\right)}\right\}$$

,

where V is chamber volume (mL), W is left ventricular wall volume (0.943 mL/g ventricular weight), and P is end diastolic pressure (dyne/cm2 = 7.5 x 10-4 mmHg). Myocardial diastolic stiffness is calculated as the diastolic stiffness constant (κ,dimensionless), the slope of the linear relation between E and σ (Mirsky & Parmley 1973).

The variables investigated included altering the perfusion pressure of the Langendorff equipment by changing the height of the column. The pressures investigated were 60, 70 and 80 mmHg twice per experiment.

The coronary flow, cardiac function and stiffness of the heart are normally calculated with the left ventricular pressure at 10 mmHg. It was investigated if different diastolic pressures (0, 5, 10, 15, 20 and 30 mmHg) showed variation in cardiac function and flow. The volume of water in the balloon at these pressures was also investigated to determine if these volumes varied between the strains at the various pressures and to determine if the increase in volume affected the function of the hearts. The impact of balloon volume on function and histological appearance of the heart was investigated.

A2.3 Results

The cardiac function of *mdx* and C57 mice was improved at the higher perfusion pressure in both the C57 and *mdx* mice.

	60 mmHg	**70 mmHg**	**80 mmHg**
C57	93.28±1.17	112.05±1.6	125.46±2.4
mdx	102.15±1.9	120.38±2.3	135.98±3.2

Table A2.1: Cardiac function of C57 and *mdx* mice at increasing perfusion pressures

In stiffness experiments, the functional data recordings used for calculations is at a left ventricular pressure of 10 mmHg, this value is the pressure at which the normal heart functions. The different pressures were investigated and it was found that the function at lower (0-5 mmHg) and higher pressures (20-30 mmHg) was decreased compared to the function at higher pressures (10-15 mmHg).

	C57	*mdx*
0 mmHg	91.33±9.0	88.54±7.4
5 mmHg	112.27±6.7	102.28±6.6
10 mmHg	135.96±3.3	134.53±1.6
15 mmHg	137.56±3.2	136.08±2.0
20 mmHg	136.42±3.6	133.07±2.6
30 mmHg	133.62±4.2	129.33±3.2

Table A2.2: Cardiac function of C57 and *mdx* mice at increasing left ventricular diastolic pressures

The coronary flow was not affected by increasing left ventricular pressures (Table A2.3) but increased with increasing perfusion pressures (Table A2.4).

	C57	*mdx*
0 mmHg	2.52±0.07	2.53±0.08
5 mmHg	2.39±0.1	2.35±0.08
10 mmHg	2.41±0.1	2.30±0.07
15 mmHg	2.40±0.1	2.28±0.07
20 mmHg	2.4±0.1	2.21±0.06
30 mmHg	2.3±0.1	2.18±0.06

Table A2.3: Coronary flow of C57 and *mdx* hearts at increasing left ventricular diastolic pressures.

	60 mmHg	70 mmHg	80 mmHg
C57	1.73±0.15	2.04±0.19	2.38±0.24
mdx	2.07±0.17	2.62±0.21	3.18±0.30

Table A2.4: Coronary flow of C57 and *mdx* hearts at increasing perfusion pressures.

NOTE:

In the initial Langendorff experiments (exercise, pirfenidone and l-arginine), the Langendorff equipment was manufactured by ADInstruments (Figure A2.1 (a) and (b)). Several problems were encountered with this apparatus, leading to difficulties in acquiring data. The mouse heart is extremely sensitive to the temperature of Krebs entering the heart. It was discovered that the Krebs was losing heat (around 5°C) from the chamber to the heart, leading to lower cardiac contractility and incorrect coronary flow. After weeks of modifying this equipment to ensure it was suitable for mouse heart experiment, it was determined not to be suitable for these experiments. It is understood subsequent modifications have been made by ADI to improve its suitability for mice.

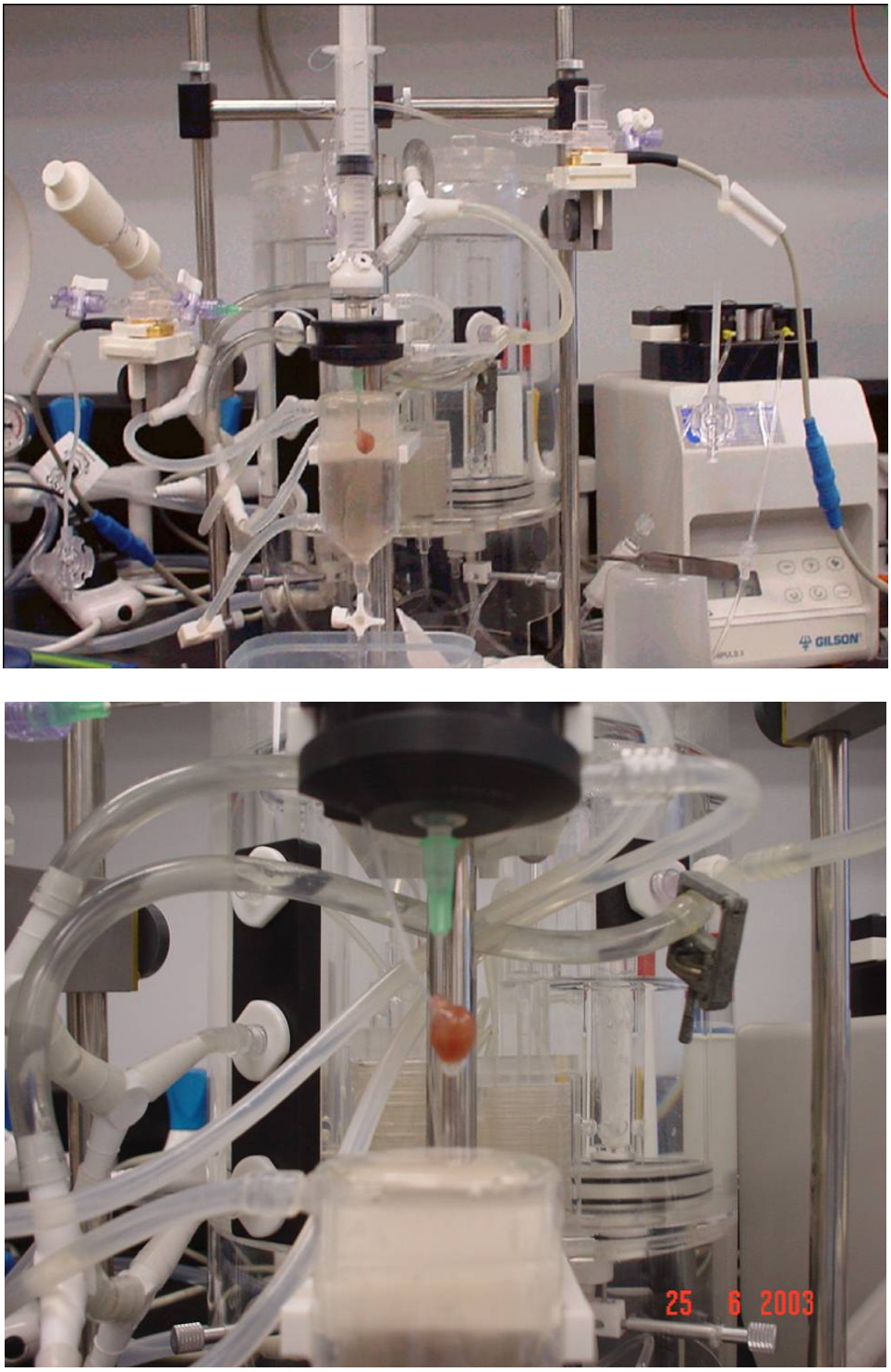

Figure A2.1: Original Langendorff equipment, note the waterjacketed lines on both sides

For the remaining Langendorff experiments, a Langendorff system similar to that developed by John Headrick was established using Radnoti glassware (Figure A2.2). A heating coil, accurate perfusion pressure and a flow probe were employed in this set up. This allowed for a constant temperature and correct perfusion pressures and accurate flow measurements to be recorded.

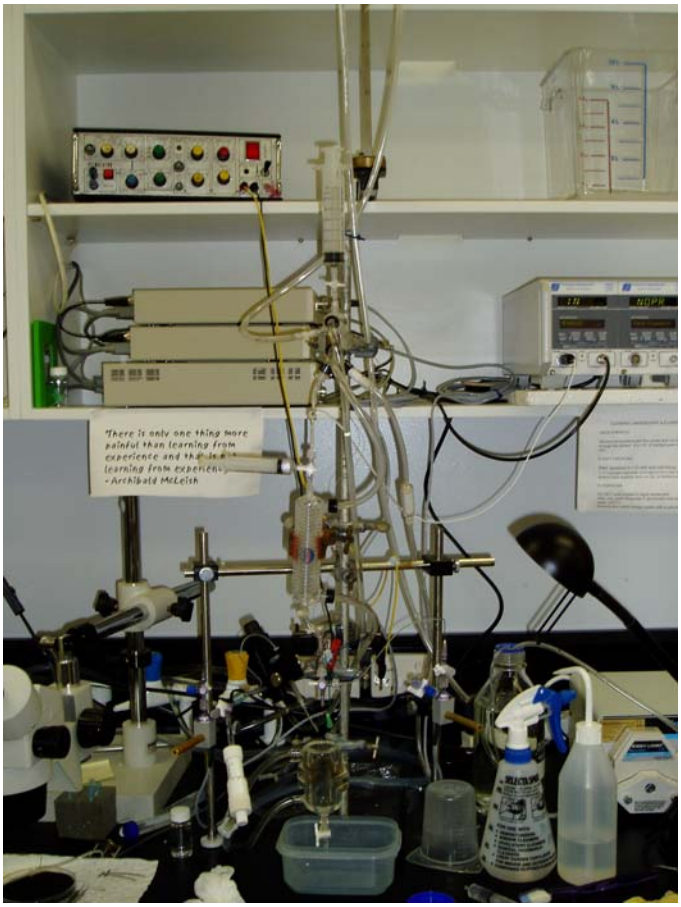

Figure A2.2: Final Langendorff set up, with heating coil to ensure correct perfusion fluid temperature.

A2.4: Discussion

The Langendorff technique had to be optimized to suit the *mdx* mouse. Initially, after the heart excision, it was placed on ice to isolate the aorta, but it was found the heart failed to function efficiently after exposure to these extreme temperatures. It is known that *mdx* mice have calcium overload and that ice cold temperatures can stress the heart, causing RCC, contributing to the excess calcium overload in the heart, leading to insufficient functioning and contracture of the heart. In previous experiments in the lab, the addition of BDM to the Krebs solution could prevent this calcium overload and cause no additional damage to the heart. Subsequent Langendorff experiments involved the addition of BDM to the Krebs. The heart functioned better if BDM was added to the chilled Krebs, rather than the heart being placed on frozen Krebs. A small volume of Krebs containing 10 mM 2,3-butanedione monoxime (temperature 21°C) in a petrie dish was used to bath the heart in while isolating the aorta.

With increasing perfusion pressures, it was found that the perfusion pressure of 80 mmHg improved supply of oxygen and nutrients to the myocardium and was optimised.

Cardiac function was highest at a diastolic pressure of 10-15 mmHg in both *mdx* and C57 mice. The diastolic pressure is at 10mmHg in normal, healthy hearts, so the left ventricular function and stiffness calculations continued to be measured at this pressure. The cardiac function was also compared in the exercise experiments between 10, 20 and 30 mmHg, similarly, the function at 10 mmHg was highest.

Coronary flow was higher at lower left ventricular pressures, in both *mdx* and C57s but this was of no concern. The flow was below 5mL/min in all readings and a higher function is of greater value in these experiments.

The optimum pressure at which to perform Langendorff experiments are at a perfusion pressure of 80 mmHg and at a left ventricular diastolic pressure of 10 mmHg.